

Iridium and rhodium pyrazolyl and carbene based catalysts for X-C bond formation

Author:

Mancano, Giulia

Publication Date:

2013

DOI:

<https://doi.org/10.26190/unsworks/2496>

License:

<https://creativecommons.org/licenses/by-nc-nd/3.0/au/>

Link to license to see what you are allowed to do with this resource.

Downloaded from <http://hdl.handle.net/1959.4/52945> in <https://unsworks.unsw.edu.au> on 2024-05-01

Iridium and Rhodium Pyrazolyl and Carbene Based Catalysts for X-C Bond Formation

A thesis submitted in fulfillment of the requirements for
admission to the degree of

Doctor of Philosophy

by

Giulia Mancano



School of Chemistry
The University of New South Wales
Australia
April 2013

PLEASE TYPE

THE UNIVERSITY OF NEW SOUTH WALES
Thesis/Dissertation Sheet

Surname or Family name: Mancano

First name: Giulia

Other name/s:

Abbreviation for degree as given in the University calendar: PhD

School: School of Chemistry

Faculty: Faculty of Science

Title: Iridium and Rhodium Pyrazolyl and Carbene Based
Catalyst for X-C Bond Formation

Abstract 350 words maximum: (PLEASE TYPE)

This thesis describes the investigation of Ir(I) and Rh(I) complexes as catalysts to facilitate the addition of X-H (X= Si, O and N) bonds across an alkyne C≡C triple bond. Towards this goal two new pincer ligands were prepared that contained a central NHC donor group linked to two pendent pyrazolyl donor groups by either a methyl (NCN^{Me}) or ethyl (NCN^{Et}) group. The longer ethyl linker of NCN^{Et} led to a higher lability of one pyrazole donor. The coordination properties of the pincer ligands also varied depending on the nature of the metal centre and the complex coligands with tridentate (k³), bidentate (k²) and monodentate (k¹) coordination modes all being observed. A bimetallic complex [Rh(NCN^{Me})CO]₂(BPh₄)₂ (2.6) was also prepared where the NCN^{Me} ligand coordinated in an unusual bridging mode.

The new pincer complexes were investigated as catalysts for the hydroamination, hydroalkoxylation and hydrosilylation of alkynes, and their reactivity was compared with two analogous complexes containing an NHC-pyrazolyl chelate. For the intramolecular hydroamination of 5-phenyl-4-pentyn-1-amine (3.1) the pincer ligand geometry was responsible for a decrease in catalyst activity, however, during the cyclisation of 4-pentynoic acid (3.6) the pincer ligands appeared to stabilise the catalyst against deactivation resulting in higher reaction conversions. A marked difference was also observed between catalysts containing the NCN^{Me} or NCN^{Et} pincer ligands.

A series of previously reported Ir(I) and Rh(I) complexes were also investigated as catalysts for the intermolecular hydroamination of terminal alkynes with primary amines. Catalysts containing the weakly coordinating BARF anion were found to be much more effective than complexes containing BPh₄. In general, catalysts containing CO coligands were more beneficial than those containing COD, with iridium catalysts significantly more active than rhodium. The nature of the chelating ligand group, either bis(pyrazolyl)methane (bpm) or 1-[2-(diphenylphosphino)ethyl]pyrazole (PyP), had little impact on catalyst activity. The bimetallic system (m-L)[Ir(CO)₂]₂(BARF)₂ (4.6) was found to be the most active catalyst of the series, particularly for the hydroamination of phenylacetylene (3.3) and aniline (3.4), for which it is one of the most efficient catalysts known to date.

Declaration relating to disposition of project thesis/dissertation

I hereby grant to the University of New South Wales or its agents the right to archive and to make available my thesis or dissertation in whole or in part in the University libraries in all forms of media, now or here after known, subject to the provisions of the Copyright Act 1968. I retain all property rights, such as patent rights. I also retain the right to use in future works (such as articles or books) all or part of this thesis or dissertation.

I also authorise University Microfilms to use the 350 word abstract of my thesis in Dissertation Abstracts International (this is applicable to doctoral theses only).


Signature


Witness

22/10/2013
Date

The University recognises that there may be exceptional circumstances requiring restrictions on copying or conditions on use. Requests for restriction for a period of up to 2 years must be made in writing. Requests for a longer period of restriction may be considered in exceptional circumstances and require the approval of the Dean of Graduate Research.

FOR OFFICE USE ONLY

Date of completion of requirements for Award:

THIS SHEET IS TO BE GLUED TO THE INSIDE FRONT COVER OF THE THESIS

COPYRIGHT STATEMENT

'I hereby grant the University of New South Wales or its agents the right to archive and to make available my thesis or dissertation in whole or part in the University libraries in all forms of media, now or here after known, subject to the provisions of the Copyright Act 1968. I retain all proprietary rights, such as patent rights. I also retain the right to use in future works (such as articles or books) all or part of this thesis or dissertation.

I also authorise University Microfilms to use the 350 word abstract of my thesis in Dissertation Abstract International (this is applicable to doctoral theses only).

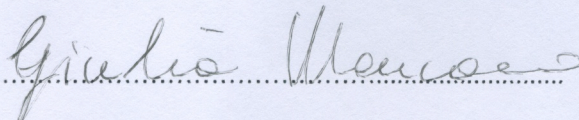
I have either used no substantial portions of copyright material in my thesis or I have obtained permission to use copyright material; where permission has not been granted I have applied/will apply for a partial restriction of the digital copy of my thesis or dissertation.'

Signed 

Date 22/10/2013

AUTHENTICITY STATEMENT

'I certify that the Library deposit digital copy is a direct equivalent of the final officially approved version of my thesis. No emendation of content has occurred and if there are any minor variations in formatting, they are the result of the conversion to digital format.'

Signed 

Date 22/10/2013

ORIGINALITY STATEMENT

'I hereby declare that this submission is my own work and to the best of my knowledge it contains no materials previously published or written by another person, or substantial proportions of material which have been accepted for the award of any other degree or diploma at UNSW or any other educational institution, except where due acknowledgement is made in the thesis. Any contribution made to the research by others, with whom I have worked at UNSW or elsewhere, is explicitly acknowledged in the thesis. I also declare that the intellectual content of this thesis is the product of my own work, except to the extent that assistance from others in the project's design and conception or in style, presentation and linguistic expression is acknowledged.'

Signed Giulia Mancini

Date 22/10/2013

ABSTRACT

This thesis describes the investigation of Ir(I) and Rh(I) complexes as catalysts to facilitate the addition of X-H (X= Si, O and N) bonds across an alkyne C \equiv C triple bond. Towards this goal two new pincer ligands were prepared that contained a central NHC donor group linked to two pendent pyrazolyl donor groups by either a methyl (NCN^{Me}) or ethyl (NCN^{Et}) group. The longer ethyl linker of NCN^{Et} led to a higher lability of one pyrazole donor. The coordination properties of the pincer ligands also varied depending on the nature of the metal centre and the complex with tridentate (κ^3), bidentate (κ^2) and monodentate (κ^1) coordination modes all being observed. A bimetallic complex [Rh(NCN^{Me})CO]₂(BPh₄)₂ was also prepared where the NCN^{Me} ligand coordinated in an unusual bridging mode.

The new pincer complexes were investigated as catalysts for the hydroamination, hydroalkoxylation and hydrosilylation of alkynes, and their reactivity was compared with two analogous complexes containing an NHC-pyrazolyl chelate. For the intra-molecular hydroamination of 5-phenyl-4-pentyn-1-amine the pincer ligand geometry was responsible for a decrease in catalyst activity, however, during the cyclisation of 4-pentynoic acid the pincer ligands appeared to stabilise the catalyst against deactivation resulting in higher reaction conversions. A marked difference was also observed between catalysts containing the NCN^{Me} or NCN^{Et} pincer ligands.

A series of previously reported Ir(I) and Rh(I) complexes were also investigated as catalysts for the inter-molecular hydroamination of terminal alkynes with primary amines. Catalysts containing the weakly coordinating BArF anion were found to be

much more effective than complexes containing BPh_4^- . In general, catalysts containing CO co-ligands were more beneficial than those containing COD, with iridium catalysts significantly more active than rhodium. The nature of the chelating ligand group, either bis(pyrazolyl)methane (bpm) or 1-[2-(diphenylphosphino)ethyl]pyrazole (PyP), had little impact on catalyst activity. The bimetallic system $(\mu\text{-L})[\text{Ir}(\text{CO})_2]_2(\text{BArF})_2$ was found to be the most active catalyst of the series, particularly for the hydroamination of phenylacetylene and aniline, for which it is one of the most efficient catalysts known to date.

ACKNOWLEDGEMENTS

I would firstly like to express my deep gratitude to my supervisor, Prof. Barbara Ann Messerle, for the incredible patience, support and understanding throughout all the years of my PhD research.

I would also like to thank Dr. Michael J. Page for sharing his great ideas and experience. I am thankful to Oanh for introducing me to the UNSW laboratory and helping to adapt to the new working environment during the beginning of my PhD research.

I owe special thanks to all BAM group members, past and present, in particular to Marina, Yeng, Sandy, Carol, Mark, Chin, Andrey and Matt for all their advice and help with my project as well as for creating a good atmosphere in the laboratory, interesting conversations and most importantly their friendship.

There are many friends who have been there for me over the past few years. Particular thanks go to the closest friends I have had in Sydney: my flatmates Darren, Alisha and Shane, Carolina, Persefoni, Stephanie, Rasmus and Mareike for the long-distance mail and cheers to the friendships we had over the years.

I want to thank my loving family: my parents for their unconditional support which allowed me to pursue my interests, their love, care, and also for their time and effort over the years that gave me the opportunity to be where I am today.

Giulia Mancano

April 2013

LIST OF ABBREVIATIONS

Ar	aryl
atm	atmosphere
BArF	<i>tetrakis</i> [3,5- <i>bis</i> (trifluoromethyl)phenyl]borate anion
BPh ₄ ⁻	tetraphenylborate anion
bpm	<i>bis</i> (1-pyrazolyl)methane
br	broad (NMR)
Bu	butyl
C ₆ D ₆	Benzene- <i>d</i> ₆
Cat.	catalyst
COD	1,5-cyclooctadiene
Conv.	conversion
COSY	Correlation Spectroscopy
Cp*	1,2,3,4,5-pentamethylcyclopentadienyl
Cy	cyclohexyl
δ	chemical shift in ppm (NMR)
d	doublet (NMR)
D	deuterium
dcm	dichloromethane
DMF	<i>N,N</i> -dimethylformamide
dmsO	dimethylsulfoxide
<i>dppe</i>	1,2-bis(diphenylphosphino)ethane
ESI-MS	ElectroSpray Ionisation Mass Spectrometry
Et	ethyl
Et ₃ SiH	triethylsilane
Et ₂ O	diethyl ether
<i>fac</i>	facial

hrs	hours
HIV	human immunodeficiency virus
Hz	hertz (s^{-1})
<i>i</i>	<i>ipso</i>
Im	Imidazole
<i>i</i> -Pr	isopropyl
IR	infrared
<i>J</i>	scalar coupling constant (NMR)
L	ligand
m	multiplet (NMR)
<i>m</i>	<i>meta</i>
M-M	metal-metal distance in bimetallic complex
[M]	metal complex
Me	methyl
MeOH	methanol
min.	minute(s)
mmol	millimoles
mol	mole
<i>m/z</i>	mass to charge ratio
N	nitrogen donor ligand
<i>n</i> -Bu	normal butyl
NHCs	N-heterocyclic carbenes
NMR	Nuclear Magnetic Resonance
NOESY	Nuclear Overhauser Effect Spectroscopy
<i>o</i>	<i>ortho</i>
O-H	hydroxyl group
<i>p</i>	<i>para</i>
Ph	phenyl

ppm	parts per million
Pyp	1-[2-(diphenylphosphino)ethyl]pyrazole
Pz	pyrazole or pyrazolyl
q	quartet (NMR)
r.t	room temperature
s	singlet (NMR)
t	triplet (NMR)
t	time
<i>t</i> -Bu	tertiary butyl
TCE-d ₂	1,1,2,2-tetrachloroethane
thf	tetrahydrofuran
TM	transition metal
TOF	turn over frequency
TON	turn over number

TABLE OF CONTENTS

<i>ABSTRACT</i>	i
<i>ACKNOWLEDGEMENTS</i>	iii
<i>LIST OF ABBREVIATIONS</i>	iv
<i>TABLE OF CONTENTS</i>	vii
<i>LIST OF FIGURES</i>	xv
<i>LIST OF TABLES</i>	xx

Chapter 1: General Introduction

1.1 Transition metals in homogeneous catalysis	1
1.2 Catalysts in organic chemistry	1
1.3 Homogeneous and heterogeneous catalysts	2
1.4 Transition metal complexes as catalysts	4
1.5 Catalyst structure	5
1.5.1 Metal properties	6
1.5.2 The nature of the ligand	7
1.5.2.1 Multitopic ligands and ligand geometry	7
1.5.2.2 Phosphorus donor ligands	9
1.5.2.3 Nitrogen donor ligands	9
1.5.2.4 N-heterocyclic carbene donor ligands	10
1.5.2.5 The carbon monoxide ligand	11

1.5.2.6 π -Coordinating ligands	11
1.6 Bimetallic complexes	12
1.7 Counter ion properties	14
1.8 H-X addition to alkynes	15
1.8.1 Hydroamination	16
1.8.2 Hydroalkoxylation	17
1.8.3 Hydrosilylation	19
1.9 Objectives of this thesis	20
1.10 References	22

Chapter 2: Complexes with NCN Pincer Ligands

2.1 Introduction	26
2.1.1 Pincer ligands	26
2.1.2 Coordination properties of pincer ligands	27
2.1.3 NHC pincer complexes	29
2.1.4 Objectives	33
2.2 Results and discussion	34
2.2.1 Synthesis of ligand precursors	34
2.2.2 Synthesis of rhodium(I) and iridium(I) complexes containing the ligand NCN^{Me} (2.1)	36
2.2.2.1 Synthesis of $[\text{Rh}(\text{NCN}^{\text{Me}})(\text{COD})]\text{BPh}_4$ (2.3)	36

2.2.2.1.1	Solid state structure of [Rh(NCN ^{Me})(COD)]BPh ₄ (2.3)	39
2.2.2.2	Synthesis of [Ir(NCN ^{Me})(COD)]BPh ₄ (2.4) and [Ir(κ^1 -NCN ^{Me}) ₂ (COD)]BPh ₄ (2.5)	41
2.2.2.2.1	Solid state structure of [Ir(NCN ^{Me})(COD)]BPh ₄ (2.4) and [Ir(κ^1 -NCN ^{Me}) ₂ (COD)]BPh ₄ (2.5)	44
2.2.2.3	Synthesis of [Rh(μ -NCN ^{Me})(CO)] ₂ (BPh ₄) ₂ (2.6)	47
2.2.2.3.1	Solid state structure of [Rh(μ - NCN ^{Me})CO] ₂ (BPh ₄) ₂ (2.6)	49
2.2.2.4	Synthesis of [Ir(NCN ^{Me})(CO)] ₂ BPh ₄ (2.7)	50
2.2.3	Synthesis of rhodium(I) and iridium(I) complexes containing the ligand NCN ^{Et} (2.2)	52
2.2.3.1	Synthesis of [Ir(κ^1 -NCN ^{Et}) ₂ (COD)]BPh ₄ (2.8)	52
2.2.3.1.1	Solid state structure of [Ir(κ^1 - NCN ^{Et}) ₂ (COD)]BPh ₄ (2.8)	53
2.2.3.2	Synthesis of [Rh(NCN ^{Et})(COD)]BPh ₄ (2.9)	55
2.2.3.2.1	Solid state structure of [Rh(NCN ^{Et})(COD)]BPh ₄ (2.9)	56
2.2.3.3	Synthesis of [Rh(NCN ^{Et})(CO)] ₂ BPh ₄ (2.10)	58
2.2.4	Synthesis of [Ir(NCN ^{Me})(PPh ₃) ₂ (CO)]BPh ₄ (2.1V) and [Ir(NCN ^{Et})(PPh ₃) ₂ (CO)]BPh ₄ (2.2V)	60
2.2.4.1	Solid state structure of [Ir(NCN ^{Me})(PPh ₃) ₂ (CO)]BPh ₄ (2.1V)	61
2.3	Summary and conclusions	62
2.4	References	64

Chapter 3: Catalysis with Pincer Complexes

3.1 Introduction	68
3.1.1 Reactivity of pincer complexes	68
3.1.2 Pincer complexes in catalysis	68
<i>3.1.2.1 Ir and Rh complexes with pincer ligands</i>	71
3.1.3 Iridium and rhodium catalysed addition of X-H bonds to alkynes	73
<i>3.1.3.1 Hydroamination</i>	73
<i>3.1.3.2 Hydroalkoxylation</i>	77
<i>3.1.3.3 Hydrosilylation</i>	79
3.1.4 Objectives	82
3.2 Results and discussion	84
3.2.1 Intra-molecular hydroamination of 5-phenyl-4-pentyn-1-amine (3.1) to 2-benzyl-1-pyrroline (3.2)	84
3.2.2 Inter-molecular hydroamination of phenylacetylene (3.3) and aniline (3.4)	89
3.2.3 Hydroalkoxylation of 4-pentynoic acid (3.6) to γ -methylene- γ -butyrolactone (3.7)	92
3.2.4 Cyclization of 2-(5-Hydroxypent-1-ynyl)benzyl alcohol (3.8)	99
3.2.5 Catalysed hydrosilylation of alkynes	99
3.3 Summary and conclusions	105
3.4 References	108

Chapter 4: Inter-molecular Hydroamination

4.1 Introduction	112
4.1.1 The inter-molecular hydroamination of alkynes	112
4.1.2 Inter-molecular hydroamination catalysts	113
4.1.2.1 Lanthanide and actinide complexes	113
4.1.2.2 Early Transition Metal Complexes	115
4.1.2.3 Late Transition Metal Complexes	116
4.1.3 Ir(I) and Rh(I) Intra-molecular Hydroamination Catalysts	120
4.1.4 Counter ion effects on Ir(I) and Rh(I) catalysts	121
4.1.5 Bimetallic Ir(I) and Rh(I) Catalysts	122
4.1.6 Objectives	123
4.2 Results and discussion	125
4.2.1 Hydroamination of phenylacetylene (3.3) and aniline (3.4)	125
4.2.1.1 Catalysts with <i>P,N</i> -donor ligand: $[Ir(PyP)(COD)]BPh_4$ (4.1), $[Ir(PyP)(COD)]BArF$ (4.2) and $[Ir(PyP)(CO)]BArF$ (4.3)	125
4.2.1.2 Catalysts with <i>N,N</i> -donor ligands: $[Ir(bpm)(CO)_2]BArF$ (4.4) and $[Rh(bpm)(CO)_2]BArF$ (4.5)	128
4.2.1.3 Bimetallic catalysts: $(\mu-L)[Ir(CO)_2]_2(BArF)_2$ (4.6) and $(\mu-L)[Rh(CO)_2]_2(BArF)_2$ (4.7)	130
4.2.2 Hydroamination of aliphatic substrates with aniline	135
4.2.3 Investigation of Imine Hydrolysis	138

4.3 Summary and Conclusions	140
4.4 References	142

Chapter 5: Summary and Conclusions

5.1 Summary and conclusions	144
-----------------------------	-----

Chapter 6: EXPERIMENTAL

PART 1: GENERAL PROCEDURE	145
----------------------------------	-----

E.1.1 General consideration	147
-----------------------------	-----

E.1.2 NMR spectroscopy	148
------------------------	-----

E.1.3 Other characterization techniques	149
---	-----

PART 2: EXPERIMENTAL FOR CHAPTER 2	150
---	-----

E.2.1 Synthesis of NCN ligands	150
--------------------------------	-----

<i>E.2.1.1 Synthesis of $\text{NCN}^{\text{Me}}\cdot\text{HBPh}_4$ (2.1)</i>	150
---	-----

<i>E.2.1.2 Synthesis of $\text{NCN}^{\text{Et}}\cdot\text{HBPh}_4$ (2.2)</i>	151
---	-----

E.2.2 Synthesis of Rh and Ir COD containing complexes with $\text{NCN}^{\text{Me}}\cdot\text{HBPh}_4$ (2.1)	152
---	-----

<i>E.2.2.1 Synthesis of $[\text{Rh}(\text{NCN}^{\text{Me}})(\text{COD})]\text{BPh}_4$ (2.3)</i>	152
--	-----

<i>E.2.2.2 Reaction of NCN^{Me} (2.1) with $[\text{Ir}(\mu\text{-Cl})(\text{COD})]_2$</i>	153
---	-----

E.2.3 Synthesis of Rh and Ir CO containing complexes with $\text{NCN}^{\text{Me}}\cdot\text{HBPh}_4$ (2.1)	155
--	-----

<i>E.2.3.1 Synthesis of $[Rh(NCN^{Me})(CO)]_2(BPh_4)_2$ (2.6)</i>	155
<i>E.2.3.2 Synthesis of $[Ir(NCN^{Me})(CO)_2]BPh_4$ (2.7)</i>	156
E.2.4 Synthesis of Ir and Rh COD containing complexes with $NCN^{Et}.HBPh_4$ (2.2)	158
<i>E.2.4.1. Synthesis of $[Ir(NCN^{Et})_2(COD)]BPh_4$ (2.8)</i>	158
<i>E.2.4.2 Synthesis of $[Rh(NCN^{Et})(COD)]BPh_4$ (2.9)</i>	159
<i>E.2.4.3 Synthesis of $[Rh(NCN^{Et})(CO)_2]BPh_4$ (2.10)</i>	160
E.2.5 Synthesis of $Ir(PPh_3)_2(CO)$ complexes with $NCN^{Me}.HBPh_4$ (2.1) and $NCN^{Et}.HBPh_4$ (2.2)	160
<i>E.2.5.1 Synthesis of $[Ir(NCN^{Me})(PPh_3)_2(CO)]BPh_4$ (2.1V)</i>	160
<i>E.2.5.2 Synthesis of $[Ir(NCN^{Et})(PPh_3)_2(CO)]BPh_4$ (2.2V)</i>	161

PART 3: EXPERIMENTAL FOR CHAPTER 3 163

E.3.1 Iridium(I) and Rhodium(I) catalysed reactions	163
<i>E.3.1.2 General procedure</i>	163
<i>E.3.1.3 Intra-molecular hydroamination of 5-phenyl-4-pentyn-1-amine (3.1) to 2-methyl-1-pyrroline (3.2)</i>	164
<i>E.3.1.4 Inter-molecular hydroamination of phenylacetylene (3.3) and aniline (3.4)</i>	165
<i>E.3.1.5 Catalysed hydroxylation of 4-pentynoic acid (3.6)</i>	166
<i>E.3.1.6 Catalysed dihydroalkoxylation of 2-(5-Hydroxypent-1-ynyl)benzyl alcohol (3.8)</i>	168
<i>E.3.1.7 Catalysed hydrosilylation of alkynes</i>	169
E.3.2 Crystallographic Data	172
	181

PART 4: EXPERIMENTAL FOR CHAPTER 4

E.4.1 Inter-molecular hydroamination catalysis of terminal alkynes with amines	181
E.4.2 Inter-molecular hydroamination of phenylacetylene (3.3) and aniline (3.4)	182
E.5 References	186

Appendix

X-ray crystallographic data

LIST OF FIGURES

- Figure 1.1: Bonding of a π -bond donor to a metal. Arrow a represents electron donation from the filled substrate π -bond to the empty d_σ orbital on the metal; arrows b represent the back donation from the filled $M(d_\pi)$ orbital to the empty substrate π^* 4
- Figure 2.1: ^1H (400 MHz, DMSO-d_6) NMR spectra of the a) bis(methylpyrazolyl)imidazolium salt (**2.1**) and b) bis(ethylpyrazolyl)imidazolium salt (**2.2**). 36
- Figure 2.2: a) ^1H NMR (400 MHz, DMSO-d_6) of the crude residue from the synthesis of Rh(I) complex **2.3**; b) three resonances due to the H^4Pz of isomeric products. 37
- Figure 2.3: ^1H (400 MHz, DMSO-d_6) NMR spectrum of $[\text{Rh}(\text{NCN}^{\text{Me}})(\text{COD})]\text{BPh}_4$ complex (**2.3**). 38
- Figure 2.4: ORTEP diagram of the cationic fragment of $[\text{Rh}(\text{NCN}^{\text{Me}})(\text{COD})]\text{BPh}_4$ complex **2.3**, with 40% probability ellipsoids for the non hydrogen atoms, as viewed from the equatorial axis a) and from the axial axis b). Selected bond lengths (\AA) and angles ($^\circ$): $\text{Rh-C}_{\text{NHC}} = 1.981(3)$, $\text{Rh-N} = 2.267(2)$, $\text{Rh-N} = 2.270(2)$, $\text{Rh-COD}_{\text{ax}} = 2.270(3)/2.273(3)$, $\text{Rh-COD}_{\text{eq}} = 2.097(3)/2.097(3)$, $\text{N-Rh-N} = 88.77(10)$. 40
- Figure 2.5: ^1H (400 MHz, DMSO-d_6) NMR spectrum of the $[\text{Ir}(\text{NCN}^{\text{Me}})(\text{COD})]\text{BPh}_4$ complex (**2.4**) 42
- Figure 2.6: Variable temperature ^1H NMR stacked spectra (600 MHz, THF-d_8) of **2.4** showing the broad alkenic COD protons resonances as temperature is decreased from a) 298.15 K to b) 268.15 K, c) 258.15 K and d) 248.15 K. 43

Figure 2.7: ^1H (400 MHz, DMSO-d_6) NMR spectrum of $[\text{Ir}(\kappa^1\text{-NCN}^{\text{Me}})_2(\text{COD})]\text{BPh}_4$ complex (2.5) 44

Figure 2.8: ORTEP diagram of the cationic fragment of $[\text{Ir}(\text{NCN}^{\text{Me}})(\text{COD})]\text{BPh}_4$ (2.4), with 40% probability ellipsoids for the non hydrogen atoms, as viewed from the equatorial axis a) and from the axial axis b). Selected bond lengths (\AA) and angles ($^\circ$): $\text{Ir-C}_{\text{NHC}} = 1.995(4)$, $\text{Ir-N} = 2.194(3)$, $\text{Ir-N} = 2.247(3)$, $\text{Ir-COD}_{\text{ax}} = 2.210(4)/2.233(4)$, $\text{Ir-COD}_{\text{eq}} = 2.093(4)/2.093(4)$, $\text{N-Ir-N} = 85.68(12)$. 45

Figure 2.9: ORTEP diagram of the cationic fragment of $[\text{Ir}(\kappa^1\text{-NCN}^{\text{Me}})_2(\text{COD})]\text{BPh}_4$ (2.5), with 40% probability ellipsoids for the non hydrogen atoms, as viewed from the equatorial axis a) and from the axial axis b). Selected bond lengths (\AA) and angles ($^\circ$): $\text{Ir-C}_{2\text{NHC}} = 2.0463(3)$, $\text{Ir-C}_{2'\text{NHC}} = 2.048(3)$, $\text{Ir-COD}_{\text{C1/2}} = 2.213(3)/2.180(3)$, $\text{Ir-COD}_{\text{C5/6}} = 2.210(3)/2.179(3)$, $\text{C2-Ir-C2'} = 97.11(12)$. 46

Figure 2.10: ^1H (400 MHz, DMSO-d_6) NMR spectrum of $[\text{Rh}(\mu\text{-NCN}^{\text{Me}})(\text{CO})]_2(\text{BPh}_4)_2$ complex (2.6) 48

Figure 2.11: ORTEP diagram of the cationic fragment of $[\text{Rh}(\mu\text{-NCN}^{\text{Me}})\text{CO}]_2(\text{BPh}_4)_2$ (2.6), with 40% probability ellipsoids for the non hydrogen atoms,, as viewed from the equatorial axis a) and from the axial axis b). Selected bond lengths (\AA) and angles ($^\circ$): $\text{Rh1-Rh2} = 3.341$, $\text{Rh1-C}_{\text{NHC}} = 1.975(7)$, $\text{Rh2-C}_{\text{NHC}} = 1.992(7)$, $\text{Rh1-CO} = 1.783(8)$, $\text{Rh2-CO} = 1.808(9)$, $\text{Rh1-N}_{\text{transCO}} = 2.074(5)$, $\text{Rh2-N}_{\text{transCO}} = 2.100(6)$, $\text{Rh1-N}_{\text{transNHC}} = 2.103(6)$, $\text{Rh2-N}_{\text{transNHC}} = 2.098(6)$. 49

Figure 2.12: Stacked ^1H NMR spectra (400 MHz, DMSO-d_6) of a) $[\text{Ir}(\text{NCN}^{\text{Me}})(\text{COD})]\text{BPh}_4$ (2.3) and b) $[\text{Ir}(\text{NCN}^{\text{Me}})(\text{CO})_2]\text{BPh}_4$ (2.7). 51

Figure 2.13: ^1H NMR (400 MHz, DMSO-d_6) NMR spectrum of $[\text{Ir}(\text{NCN}^{\text{Et}})_2(\text{COD})]\text{BPh}_4$ (**2.8**) 53

Figure 2.14: ORTEP diagram of the cationic fragment of $[\text{Ir}(\text{NCN}^{\text{Et}})_2(\text{COD})]\text{BPh}_4$ (**2.8**), with 40% probability ellipsoids for the non hydrogen atoms, as viewed from the equatorial axis a) and from the axial axis b). Selected bond lengths (\AA) and angles ($^\circ$): Ir-C1A_{NHC} = 2.041(2), Ir-C1B_{NHC} = 2.052(3), Ir-COD_{C1C/C2C} = 2.200(3)/2.185(3), Ir-COD_{C5C/C6C} = 2.193(3)/2.185(3), C1A-Ir-C1B = 93.79(10).

Figure 2.15: ^1H (400 MHz, acetone- d_6) NMR spectrum of $[\text{Rh}(\text{NCN}^{\text{Et}})(\text{COD})]\text{BPh}_4$ complex (**2.9**). 56

Figure 2.16: ORTEP diagram of the cationic fragment of $[\text{Rh}(\text{NCN}^{\text{Et}})(\text{COD})]\text{BPh}_4$ complex (**2.9**), with 40% probability ellipsoids for the non hydrogen atoms, as viewed from the axial axis a) and from the equatorial axis b). Selected bond lengths (\AA) and angles ($^\circ$): Rh-C_{NHC} = 2.037(2), Rh-N2A = 2.089(2), Rh-COD_{transNHC} = 2.213(3)/2.179(2), Rh-COD_{transN} = 2.159(2)/2.122(2), C_{NHC}-Rh-N2A = 85.37(8).

Figure 2.17: ^1H (500 MHz, acetone- d_6) NMR spectrum of $[\text{Rh}(\text{NCN}^{\text{Et}})(\text{CO})_2]\text{BPh}_4$ complex (**2.10**). 59

Figure 2.18: ^1H (400 MHz, THF- d_8) NMR spectrum of $[\text{IrNCN}^{\text{Et}}(\text{PPh}_3)_2(\text{CO})](\text{BPh}_4)$ complex (**2.1V**). 61

Figure 2.19: ORTEP diagram of the cationic fragment of complex $[\text{Ir}(\text{NCN}^{\text{Me}})(\text{PPh}_3)_2(\text{CO})]\text{BPh}_4$ (**2.1V**), with 40% probability ellipsoids for the non hydrogen atoms, as viewed from the equatorial axis. Selected bond lengths (\AA) and angles ($^\circ$): Ir-C_{NHC} = 2.0711(19), Ir-CO = 1.863(2), Ir-P_{1A} = 2.3240(5), Ir-P_{1B} = 2.3416(5), P_{1A}-Ir-C_{NHC} = 92.56(5), P_{1B}-

Ir-C_{NHC} = 90.05(5).

Figure 3.1: Reaction profile for the hydroamination of 5-phenyl-4-pentyn-1-amine (**3.1**) to 2-benzyl-1-pyrroline (**3.2**) in 1,4-dioxane-d₈ at 100 °C using 5 mol % catalyst loading of [Rh(NCN^{Me})(COD)]BPh₄ (**2.3**), [Ir(NCN^{Me})(COD)]BPh₄ (**2.4**), [Rh(NCN^{Et})(COD)]BPh₄ (**2.9**) and [Rh(NC^{Me})(COD)]BPh₄ (**2.11**). 85

Figure 3.2: Reaction profile for the hydroamination of 5-phenyl-4-pentyn-1-amine (**3.1**) to 2-benzyl-1-pyrroline (**3.2**) in 1,4-dioxane-d₈ at 100 °C using 5 mol% catalyst loading of [Rh(NCN^{Me})(CO)]₂(BPh₄)₂ (**2.6**), [Ir(NCN^{Me})(CO)]₂BPh₄ (**2.7**), [Rh(NCN^{Et})(CO)]₂BPh₄ (**2.10**) and [Rh(NC^{Me})(CO)]₂BPh₄ (**2.12**). 87

Figure 3.3: Stacked ¹H NMR spectra (THF-d₈, 600 MHz, 333K) of hydroxylation of 4-pentynoic acid (**3.6**) to γ-methylene-γ-butyrolactone (**3.7**) in THF-d₈ at 80 °C at fixed time intervals: a) t=0; b) t= 4.3 hrs; c) t= 5.6 hrs; d) t= 12 hrs; e) t= 29 hrs. 93

Figure 3.4: Reaction profile for the cyclisation of 4-pentynoic acid (**3.6**) in 1,4-dioxane-d₈ at 100 °C using 5 mol% of [Rh(NCN^{Me})(COD)]BPh₄ (**2.3**), [Ir(NCN^{Me})(COD)]BPh₄ (**2.4**), [Rh(NCN^{Et})(COD)]BPh₄ (**2.9**) and [Rh(NC^{Me})(COD)]BPh₄ (**2.11**). 94

Figure 3.5: Reaction profile for the cyclisation of 4-pentynoic acid (**3.6**) in 1,4-dioxane-d₈ at 100 °C using 5 mol% of [Rh(NCN^{Me})(CO)]₂(BPh₄)₂ (**2.6**), [Ir(NCN^{Me})(CO)]₂BPh₄ (**2.7**), [Rh(NCN^{Et})(CO)]₂BPh₄ (**2.10**) and [Rh(NC^{Me})(CO)]₂BPh₄ (**2.12**). 96

Figure 3.6: ¹H NMR spectrum (acetone-d₆, 400 MHz, 333K) showing the three vinylsilanes product from the hydrosilylation of phenylacetylene (**3.3**) with triethylsilane using [Rh(NCN^{Me})(COD)]BPh₄ (**2.3**). 100

Figure 3.7: Product distribution at 24 hours for the hydrosilylation of phenylacetylene (**3.3**) in 101
acetone-d₆ at 55 °C with 5 mol% of the pincer complexes [Rh(NCN^{Me})(COD)]BPh₄ (**2.3**),
[Ir(NCN^{Me})(COD)]BPh₄ (**2.4**), [Rh(NCN^{Me})(CO)]₂(BPh₄)₂ (**2.6**) and [Ir(NCN^{Me})(CO)]₂BPh₄
(**2.7**).

Figure 3.8: Product distribution at 24 hours for the hydrosilylation of 1-phenylpropyne (**3.11**) in 102
acetone-d₆ at 55 °C with 5 mol% of the pincer complexes [Rh(NCN^{Me})(COD)]BPh₄ (**2.3**),
[Ir(NCN^{Me})(COD)]BPh₄ (**2.4**), [Rh(NCN^{Me})(CO)]₂(BPh₄)₂ (**2.6**) and [Ir(NCN^{Me})(CO)]₂BPh₄
(**2.7**).

Figure 4.1: Reaction profile of the inter-molecular hydroamination of phenylacetylene (**3.3**) and 131
aniline (**3.4**) into *E-N*-(1-phenylethylidene)benzeneamine (**3.5**) catalysed by 1.5 mol% of
complexes (μ-L)[Ir(CO)₂]₂(BArF)₂ (**4.6**) and (μ-L)[Rh(CO)₂]₂(BArF)₂ (**4.7**) at 100 °C in TCE-
d₂ and toluene-d₈.

Figure 4.2 Reaction profile of the inter-molecular hydroamination of phenylacetylene (**3.3**) and 132
aniline (**3.4**) into *E-N*-(1-phenylethylidene)benzeneamine (**3.5**) catalysed by 3.0 mol% metal
loading [Ir(PyP)(COD)]BPh₄ (**4.1**), [Ir(bpm)(CO)]₂BArF₄ (**4.4**) and (μ-L)[Ir(CO)₂]₂(BArF)₂
(**4.6**) at 100 °C in TCE-d₂.

Figure 4.3: Inter-molecular hydroamination of phenylacetylene (**3.3**) and aniline (**3.4**) into *E-* 140
N-(1-phenylethylidene)benzeneamine (**3.5**) and acetophenone (**4.13**) with addition of
deionized H₂O performed in TCE-d₂ at 100 °C using 1.5 mol % of (μ-L)[Ir(CO)₂]₂(BArF)₂
(**4.6**).

LIST OF TABLES

Table 3.1: Catalytic efficiency of $[\text{Rh}(\text{NCN}^{\text{Me}})(\text{COD})]\text{BPh}_4$ (**2.3**), $[\text{Ir}(\text{NCN}^{\text{Me}})(\text{COD})]\text{BPh}_4$ (**2.4**), $[\text{Rh}(\text{NCN}^{\text{Me}})(\text{CO})]_2(\text{BPh}_4)_2$ (**2.6**), $[\text{Ir}(\text{NCN}^{\text{Me}})(\text{CO})_2]\text{BPh}_4$ (**2.7**), $[\text{Rh}(\text{NCN}^{\text{Et}})(\text{COD})]\text{BPh}_4$ (**2.9**), $[\text{Rh}(\text{NCN}^{\text{Et}})(\text{CO})_2]\text{BPh}_4$ (**2.10**), $[\text{Rh}(\text{NC}^{\text{Me}})(\text{COD})]\text{BPh}_4$ (**2.11**) and $[\text{Rh}(\text{NC}^{\text{Me}})(\text{CO})_2]\text{BPh}_4$ (**2.12**) for the cyclisation of 5-phenyl-4-pentyn-1-amine (**3.1**).^[a] 88

Table 3.2: Catalytic efficiency of $[\text{Rh}(\text{NCN}^{\text{Me}})(\text{COD})]\text{BPh}_4$ (**2.3**), $[\text{Ir}(\text{NCN}^{\text{Me}})(\text{COD})]\text{BPh}_4$ (**2.4**), $[\text{Rh}(\text{NCN}^{\text{Me}})(\text{CO})]_2(\text{BPh}_4)_2$ (**2.6**), $[\text{Ir}(\text{NCN}^{\text{Me}})(\text{CO})_2]\text{BPh}_4$ (**2.7**), $[\text{Rh}(\text{NCN}^{\text{Me}})(\text{COD})]\text{BArF}$ (**2.3.BArF**), $[\text{Ir}(\text{NCN}^{\text{Me}})(\text{COD})]\text{BArF}$ (**2.4.BArF**), $[\text{Rh}(\text{NCN}^{\text{Me}})(\text{CO})]_2(\text{BArF})_2$ (**2.6.BArF**) and $[\text{Ir}(\text{NCN}^{\text{Me}})(\text{CO})_2]\text{BArF}$ (**2.7.BArF**) for the addition of phenylacetylene (**3.3**) to aniline (**3.4**).^[a] 91

Table 3.3: Catalytic efficiency of $[\text{Rh}(\text{NCN}^{\text{Me}})(\text{COD})]\text{BPh}_4$ (**2.3**), $[\text{Ir}(\text{NCN}^{\text{Me}})(\text{COD})]\text{BPh}_4$ (**2.4**), $[\text{Rh}(\text{NCN}^{\text{Me}})(\text{CO})]_2(\text{BPh}_4)_2$ (**2.6**), $[\text{Ir}(\text{NCN}^{\text{Me}})(\text{CO})_2]\text{BPh}_4$ (**2.7**), $[\text{Rh}(\text{NCN}^{\text{Et}})(\text{COD})]\text{BPh}_4$ (**2.9**), $[\text{Rh}(\text{NCN}^{\text{Et}})(\text{CO})_2]\text{BPh}_4$ (**2.10**), $[\text{Rh}(\text{NC}^{\text{Me}})(\text{COD})]\text{BPh}_4$ (**2.11**) and $[\text{Rh}(\text{NC}^{\text{Me}})(\text{CO})_2]\text{BPh}_4$ (**2.12**) for the cyclisation 4-pentynoic acid (**3.6**) to γ -methylene- γ -butyrolactone (**3.7**).^[a] 98

Table 3.4: Hydrosilylation of phenylacetylene ($\text{R} = \text{H}$) (**3.3**) with Et_3SiH and 1-phenylpropyne ($\text{R} = \text{CH}_3$) (**3.11**) with Et_3SiH using $[\text{Rh}(\text{NCN}^{\text{Me}})(\text{COD})]\text{BPh}_4$ (**2.3**), $[\text{Ir}(\text{NCN}^{\text{Me}})(\text{COD})]\text{BPh}_4$ (**2.4**), $[\text{Rh}(\text{NCN}^{\text{Me}})(\text{CO})]_2(\text{BPh}_4)_2$ (**2.6**) and $[\text{Ir}(\text{NCN}^{\text{Me}})(\text{CO})_2]\text{BPh}_4$ (**2.7**).^[a] 105

Table 4.1: Comparison of the catalytic activity of $[\text{Ir}(\text{PyP})(\text{COD})]\text{BPh}_4$ (**4.1**), $[\text{Ir}(\text{PyP})(\text{COD})]\text{BArF}_4$ (**4.2**) and $[\text{Ir}(\text{PyP})(\text{CO})_2]\text{BArF}_4$ (**4.3**) for the inter-molecular hydroamination of phenylacetylene (**3.3**) and aniline (**3.4**).^[a] 126

Table 4.2: Comparison of the catalytic activity of $[\text{Ir}(\text{bpm})(\text{CO})_2]\text{BArF}$ (**4.4**) and $[\text{Rh}(\text{bpm})(\text{CO})_2]\text{BArF}$ (**4.5**) for the inter-molecular hydroamination of phenylacetylene (**3.3**) and aniline (**3.4**).^[a] 129

Table 4.3: Comparison of the catalytic efficiency of $(\mu\text{-L})[\text{Ir}(\text{CO})_2]_2(\text{BArF})_2$ (**4.6**) with literature precedents for the inter-molecular hydroamination of phenylacetylene (**3.3**) and aniline (**3.4**) into *E-N*-(1-phenylethylidene)benzeneamine (**3.5**). 134

Table 4.4: Comparison of the catalytic activity of $[\text{Ir}(\text{bpm})(\text{CO})_2]\text{BArF}$ (**4.4**), $[\text{Rh}(\text{bpm})(\text{CO})_2]\text{BArF}$ (**4.5**) and $(\mu\text{-L})[\text{Ir}(\text{CO})_2]_2(\text{BArF})_2$ (**4.6**) for the inter-molecular hydroamination of aniline (**3.4**) and 1-heptyne (**4.8**). 136

Table 4.5: Comparison of the catalytic activity of $[\text{Ir}(\text{bpm})(\text{CO})_2]\text{BArF}$ (**4.4**), and $(\mu\text{-L})[\text{Ir}(\text{CO})_2]_2(\text{BArF})_2$ (**4.6**) complexes for the inter-molecular hydroamination of phenylacetylene (**3.3**) and 1-hexylamine (**4.11**). 137

Table E.1: Quantity of catalysts and substrates used for the intra-molecular hydroamination of 5-phenyl-4-pentyn-1-amine (**3.1**) to 2-benzyl-1-pyrroline (**3.2**) in dioxane- d_8 at 100 °C using pincer complexes with BPh_4 counter ion. 164

Table E.2: Quantity of catalysts and substrates used for the inter-molecular hydroamination of phenylacetylene (**3.3**) and aniline (**3.4**) into *E-N*-(1-phenylethylidene)benzeneamine imine (**3.5**) in dioxane at 100 °C using pincer complexes. 167

Table E.3: Quantity of catalysts and substrates used for the hydroalkoxylation 4-pentynoic acid (**3.6**) to γ -methylene- γ -butyrolactone (**3.7**) 100 °C using pincer complexes with BPh_4 counter ion. 167

Table E.4: Quantity of catalysts and substrates used for the dihydroalkoxylation of 169
2-(5-Hydroxypent-1-ynyl)benzyl alcohol (**3.8**) into 5,6- (**3.9A**) and 6,5- (**3.9B**) spiroketals in
dioxane-d₈ at 100 °C using pincer complexes with BPh₄ counter ion.

Table E.5: Quantity of catalysts and substrates used for the hydrosilylation of phenylacetylene 170
(**3.3**) and Et₃SiH in acetone-d₆ at 60 °C using pincer complexes with BPh₄ counter ion.

Table E.6: Quantity of catalysts and substrates used for the hydrosilylation of 1-phenylpropyne 171
(**3.11**) and Et₃SiH in acetone-d₆ at 60 °C using pincer complexes with BPh₄ counter ion.

Table E.7: Catalysed conversion of aniline (**3.4**) and 1-heptyne (**4.8**) in toluene-d₈ at 100 °C 181
using bimetallic complexes with *N,N*- bidentate ligands.

Table E.8: Catalysed conversion of phenylacetylene (**3.3**) and 1-hexylamine (**4.11**) in toluene- 182
d₈ at 100 °C using bimetallic complexes with *N,N*- bidentate ligands.

Table E.9: Catalysed conversion of 1-heptyne (**4.8**) and 1-hexylamine (**4.11**) in toluene-d₈ at 182
100 °C using bimetallic complex (μ-L)[Ir(CO)₂]₂(BArF)₂ (**4.6**).

Table E.10: Quantity of catalysts and substrates used for the inter-molecular hydroamination of 183
phenylacetylene (**3.3**) and aniline (**3.4**) into *E-N*-(1-phenylethylidene)benzeneamine imine (**3.5**)
at 100 °C using Ir(I) complexes with *P,N*- and *N,N*- bidentate ligands in various solvents.

Table E.11: Quantity of catalysts and substrates used for the inter-molecular hydroamination of 184
phenylacetylene (**3.3**) and aniline (**3.4**) into *E-N*-(1-phenylethylidene)benzeneamine imine (**3.5**)
at 100 °C using complexes with *N,N*- bidentate ligands in various solvents.

Table E.12: Quantity of catalysts and substrates used for the inter-molecular hydroamination of 185
phenylacetylene (**3.3**) and aniline (**3.4**) into *E-N*-(1-phenylethylidene)benzeneamine imine (**3.5**)
at 100 °C using bimetallic complexes with *N,N*- bidentate ligands.

Table E.13: Quantity of catalysts and substrates used for the inter-molecular hydroamination of 185
phenylacetylene (**3.3**) and aniline (**3.4**) into *E-N*-(1-phenylethylidene)benzeneamine imine (**3.5**)
in TCE-d₂ at 100 °C using complexes with *P,N*- and *N,N*- bidentate ligands.

General Introduction

1.1 Transition metals in homogeneous catalysis

Organometallic chemistry is based on the observation that the association between a metal centre and an organic fragment is able to significantly modify the properties of both components. The origins of this field are dated 1757, when the French pharmacist-chemist Louis Claude Cadet de Gassicourt, prepared the first organometallic complex.¹ The industrial application of organometallic chemistry was then established as early as the 1880s when Ludwig Mond discovered that nickel easily reacted with CO to form gaseous Ni(CO)_4 , which could be then collected and under thermal decomposition would give pure nickel in return. Fifty years later, in the 1930s, the first catalytic application of an organometallic compound was explored and $\text{Co}_2(\text{CO})_8$ was applied in hydroformylation catalysis.² Later on, the significant development of metal complexes in catalysis, such as Wilkinson's catalyst $[\text{RhCl(PPh}_3)_3]$ (where no M-C bond is present), has greatly expanded the field.³

1.2 Catalysts in organic chemistry

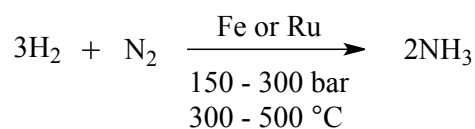
A catalyst is a substance able to lower the energy barrier between reactants and products without being consumed by the reaction. Because of the lower energy barrier a catalyst allows reactions to proceed at lower temperatures. A catalyst, nevertheless, doesn't affect the reaction equilibrium but only the reaction rate, therefore a catalyst can accelerate only thermodynamically favoured reactions. For a reaction where various pathways may proceed to the formation of a number of different products a catalyst may also be used to preferentially accelerate one pathway over others, providing a route towards more selective reactions. The advantage of lower reaction temperatures and more selective product formation address important economical and environmental

concerns. Catalysts in particular address the "Green Chemistry"⁴ principle of *atom economy*, according to which the formation of by-products is eliminated or reduced to minimise the environmental impact of a chemical process.⁵

1.3 Homogeneous and heterogeneous catalysts

Catalysts can be divided into two major groups: *homogeneous* and *heterogeneous*. Homogeneous catalysts are in the same phase as the substrates, usually within the same solution, while heterogeneous catalysts are in a different phase, usually a solid catalyst suspended in solution. Heterogeneous catalysts are typically stable solids, relatively easy to handle and easily recyclable. They are also usually tolerant of extremely harsh reaction conditions. However, understanding heterogeneous catalyst structure and reaction mechanisms is difficult due to a poorly defined surface structure and a limited ability to observe the chemistry of surfaces. Therefore improvement of heterogeneous catalyst design is still very empirical.⁶

An important application of heterogeneous catalyst is the Haber-Bosch process, where under very high temperature (300-500 °C) and high pressure (150-200 bar), metallic iron or ruthenium are used to catalyse the combination of N₂ and H₂ gas to produce ammonia, NH₃ (Scheme 1.1).⁷



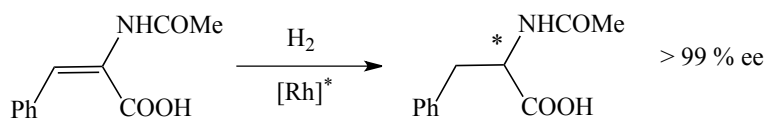
Scheme 1.1

Most new cars are also equipped with a catalytic converter, which consists of a heterogeneous catalyst (usually platinum or palladium) able to absorb and dissociate NO into molecular N₂ and oxidize CO to CO₂ to minimise pollution.⁸

Homogeneous catalysts are much less simple to use. They are often highly sensitive to extreme temperatures and deactivation by exposure to air or other contaminants. Separation of the catalyst from a reaction mixture is also typically problematic. Nevertheless, homogeneous catalysts have been found to be very useful, often able to reach much higher product selectivity and requiring the use milder reaction conditions than heterogeneous systems. A key advantage of homogeneous catalysts is their ability to be easily characterized via spectroscopic techniques. Plus, due to their molecular nature variations of steric and electronic properties can be easily introduced and the catalyst reactivity tailored to design.²

An important commercial use of homogeneous catalyst is the Monsanto process. This process has been the source of 60% of the 3.5 Mt of acetic acid produced worldwide every year. Developed in 1966, the process utilizes a Rh(I) catalyst *cis*-[Rh(CO)₂I₂]⁻ to synthesise acetic acid from MeOH and CO with extremely high selectivity >99% and using only 0.001 mol L⁻¹ of catalyst.^{7,9,10}

The hydrogenation of alkenes has also benefitted greatly from the application of homogeneous catalysts. Wilkinson's catalyst RhCl(PPh₃)₃ for example was one of the first systems developed to efficiently catalyse the reduction of simple alkenes.⁷ This led to the development of related systems that contained chiral phosphine ligands which were able to catalyse the reduction of prochiral alkenes into enantiomerically enriched alkanes (Scheme 1.2).¹¹



Scheme 1.2

1.4 Transition metal complexes as catalysts

Transition metals are able to accommodate a variety of coordination geometries and support a number of stable oxidation states, which makes them versatile metals for use in homogenous catalysis.¹² Transition metals are also potent Lewis acids able to accept electron density from their surrounding ligands. For a substrate molecule coordinated to a metal complex, this Lewis acidity can result in the polarisation of a bond and/or the weakening of a bond by withdrawing electrons from a bonding orbital, thereby activating the substrate towards reaction. At the same time back donation of electron density from filled metal d-orbitals to antibonding π^* or σ^* orbitals of the substrate can further activate the coordinated substrate (Figure 1.1).²

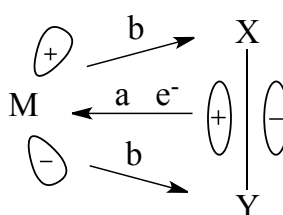
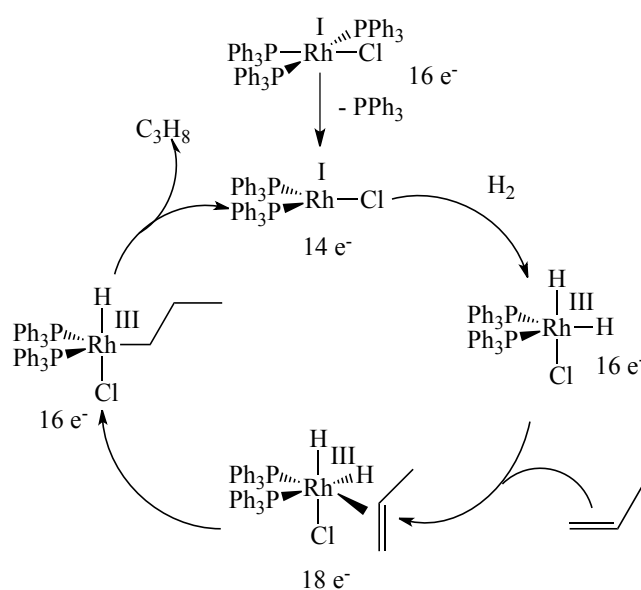


Figure 1.1: Bonding of a π -bond donor to a metal. Arrow **a** represents electron donation from the filled substrate π -bond to the empty d_σ orbital on the metal; arrows **b** represent the back donation from the filled $M(d_\pi)$ orbital to the empty substrate π^*

The hydrogenation of an alkene by Wilkinson's catalyst $[\text{Rh}(\text{PPh}_3)_3\text{Cl}]$ provides an excellent example of how various oxidation states, coordination geometries and valence electron counts can combine to facilitate a catalytic reaction (Scheme 1.3). The initial

$16e^-$ Rh(I) species at first undergoes ligand loss to yield a $14e^-$ intermediate. This is followed by the oxidative addition of H_2 , resulting in a change of oxidation number at the metal centre from I to III and an increase in coordination number from 3 to 5. Alkene coordination and insertion of the alkene into the Rh-H bond follow and the cycle concludes with the reductive elimination of the product and regeneration of the active $14e^-$ Rh(I) species.⁷



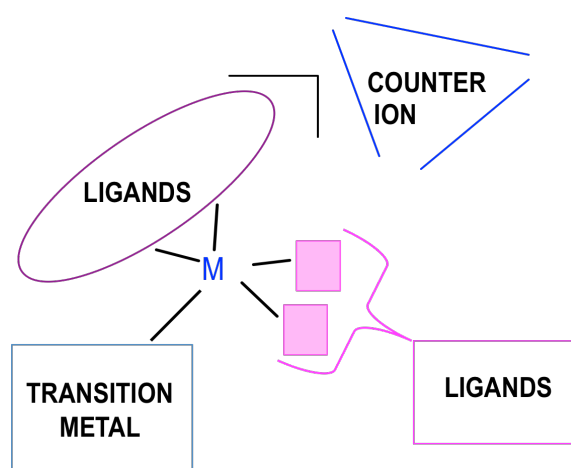
Scheme 1.3

Each catalytic cycle is called a turnover. The turnover number (TON) corresponds to the moles of product formed per moles of catalyst and gives a measure of catalyst lifetime. When the turnover is measured against time, usually in hours, then the turnover frequency (TOF) is obtained, which provides a measure of the catalytic rate.²

1.5 Catalyst structure

The structure of a homogeneous catalytic system can be well-understood using spectroscopic techniques, which then allows us to tailor the electronic and steric

properties of the catalyst to suit the reaction needs. The catalytic activity of a metal complex is based on fine-tuning the three main complex components: the identity of the metal centre, the electronic and steric proprieties of the ligands and the properties of any uncoordinated counterion associated with a charged complex (Scheme 1.4).



Scheme 1.4

1.5.1 Metal properties

Transition metal (TM) properties vary greatly across the periodic table. The early TMs are highly electropositive and therefore quite π -basic, resulting in a strong backdonation of electron density from the metal to the π^* orbitals of unsaturated ligand groups such as CO, arenes, alkenes and alkynes.² The lower oxidation states of the early TMs are also highly sensitive to oxidation and are therefore readily deactivated in the presence of air or other oxidising constituents. The greater stability of the higher oxidation states makes these metals reluctant to participate in reductive processes that are often necessary to facilitate the elimination of a product molecule from the metal complex.²

Late transition metals, on the other hand, are more electronegative retaining their electrons more strongly. They are able to withdraw electrons from coordinated bonds

and thereby increase ligands susceptibility towards nucleophilic attack. Late transition metals are also considerably less sensitive to oxidation by air and the smaller difference in energy between oxidation states makes multiple oxidation states more available to participate in a catalytic cycle.²

1.5.2 The nature of the ligand

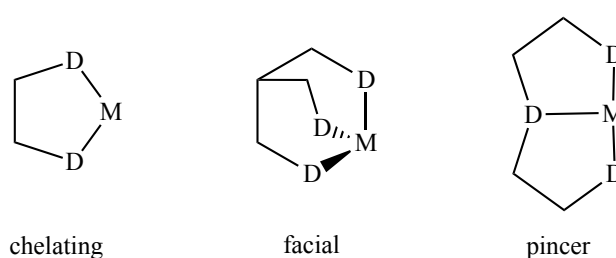
The nature of the ligand can greatly influence the electronic and steric properties of a metal complex depending on the geometry of the ligand, the number of coordinating groups and how strongly the ligand groups donate or withdraw electron density from the metal centre.^{2,13} The ligand therefore represents the most variable fragment in the complex design. While strongly coordinating ligands may stabilize electron deficient metal centers, more labile ligands are often necessary to create vacant coordination sites on the metal through which a substrate may bind. The steric bulk of a ligand can also influence the activity of a catalyst. Indeed, steric crowding around a complex may enhance the lability of a ligand or shield reactive sites on the metal from unwanted side reactions.¹⁴ For multitopic ligands that contain more than one donor group the lability and steric properties of the ligand can be tailored even further depending on what coordination geometry the donor groups adopt and the rigidity and steric bulk of the ligand scaffold.

1.5.2.1 Multitopic ligands and ligand geometry

In comparison to monodentate ligands, multitopic ligands are kinetically much less labile and thermodynamically more stable. This is due to the entropic penalty of displacing a single multitopic ligand with two or more monodentate ligands. As a result of the stronger metal ligand interaction multitopic ligands tend to yield complexes of

higher thermal stability. They also tend to inhibit unwanted decomposition pathways by occupying multiple coordination sites through which such reactions may otherwise proceed. Increasing the number of donor groups increases the degree of complex stabilization, however for a catalytic metal complex this can come at the cost of catalytic activity. A balance therefore needs to be established between these two opposing influences in order to generate an effective catalyst.²

Multitopic ligands can be classified according to the number of donor groups they contain and the geometry of their coordination mode. Bidentate ligands have the simplest geometry coordinating in a chelating fashion to a metal centre, whereas tridentate ligands can coordinate to a metal centre in either a facial or pincer fashion (Scheme 1.5), all of which have been extensively utilized in homogeneous catalysis. Pincer ligands in particular have shown an extraordinary ability to stabilize highly reactive metal complexes and to dramatically improve the thermal stability of many catalysts.^{15,16}



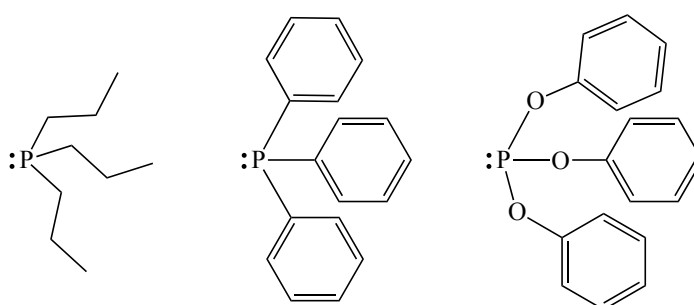
Scheme 1.5

A particular advantage of using multitopic ligand architectures is the ability to combine both strong and weak donor groups. Weakly coordinating ligands are often necessary as their high lability provides access to vacant coordination sites on the metal through which a reaction may proceed. However complete loss of the ligand can result in an

electron deficient metal centre that is more susceptible to decomposition. By combining both strong and weak donor groups it is possible for the weaker donor to dissociate temporarily while the stronger donor anchors the ligand to the complex thereby maintaining both catalyst reactivity and stability, a process known as hemilability.¹⁴

1.5.2.2 Phosphorus donor ligands

Phosphine donor ligands of the type PR_3 (R = alkyl, aryl, O-alkyl/aryl) (Scheme 1.6) are one of the most widely used and versatile ligands with their electronic and steric properties easily altered over a wide range by varying the nature of the substituents (R). Phosphines are strong two electrons σ -donor ligands and generally weak π -acceptor ligands.¹⁷ They form strong metal-ligand bonds particularly with the late TM's where they are compatible with metals in both high and low oxidation states. They also exhibit a moderate trans influence, which increases the lability of ligands coordinated trans to the phosphine.²

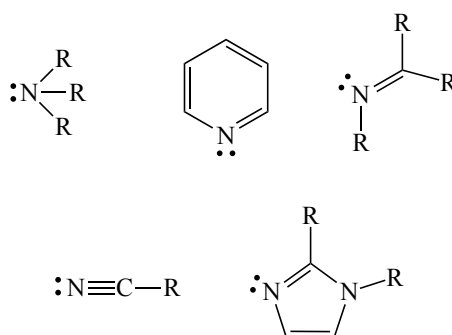


Scheme 1.6

1.5.2.3 Nitrogen donor ligands

The possibility of sp^3 , sp^2 and sp hybridization for N-donor ligands gives a wide variation of steric and electronic properties for this donor group (Scheme 1.7). Nitrogen

donor ligands are good 2-electron σ -donors but very poor π -acceptors.¹³ Ligands with sp^2 hybridized N-donors such as those found in imines and the N-heterocycles, imidazole, pyrazole, oxazole, pyridine etc., are particularly useful moieties for the coordination of transition metal complexes. They are stronger 2-electron σ -donors than sp^3 N-donor groups and are easily incorporated into larger ligand structures. Compared to phosphines, N-donor ligands form weaker more labile metal-ligand bonds and for this reason their incorporation into larger multidentate ligand structures is often desirable.

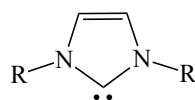


Scheme 1.7

1.5.2.4 N-heterocyclic carbene donor ligands

N-heterocyclic carbenes (NHCs) are compounds that contain an sp^2 hybridized 6-electron carbene moiety incorporated into an N-heterocyclic ring.¹⁸ In contrast to non-heterocyclic carbenes, NHCs are significantly more stable. For the most common NHC motif based on an imidazole ring structure (Scheme 1.8), the interaction between the electron lone pairs of the two neighbouring nitrogen π -orbitals and the empty π -orbital of the carbene help stabilize the electron deficient carbon centre, allowing the coordination chemistry of the carbene's lone electron pair to be exploited.¹⁹ Overall, carbenes are very strong σ -donor ligands and very poor π -acceptor ligands. Because of

their strong σ -bonding character, NHCs are often compared to phosphines in term of their coordination chemistry, however NHCs are much stronger ligands than even the most basic phosphine ligand²⁰ resulting in ligand-metal bonds of very low kinetic lability.^{21,22} Their complexes are therefore more tolerant of higher reaction temperatures and the coordinated carbene ligand itself is less susceptible to oxidation.



Scheme 1.8

1.5.2.5 The carbon monoxide ligand

Carbon monoxide coordinates to a metal centre through both σ -bond donation of electron density from the lone electron pair on carbon and π -backbonding from filled metal d orbitals to the empty π^* orbitals of the CO triple bond. CO is in fact an exceptionally π -acidic ligand in combination with electron rich late TMs (such as Rh(I) and Ir(I)). By removing electron density from the metal centre CO ligands not only stabilize lower oxidation states of the complex but also increases its Lewis acidity. The IR stretching frequency of the CO triple bond also provides a useful spectroscopic handle for the characterization of CO containing complexes.

1.5.2.6 π -Coordinating ligands

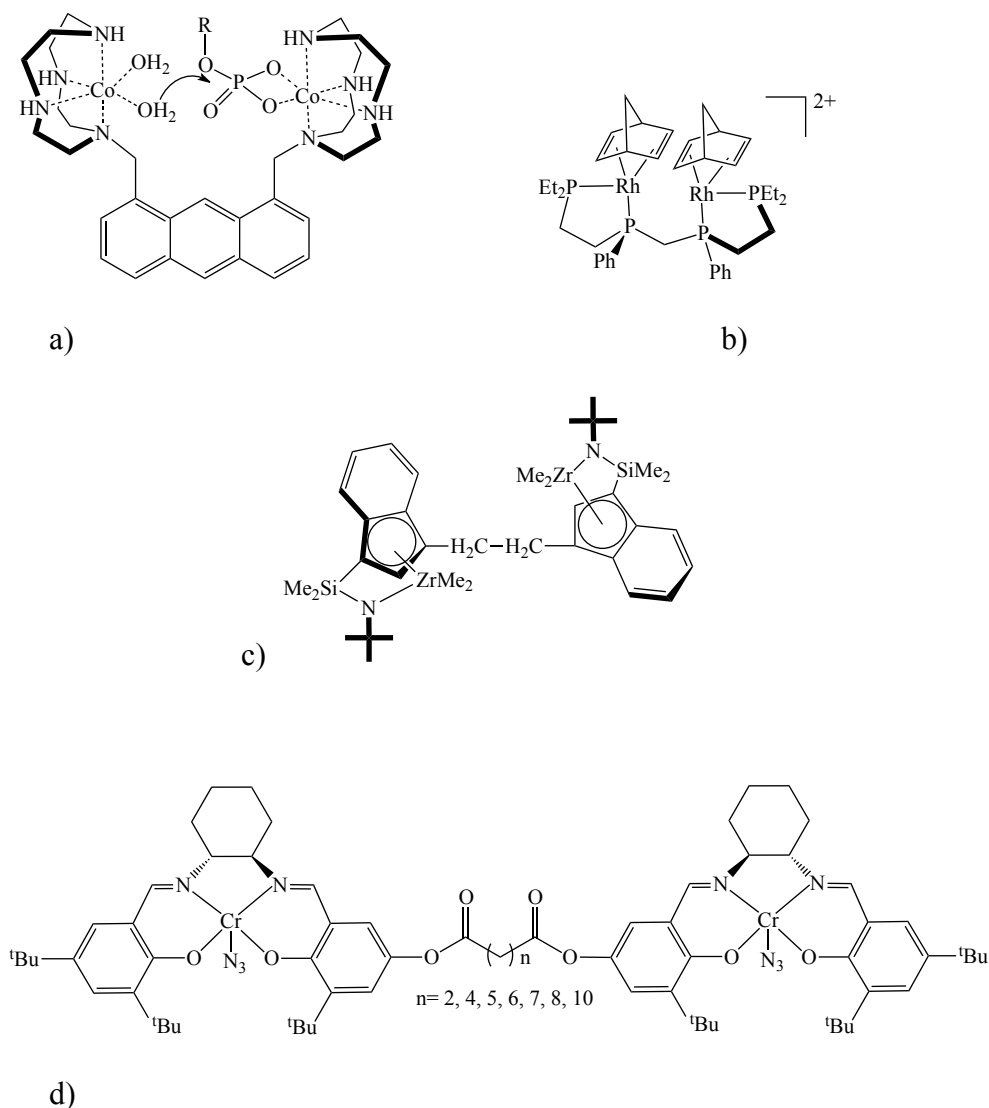
π -Coordinating ligands bond to a metal centre via donation of e^- density from the π -electrons shared between a pair of multiply bonded atoms, such as in alkenes and alkynes. They also have the potential to accept e^- density from the metal into their

π^* -orbitals, however to a much lesser degree than CO. The combination of σ -donation and π -back bonding can weaken the π -bond of a coordinated substrate and increases its susceptibility to both nucleophilic and electrophilic attack depending on the oxidation state of the metal and the amount of back-bonding.

1.6 Bimetallic complexes

The use of bimetallic complexes in homogeneous catalysis has only recently received much attention. Bimetallic complexes contain two metals immobilized within one ligand scaffold. By bringing the two metal centres into close proximity an enhancement of catalyst activity is often observed which is greater than the sum of the individual monometallic units. Such enhancement is termed intermetallic “cooperativity”^{23,24} Early work into developing bimetallic catalysts was aimed at developing enzyme mimics for the hydrolysis of phosphoesters.²⁵ The anthracene bridged di-Cobalt complex (Scheme 1.9 a) for example was shown to promote the hydrolysis of phosphoesters at a tenfold greater rate than the analogous mononuclear complex.²⁶ The first example of a bimetallic catalyst promoting an organic reaction was reported by Stanley and co-workers who demonstrated that the Rh_2 complex (Scheme 1.9 b) was a far superior catalyst for the hydroformylation of 1-hexene compared to its monometallic analogues.²⁷ *Bis*-metallo-salen complexes of Cr_2 (Scheme 1.9 d), Al_2 and Co_2 have also been used for the asymmetric ring opening of epoxides resulting in increased enantioselectivities and catalyst activities up to several orders of magnitude greater compared to the monometallic analogues.²⁵ Marks and coworkers have also reported half-sandwich indenyl Zr_2 (Scheme 1.9 c) and Ti_2 catalysts for the polymerisation of alkenes, which were up to 600 times more active than the related monometallic

catalysts. Bimetallic systems have been used as catalyst for a wide range of organic reactions such as the polymerization of olefins,^{28,29,30} the Heck coupling of aryl halides³⁰ and the hydrogenation of alkenes.³¹



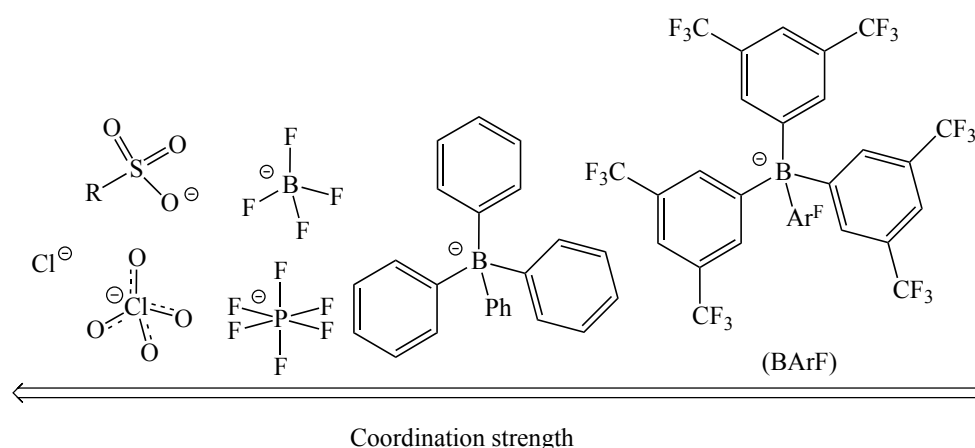
Scheme 1.9

As can be seen from the examples described above a variety of bimetallic arrangements can be used to enhance the catalyst activity. Typically such enhancement is highly sensitive to small changes in catalyst structure and is often

highly specific to a certain reaction or substrate. The application of bimetallic complexes across a broader range of catalytic transformations remains a significant challenge.

1.7 Counter ion properties

The nature of the counter ion is known to affect the catalytic efficiency of charged metal complexes.³² Coordinating anions such as halides and those containing basic oxygen groups such as sulfonates and ClO_4^- readily bind to electrophilic metal centers and can therefore compete with substrates for coordination sites on the metal.³³ Even anions with weakly basic fluorine substituents such as BF_4^- and PF_6^- have been shown on many occasions to bind to coordinatively unsaturated metal centres. In order to produce a more weakly coordinating anion the delocalization of the negative charge over a large area of non-nucleophilic moieties is desirable. Exchange of the fluorine atoms in BF_4^- for phenyl groups therefore gave the larger BPh_4^- ion. This anion was shown to be considerably less nucleophilic leading to a better separation of the complex ions and greater availability of the metal centre for substrate binding. However BPh_4^- is still able to coordinate to a metal through its phenyl rings and was also shown to undergo B-Ph bond cleavage in the presence of strong Lewis acids.³⁴

**Scheme 1.10**

The addition of CF_3 substituents onto the phenyl rings of BPh_4^- gives the tetrakis(3,5-trifluoromethylphenyl)borate anion (BArF^-). The incorporation of electron-withdrawing and sterically bulky substituents has been shown to inhibit the π -coordinating ability of the arene substituents and also reduce the tendency for B-Ar cleavage. Since its development the BArF^- anion and related fluorinated aromatic borates have been widely applied in homogeneous catalysis. The weakly coordinating nature of this anion has led in many cases to significant improvements to both the catalysts efficiency and selectivity.³⁴

1.8 H-X addition to alkynes

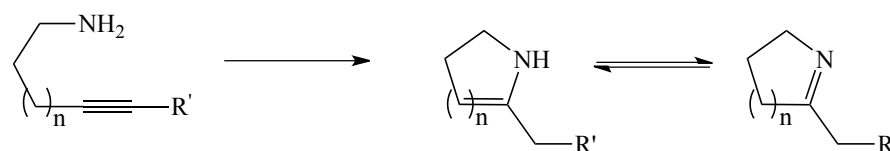
The development of catalysts that facilitate the addition of X-H bonds across the $\text{C}\equiv\text{C}$ triple bond of an alkyne is an important challenge in modern synthetic chemistry. This reaction is a highly atom economical method towards the synthesis of new X-C bonds, leading to the formation of no wasteful by-products. It is also a fundamental tool for the synthesis of many valuable complex organic molecules. The types of reactions

considered here are classified by the nature of atom X, namely: hydroamination ($X = N$), hydroalkoxylation ($X = O$) and hydrosilylation ($X = Si$).

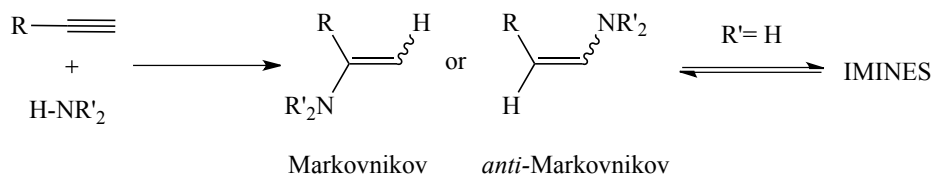
1.8.1 Hydroamination

The hydroamination of alkynes involves the addition of an amine N-H bond across an alkyne $C \equiv C$ triple bond. This leads to the formation of new N-containing compounds (Scheme 1.11).³⁵ This reaction can be performed with both primary and secondary amines to give enamines, however for primary amines the final product is typically the more thermodynamically stable imine tautomer. The reaction can be performed in either an inter- or intra-molecular fashion, with both Markovnikov and *anti*-Markovnikov regioisomers being possible.

a) INTRA-MOLECULAR HYDROAMINATION



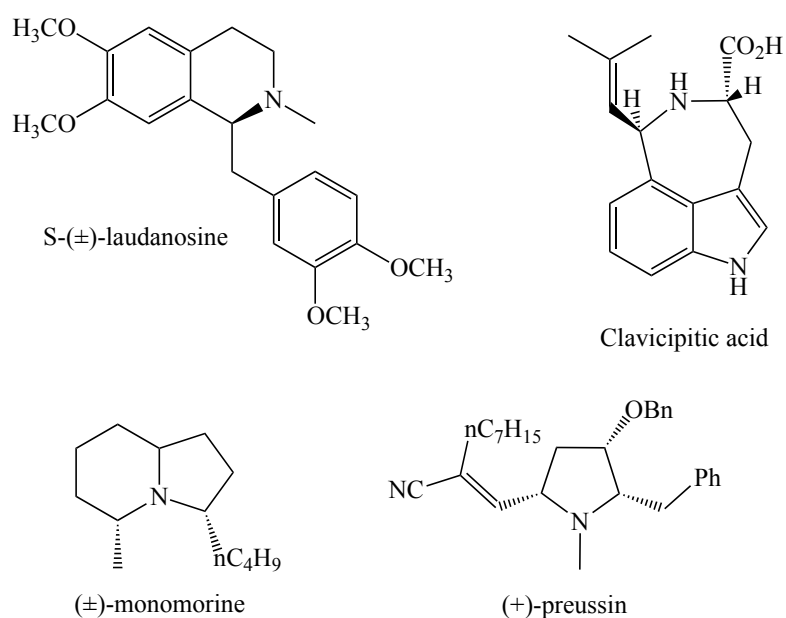
b) INTER-MOLECULAR HYDROAMINATION



Scheme 1.11

The amine, enamine and imine products of this reaction are of tremendous importance in the bulk and fine chemical industries. The intra-molecular hydroamination reaction in particular is very useful for the synthesis of N-heterocycles. N-heterocycles are

ubiquitous constituents of biological systems and are therefore prime synthetic targets for the pharmaceutical and agrochemical industries. Prominent examples include the alkaloids (\pm)-monomorphine,³⁶ S-(+)-laudanosine,³⁷ clavicipitic acid^{38,39} as well as the anti-fungal agent (+)-preussin (Scheme 1.12).⁴⁰

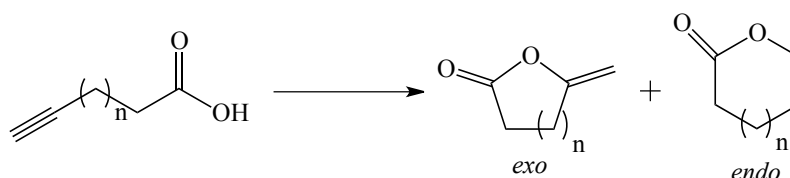


Scheme 1.12

1.8.2 Hydroalkoxylation

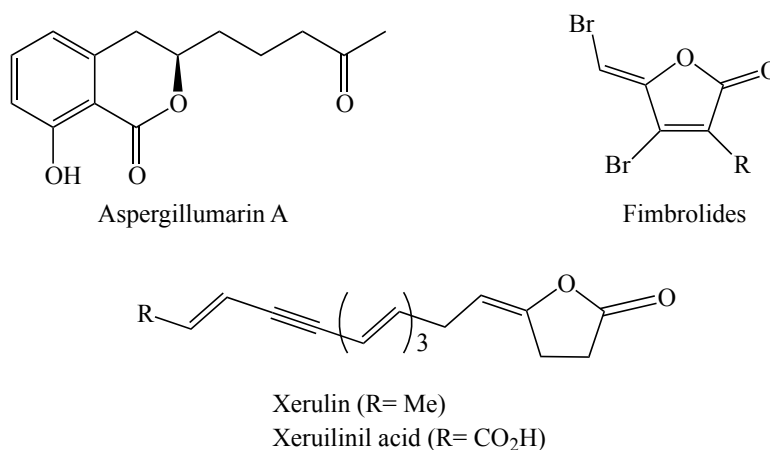
The hydroalkoxylation of alkynes involves the addition of an O-H bond across the alkyne $C\equiv C$ triple bond. This leads to the formation of new O-containing compounds. Most commonly it is the intra-molecular cyclisation of alkynyl alcohols or alkynoic acids that is of interest. The cyclisation of alkynoic acids gives alkylidene lactones with two potential isomers being formed depending on whether the alkene bond is present

exo- or *endo*- to the heterocycle (Scheme 1.13). Both isomers have similar thermodynamic stability with the regioselectivity of the reaction being determined by the type of catalyst used to perform the cyclisation.



Scheme 1.13

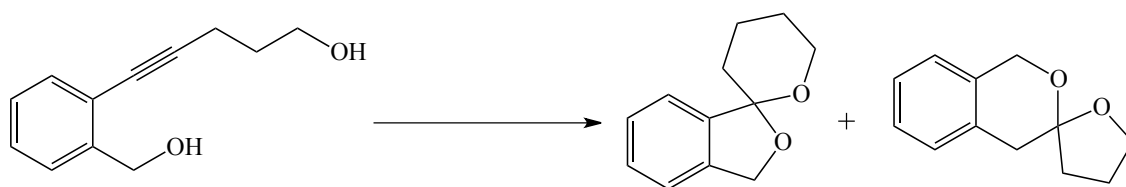
The synthesis of lactone containing compounds is highly desirable due to the high biological activity of this class of molecules. For example, compounds such as xerulinic acid have been shown to inhibit cholesterol production,⁴¹ fimbrolides have been investigated as anti-bacterials^{42,43} and aspergillumarin A⁴⁴ has been applied as an anti-fungal agent (Scheme 1.14).



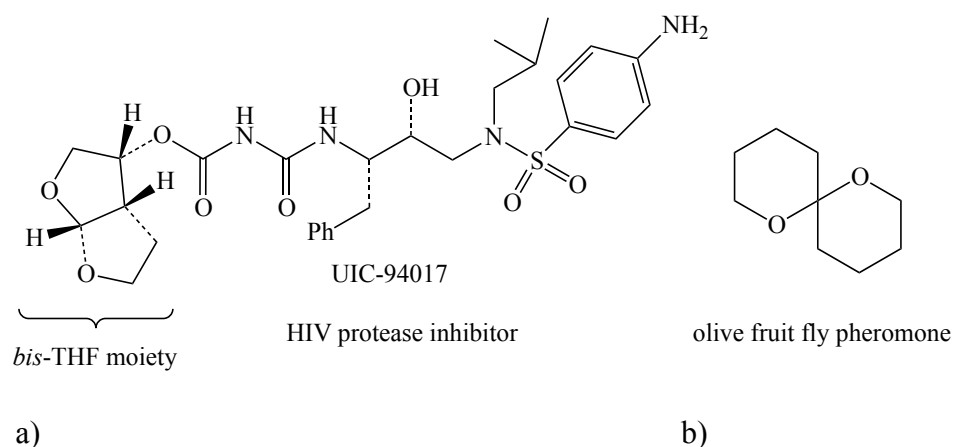
Scheme 1.14

The cyclization of alkyndiols provides a particularly attractive method towards the synthesis of spiroketals (Scheme 1.15). Spiroketals are also present in a large number of

biologically active products such as the HIV protease inhibitor UIC-94017 (Scheme 1.16 a)⁴⁵ and the fruit fly pheromone 1,7-dioxaspiro[5.5]undecane (Scheme 1.16 b).⁴⁶



Scheme 1.15



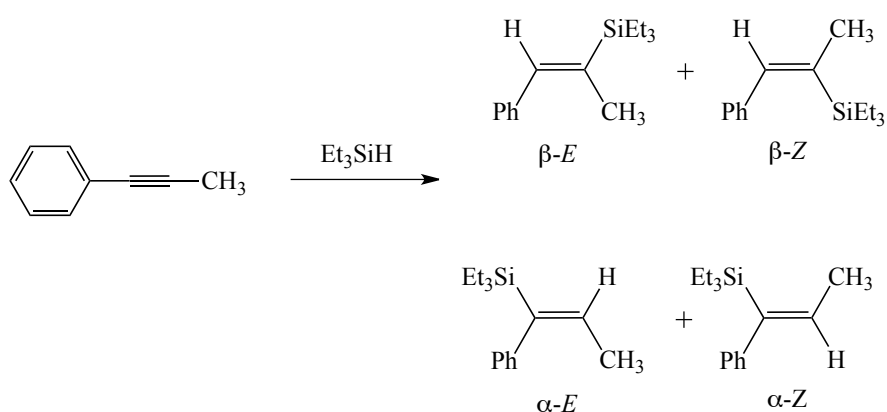
Scheme 1.16

1.8.3 Hydrosilylation

The hydrosilylation of alkynes involves the addition of a Si-H bond across an alkyne $C\equiv C$ triple bond. Hydrosilylation of carbon-carbon multiple bonds has been one of the most important laboratory and industrial methods for the formation of silicon-carbon bonds.⁴⁷ The hydrosilylation of alkynes provides access to vinylsilanes which are useful intermediates in organic synthesis.^{48,49,50} Organosilane products have been extensively used in adhesives, binders, silicone polymers and self-curing rubber formulations.

The hydrosilylation of alkynes can result in multiple regioisomeric products. For example the hydrosilylation of 1-phenylpropyne can give four possible products

depending on whether the silicon adds to the α or β carbon of the alkyne and the relative arrangement *E* or *Z* of the substituents (Scheme 1.17). Therefore the development of catalysts that are not only highly active but also achieve a high regioselectivity is quite challenging.



Scheme 1.17

1.9 Objectives of this thesis

The work described in this thesis involves the design and synthesis of rhodium and iridium organometallic complexes and their application as homogeneous catalysts for the addition of X-H bonds ($\text{X} = \text{S}, \text{O}$ and N) to alkynes. The specific objectives were to:

- Exploit the excellent coordination properties of NHCs in combination with weaker, more labile pyrazole ligands by synthesizing novel NCN pincer ligand motifs;
- Explore the coordination chemistry of these NCN pincer ligands towards Rh(I) and Ir(I) metal complexes;
- Investigate the efficiency of the new Rh(I) and Ir(I) pincer complexes as

catalysts for promoting the hydroamination (C-N bond formation), hydroalkoxylation (C-O bond formation) and hydrosilylation (C-Si bond formation) of alkynes;

- d. Compare the activity of these pincer complexes with analogous Rh(I) complexes containing a bidentate NHC-pyrazolyl ligand;
- e. Develop known Ir(I) and Rh(I) complexes as catalysts for the inter-molecular hydroamination of alkynes. The influence of the ligands, co-ligands and counter ions on the catalysts reactivity will be investigated and optimised under various solvent and temperature regimes with the aim of putting in place the most efficient catalyst. Bimetallic catalyst motifs will also be explored

This thesis will be divided into three main parts. The first part, chapter 2, will focus on the synthesis of new pincer ligands and their complexes with Rh(I) and Ir(I). Chapter 3 will focus on the application of these complexes and related systems in catalysis. Chapter 4 will be focused on the development of other Rh(I) and Ir(I) catalysts for the inter-molecular hydroamination reaction.

1.10 References

- (1) Seyferth, D. *Organometallics* **2001**, 20, 1488.
- (2) Crabtree, R. H. *The organometallic chemistry of the transition metals*; John Wiley & Sons, Inc., Hoboken, New Jersey, **2009**.
- (3) Osborn, J. A.; Jardine, F. H.; Young, J. F.; Wilkinson, G. *J. Chem. Soc. A* **1966**, 1711.
- (4) Anastas, P. W., J. *Green Chemistry: Theory and Practice*; Oxford University Press Oxford, **1998**.
- (5) Trost, B. M. *Acc. Chem. Res.* **2002**, 35, 695.
- (6) Cornils, B. H., W. A.; Schlogl, R.; Wong, C. H. *Catalysis from A to Z. A Concise Encyclopedia*; WILEY-VCH: Weinheim, **2003**.
- (7) Housecroft, C. E.; Sharpe, A. G. *Inorganic Chemistry-second edition*; Pearson Education Limited, **2005**.
- (8) Blackman, A., Bottle S. E., Schmid S., Mocerino M., Wille U. *Chemistry, 2nd Edition*; Wiley: Milton, Qld, Australia, **2012**.
- (9) Trost, B. M., Fleming, I., Paquette, L. A., Oppolzer, W. *In Comprehensive Organic Synthesis*; Eds.; Pergamon: Oxford, **1991**; Vol. 5, Chapter 4.1, 315-400.
- (10) Roush, W. R. I. C. O. S.; Trost, B. M., Fleming, I., Paquette, L. A., Eds.; Pergamon: Oxford, **1991**; Vol. 5, Chapter 4.4, 513-550.
- (11) Knowles, W. S. *Adv. Synth. Catal.* **2003**, 345, 3.
- (12) Leigh, G. J. *IUPAC: Nomenclature of Inorganic Chemistry (Recommandation 1990)*; Blackwell Scientific Publication, Oxford.
- (13) Togni, A.; Venanzi, L. M. *Angew. Chem., Int. Ed. Engl.* **1994**, 33, 497.
- (14) Golovin, M. N.; Rahman, M. M.; Belmonte, J. E.; Giering, W. P. *Organometallics* **1985**, 4, 1981.

-
- (15) Bassetti, M.; Capone, A.; Salamone, M. *Organometallics* **2004**, *23*, 247.
- (16) Wehman-Ooyevaar, I. C. M.; Kapteijn, G. M.; Grove, D. M.; Smeets, W. J. J.; Spek, A. L.; van Koten, G. *J. Chem. Soc., Dalton Trans.* **1994**, 703.
- (17) Noyori, R. *Asymmetric Catalysis in Organic Synthesis*; John Wiley and Sons, Inc., **1994**.
- (18) Arduengo, A. J.; Harlow, R. L.; Kline, M. *J. Am. Chem. Soc.* **1991**, *113*, 361.
- (19) Glorius, F. *N-Heterocyclic Carbenes in Catalysis- An Introduction from Metal Catalysis N-Heterocyclic Carbenes in Transition Metal Catalysis*; Springer Berlin Heidelberg, **2007**; Vol. 21.
- (20) Chianese, A. R.; Li, X.; Janzen, M. C.; Faller, J. W.; Crabtree, R. H. *Organometallics* **2003**, *22*, 1663.
- (21) Nielsen, M.; Kammer, A.; Cozzula, D.; Junge, H.; Gladiali, S.; Beller, M. *Angew. Chem., Int. Ed.* **2011**, *50*, 9593.
- (22) Herrmann, W. A. *Angew. Chem. Int. Ed.* **2002**, *41*, 1290.
- (23) Steinhagen, H.; Helmchen, G. *Angew. Chem., Int. Ed. Engl.* **1996**, *35*, 2339.
- (24) Rowlands, G. J. *Tetrahedron* **2001**, *57*, 1865.
- (25) Cacciapaglia, R.; Casnati, A.; Mandolini, L.; Reinhoudt, D. N.; Salvio, R.; Sartori, A.; Ungaro, R. *J. Am. Chem. Soc.* **2006**, *128*, 12322.
- (26) David, H. V.; Anthony, W. C. *J. Am. Chem. Soc.* **1993**, *115*.
- (27) Broussard, M.; Juma, B.; Train, S.; Peng, W.; Laneman, S.; Stanley, G. *Science* **1993**, *260*, 1784.
- (28) Li, H.; Stern, C. L.; Marks, T. J. *Macromolecules* **2005**, *38*, 9015.
- (29) Li, H.; Li, L.; Schwartz, D.; Metz, M.; Marks, T.; Liable-Sands, L.; Rheingold, A. J. *J. Am. Chem. Soc.* **2005**, *127*, 14756.

-
- (30) Li, H.; Li, L.; Marks, T. J. *Angew. Chem., Int. Ed.* **2004**, *43*, 4937.
- (31) Maitlis, P. M. *Acc. Chem. Res.* **1978**, *11*, 301.
- (32) Macchioni, A. *Chem. Rev.* **2005**, *105*, 2039.
- (33) Honeychuck, R. V.; Hersh, W. H. *Inorg. Chem.* **1989**, *28*, 2869.
- (34) Strauss, S. H. *Chem. Rev.* **1993**, *93*, 927.
- (35) Pohlki, F.; Doye, S. *Chem. Soc. Rev.* **2003**, *32*, 104.
- (36) McGrane, P. L.; Livinghouse, T. *J. Org. Chem.* **1992**, *57*, 1323.
- (37) Mujahidin, D.; Doye, S. *Eur. J. Org. Chem.* **2005**, *2005*, 2689.
- (38) Harrington, P. J.; Hegedus, L. S. *J. Org. Chem.* **1984**, *49*, 2657.
- (39) Harrington, P. J.; Hegedus, L. S.; McDaniel, K. F. *J. Am. Chem. Soc.* **1987**, *109*, 4335.
- (40) McGrane, P. L.; Livinghouse, T. *J. Am. Chem. Soc.* **1993**, *115*, 11485.
- (41) Kuhnt, D. A., T.; Besl, H.; Bross, M.; Herrmann, R.; Mocek, U.; Steffan, B.; Steglich, W. *J. Antibiot.* **1990**, 1413.
- (42) Kazlauskas, R.; Murphy, P. T.; Quinn, R. J.; Wells, R. J. *Tetrahedron Lett.* **1977**, *18*, 37.
- (43) Suga, H.; Smith, K. M. *Curr. Opin. Chem. Biol.* **2003**, *7*, 586.
- (44) Hill, R. A.; Sutherland, A. *Nat. Prod. Rep.* **2012**, *29*, 1377.
- (45) Ghosh, A. K.; Leshchenko, S.; Noetzel, M. *J. Org. Chem.* **2004**, *69*, 7822.
- (46) Schwartz, B. D.; Hayes, P. Y.; Kitching, W.; De Voss, J. J. *J. Org. Chem.* **2005**, *70*, 3054.
- (47) Ojima, I.; Clos, N.; Donovan, R. J.; Ingallina, P. *Organometallics* **1990**, *9*, 3127.
- (48) Lee, H. M.; Nolan, S. P. *Org. Lett.* **2000**, *2*, 2053.
- (49) Colvin, E. W. *Silicon Reagents in Organic Synthesis*; Academic Press: London, **1998**; Vol 48.

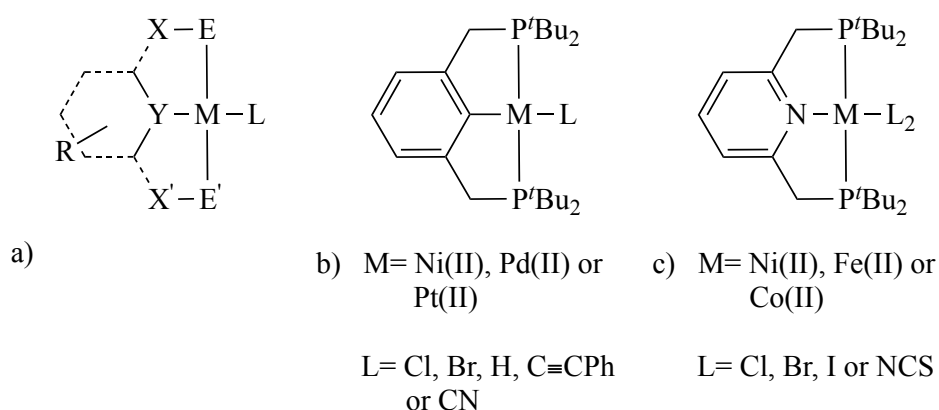
- (50) Langkopf, E.; Schinzer, D. *Chem. Rev.* **1995**, 95, 1375.

Complexes with NCN
Pincer Ligands

2.1 Introduction

2.1.1 Pincer ligands

Pincer ligands are tridentate ligands of the general formula EYE' , where Y denotes the central donor atom and E/E' the two pendant donor atoms. These ligands are typically composed of a central phenyl or pyridyl ring joined at the ortho positions by a short linker X/X' to the pendant donor groups (Scheme 2.1 a). This results in a relatively rigid ligand conformation that usually coordinates to a metal centre in a meridional (or pincer) fashion. The earliest complexes synthesised with pincer ligands were the square planar PCP^1 and PNP^2 metal halide complexes shown in Scheme 2.1(b) and (c).



Scheme 2.1

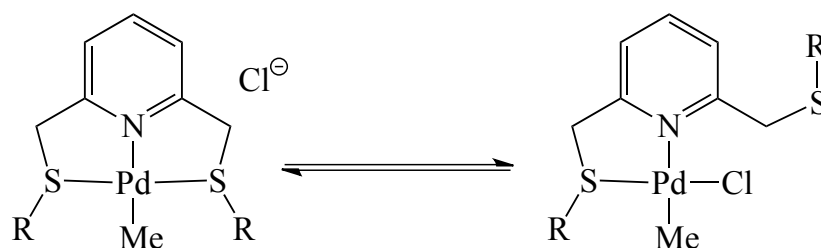
Since then the general structure of pincer ligands has diversified considerably. The central core is no longer restricted to a phenyl or pyridyl ring and a range of alternative heterocyclic and acyclic structures containing amide, carbene, alkyl, silyl or boryl donor groups have been reported. The nature of the pendant donors E/E' have been extensively modified as well with amine (NR_3),³⁻⁵ imine (NR_2),^{6,7} phosphine (PR_2),^{5,7-11} phosphite (P(OR)_2),¹²⁻¹⁴ ether (OR),¹⁵ thioether (SR),^{16,17} *N*-heterocyclic carbene (NHCs),¹⁸⁻²² and selenoether (SeR)²³ donor groups having all been used.^{24,25} Further structural modifications have also been achieved through variation of the spacer groups X/X' from

alkyl chains of various length ((-CH₂-)_n) to heteroatom linkers such as amines (-NR-)²⁶ and ethers (-O-).³ Finally, the two spacers X/X' and the pendant donor atoms E/E' may not necessarily be identical, and asymmetric systems have been routinely synthesised^{25-34,21,3,11} The facility through which a wide range of functional groups can be varied has made it possible to easily tune the electronic and steric properties of the pincer ligand and hence the reactivity of a coordinated metal centre. Such a great diversity of functionality has therefore led to the application of pincer ligand containing metal complexes as homogeneous catalysts for numerous transformations.

2.1.2 Coordination properties of pincer ligands

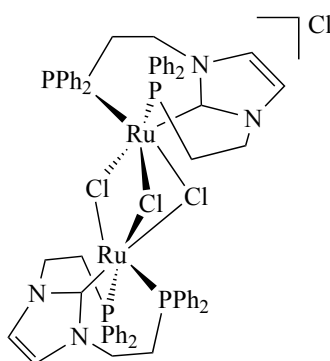
Pincer ligands first attracted attention due to the high thermal stability associated with many of their complexes, such as the PCP nickel(II) chloride complex synthesised by Shaw *et al.* (Scheme 2.1 b), which sublimes at 240 °C at 1 atmosphere without apparent signs of decomposition.¹ The stability imparted by pincer ligands to the metal complex is thought in part to emerge from the rigid meridional coordination geometry that such a structure enforces. This limits the number of open coordination sites on the metal and the available coordination geometries of the complex, which can inhibit unwanted decomposition pathways.³⁵

A tridentate coordination is not always observed upon use of pincer ligands and several other coordination modes are also possible. A bidentate (κ^2) coordination mode is often observed when weakly coordinating side arms are present.^{36,37} Such binding was reported by Canovese *et al.* with an SNS palladium complex containing thioether sidearms (Scheme 2.2). This complex forms an equilibrium between the bidentate and pincer coordination modes in solution.³⁸ Notably such hemilability had a beneficial impact on the rate of allene insertion into the Pd-Me bond.



Scheme 2.2

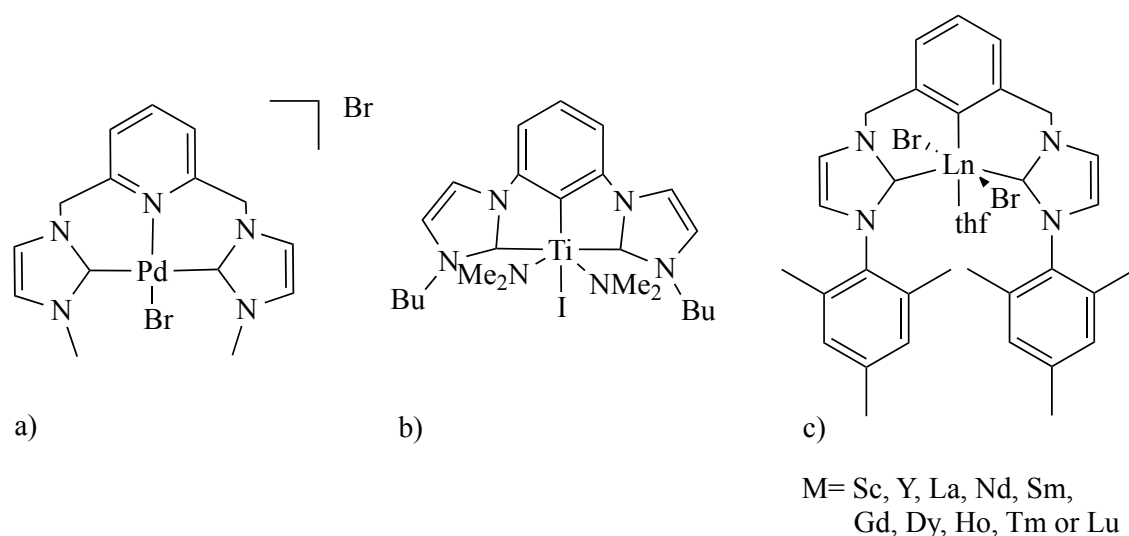
Increasing the flexibility of the ligand by increasing the length of the linker groups X/X' can lead to a facial coordination of the three donor groups. For example the dimeric ruthenium complex in Scheme 2.3 contains two PCP pincer ligands that are bound in a facial coordination manner. This is possible due to the longer ethylene linking groups between the central NHC ring and the pendant phosphorus donor atoms. It is interesting to note that with the *fac*-coordination mode the 6-electron pincer ligand is able to mimic the η^5 -binding mode of the cyclopentadienyl anion, which is a well established 'privileged' ligand with proven potential in a wide range of applications.³⁹



Scheme 2.3

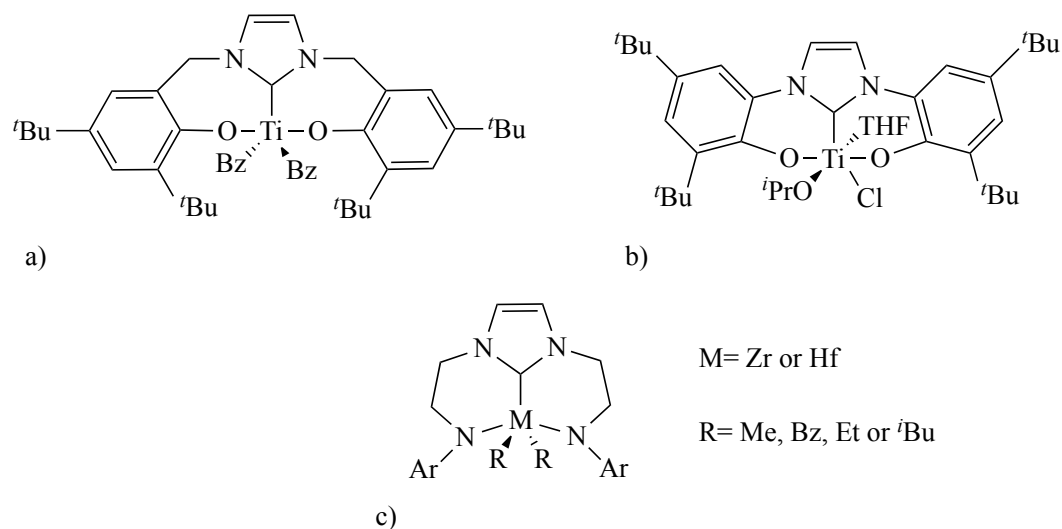
2.1.3 NHC pincer complexes

N-heterocyclic carbenes (NHCs) are very strong σ -donor ligands that have a low kinetic lability and are able to confer a high thermal stability to a metal complex.^{40,41} For this reason the incorporation of NHCs into pincer ligand scaffolds is highly desirable. Typically, NHCs have been incorporated as the pendant donor groups about a central phenyl or pyridyl core and such CCC and CNC pincer ligands have been used in combination with a variety of metals for catalytic applications. Selected examples include the PdCNC complex (Scheme 2.4 a) which is an effective catalyst for the Heck reaction,⁴² the TiCCC complex (Scheme 2.4 b) which efficiently catalyses the intra-molecular hydroamination of amino alkenes,⁴³ as well as the series of lanthanide CCC isoprene polymerisation catalysts (Scheme 2.4 c).⁴⁴



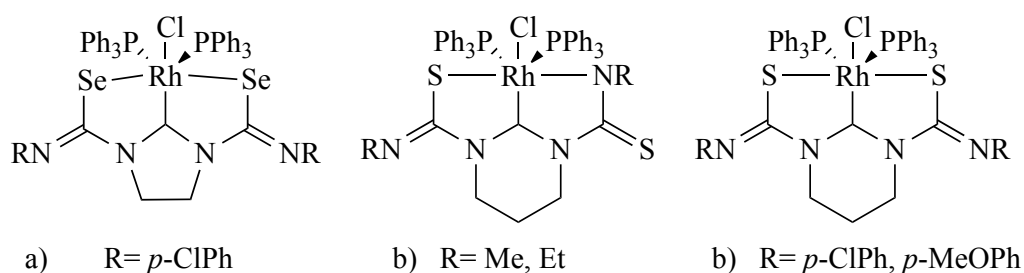
Scheme 2.4

Much less explored are pincer systems that contain a central NHC donor group. Such systems have only been investigated in the last decade with much initial interest focused on dianionic NCN or OCO pincer complexes of the early transition metals, particularly group 4 (Ti, Zr and Hf) (Scheme 2.5).⁴⁵⁻⁴⁷



Scheme 2.5

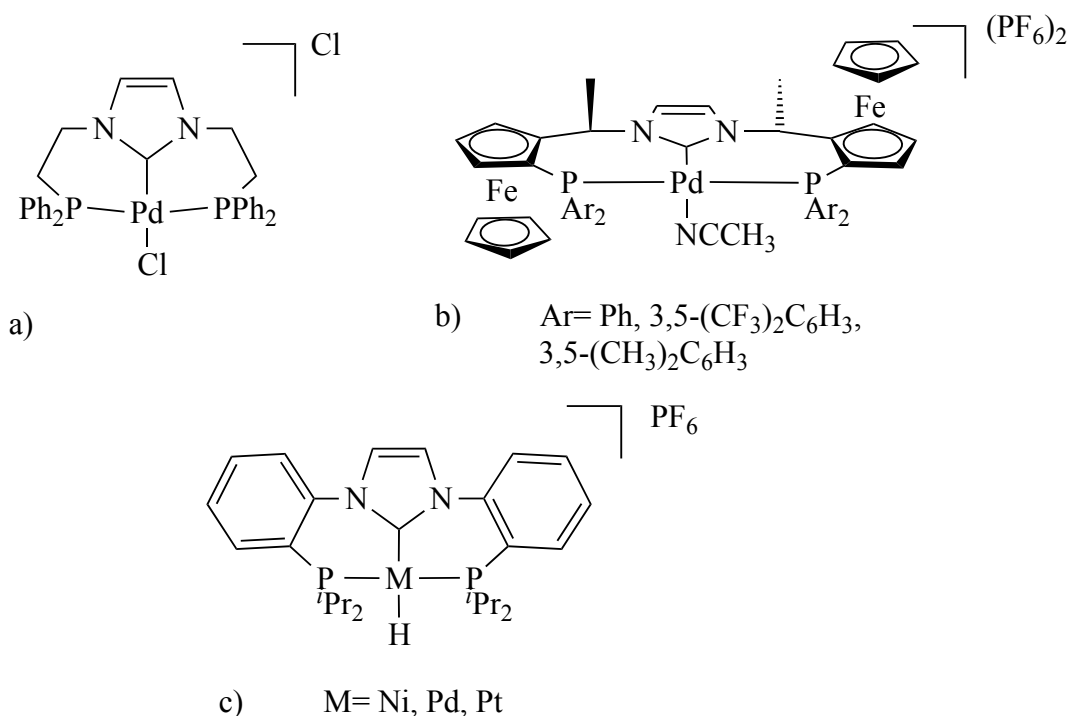
Dianionic selenolate (SeCSe)⁴⁸ and thiolate (SCS) NHC pincer ligands have also been complexed to the late transition metals such as Rh, Pd and Pt (Scheme 2.6).⁴⁵ Note for the rhodium SCS complexes, which contain an unusual ring-expanded NHC as the central donor group, both amidate⁴⁹ and thiolate⁵⁰ coordination modes can occur depending on the size of the substituent R.



Scheme 2.6

Neutral NHC centred PCP ligands have also been investigated. The first reported examples were the palladium complexes shown in Scheme 2.7 (a) and (b) which contain ethylene and ferrocenyl linkers, respectively.⁵¹ A related PCP ligand containing ortho-

phenyl linkers between the NHC and phosphine donor groups has also been published with complexes of Ni, Pd and Pt (Scheme 2.7 c).⁵²



Scheme 2.7

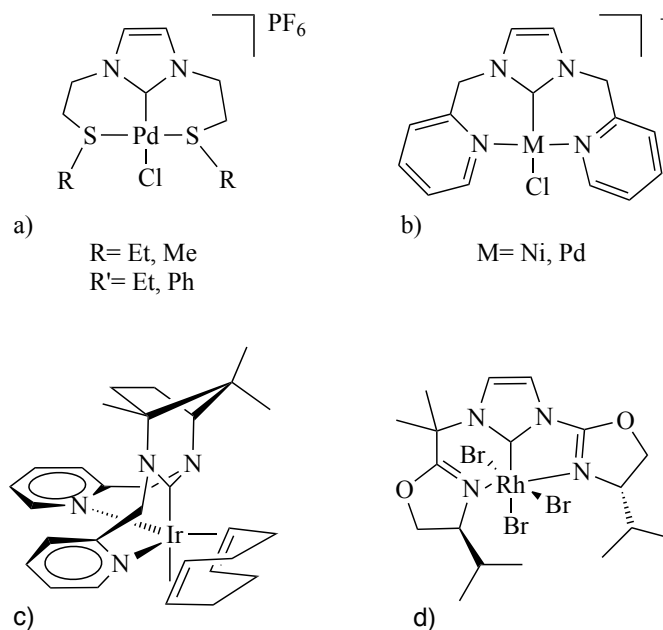
The ethylene and *ortho*-phenyl linked PCP pincer ligands have also been coordinated to rhodium (Scheme 2.8). It is interesting to note that despite a very similar structure these two Rh complexes showed quite different reactivity. For example the structure of the ethyl linked complex⁵³ (Scheme 2.8 a) could only be inferred due to its highly unstable nature which led to its oxidative degradation to yield a Rh(III) trichloride complex (Scheme 2.8 b). Alternatively, the analogous *ortho*-phenyl linked complex (Scheme 2.8 c, X = Cl)⁵⁴ is perfectly stable. However, if the *ortho*-phenyl linked complex contains a methyl or hydride ligand in place of chloride (Scheme 2.8 c, X = Me or H) then the complex undergoes an intra-molecular P-C bond cleavage to yield cyclometallated complexes (Scheme 2.8 d).



ligand with a ring-expanded NHC as the central donor group (Scheme 2.9).^{55,56}



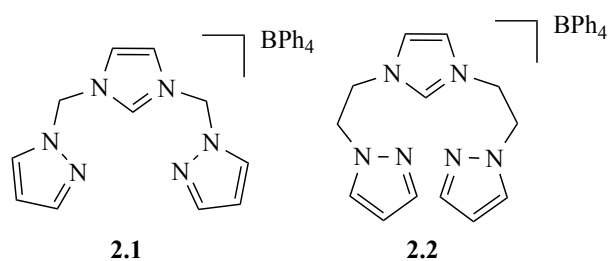
bis-oxazolyl (Scheme 2.10 d) side arms were also reported.^{57,58}



Scheme 2.10

2.1.4 Objectives

The aims of this chapter were to synthesise two new pincer ligand structures (Scheme 2.11), which contain a strongly coordinating NHC as the central donor group and two weakly coordinating pyrazole arms. The pyrazole groups were to be joined to the central NHC donor by methyl or ethyl linker groups.

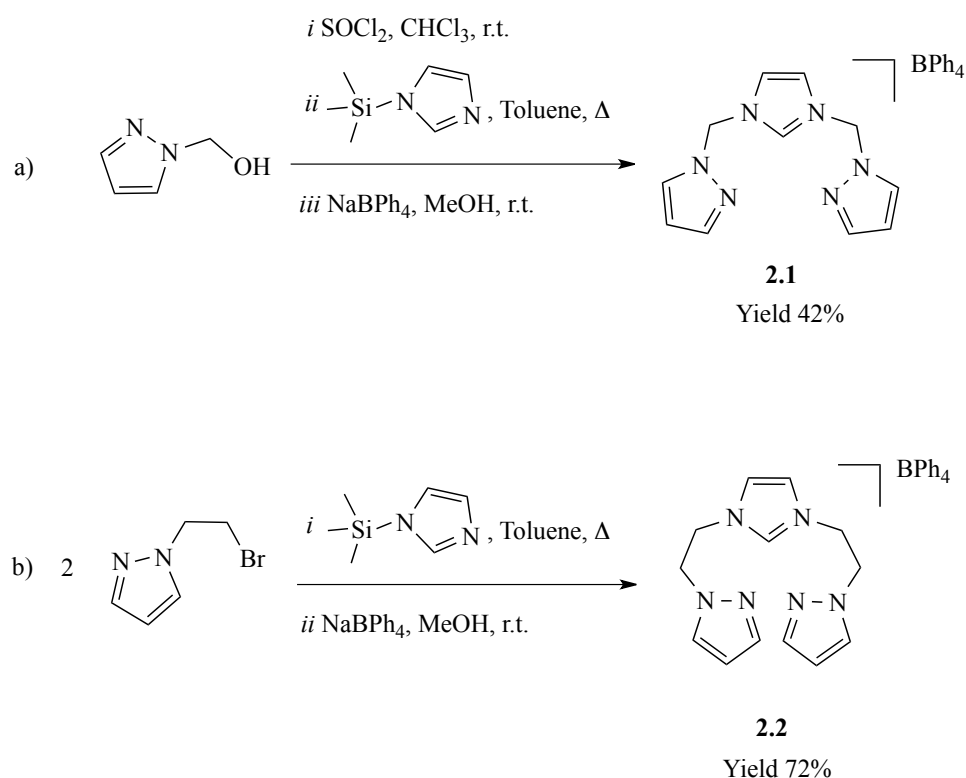


Scheme 2.11

We wished to investigate the coordination properties of these ligands with complexes of Rh(I) and Ir(I) containing either 1,5-cyclooctadiene (COD) or CO co-ligands.

2.2 Results and discussion

2.2.1 Synthesis of ligand precursors



Scheme 2.12

The ligand precursor bis(methylpyrazolyl)imidazolium tetraphenylborate $\text{NCN}^{\text{Me}}\cdot\text{HBPh}_4$ (**2.1**) was synthesised in three steps (Scheme 2.12 a). First the reaction of N-hydroxymethylpyrazole with thionyl chloride afforded the HCl salt of N-chloromethylpyrazole. The crude product was then suspended in dry toluene and reacted with half an equivalent of trimethylsilyl imidazole at reflux for 20 hours to yield a viscous brown oil of the imidazolium chloride product. Anion exchange with NaBPh_4 in methanol gave the desired product (**2.1**) as a crystalline white solid in 42% yield. Unfortunately, the efficiency of this synthesis was affected by the undesired protonation of imidazole nitrogen from the hydrochloric pyrazole salt. However, isolation of the

free pyrazole base was not possible. Synthesis of the ligand precursor bis(ethylpyrazolyl)imidazolium tetraphenylborate $\text{NCN}^{\text{Et}}\cdot\text{HBPh}_4$ (**2.2**) was achieved following an analogous procedure from the reaction of N-(2-bromoethyl)pyrazole with trimethylsilyl imidazole (Scheme 2.12 b). After anion exchange with NaBPh_4 the desired product (**2.2**) was obtained in 72% yield.

The ^1H NMR spectrum of **2.1** (Figure 2.1 a) contains a characteristic high frequency singlet resonance at 9.62 ppm due to the imidazolium H^2 proton, clearly indicating successful synthesis of the ligand precursor. A large singlet resonance at 6.58 ppm due to the four methylene protons and a characteristic triplet at 6.40 ppm due to the pyrazole H^4 proton were also observed. Similarly, the ^1H NMR spectrum of ligand precursor **2.2** (Figure 2.1 b) contains a characteristic high frequency resonance for the imidazolium H^2 proton at 8.72 ppm. This slightly lower frequency, compared with that of 9.62 ppm for the equivalent proton of compound **2.1**, suggests there is a significant electronic impact on the imidazolium ring by increasing the length of the alkyl linkers from methyl to ethyl.

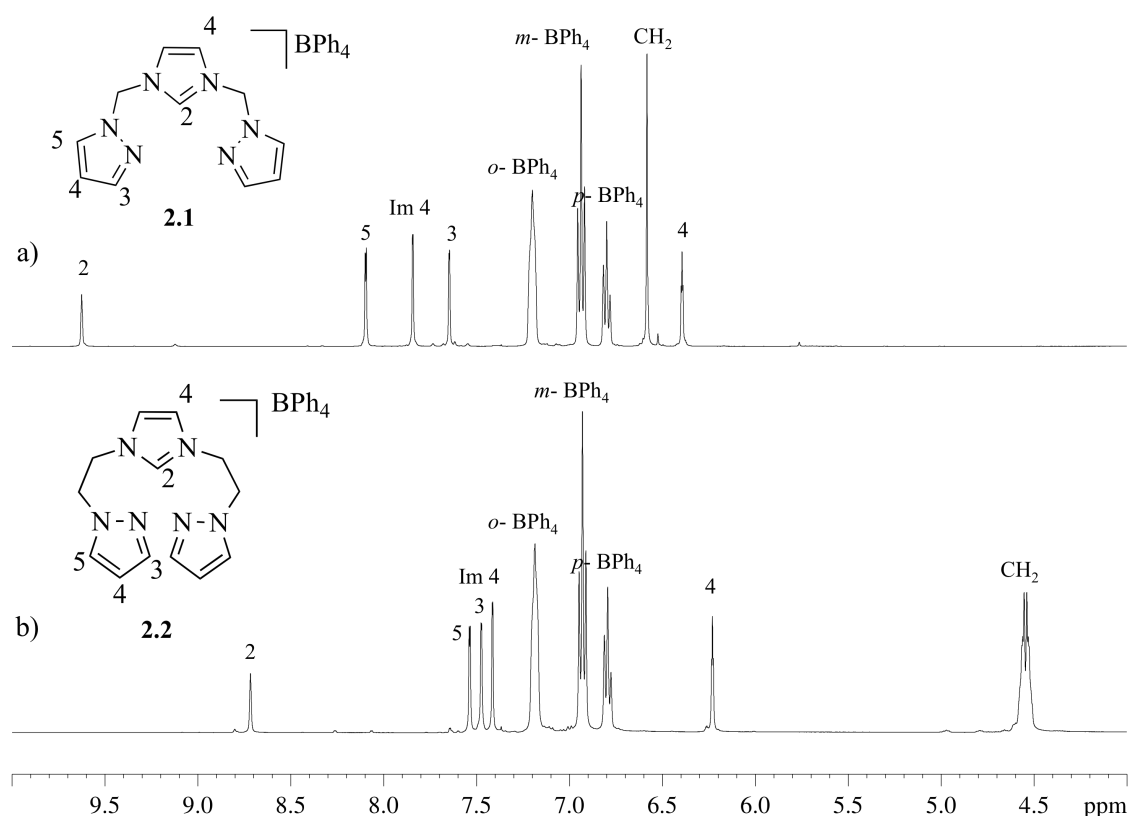
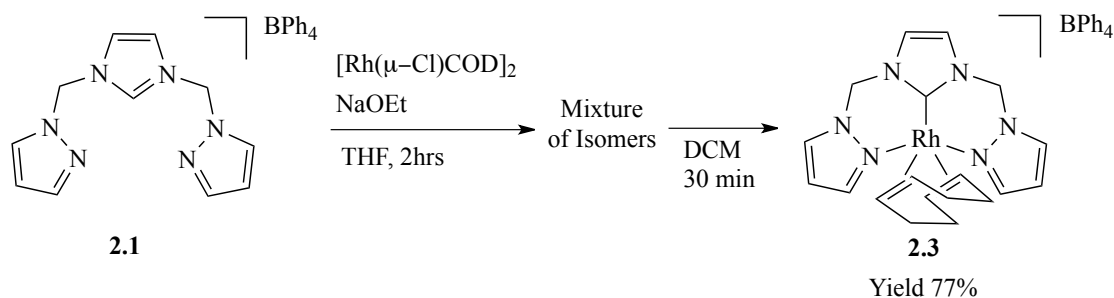


Figure 2.1: ^1H (400 MHz, DMSO-d_6) NMR spectra of the a) bis(methylpyrazolyl)imidazolium salt (2.1) and b) bis(ethylpyrazolyl)imidazolium salt (2.2).

2.2.2 Synthesis of rhodium(I) and iridium(I) complexes containing the ligand NCN^{Me} (2.1)

2.2.2.1 Synthesis of $[\text{Rh}(\text{NCN}^{\text{Me}})(\text{COD})]\text{BPh}_4$ (2.3)



Scheme 2.13

The Rh(I) complex $[\text{Rh}(\text{NCN}^{\text{Me}})(\text{COD})]\text{BPh}_4$ (**2.3**) (where COD= 1,5-cyclooctadiene) was synthesized by generating the pincer carbene ligand (NCN^{Me}) *in situ* via reaction of the ligand precursor $\text{NCN}^{\text{Me}}.\text{HBPh}_4$ (**2.1**) with $[\text{Rh}(\mu\text{-Cl})\text{COD}]_2$ and NaOEt in THF at room temperature for two hours. Removal of the volatiles and analysis of the crude residue by ^1H NMR spectroscopy revealed the formation of multiple species (Scheme 2.13). No trace of unreacted ligand precursor was detected but three new ligand containing products were observed, as clearly indicated by the presence of three distinct triplet resonances characteristic of the pyrazole H^4 protons (Figure 2.2).

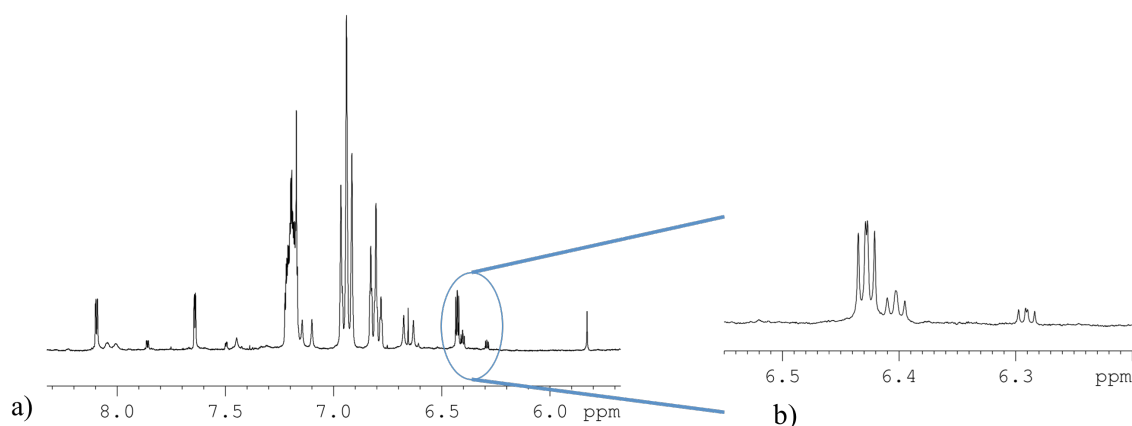


Figure 2.2: a) ^1H NMR (400 MHz, DMSO-d_6) of the crude residue from the synthesis of Rh(I) complex **2.3**; b) three resonances due to the H^4 Pz of isomeric products.

Despite a series of recrystallization attempts using different solvent combinations, isolation of a single species was not achievable. The composition of the mixture however was revealed to be solvent dependent and stirring the crude product mixture in dichloromethane for 30 minutes gave a single new species. Such a transformation suggests that the three species present initially were in fact geometrical or structural isomers of each other, although further characterisation of these intermediates was not attempted. After stirring the crude mixture of unidentified isomers in dichloromethane,

addition of *n*-pentane afforded the desired product $[\text{Rh}(\text{NCN}^{\text{Me}})(\text{COD})]\text{BPh}_4$ (**2.3**) as a bright yellow powder (77 % yield).

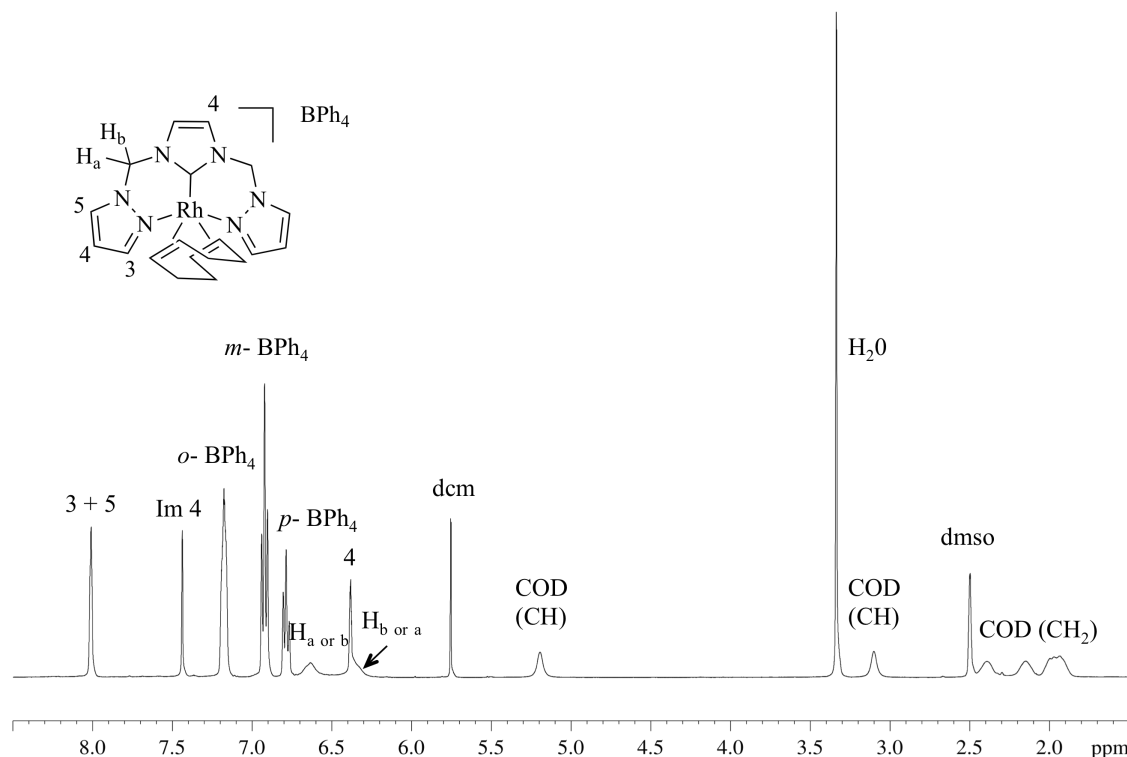


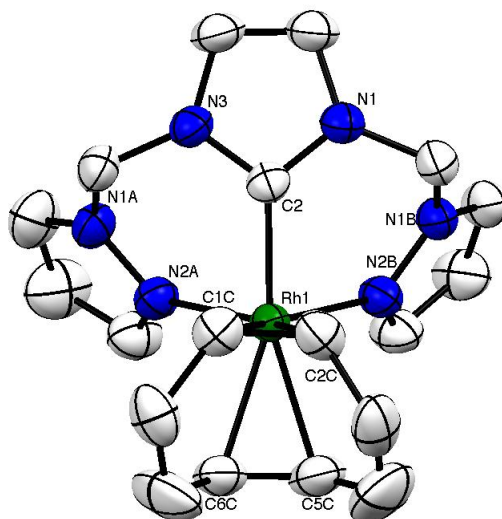
Figure 2.3: ^1H (400 MHz, DMSO-d_6) NMR spectrum of $[\text{Rh}(\text{NCN}^{\text{Me}})(\text{COD})]\text{BPh}_4$ complex (**2.3**).

In the ^1H NMR spectrum of **2.3** (Figure 2.3) only one set of resonances is present for the pyrazolyl protons and one singlet resonance for the imidazole H^4 protons indicating that there is a plane of symmetry through the centre of the ligand. The resonances due to the methylene protons of the bridging ligand arms appear as two very broad singlets at 6.63 and 6.36 ppm, one for each of the magnetically inequivalent geminal protons CH^aH^b . The width of these two peaks indicates that the geminal protons are undergoing exchange over the time frame of the signal acquisition, suggesting a relatively fluxional complex conformation. The resonances of the 1,5-cyclooctadiene (COD) ligand are also broadened. Notably, a large separation is observed for the two COD resonances

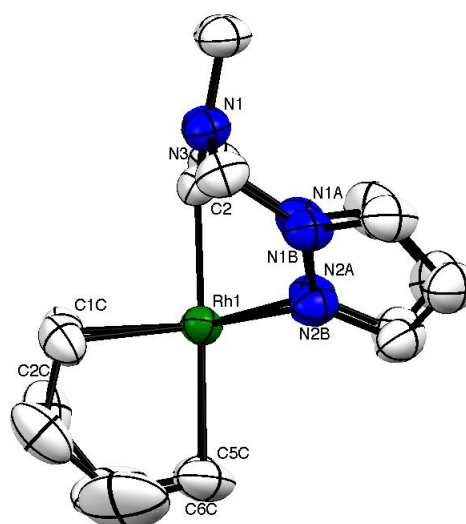
assigned to the alkene protons at 5.19 and 3.11 ppm, indicating a significant difference in the magnetic environment of these two groups.

2.2.2.1.1 Solid state structure of [Rh(NCN^{Me})(COD)]BPh₄ (**2.3**)

Crystals of [Rh(NCN^{Me})(COD)]BPh₄ (**2.3**) suitable for x-ray diffraction analysis were obtained by slow diffusion of *n*-pentane into a concentrated solution of the complex in dichloromethane. In contrast with pincer ligands of a similar geometry, which typically coordinate in a meridional fashion, the bis(methylpyrazolyl)carbene ligand (NCN^{Me}) of complex **2.3** coordinates to the metal centre in a facial fashion (Figure 2.4). In combination with the COD co-ligand, the complex assumes a distorted trigonal bipyramidal geometry, where the axial plane is occupied by the carbene and one COD alkene donor, while the second COD alkene and the two pyrazole donors lay on a distorted equatorial plane. Note, the angle N-Rh-N of 88.77(10)° is far from the ideal trigonal bipyramidal angle of 120°. An axial plane of symmetry bisecting the two *N*-donor groups is consistent with the symmetry shown in the ¹H NMR spectrum suggesting a similar structure predominates in solution.



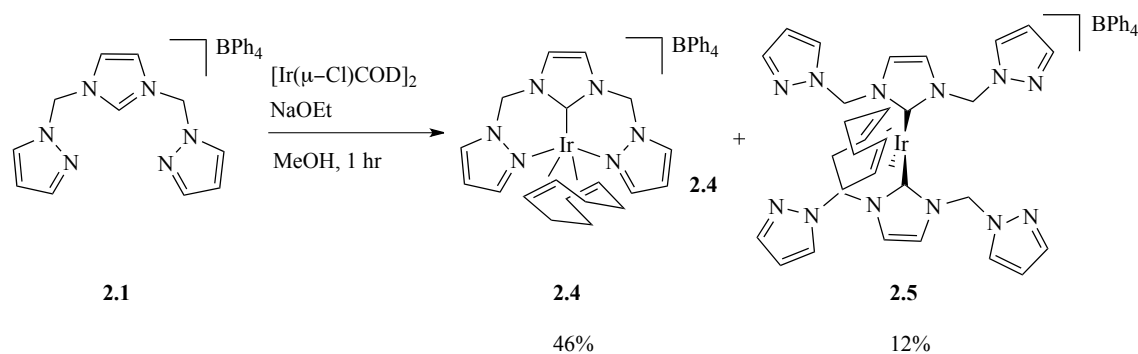
a)



b)

Figure 2.4: ORTEP diagram of the cationic fragment of $[\text{Rh}(\text{NCN}^{\text{Me}})(\text{COD})]\text{BPh}_4$ complex **2.3**, with 40% probability ellipsoids for the non hydrogen atoms, as viewed from the equatorial axis a) and from the axial axis b). Selected bond lengths (Å) and angles (°): Rh-C_{NHC} = 1.981(3), Rh-N = 2.267(2), Rh-N = 2.270(2), Rh-COD_{ax} = 2.270(3)/2.273(3), Rh-COD_{eq} = 2.097(3)/2.097(3), N-Rh-N = 88.77(10).

2.2.2.2 Synthesis of $[\text{Ir}(\text{NCN}^{\text{Me}})(\text{COD})]\text{BPh}_4$ (**2.4**) and $[\text{Ir}(\kappa^1\text{-NCN}^{\text{Me}})_2(\text{COD})]\text{BPh}_4$ (**2.5**)



Scheme 2.14

The reaction of the imidazolium ligand precursor $\text{NCN}^{\text{Me}}.\text{HBPh}_4$ (**2.1**) with $[\text{Ir}(\mu\text{-Cl})\text{COD}]_2$ and NaOEt in MeOH at room temperature for two hours gave a pale yellow precipitate and a bright orange solution (Scheme 2.14). The yellow precipitate was collected and recrystallized from THF/diethyl ether to give the desired pincer bound product $[\text{Ir}(\text{NCN}^{\text{Me}})(\text{COD})]\text{BPh}_4$ (**2.4**) in 46% yield. Reduction of the orange solution to dryness and recrystallization of the residue from dichloromethane/pentane gave a bright orange precipitate of the bis-carbene complex $[\text{Ir}(\kappa^1\text{-NCN}^{\text{Me}})_2(\text{COD})]\text{BPh}_4$ (**2.5**) in 12% yield.

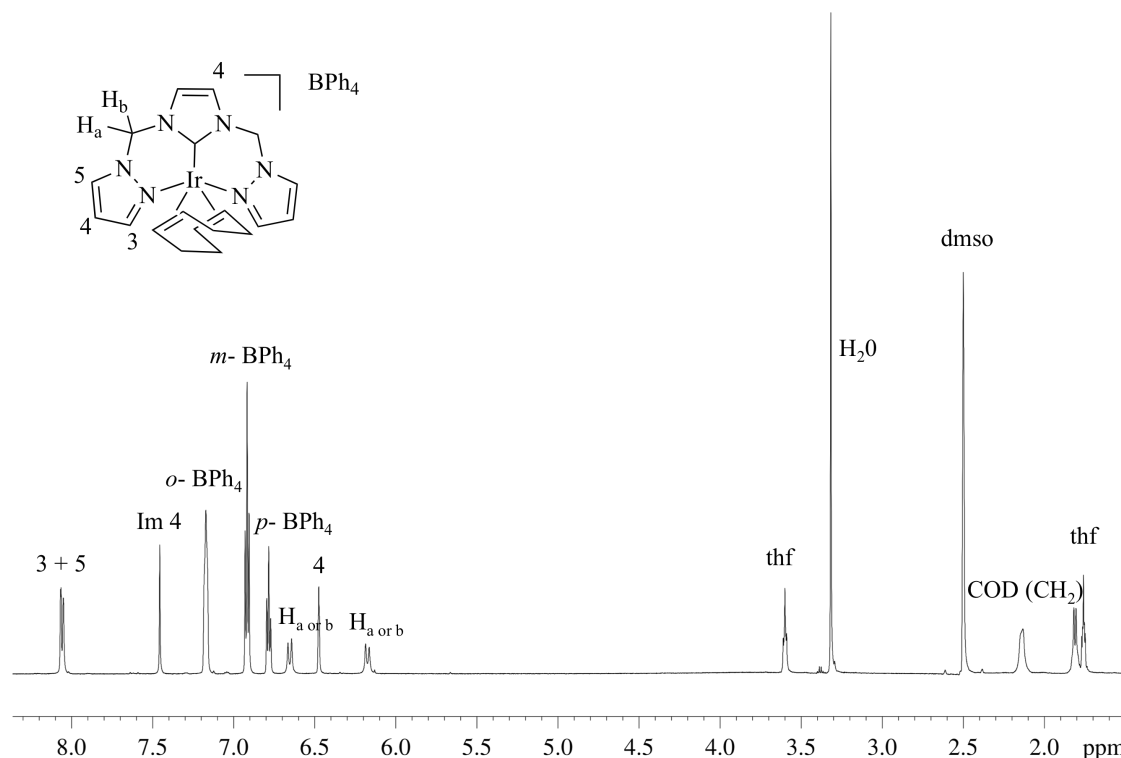


Figure 2.5: ^1H (400 MHz, DMSO-d_6) NMR spectrum of the $[\text{Ir}(\text{NCN}^{\text{Me}})(\text{COD})]\text{BPh}_4$ complex (**2.4**).

The ^1H NMR spectrum of the pincer complex **2.4** (Figure 2.5) contains a single set of resonances due to the pyrazole protons and one singlet resonance due to the imidazole H^4 protons indicating a plane of symmetry through the centre of the ligand. The resonances assigned to the methylene protons are resolved as two sharp geminally coupled doublets at 6.65 and 6.16 ppm ($^2J_{\text{HH}} = 13.4$ Hz). Unusually, only 8 of the expected 12 COD proton resonances could be observed at room temperature. These were assigned to the alkyl ($-\text{CH}_2\text{CH}_2-$) COD protons, which appeared as two broad multiplets at 2.12 and 1.81 ppm. In an effort to identify the missing COD protons the ^1H NMR spectrum of complex **2.4** was acquired at 268.15 K, 258.15 K and 248.15 K. As can be seen in Figure 2.6 (b-d) two broad singlets for the missing alkenic ($-\text{CH}=\text{CH}-$) protons resolve from the baseline of the spectrum as the temperature decreases. The broadness of the COD resonances at room temperature indicate a fluxional

conformation of the complex, similar to that observed for the analogous rhodium complex $[\text{Rh}(\text{NCN}^{\text{Me}})(\text{COD})]\text{BPh}_4$ (**2.3**).

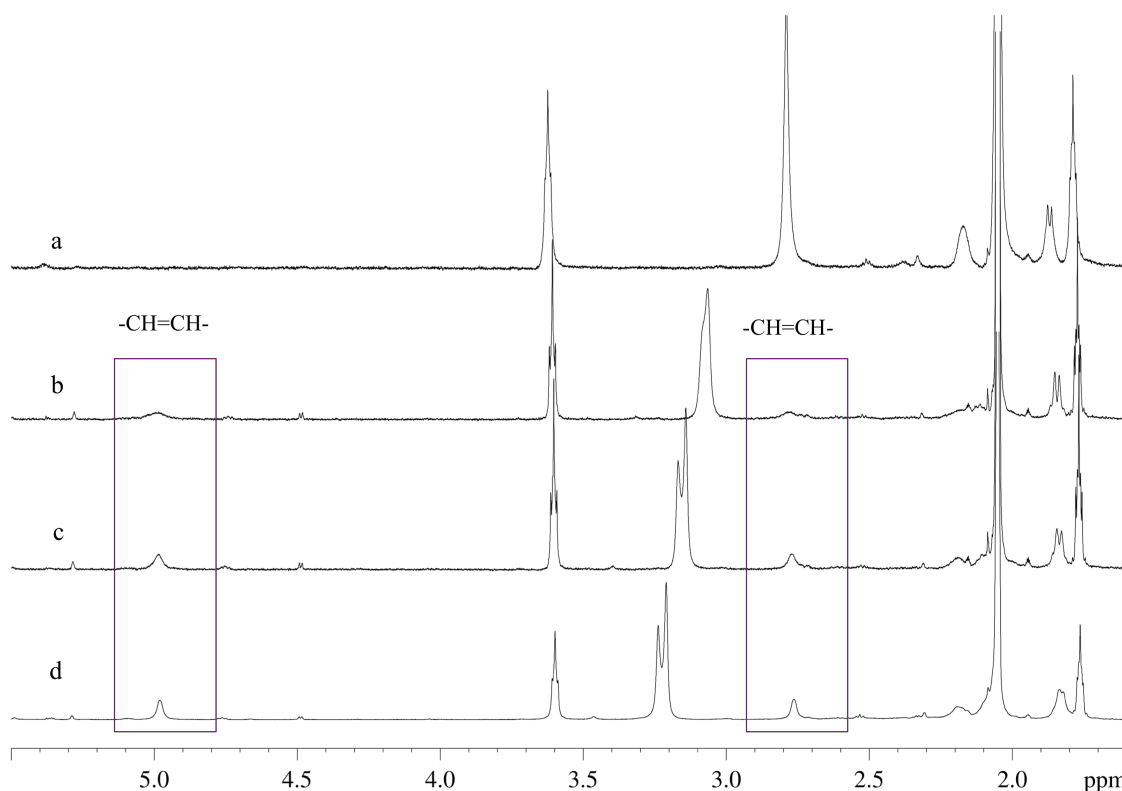


Figure 2.6: Variable temperature ^1H NMR stacked spectra (600 MHz, THF-d_8) of **2.4** showing the broad alkenic COD protons resonances as temperature is decreased from a) 298.15 K to b) 268.15 K, c) 258.15 K and d) 248.15 K.

The ^1H NMR spectrum of the biscarbene complex $[\text{Ir}(\kappa^1\text{-NCN}^{\text{Me}})_2(\text{COD})]\text{BPh}_4$ (**2.5**) is characterised by a ligand:COD: BPh_4 ratio of 2:1:1 indicating the coordination of two ligand groups to the iridium metal centre (Figure 2.7). As only one set of ligand resonance is observed the two ligands must occupy equivalent environments. Despite the pyrazole donor groups remaining uncoordinated, splitting of the methylene protons into geminally coupled doublet pairs (6.92 and 6.51 ppm, $^2J_{\text{HH}} = 13.4$ Hz) is observed. Therefore, rotation of the ligand around the Ir-carbene bond must be impaired due to the steric bulk of the uncoordinated pyrazole arms. A single broad resonance for the COD

alkenic protons (-CH=CH-) also indicates a plane of symmetry bisecting these two donor groups.

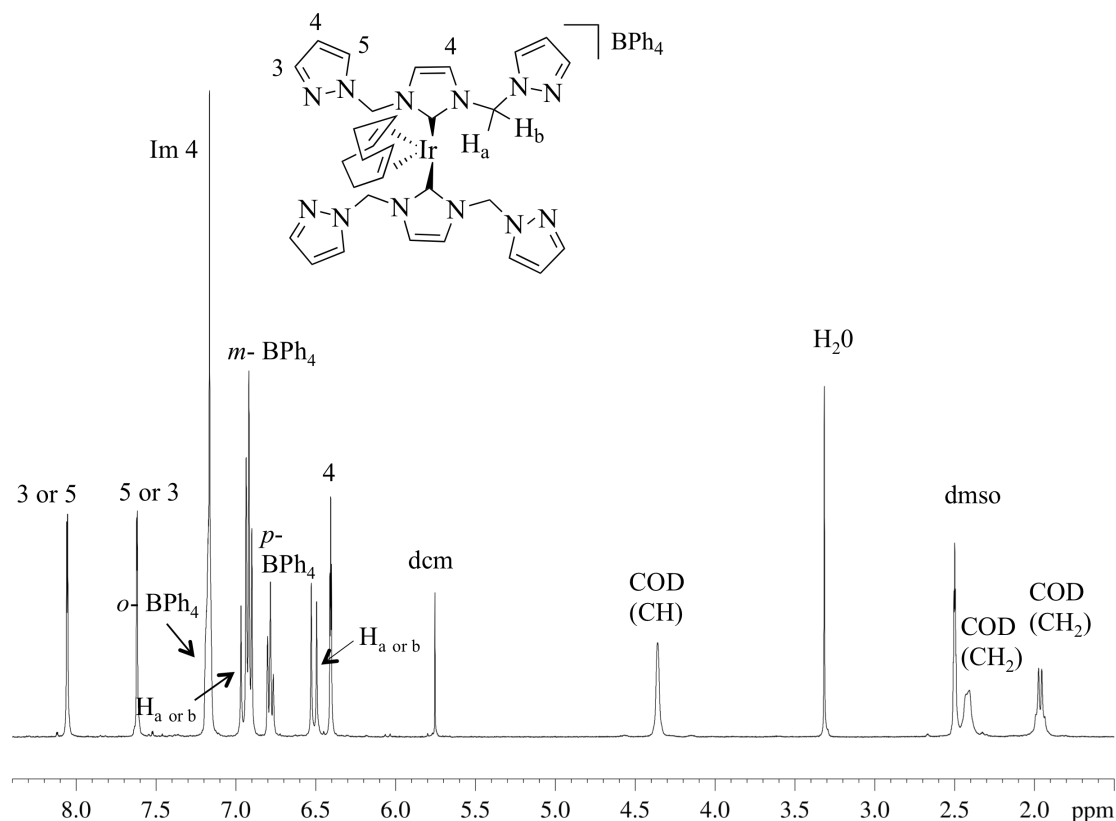
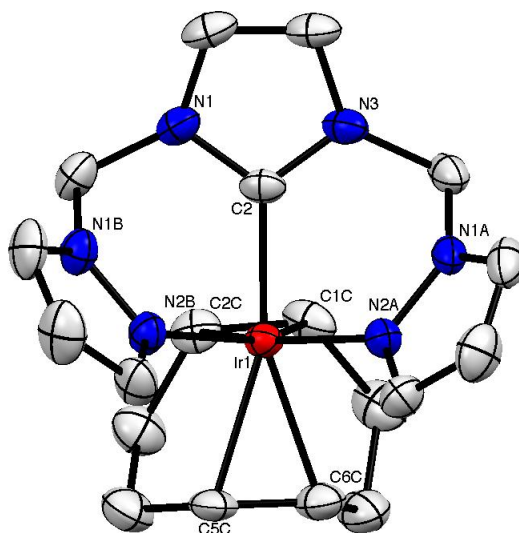


Figure 2.7: ^1H (400 MHz, $\text{DMSO}-d_6$) NMR spectrum of $[\text{Ir}(\kappa^1\text{-NCN}^{\text{Me}})_2(\text{COD})]\text{BPh}_4$ complex (**2.5**).

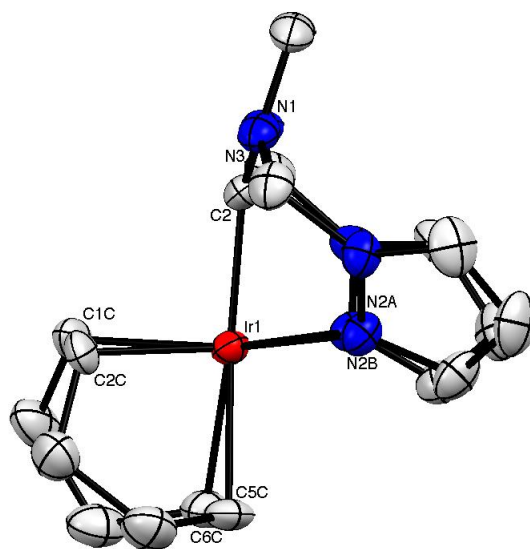
2.2.2.2.1 Solid state structure of $[\text{Ir}(\text{NCN}^{\text{Me}})(\text{COD})]\text{BPh}_4$ (**2.4**) and $[\text{Ir}(\kappa^1\text{-NCN}^{\text{Me}})_2(\text{COD})]\text{BPh}_4$ (**2.5**)

X-ray diffraction quality crystals of both complexes **2.4** (Figure 2.9) and **2.5** (Figure 2.10) were grown by slow diffusion of *n*-pentane into a concentrated dichloromethane solution of the desired complex. The pincer coordinated iridium complex **2.4** adopts a similar structure to its rhodium analogue **2.3**, as described above. The NCN^{Me} ligand coordinates to iridium in a facial fashion to yield a distorted trigonal bipyramidal geometry. The carbene and one COD alkene group occupy the axial positions and the

second COD alkene and the two pyrazole donors lay on a distorted equatorial plane (N-Ir-N= 85.68(12)°).

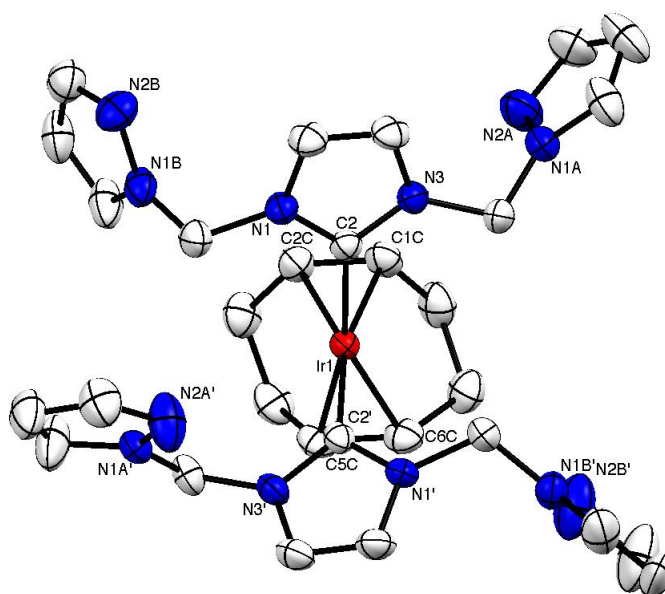


a)

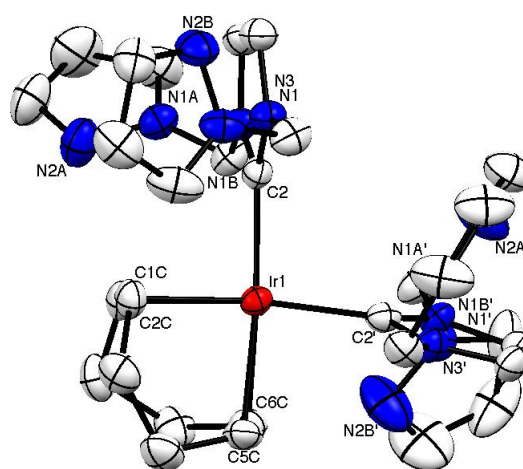


b)

Figure 2.8: ORTEP diagram of the cationic fragment of $[\text{Ir}(\text{NCN}^{\text{Me}})(\text{COD})]\text{BPh}_4$ (**2.4**), with 40% probability ellipsoids for the non hydrogen atoms, as viewed from the equatorial axis a) and from the axial axis b). Selected bond lengths (Å) and angles (°): Ir-C_{NHC}= 1.995(4), Ir-N= 2.194(3), Ir-N= 2.247(3), Ir-COD_{ax}= 2.210(4)/2.233(4), Ir-COD_{eq}= 2.093(4)/ 2.093(4), N-Ir-N= 85.68(12).



a)

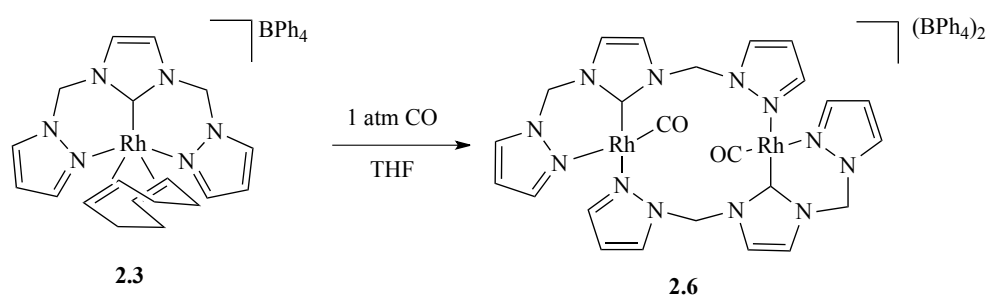


b)

Figure 2.9: ORTEP diagram of the cationic fragment of $[\text{Ir}(\kappa^1\text{-NCN}^{\text{Me}})_2(\text{COD})]\text{BPh}_4$ (**2.5**), with 40% probability ellipsoids for the non hydrogen atoms, as viewed from the equatorial axis a) and from the axial axis b). Selected bond lengths (Å) and angles ($^\circ$): Ir-C2_{NHC} = 2.0463(3), Ir-C2'_{NHC} = 2.048(3), Ir-COD_{C1/2} = 2.213(3)/2.180(3), Ir-COD_{C5/6} = 2.210(3)/2.179(3), C2-Ir-C2' = 97.11(12).

The X-ray structure of the bis-NHC complex $[\text{Ir}(\kappa^1\text{-NCN}^{\text{Me}})_2(\text{COD})]\text{BPh}_4$ (**2.5**) confirmed the ^1H NMR analysis, revealing a square planar geometry where two carbene ligands (NCN^{Me}) and a chelating 1,5-cyclooctadiene co-ligand are coordinated to the Ir(I) centre. The two NCN^{Me} ligands are coordinated to the metal centre only through the carbene donor with the two pyrazole arms remaining uncoordinated. The carbene-metal bond lengths $\text{Ir-C2}_{\text{NHC}}$ and $\text{Ir-C2'}_{\text{NHC}}$, were 2.0463(3) and 2.048(3) Å, respectively, which are comparable with the carbene-iridium bond lengths reported in the literature for other monodentate biscarbene iridium complexes (2.074(4) and 2.076(3) Å).⁵⁹ However, in comparison to the pincer complex **2.4**, the Ir-C bond lengths of **2.5**, $\text{Ir-C2}_{\text{NHC}}$ and $\text{Ir-C2'}_{\text{NHC}}$, are longer which is an indication of a weaker carbene-iridium bond strength.

2.2.2.3 Synthesis of $[\text{Rh}(\mu\text{-NCN}^{\text{Me}})(\text{CO})]_2(\text{BPh}_4)_2$ (**2.6**)



Scheme 2.16

The bimetallic Rh(I) complex $[\text{Rh}(\mu\text{-NCN}^{\text{Me}})(\text{CO})]_2(\text{BPh}_4)_2$ (**2.6**) was synthesised by displacement of COD from $[\text{Rh}(\text{NCN}^{\text{Me}})(\text{COD})]\text{BPh}_4$ (**2.3**) under an atmosphere of CO (Scheme 2.16). Instead of the expected monomeric dicarbonyl complex the reaction led to the formation of a dinuclear species where each of the two NCN^{Me} ligands coordinate

to two Rh(I) centres. The structure of **2.6** was confirmed by x-ray crystallography (see Section 2.3.3.1).

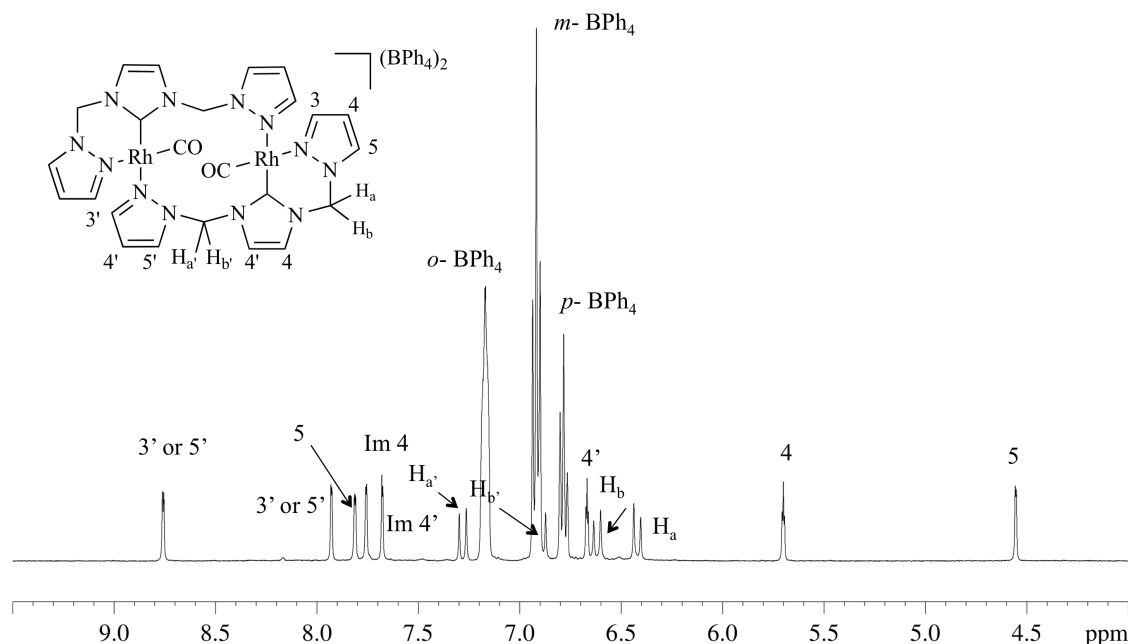


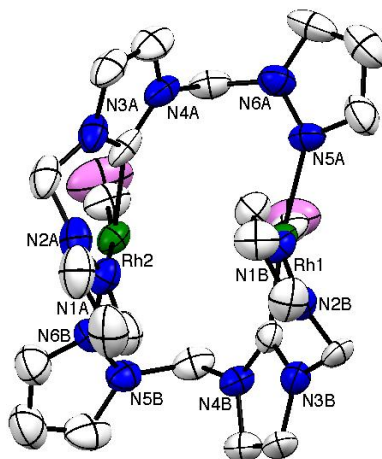
Figure 2.10: ^1H (400 MHz, DMSO-d_6) NMR spectrum of $[\text{Rh}(\mu\text{-NCN}^{\text{Me}})(\text{CO})]_2(\text{BPh}_4)_2$ complex (**2.6**).

In the ^1H NMR spectrum of **2.6** (Figure 2.10) only one set of ligand resonances is observed indicating that the two ligand groups are in equivalent environments. An unusually low frequency is observed for the pyrazole H^3 proton indicative of strong magnetic shielding. In the ^{13}C NMR spectrum of **2.6** at room temperature the resonance for the Rh-CO group could not be detected. The $^{13}\text{C}\{^1\text{H}\}$ NMR spectrum was therefore acquired at 193K, which revealed a single Rh-CO group resonance at 175.3 ppm (d, $^1J_{\text{Rh-C}} = 51.8$ Hz), indicating that only one CO ligand is coordinated to each Rh nucleus and that both CO groups occupy equivalent environments.

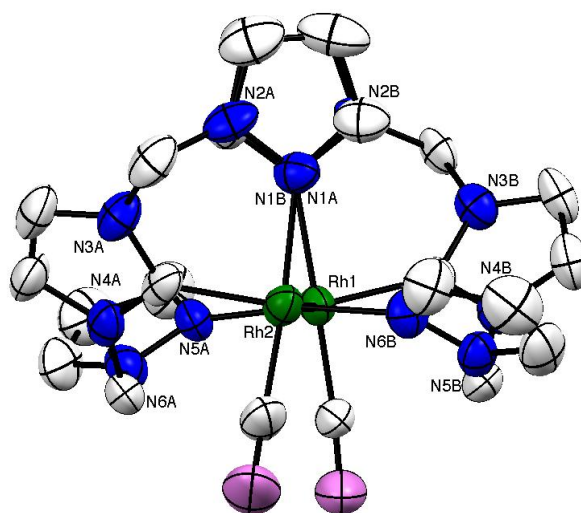
The IR spectrum of **2.6** was acquired in both the solid state (KBr) and in solution (DMSO). In both cases only a single CO stretching frequency was observed at 1998 cm^{-1} .

2.2.2.3.1 Solid state structure of $[\text{Rh}(\mu\text{-NCN}^{\text{Me}})\text{CO}]_2(\text{BPh}_4)_2$ (**2.6**)

X-ray quality crystals of complex **2.6** (Figure 2.11) were grown by slow diffusion of pentane into a concentrated solution of acetone.



a)

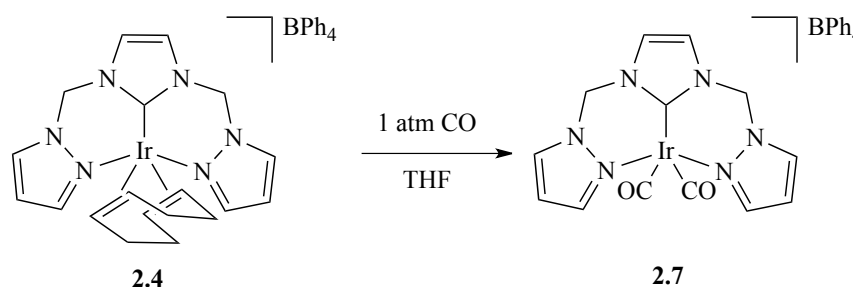


b)

Figure 2.11: ORTEP diagram of the cationic fragment of $[\text{Rh}(\mu\text{-NCN}^{\text{Me}})\text{CO}]_2(\text{BPh}_4)_2$ (**2.6**), with 40% probability ellipsoids for the non hydrogen atoms, as viewed from the equatorial axis a) and from the axial axis b). Selected bond lengths (Å) and angles (°): Rh1-Rh2= 3.341, Rh1-C_{NHC}= 1.975(7), Rh2-C_{NHC}= 1.992(7), Rh1-CO= 1.783(8), Rh2-CO= 1.808(9), Rh1-N_{transCO}= 2.074(5), Rh2-N_{transCO}= 2.100(6), Rh1-N_{transNHC}= 2.103(6), Rh2-N_{transNHC}= 2.098(6).

The solid state structure of **2.6** was determined by X-ray crystallography which revealed the unusual dimeric nature of this complex. The solid state structure of **2.6** shows two square planar Rh centres bridged by two NCN^{Me} ligands. Each NCN^{Me} ligand forms a pyrazolyl-carbene chelate with one Rh centre while the second pyrazolyl donor coordinates to the other Rh centre. Each Rh centre is therefore coordinated by two pyrazolyl donor groups, one from each ligand, a carbene donor group and a CO ligand. The two Rh atoms are 3.341 Å apart which is too long to be considered a formal Rh-Rh bond.⁶⁰⁻⁶² The pyrazole H^3 proton can be seen to reside over the ring of another pyrazole group which accounts for the strong shielding observed in the ^1H NMR spectrum. This correlation also confirms congruence between the solid state and solution structures of **2.6**.

2.2.2.4 Synthesis of $[\text{Ir}(\text{NCN}^{\text{Me}})(\text{CO})_2]\text{BPh}_4$ (**2.7**)



Scheme 2.18

The complex $[\text{Ir}(\text{NCN}^{\text{Me}})(\text{CO})_2]\text{BPh}_4$ (**2.7**) was synthesised by displacement of the COD co-ligand from the complex $[\text{Ir}(\text{NCN}^{\text{Me}})(\text{COD})]\text{BPh}_4$ (**2.4**) under 1 atmosphere of CO (Scheme 2.18). Unlike the analogous Rh complex **2.6** which formed a dimeric species with only one CO molecule bound to Rh, the displacement of COD from **2.4** led to the expected dicarbonyl product. Unfortunately, the complex could not be isolated as

it was found to be unstable in the absence of a CO atmosphere, therefore the product could only be characterized *in situ*.

Figure 2.12 shows the ^1H NMR spectrum of a THF-d_8 solution of $[\text{Ir}(\text{NCN}^{\text{Me}})(\text{COD})]\text{BPh}_4$ (**2.4**) before a) and after b) the introduction of a CO atmosphere.

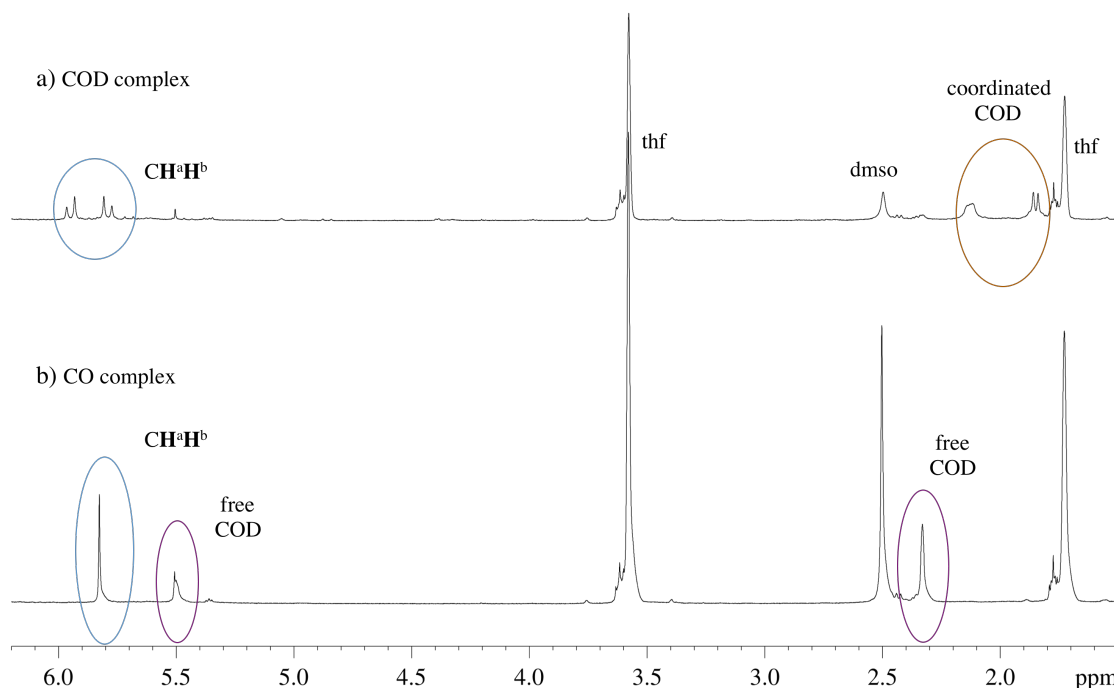


Figure 2.12: Stacked ^1H NMR spectra (400 MHz, DMSO-d_6) of a) $[\text{Ir}(\text{NCN}^{\text{Me}})(\text{COD})]\text{BPh}_4$ (**2.3**) and b) $[\text{Ir}(\text{NCN}^{\text{Me}})(\text{CO})_2]\text{BPh}_4$ (**2.7**).

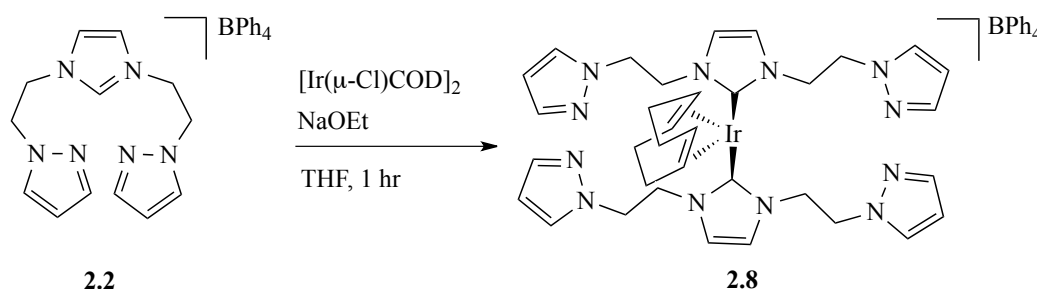
Upon carbonylation the characteristic peaks of coordinated COD at 2.13 ppm and 1.85 ppm disappear and two new resonances at 2.33 ppm and 5.5 ppm characteristic of free COD are observed. Upon carbonylation the two doublet resonances at 6.66 and 5.18 ppm for the ligand methylene protons ($\text{CH}^{\text{a}}\text{H}^{\text{b}}$) also coalesced to give a large singlet at 5.83 ppm. At 193 K this singlet resonance resolved back into two doublets (5.90 and 5.79 ppm, $^2J_{\text{HH}} = 13.1$ Hz), which indicated that fluctuation of the complex conformation is averaging these two signals at room temperature. The $^{13}\text{C}\{^1\text{H}\}$ NMR spectrum didn't

show any characteristic resonances due to the coordinated CO groups, possibly due to line broadening as a result of structural fluxionality of the complex.

The solution state IR spectrum (THF) showed two intense bands at 2081 and 2013 cm^{-1} for the CO stretching frequencies of complex **2.7**, confirming that two CO ligands are bound to the metal centre.

2.2.3 Synthesis of rhodium(I) and iridium(I) complexes containing the ligand NCN^{Et} (**2.2**)

2.2.3.1 Synthesis of $[\text{Ir}(\kappa^1\text{-NCN}^{\text{Et}})_2(\text{COD})]\text{BPh}_4$ (**2.8**)



Scheme 2.19

The reaction of the imidazolium ligand precursor $\text{NCN}^{\text{Et}}.\text{HBPh}_4$ (**2.2**) with $[\text{Ir}(\mu\text{-Cl})\text{COD}]_2$ and NaOEt was attempted under a series of different reaction conditions. Both THF and methanol were used as solvent, and the reaction performed at room temperature or reflux, for either a few hours or overnight. In each case the only product that was isolated was the Ir(I) biscarbene complex $[\text{Ir}(\kappa^1\text{-NCN}^{\text{Et}})_2(\text{COD})]\text{BPh}_4$ (**2.8**). The ^1H NMR spectrum of **2.8** (Figure 2.13) revealed a ligand: BPh_4 :COD ratio of 2:1:1 consistent with two carbene ligands coordinated to iridium. A single set of resonances for the NCN^{Et} ligand protons is also observed indicating that both ligands

are in equivalent environments. Diastereotopic splitting of the ethyl proton resonances is also consistent with a restricted rotation of the Ir-carbene bond.

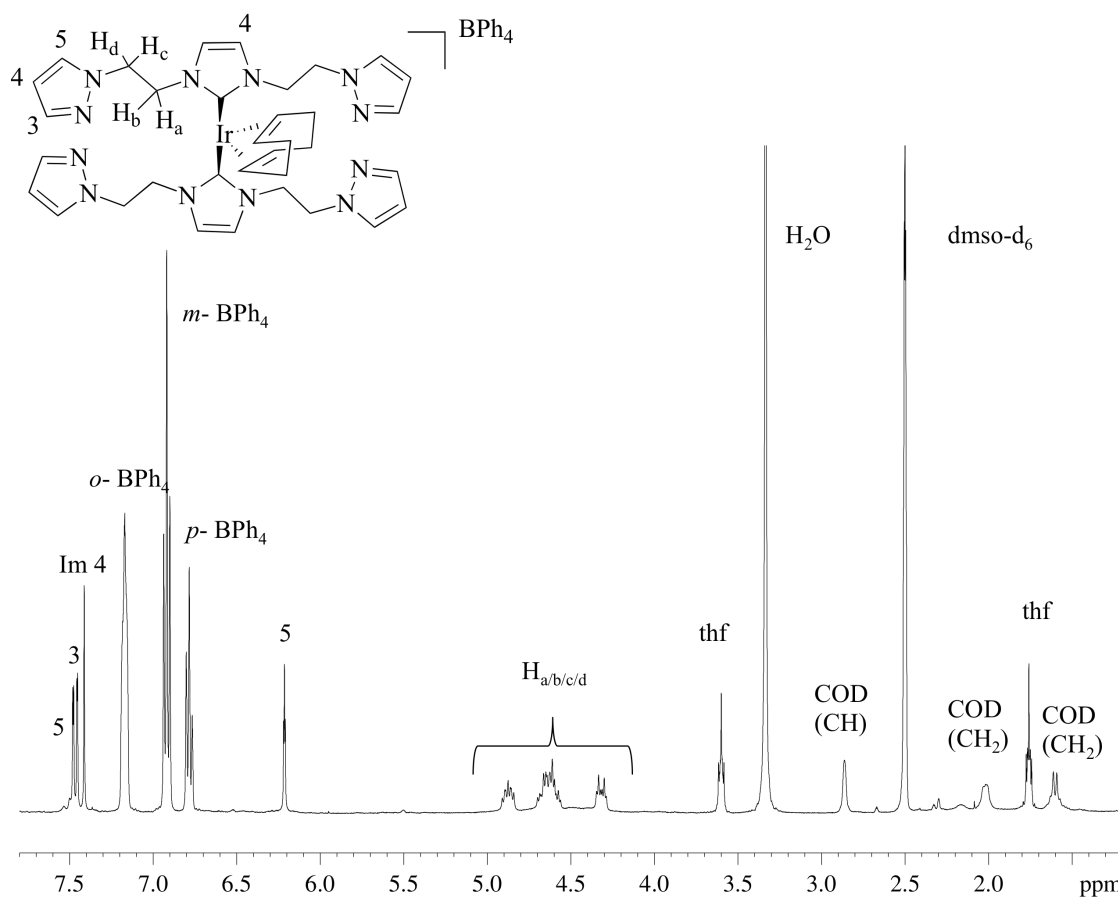
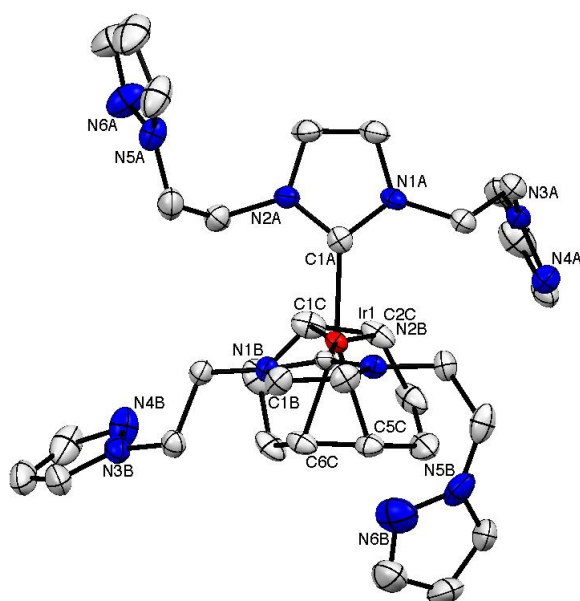


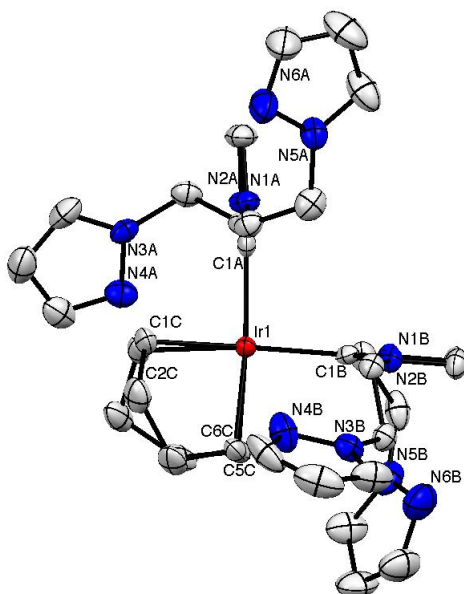
Figure 2.13: ^1H NMR (400 MHz, DMSO- d_6) NMR spectrum of $[\text{Ir}(\kappa^1\text{-NCN}^{\text{Et}})_2(\text{COD})]\text{BPh}_4$ (**2.8**).

2.2.3.1.1 Solid state structure of $[\text{Ir}(\kappa^1\text{-NCN}^{\text{Et}})_2(\text{COD})]\text{BPh}_4$ (**2.8**)

X-ray diffraction analysis of single crystals of complex **2.8** revealed its solid state structure (Figure 2.14). The complex forms a distorted square planar configuration with both NCN^{Et} ligands coordinated to Ir through only the carbenic carbon of the NHC donor. This is analogous to the structure obtained with $[\text{Ir}(\kappa^1\text{-NCN}^{\text{Me}})_2(\text{COD})]\text{BPh}_4$ (**2.5**), described above.



a)

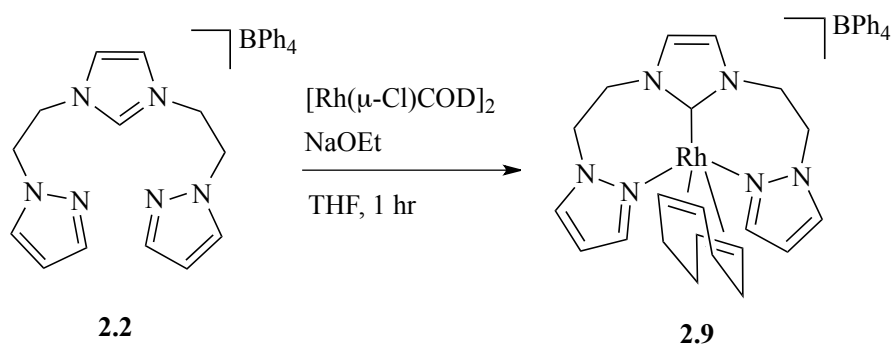


b)

Figure 2.14: ORTEP diagram of the cationic fragment of $[\text{Ir}(\kappa^1\text{-NCN}^{\text{Et}})_2(\text{COD})]\text{BPh}_4$ (**2.8**), with 40% probability ellipsoids for the non hydrogen atoms, as viewed from the equatorial axis a) and from the axial axis b). Selected bond lengths (Å) and angles (°): Ir-C1A_{NHC} = 2.041(2), Ir-C1B_{NHC} = 2.052(3), Ir-COD_{C1C/C2C} = 2.200(3)/2.185(3), Ir-COD_{C5C/C6C} = 2.193(3)/2.185(3), C1A-Ir-C1B = 93.79(10).

The carbene-iridium bond length of 2.041(2) and 2.052(3) Å in **2.8** are consistent with the carbene-iridium lengths reported in the literature for monodentate biscarbene complexes.⁵⁹ However, the carbene-iridium bond length is extended with comparison to the carbene-iridium bond length in the pincer carbene complexes (**2.4**), indication of a weaker carbene-iridium bond strength in complex **2.8**.

2.2.3.2 Synthesis of $[\text{Rh}(\text{NCN}^{\text{Et}})(\text{COD})]\text{BPh}_4$ (**2.9**)



Scheme 2.20

Coordination of the ethyl bridged pincer ligand NCN^{Et} to Rh(I) was achieved by reaction of the ligand precursor $\text{NCN}^{\text{Et}}.\text{HBPh}_4$ (**2.2**), $[\text{Rh}(\mu\text{-Cl})\text{COD}]_2$ and an excess of NaOEt in THF at room temperature. The volatiles were removed in vacuo and recrystallization of the residue from dichloromethane/pentane gave pure $[\text{Rh}(\text{NCN}^{\text{Et}})(\text{COD})]\text{BPh}_4$ (**2.9**) in 37 % yield. The ^1H NMR spectrum of **2.9** (Figure 2.15) is consistent with a symmetric ligand with only a single set of pyrazolyl resonances and one singlet resonance for the imidazole H^4 backbone (7.11 ppm). A series of overlapping multiplets were observed between 4.3 and 5.2 ppm due to the diastereotopic protons of the ethylene ligand arms. These spectral features are consistent with a solution state structure where both pyrazole donors are coordinated to Rh in an equivalent environment.

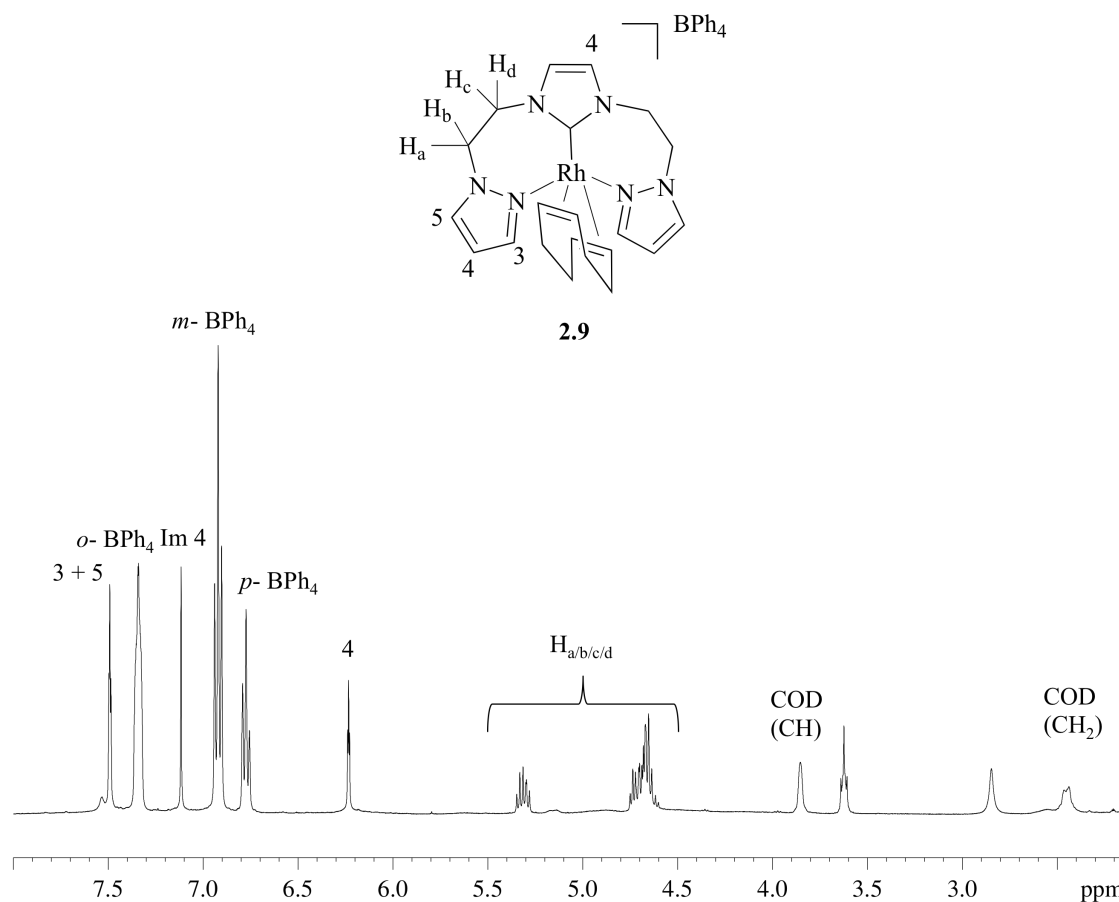


Figure 2.15: ^1H (400 MHz, acetone- d_6) NMR spectrum of $[\text{Rh}(\text{NCN}^{\text{Et}})(\text{COD})]\text{BPh}_4$ complex (**2.9**).

2.2.3.2.1. Solid state structure of $[\text{Rh}(\text{NCN}^{\text{Et}})(\text{COD})]\text{BPh}_4$ (**2.9**)

X-ray quality crystals of **2.9** were grown by slow diffusion of *n*-pentane into a concentrated dichloromethane solution of the complex. Despite the symmetry revealed in the ^1H NMR spectrum, the crystal structure of **2.9** revealed an unsymmetric coordination environment where only one of the pyrazolyl donors was coordinated to the Rh centre to give a square planar complex (Figure 2.16). The fact that both tridentate (κ^3) and bidentate (κ^2) coordination modes are observed for the ligand (in solution and the solid state respectively) suggests that a relatively small difference in energy between the two configurations exists. Therefore it is possible that the κ^2 -coordination mode may be readily accessible in solution. Such a hemilabile character of one of the pyrazolyl donors could have important consequences for the catalytic activity

of this complex where the creation of vacant coordination sites is often fundamental to the binding and activation of organic substrates.⁶³

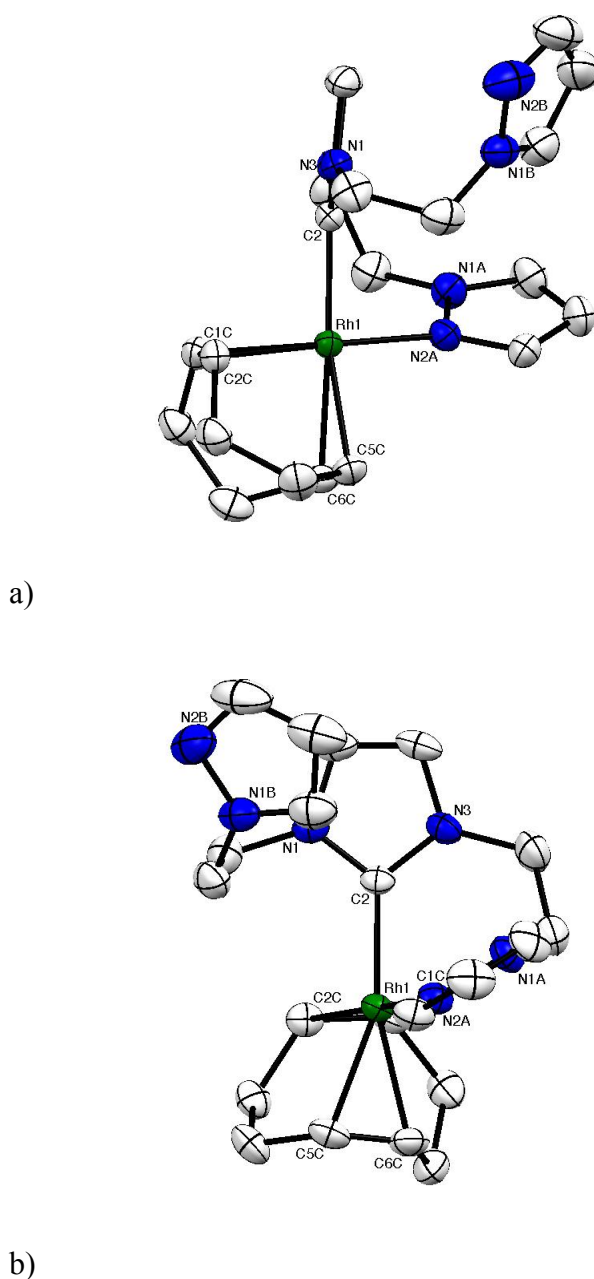
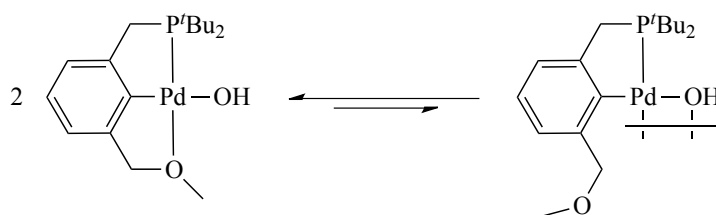


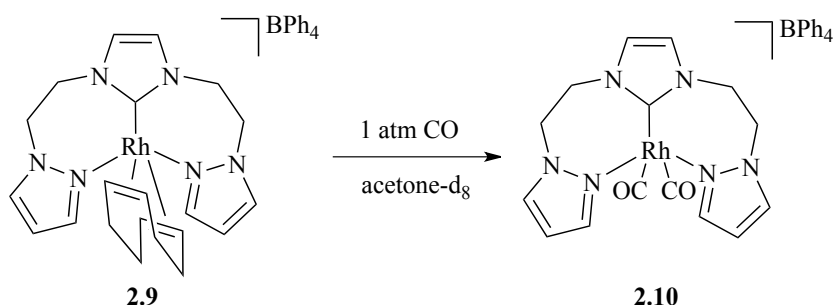
Figure 2.16: ORTEP diagram of the cationic fragment of $[\text{Rh}(\text{NCN}^{\text{Et}})(\text{COD})]\text{BPh}_4$ complex **2.9**, with 40% probability ellipsoids for the non hydrogen atoms, as viewed from the axial axis a) and from the equatorial axis b). Selected bond lengths (\AA) and angles ($^\circ$): $\text{Rh}-\text{C}_{\text{NHC}} = 2.037(2)$, $\text{Rh}-\text{N2A} = 2.089(2)$, $\text{Rh}-\text{COD}_{\text{transNHC}} = 2.213(3)/2.179(2)$, $\text{Rh}-\text{COD}_{\text{transN}} = 2.159(2)/2.122(2)$, $\text{C}_{\text{NHC}}-\text{Rh}-\text{N2A} = 85.37(8)$.

Another example of a pincer ligand that displayed an equilibrium between tridentate and bidentate coordination was reported by Goldberg *et al.*⁶³ The κ^3 bound PCO pincer complex in Scheme 2.21 was observed to be in equilibrium with a dimeric κ^2 bound complex. While the dimeric complex was present in <5 % abundance in solution, it was the only product that could be crystallised from the mixture.



Scheme 2.21

2.2.3.3 Synthesis of $[\text{Rh}(\text{NCN}^{\text{Et}})(\text{CO})_2]\text{BPh}_4$ (**2.10**)



Scheme 2.22

The complex $[\text{Rh}(\text{NCN}^{\text{Et}})(\text{CO})_2]\text{BPh}_4$ (**2.10**) was synthesised by displacement of the COD coligand from the complex $[\text{Rh}(\text{NCN}^{\text{Et}})(\text{COD})]\text{BPh}_4$ (**2.9**) under 1 atmosphere of CO (Scheme 2.22). When this reaction was performed in situ in acetone- d_6 displacement of the COD ligand could be clearly observed by replacement of coordinated COD resonances with those of free uncoordinated COD (Figure 2.17). The diastereotopic ethyl protons of **2.9** also resolved into a broad singlet at 5.10 ppm and a

triplet at 4.78 ppm ($^3J_{\text{HH}} = 5.7$ Hz). The broadness of the resonance at 5.10 ppm is consistent with a fluxional complex conformation. The observation of a single set of pyrazole resonances and only one singlet for the imidazole H^4 protons (7.17 ppm) indicates a plane of symmetry bisects the pincer ligand.

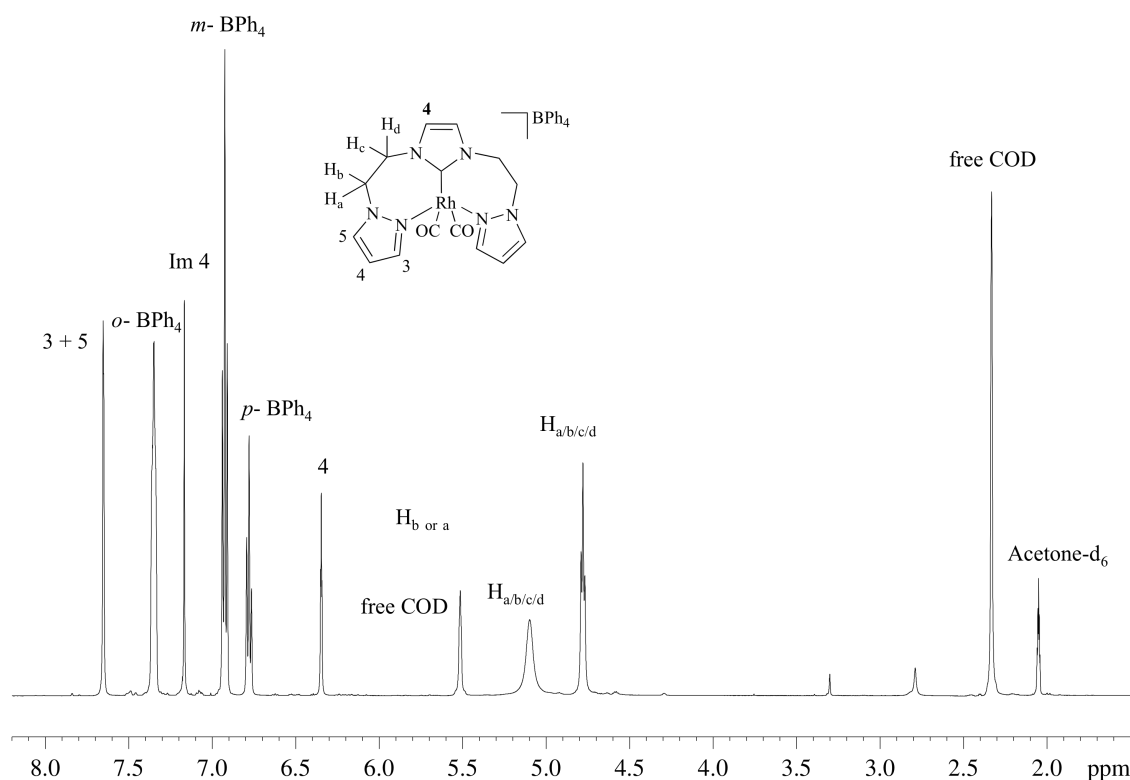


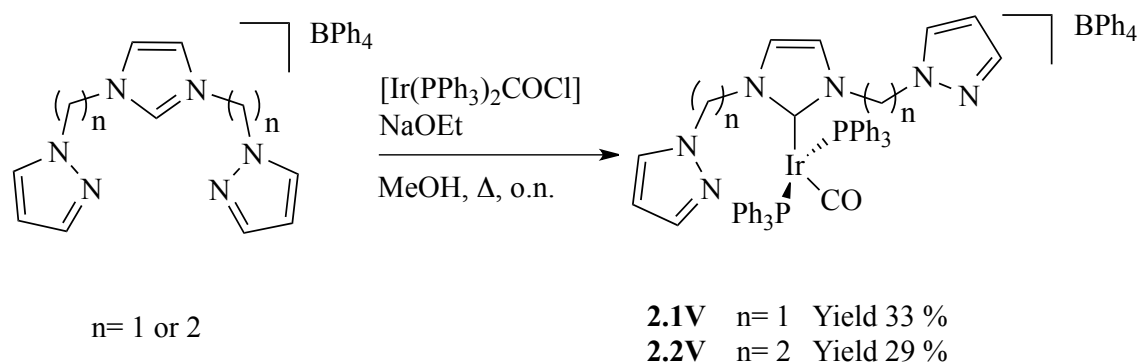
Figure 2.17: ^1H (500 MHz, acetone- d_6) NMR spectrum of $[\text{Rh}(\text{NCN}^{\text{Et}})(\text{CO})_2]\text{BPh}_4$ complex (**2.10**).

The presence of two CO groups was confirmed by IR spectroscopy ($\nu_{\text{CO}} = 2098$ and 2034 cm^{-1}). Unfortunately, $[\text{Rh}(\text{NCN}^{\text{Et}})(\text{CO})_2]\text{BPh}_4$ (**2.10**) was observed to decompose in the absence of a CO atmosphere precluding the isolation of this complex. A similar instability was also observed for the iridium dicarbonyl complex $[\text{Ir}(\text{NCN}^{\text{Me}})(\text{CO})_2]\text{BPh}_4$ (**2.7**).

This is a clear example of how the length of the alkyl chain between pyrazole and NHC donor groups can effect the reactivity of $[\text{Rh}(\text{NCN}^{\text{Me}})(\text{COD})]\text{BPh}_4$ (**2.3**) and $[\text{Rh}(\text{NCN}^{\text{Et}})(\text{COD})]\text{BPh}_4$ (**2.9**). While the dicarbonyl complex $[\text{Rh}(\text{NCN}^{\text{Et}})(\text{CO})_2]\text{BPh}_4$

(**2.10**) is formed upon reaction of **2.9** with CO, the unusual bimetallic complex $[\text{Rh}(\mu\text{-NCN}^{\text{Me}})(\text{CO})]_2(\text{BPh}_4)_2$ (**2.6**) is formed when the shorter methylene bridged ligand (NCN^{Me}) is present.

2.2.4 Synthesis of $[\text{Ir}(\text{NCN}^{\text{Me}})(\text{PPh}_3)_2(\text{CO})\text{BPh}_4]$ (**2.1V**) and $[\text{Ir}(\text{NCN}^{\text{Et}})(\text{PPh}_3)_2(\text{CO})]\text{BPh}_4$ (**2.2V**)



Scheme 2.23

The synthesis of complexes $[\text{IrNCN}^{\text{Me}}(\text{PPh}_3)_2(\text{CO})]\text{BPh}_4$ (**2.1V**) and $[\text{IrNCN}^{\text{Et}}(\text{PPh}_3)_2(\text{CO})]\text{BPh}_4$ (**2.2V**) was achieved by reaction of one equivalent of the ligand precursor $\text{NCN}^{\text{Me}}\cdot\text{HBPh}_4$ (**2.1**) or $\text{NCN}^{\text{Et}}\cdot\text{HBPh}_4$ (**2.2**) with one equivalent of Vaska's complex $[\text{Ir}(\text{PPh}_3)_2(\text{CO})\text{Cl}]$ and an excess of NaOEt in methanol under reflux. Both product **2.1V** and **2.2V** were isolated and recrystallized from thf/pentane to give bright yellow precipitates in each case.

For the NCN^{Et} containing complex **2.2V** the ^1H NMR spectrum (Figure 2.18) clearly indicated that two PPh_3 groups were retained on the complex (br multiplet, 30H, 7.52-7.37 ppm). The $^{31}\text{P}\{^1\text{H}\}$ NMR spectrum of **2.2V** also contained a singlet resonance at 21.8 ppm for the two chemically equivalent PPh_3 groups. The $^{13}\text{C}\{^1\text{H}\}$ NMR spectrum of complex **2.2V** supports the coordination of a carbonyl group to the Ir(I)

centre with a resonance observed at 176.6 ppm (t, $^2J_{\text{CP}} = 13.6$ Hz). The CO group was also identified in the IR spectrum as an intense band at 2002 cm^{-1} .

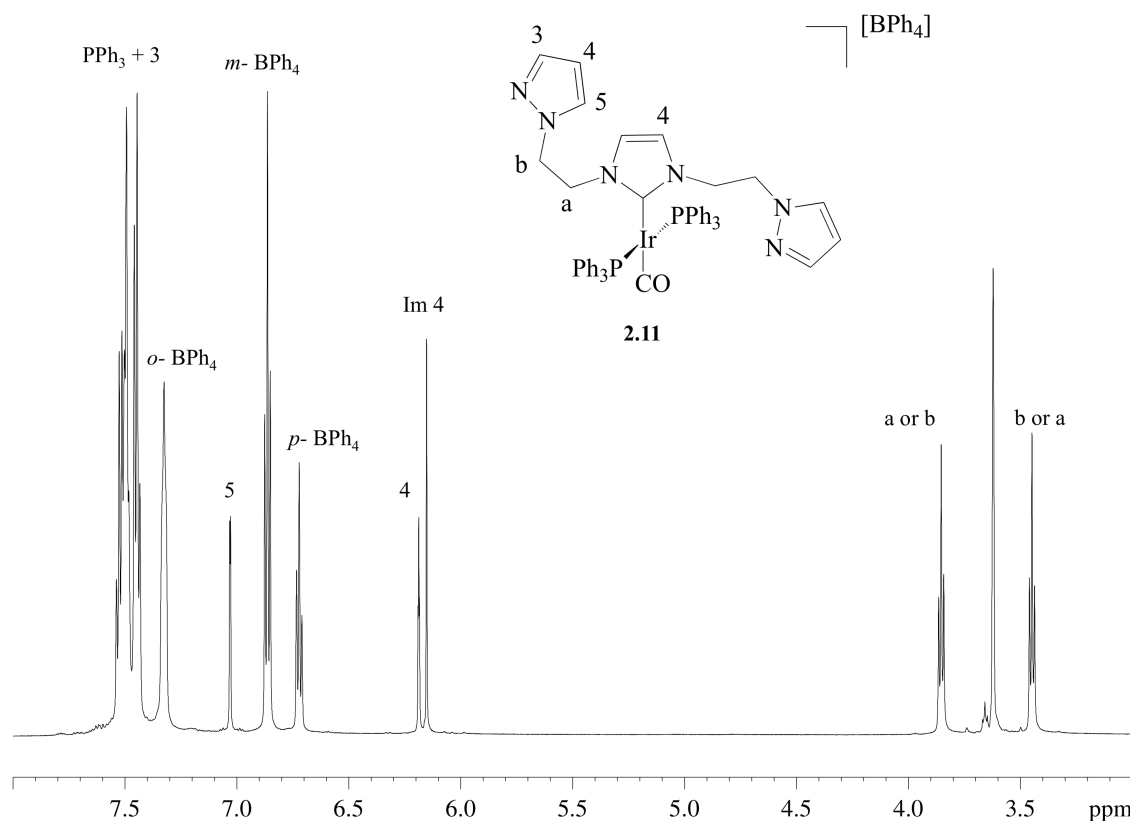


Figure 2.18: ^1H (400 MHz, THF-d_8) NMR spectrum of $[\text{IrNCN}^{\text{Et}}(\text{PPh}_3)_2(\text{CO})](\text{BPh}_4)$ complex (**2.1V**).

The spectral features of the NCN^{Me} containing complex **2.1V** were similar to **2.2V** ($^3\text{J}_{\text{PPH}_3} = 17.4$ ppm, $\text{CO} = 1997\text{ cm}^{-1}$). The ^1H NMR spectrum, however, showed considerable broadening, possibly due to restricted rotation of the Ir-NHC bond due to a closer proximity of the pyrazole groups to the bulky PPh_3 ligands.

2.2.4.1 Solid state structure of $[\text{Ir}(\text{NCN}^{\text{Me}})(\text{PPh}_3)_2(\text{CO})]\text{BPh}_4$ (**2.1V**)

An X-ray diffraction study on single crystals of $[\text{Ir}(\text{NCN}^{\text{Me}})(\text{PPh}_3)_2(\text{CO})]\text{BPh}_4$ (**2.1V**, Figure 2.18) showed a square planar coordination of the complex. The observed bond lengths are within the range expected for such ligands with very little distortion

observed on the complex geometry ($P_{1A}-Ir-C_{NHC}= 92.56(5)$, $P_{1B}-Ir-C_{NHC}= 90.05(5)$). The iridium-carbene bond length is also within the range of monodentate carbene iridium complexes⁵⁹ measuring $2.0711(19)$ Å.

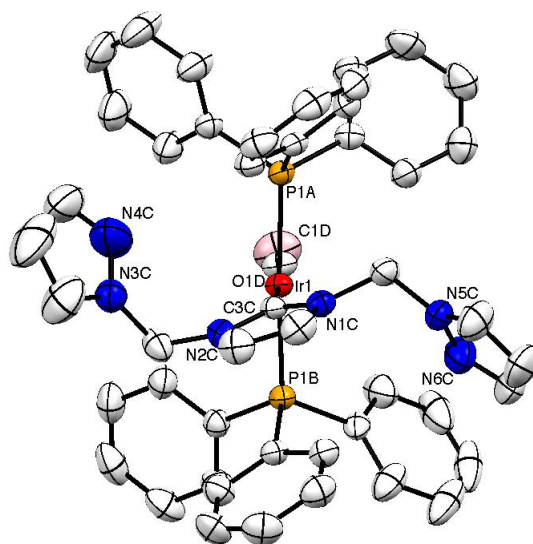


Figure 2.19: ORTEP diagram of the cationic fragment of complex $[Ir(NCN^{Me})(PPh_3)_2(CO)]BPh_4$ (**2.1V**), with 40% probability ellipsoids for the non hydrogen atoms, as viewed from the equatorial axis. Selected bond lengths (Å) and angles ($^\circ$): $Ir-C_{NHC}= 2.0711(19)$, $Ir-CO= 1.863(2)$, $Ir-P_{1A}= 2.3240(5)$, $Ir-P_{1B}= 2.3416(5)$, $P_{1A}-Ir-C_{NHC}= 92.56(5)$, $P_{1B}-Ir-C_{NHC}= 90.05(5)$.

2.3 Summary and conclusions

Two new pincer ligand precursors $NCN^{Me}.HBPh_4$ (**2.1**) and $NCN^{Et}.HBPh_4$ (**2.2**) were successfully synthesised. The coordination chemistry of the N-heterocyclic carbene derivatives NCN^{Me} and NCN^{Et} with rhodium(I) and iridium(I) was explored. The binding mode of these ligands was shown to be dependent on the nature of the metal centre (Rh or Ir), the length of the alkyl chain linking the NHC and pyrazole donor groups (methyl or ethyl) and the nature of the complex co-ligands (COD, CO or PPh_3). Some of the divergent coordination properties are described below:

- In the solid state structure of $[\text{Rh}(\text{NCN}^{\text{Me}})(\text{COD})]\text{BPh}_4$ (**2.3**) the methylene linked ligand NCN^{Me} coordinates in a facial κ^3 -manner. In contrast, the solid state structure of $[\text{Rh}(\text{NCN}^{\text{Et}})(\text{COD})]\text{BPh}_4$ (**2.9**) contains the ethylene linked ligand NCN^{Et} coordinated in a chelating κ^2 -manner.
- Upon carbonylation of $[\text{Rh}(\text{NCN}^{\text{Me}})(\text{COD})]\text{BPh}_4$ (**2.3**) the dimeric complex $[\text{Rh}(\text{NCN}^{\text{Me}})(\text{CO})_2](\text{BPh}_4)_2$ (**2.6**) is formed where the NCN^{Me} ligand bridges the two Rh centres in an unusual κ^2/κ^1 coordination mode. However, upon carbonylation of $[\text{Rh}(\text{NCN}^{\text{Et}})(\text{COD})]\text{BPh}_4$ (**2.9**) or the analogous iridium complex $[\text{Ir}(\text{NCN}^{\text{Me}})(\text{COD})]\text{BPh}_4$ (**2.4**), then the monomeric dicarbonyl complexes $[\text{Rh}(\text{NCN}^{\text{Et}})(\text{CO})_2]\text{BPh}_4$ (**2.10**) and $[\text{Ir}(\text{NCN}^{\text{Me}})(\text{CO})_2]\text{BPh}_4$ (**2.7**) are formed with κ^3 coordination of the pincer ligand.
- In a reaction of the methylene linked ligand NCN^{Me} with $[\text{Ir}(\mu\text{-Cl})\text{COD}]_2$ the κ^3 pincer coordinated complex $[\text{Ir}(\text{NCN}^{\text{Me}})(\text{COD})]\text{BPh}_4$ (**2.4**) is formed as the major product. Whereas upon reaction of the ethylene linked ligand NCN^{Et} with $[\text{Ir}(\mu\text{-Cl})\text{COD}]_2$ only the bis-NHC product $[\text{Ir}(\text{NCN}^{\text{Me}})_2(\text{COD})]\text{BPh}_4$ (**2.5**) could be isolated, where the two NCN^{Et} ligands coordinate to Ir in a κ^1 fashion through the NHC donor only.
- When strongly coordinating co-ligands such as PPh_3 are used then only monodentate (κ^1) coordination of the pincer ligands is obtained, as was observed in $[\text{Ir}(\text{NCN}^{\text{Me}})(\text{PPh}_3)_2(\text{CO})]\text{BPh}_4$ (**2.1V**) and $[\text{Ir}(\text{NCN}^{\text{Et}})(\text{PPh}_3)_2(\text{CO})]\text{BPh}_4$ (**2.2V**)

Subsequent work looking at how these diverse structures and coordination properties impact the catalytic activity of these complexes is described in Chapter 3.

2.4 References

- (1) Moulton, C. J.; Shaw, B. L. *J. Chem. Soc., Dalton Trans.* **1976**, 1020.
- (2) Dahlhoff, W. V.; Nelson, S. M. *J. Chem. Soc. A* **1971**, 2184.
- (3) Poverenov, E.; Gandelman, M.; Shimon, L. J. W.; Rozenberg, H.; Ben-David, Y.; Milstein, D. *Organometallics* **2005**, *24*, 1082.
- (4) Beleaga, A.; Bojan, V. R.; Pollnitz, A.; Rat, C. I.; Silvestru, C. *Dalton Trans.* **2011**, *40*, 8830.
- (5) Albrecht, M.; Gossage, R. A.; Spek, A. L.; van Koten, G. *J. Am. Chem. Soc.* **1999**, *121*, 11898.
- (6) Ionkin, A. S.; Marshall, W. J.; Adelman, D. J.; Shoe, A. L.; Spence, R. E.; Xie, T. *Journal of Polymer Science Part A: Polymer Chemistry* **2006**, *44*, 2615.
- (7) Hollas, A. M.; Gu, W.; Bhuvanesh, N.; Ozerov, O. V. *Inorg. Chem.* **2011**, *50*, 3673.
- (8) Gnanaprakasam, B.; Zhang, J.; Milstein, D. *Angew. Chem., Int. Ed.* **2010**, *49*, 1468.
- (9) Leis, W.; Mayer, H. A.; Kaska, W. C. *Coord. Chem. Rev.* **2008**, *252*, 1787.
- (10) Kossoy, E.; Rybtchinski, B.; Diskin-Posner, Y.; Shimon, L. J. W.; Leituss, G.; Milstein, D. *Organometallics* **2008**, *28*, 523.
- (11) Winston, M. S.; Bercaw, J. E. *Organometallics* **2010**, *29*, 6408.
- (12) Sokolov, V. I.; Bulygina, L. A. *Russ. Chem. Bull.* **2004**, *53*, 2355.
- (13) Baber, R. A.; Bedford, R. B.; Betham, M.; Blake, M. E.; Coles, S. J.; Haddow, M. F.; Hursthouse, M. B.; Orpen, A. G.; Pilarski, L. T.; Pringle, P. G.; Wingad, R. L. *Chem. Commun.* **2006**, 3880.
- (14) Bedford, R. B.; Chang, Y.-N.; Haddow, M. F.; McMullin, C. L. *Dalton Trans.* **2011**, *40*, 9034.

-
- (15) Romain, C.; Brelot, L.; Bellemin-Laponnaz, S. p.; Dagorne, S. *Organometallics* **2010**, *29*, 1191.
- (16) Page, M. J.; Wagler, J. r.; Messerle, B. A. *Organometallics* **2010**, *29*, 3790.
- (17) Bassetti, M.; Capone, A.; Mastrofrancesco, L.; Salamone, M. *Organometallics* **2003**, *22*, 2535.
- (18) Danopoulos, A. A.; Tsoureas, N.; Wright, J. A.; Light, M. E. *Organometallics* **2003**, *23*, 166.
- (19) Wong, C.-Y.; Lai, L.-M.; Pat, P.-K.; Chung, L.-H. *Organometallics* **2010**, *29*, 2533.
- (20) Raynal, M.; Pattacini, R.; Cazin, C. S. J.; Vallée, C.; Olivier-Bourbigou, H.; Braunstein, P. *Organometallics* **2009**, *28*, 4028.
- (21) Zuo, W.; Braunstein, P. *Organometallics* **2011**, *31*, 2606.
- (22) Caballero, A.; Díez-Barra, E.; Jalón, F. A.; Merino, S.; Tejeda, J. J. *Organomet. Chem.* **2001**, *617–618*, 395.
- (23) Yao, Q.; Kinney, E. P.; Zheng, C. *Org. Lett.* **2004**, *6*, 2997.
- (24) Benito-Garagorri, D.; Kirchner, K. *Acc. Chem. Res.* **2008**, *41*, 201.
- (25) Albrecht, M.; van Koten, G. *Angew. Chem., Int. Ed.* **2001**, *40*, 3750.
- (26) Benito-Garagorri, D.; Kirchner, K. *Acc. Chem. Res.* **2008**, *41*, 201.
- (27) Chuchuryukin, A. V.; Huang, R.; van Faassen, E. E.; van Klink, G. P. M.; Lutz, M.; Chadwick, J. C.; Spek, A. L.; van Koten, G. *Dalton Trans.* **2011**, *40*, 8887.
- (28) Huff, C. A.; Kampf, J. W.; Sanford, M. S. *Organometallics* **2012**, *31*, 4643.
- (29) Jing Zhang, E. B., Gregory Leitus, and David Milstein *Organometallics* **2011** *30* 5716.
- (30) Gunanathan, C.; Ben-David, Y.; Milstein, D. *Science* **2007**, *317*, 790.
- (31) del Pozo, C.; Iglesias, M.; Sánchez, F. I. *Organometallics* **2011**, *30*, 2180.

- (32) Schaub, T.; Radius, U.; Diskin-Posner, Y.; Leitus, G.; Shimon, L. J. W.; Milstein, D. *Organometallics* **2008**, *27*, 1892.
- (33) Kozlov, V. A.; Aleksanyan, D. V.; Korobov, M. V.; Avramenko, N. V.; Aysin, R. R.; Maloshitskaya, O. A.; Korlyukov, A. S.; Odinet, I. L. *Dalton Trans.* **2011**, *40*, 8768.
- (34) Kozlov, V. A.; Aleksanyan, D. V.; Nelyubina, Y. V.; Lyssenko, K. A.; Petrovskii, P. V.; Vasil'ev, A. A.; Odinet, I. L. *Organometallics* **2011**, *30*, 2920.
- (35) van der Boom, M. E.; Milstein, D. *Chem. Rev.* **2003**, *103*, 1759.
- (36) Bassetti, M.; Capone, A.; Salamone, M. *Organometallics* **2004**, *23*, 247.
- (37) Wehman-Ooyevaar, I. C. M. K.; Grove, D. M.; Smeets, W. J. J.; Spek, A. L.; van Koten, G. *J. Chem. Soc., Dalton Trans.* **1994**, *0*, 703.
- (38) Canovese, L.; Visentin, F.; Chessa, G.; Uguagliati, P.; Santo, C.; Bandoli, G.; Maini, L. *Organometallics* **2003**, *22*, 3230.
- (39) van Koten, G.; Gebbink, R. J. M. K. *Dalton Trans.* **2011**, *40*, 8731.
- (40) Díez-González, S.; Marion, N.; Nolan, S. P. *Chem. Rev.* **2009**, *109*, 3612.
- (41) Zinn, F. K.; Viciu, M. S.; Nolan, S. P. *Annu. Rep. Prog. Chem., Sect. "B"* **2004**, *100*, 231.
- (42) Gründemann, S.; Albrecht, M.; Loch, J. A.; Faller, J. W.; Crabtree, R. H. *Organometallics* **2001**, *20*, 5485.
- (43) Theodore, R. H.; Hollis, T. K.; Edward, J. V. *Organometallics* **2012**, *31*, 3002.
- (44) Lv, K.; Cui, D. *Organometallics* **2010**, *29*, 2987.
- (45) Pugh, D.; Danopoulos, A. A. *Coord. Chem. Rev.* **2007**, *251*, 610.
- (46) Romain, C.; Miqueu, K.; Sotiropoulos, J.-M.; Bellemin-Laponnaz, S.; Dagorne, S. *Angew. Chem., Int. Ed.* **2010**, *49*, 2198.

-
- (47) Romain, C.; Brelot, L.; Bellemin-Laponnaz, S. p.; Dagorne, S. *Organometallics* **2010**, *29*, 1191.
- (48) Iwasaki, F.; Manabe, N.; Nishiyama, H.; Takada, K.; Yasui, M.; Kusamiya, M.; Matsumura, N. *Bull. Chem. Soc. Jpn.* **1997** *70*, 1267.
- (49) Duan, W.-L.; Shi, M.; Rong, G.-B. *Chem. Commun.* **2003**, 2916.
- (50) Iwasaki, F.; Yasui, M.; Yoshida, S.; Nishiyama, H.; Shimamoto, S.; Matsumura, N. *Bull. Chem. Soc. Jpn.* **1996**, *69*, 2759.
- (51) Gischig, S.; Togni, A. *Eur. J. Inorg. Chem.* **2005**, *2005*, 4745.
- (52) Steinke, T.; Shaw, B. K.; Jong, H.; Patrick, B. O.; Fryzuk, M. D. *Organometallics* **2009**, *28*, 2830.
- (53) Zeng, J. Y.; Hsieh, M.-H.; Lee, H. M. *J. Organomet. Chem.* **2005**, *690*, 5662.
- (54) Shaw, B. K.; Patrick, B. O.; Fryzuk, M. D. *Organometallics* **2012**, *31*, 783.
- (55) Hill, A. F.; McQueen, C. M. A. *Organometallics* **2012**, *31*, 8051.
- (56) Fliedel, C.; Sabbatini, A.; Braunstein, P. *Dalton Trans.* **2010**, *39*, 8820.
- (57) Chen, C.; Qiu, H.; Chen, W. *J. Organomet. Chem.* **2012**, *696*, 4166.
- (58) Newman, P.; Cavell, K.; Hallett, A.; Kariuki, B. *Dalton Trans.* **2011**, *40*, 8807.
- (59) Frey, G. D.; Rentzsch, C. F.; von Preysing, D.; Scherg, T.; Mühlhofer, M.; Herdtweck, E.; Herrmann, W. A. *J. Organomet. Chem.* **2006**, *691*, 5725.
- (60) DeHaven, P. W.; Goedken, V. L. *Inorg. Chem.* **1979**, *18*, 827.
- (61) Gordon, G. C.; DeHaven, P. W.; Weiss, M. C.; Goedken, V. L. *J. Am. Chem. Soc.* **1978**, *100*, 1003.
- (62) Yamamoto, Y.; Wakatsuki, Y.; Yamazaki, H. *Organometallics* **1983**, *2*, 1604.
- (63) Fulmer, G. R.; Kaminsky, W.; Kemp, R. A.; Goldberg, K. I. *Organometallics* **2011**, *30*, 1627.

*Catalysis with Pincer
Complexes*

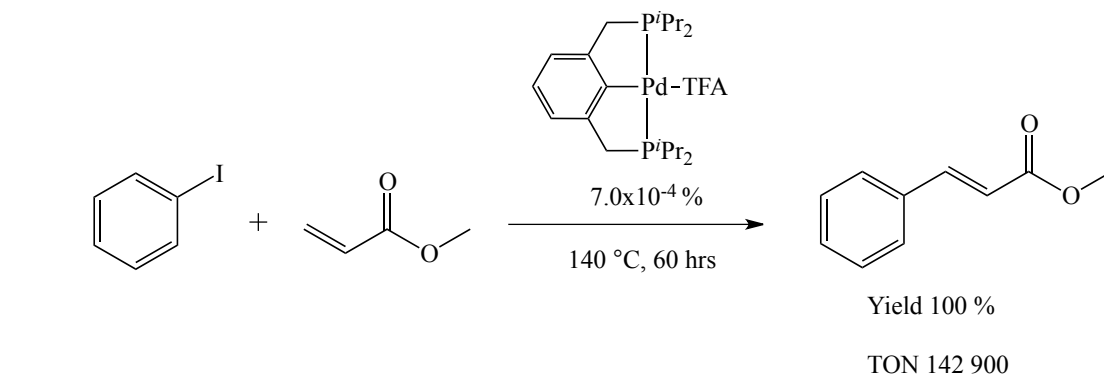
3.1 Introduction

3.1.1 Reactivity of pincer complexes

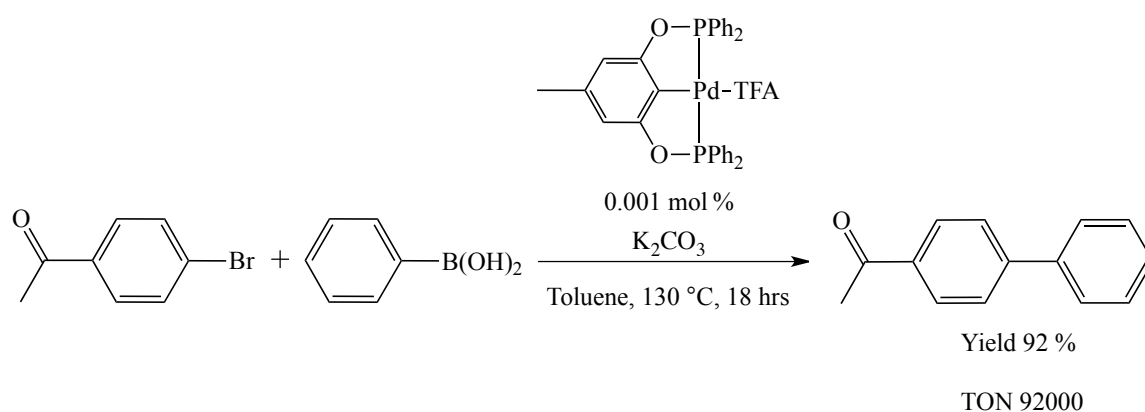
In organometallic catalysis pincer ligands have attracted much attention due to the stability they are able to confer to a metal complex, their compatibility with a wide range of metal atoms and their structural versatility, which makes their steric and electronic properties easily tuneable over a wide range of functional groups.¹ Numerous studies have revealed a diverse reactivity for pincer bound complexes that have led to the application of pincer complexes in numerous catalytic reactions.²⁻⁵

3.1.2 Pincer complexes in catalysis

Pincer complexes have been used as catalysts in a huge variety of organic transformations. One of the first pincer complexes used in catalysis, synthesised in 1976 by Shaw *et al.*,⁶ consisted of an aromatic-PCP ligand coordinated to a palladium metal centre and since then palladium in combination with aromatic-ECE (E= P, S, N) pincer ligands has been the most widely investigated pincer motif for catalysis. Palladium PCP pincer complexes have proved to be particularly effective catalysts for the coupling of aryl halides to olefins and aryl boronic acids, in the Heck⁷ (Scheme 3.1 a) and Suzuki⁸ (Scheme 3.1 b) reactions respectively.⁹ These catalysts are notable for their high turnover numbers and their resistance to degradation at high temperature during catalysis.



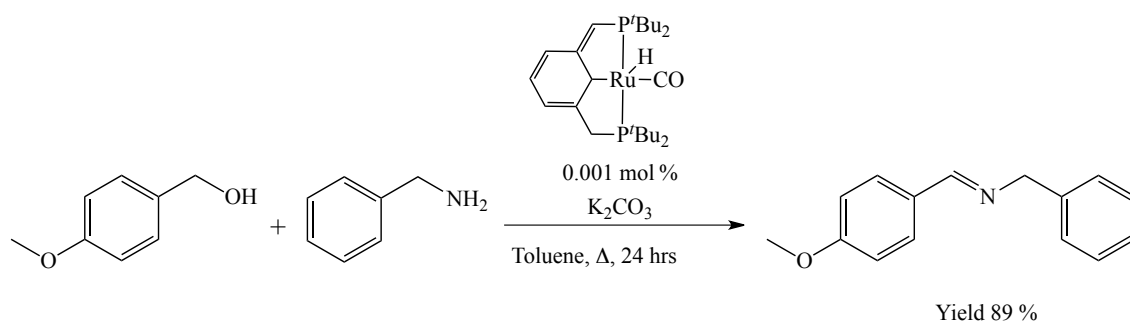
a)



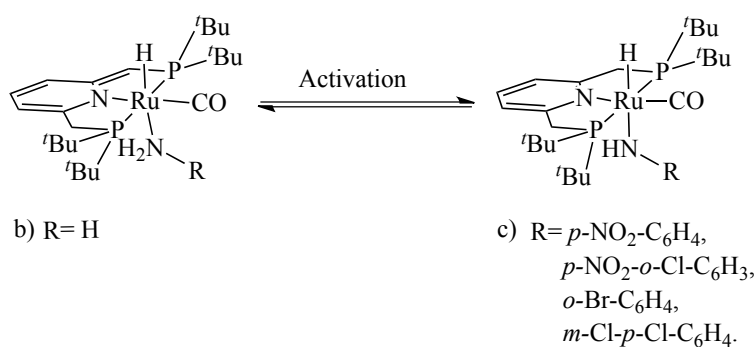
b)

Scheme 3.1

Ruthenium pincer complexes have also received considerable attention, particularly by Milstein and co-workers. Milstein *et al.* were responsible for the development of pyridyl centred PNP and PNN ruthenium complexes, which proved to be very active catalysts for a range of novel transformations, such as the dehydrogenative coupling of alcohols to form esters,¹⁰ amides¹¹ and imines¹² (Scheme 3.2 a) as well as the NH activation of amines. A key factor in the reactivity of these systems was attributed to the non-innocent nature of the PNP and PNN ligands which undergo an aromatization/dearomatization cycle of the aromatic backbone (Scheme 3.2 b).¹³⁻¹⁵



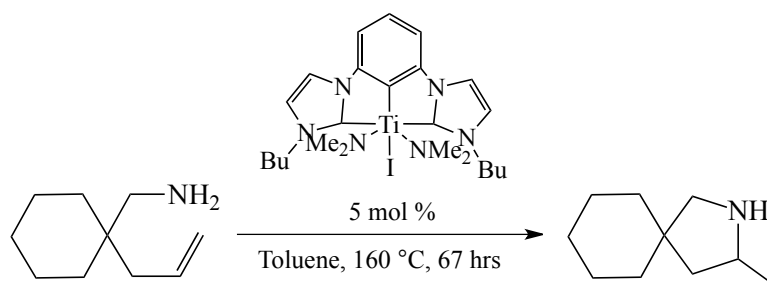
a)



b)

Scheme 3.2

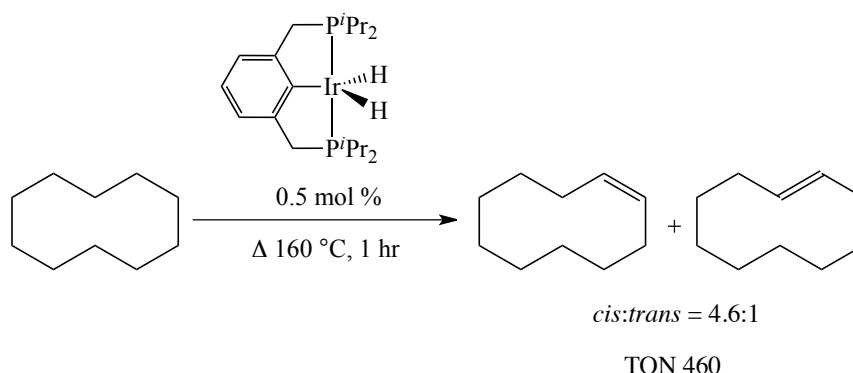
A diverse range of rare earth and early transition metal pincer complexes have also been investigated as catalysts. Lanthanide bis-carbene CCC pincer complexes were successfully applied in the highly selective polymerisation of isoprene, where exceptional thermal stabilities were exhibited.¹⁶⁻¹⁸ Analogous CCC pincer complexes of the group 4 metals (Scheme 3.3) have proved to be active catalysts for the intra-molecular hydroamination of amino alkenes, although very high reaction temperatures (up to 160 °C) and long reaction times (up to 90 hours) were required.¹⁹



Scheme 3.3

3.1.2.1 Ir and Rh complexes with pincer ligands

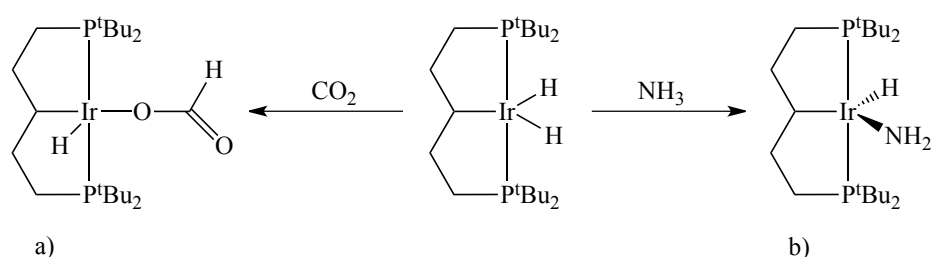
Rhodium and iridium pincer complexes have proven to be exceptionally robust catalysts capable of activating highly unreactive bonds. The Iridium PCP complex [IrPCP^{iPr}(H)₂] (Scheme 3.4 a), for example, was the first catalyst to demonstrate the efficient dehydrogenation of an alkane in the absence of a H₂ acceptor.^{20,21} The related PCP Rh pincer complex on the other hand, is an efficient catalyst for the Kumada coupling of aryl halides with aryl Grignards.²² This reaction was shown to proceed via a reactive Rh(I) intermediate which oxidatively cleaves the Ar-X bond.



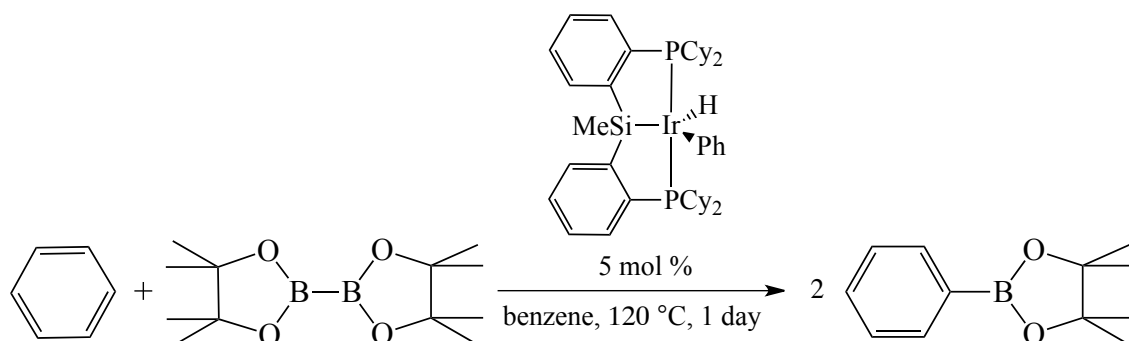
Scheme 3.4

Rh and Ir pincer complexes containing a more electron donating aliphatic alkylidene backbone were synthesised and noted for the activation of small molecules, such as CO₂ (Scheme 3.5 a).²³ Hartwig *et al.* also reported the oxidative addition of the N-H bond of

ammonia to an iridium (I) complex containing an aliphatic pincer ligand (Scheme 3.5 b). This achievement has the potential to lead to the use of ammonia as a starting material in catalytic hydroamination reactions.^{24,25} A similar result was later achieved using a silyl centred PSiP iridium complex,²⁶ while its hydride-phenyl derivative (Scheme 3.6) was shown to catalyse the borylation of benzene via cleavage of an unreactive aryl C-H bond.²⁷

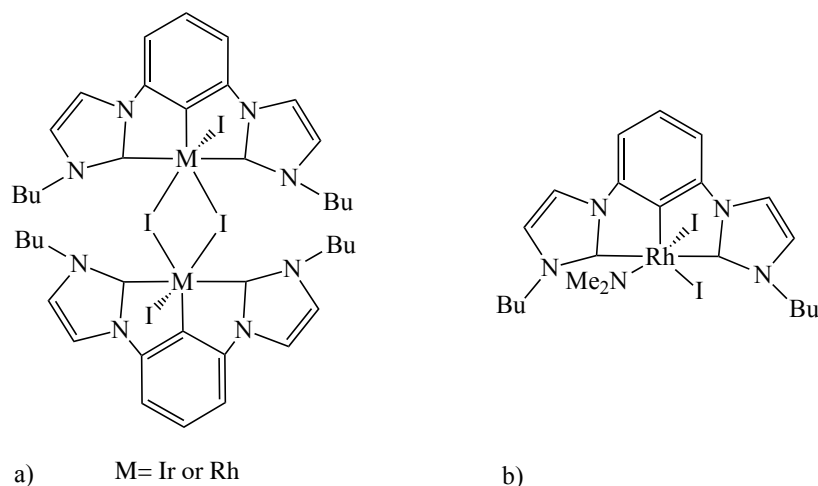


Scheme 3.5



Scheme 3.6

Rh and Ir complexes containing bis-NHC CCC pincer ligands (Scheme 3.7) have been synthesised and applied as highly active catalysts for a variety of transformations, such as the intra-molecular hydroamination of amino alkenes,²⁸ the hydrosilylation of alkynes (Scheme 3.7 b),²⁹ and the dehydrogenation of alkanes.³⁰



Scheme 3.7

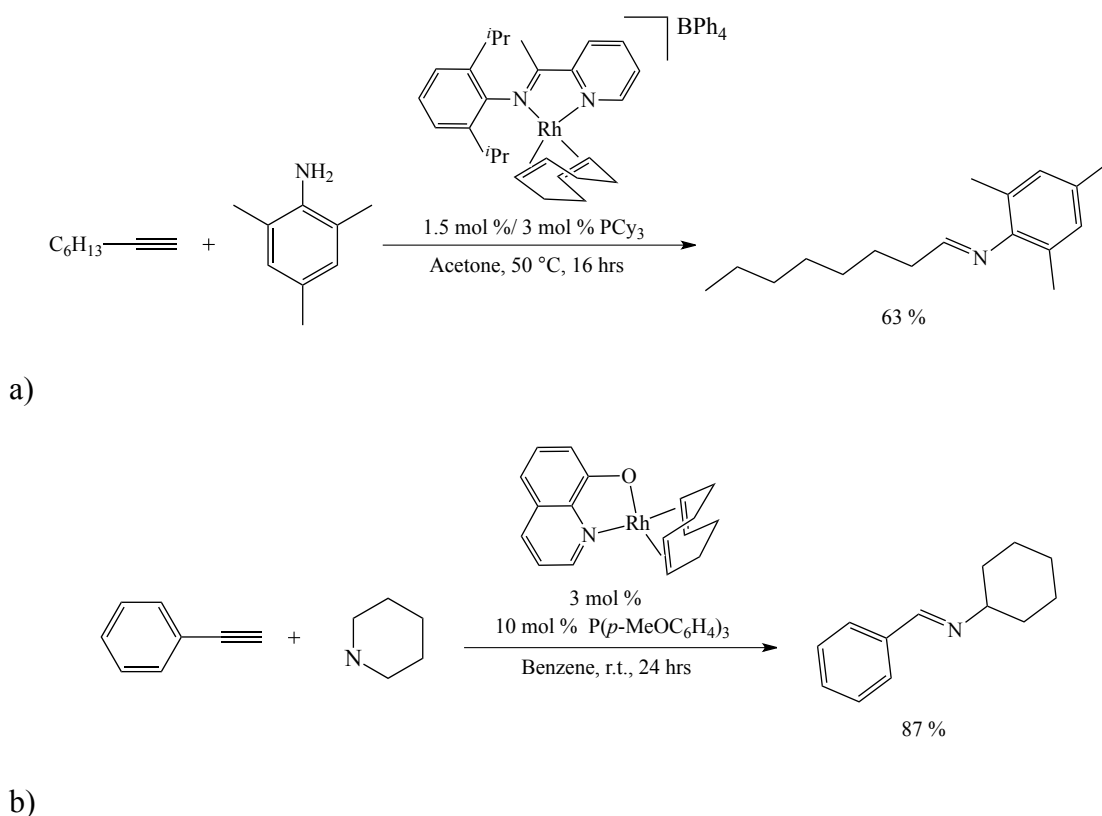
3.1.3 Iridium and rhodium catalysed addition of X-H bonds to alkynes

The development of catalysts that facilitate the addition of X-H bonds across the $C\equiv C$ triple bond of an alkyne is an important challenge in modern synthetic chemistry. This reaction is a highly atom economical method towards the synthesis of new X-C bonds, leading to the formation of no wasteful by-products. It is also a fundamental tool for the synthesis of many valuable complex organic molecules (see section 1.8, Chapter 1). Iridium and rhodium catalysts have proven to be particularly effective at facilitating the activation of alkynes towards X-H bond addition. The effectiveness of Rh and Ir metal complexes at catalysing the hydroamination (X= N), hydroalkoxylation (X= O) and hydrosilylation (X= Si) reactions is described below.

3.1.3.1 Hydroamination

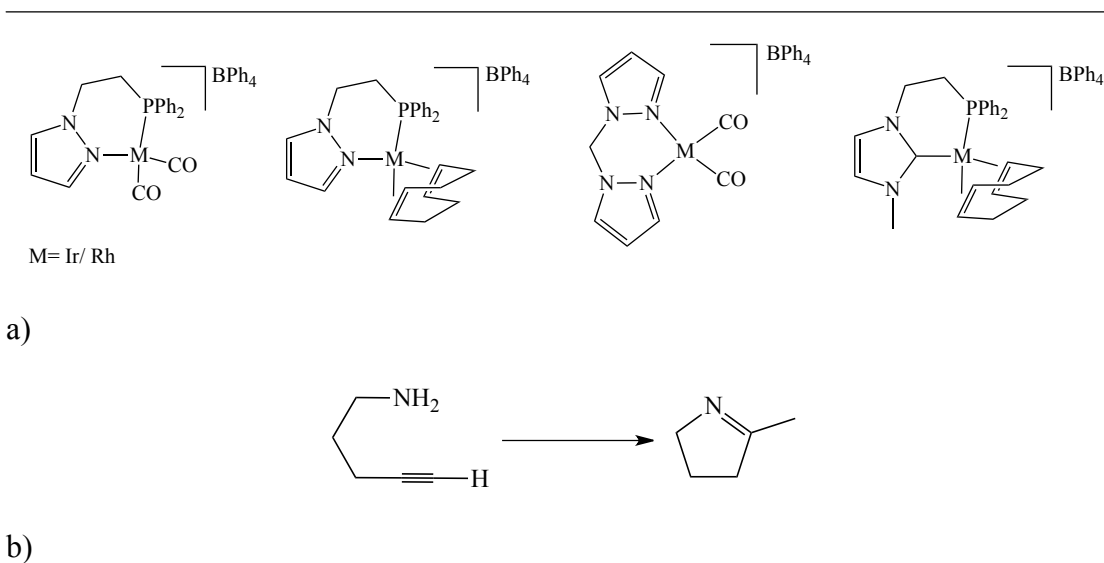
In 2001 a simple *in situ* generated catalyst formed by combining $[Rh(COD)_2]BF_4$ and PCy_3 was found to facilitate the inter-molecular hydroamination of terminal alkynes and anilines under mild conditions.³¹ Related Rh(I)COD catalysts containing neutral pyridyl-imine³² (Scheme 3.8 a) or anionic phenoxy-quinoline³³ (Scheme 3.8 b) ligands

have also been used for the inter-molecular hydroamination of terminal alkynes. The phenoxy-quinoline containing complex, in analogy with the $[\text{Rh}(\text{COD})_2]\text{BF}_4$ system, was effective at catalysing this reaction upon the addition of excess phosphine ligand to the solution.



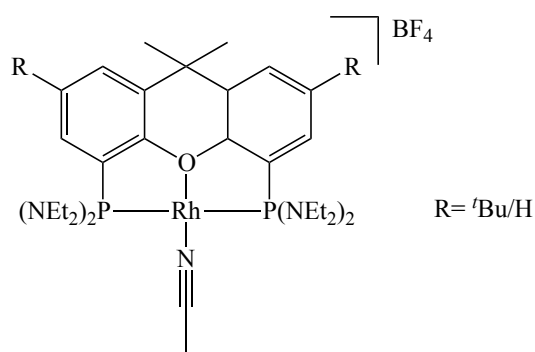
Scheme 3.8

Messerle *et al.* have developed a series of Ir(I) and Rh(I) catalysts featuring a selection of bidentate ligands containing nitrogen, phosphorus and N-heterocyclic carbene donor groups with COD and CO co-ligands (Scheme 3.9 a).³⁴⁻³⁶ These complexes were shown to efficiently catalyse the intra-molecular hydroamination reaction of 4-pentyn-1-amine (Scheme 3.9 b).



Scheme 3.9

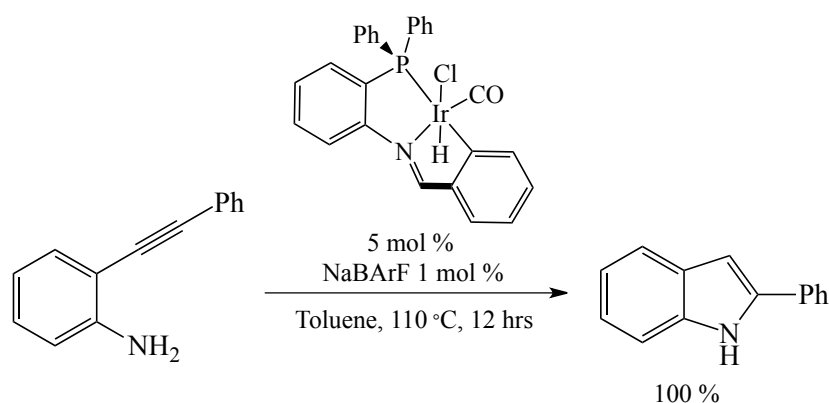
An in situ generated catalyst formed from combining $[\text{Rh}(\text{COD})(\text{MeCN})_2]\text{BF}_4$ and Xantphos ligands was effective at catalysing the cyclisation of amino-alkenes.³⁷ The Xantphos ligand in this system was shown to bind to rhodium in a POP pincer fashion (Scheme 3.10).



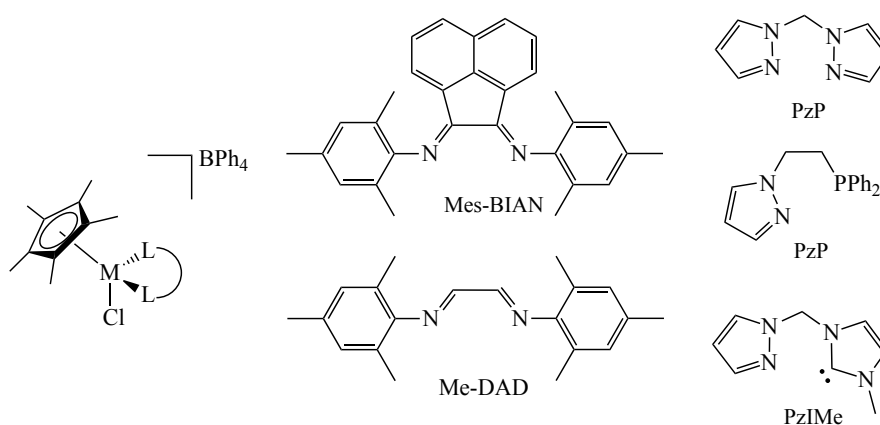
Scheme 3.10

An Ir(III) pincer catalyst containing a cyclometallated PNC ligand (Scheme 3.11) was found to be effective for the intra-molecular hydroamination of 2-alkynylanilines to yield indoles. This catalyst was only found to be effective upon abstraction of the chloride ligand via addition of NaBARF to the reaction.³⁸ Messerle *et al.* have also

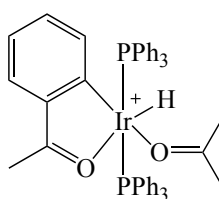
shown that halide abstraction is essential for generating an active catalyst when Ir(III) and Rh(III) Cp* catalysts (Scheme 3.12) are used for the same reaction.³⁹ Alternatively Crabtree *et al.* demonstrated that a cationic Ir(III) complex containing a weakly coordinating acetone ligand (Scheme 3.13) gave excellent hydroamination efficiencies without the need for any additives.⁴⁰



Scheme 3.11



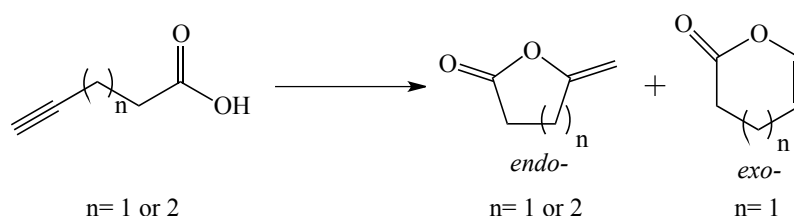
Scheme 3.12



Scheme 3.13

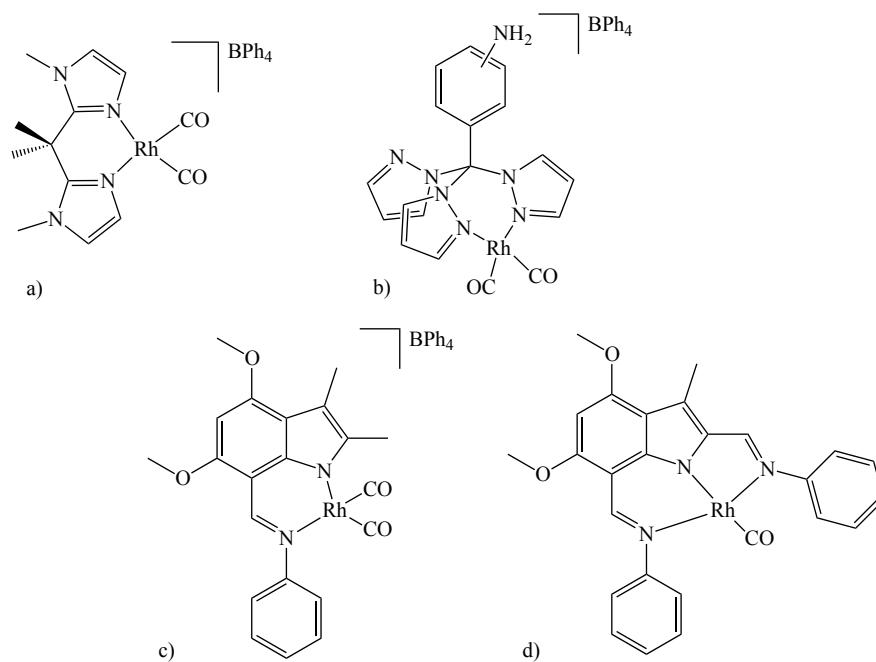
3.1.3.2 Hydroalkoxylation

a) Cyclisation of alkynoic acids

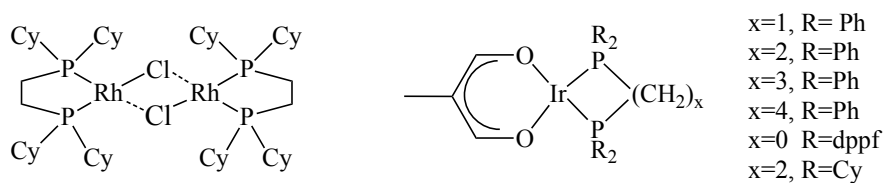


Scheme 3.14

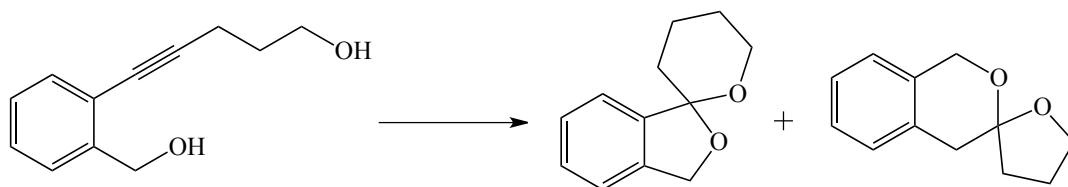
A number of Rh(I) and Ir(I) catalysts have been used for the cyclisation of alkynoic acids. Messerle *et al.* have utilised Rh(I)(CO)₂ catalysts containing a variety of multitopic *N*-donor ligands (Scheme 3.14) for the cyclisation of 4-pentynoic and 5-hexynoic acid. The *bis*(imidazolyl)methane complex (Scheme 3.15 a) was relatively slow achieving only 88% conversion for the cyclisation of 4-pentynoic acid after 15.5 hours at 50 °C and 0.35 mol% catalyst.⁴¹ In comparison the complexes containing a third unbound *N*-donor group pendent to the chelate (Scheme 3.15 b) were slower catalysts, possibly via in situ κ^3 -coordination of the ligand inhibiting substrate coordination.⁴² The indolide complex (Scheme 3.15 c) was also a relatively efficient catalyst for the cyclisation of 4-pentynoic acid, achieving >95 % conversion after 3 hours at 65 °C and 2 mol% catalyst. The analogous κ^3 -pincer complex (Scheme 3.15 d) achieved only 61 % conversion after 20 hours.⁴³

**Scheme 3.15**

The Rh(I)⁴⁴ and Ir(I)⁴⁵ phosphine containing systems (Scheme 3.16) were also reported to facilitate this reaction achieving quantitative conversion under mild conditions (24 hours, room temperature, 5 mol% catalyst).

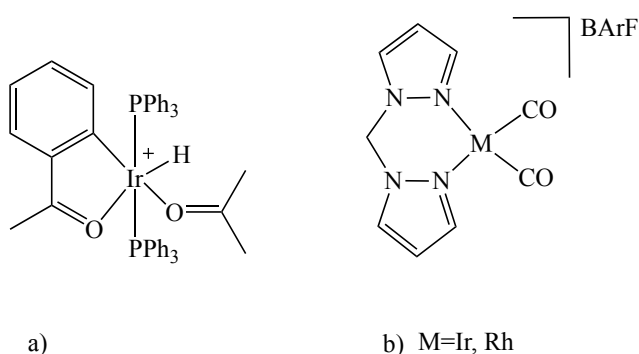
**Scheme 3.16**

b) Dihydroalkoxylation of alkyne diols



Scheme 3.17

Many of the same systems found to be effective for the intra-molecular hydroamination of alkynyl amines have also been applied as catalysts for the hydroalkoxylation of alkynols. For example, the cyclometallated Ir(III) complex (Scheme 3.18 a) reported by Crabtree *et al.*⁴⁰ was found to be an excellent catalyst for the cyclisation of a series of 2-alkynylbenzyl alcohols, while Rh(I) and Ir(I) complexes of the type $[M(\text{bpm})(\text{CO})_2]\text{BArF}$ ($M=\text{Rh}, \text{Ir}$) (Scheme 3.18 b), reported by Messerle *et al.*,⁴⁶ were highly efficient catalysts for the dihydroalkoxylation of alkynediols.

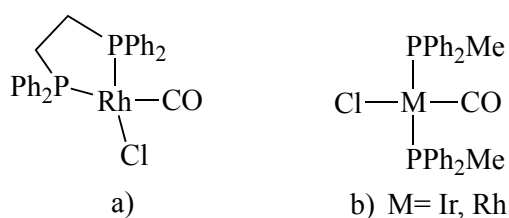


Scheme 3.18

3.1.3.3 Hydrosilylation

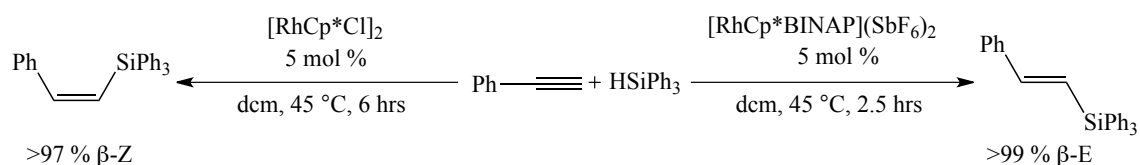
One of the earliest Rh and Ir catalyst systems used for the hydrosilylation of acetylenes

was reported by Field and Ward in 2003.⁴⁷ They used neutral Ir(I) and Rh(I) complexes, containing either a chelating dppe ligand (Scheme 3.19 a) or two monodentate PPh₂Me ligands (Scheme 3.19 b), for the hydrosilylation of both phenylacetylene and 1-phenylpropyne using Et₃SiH. The [Rh(dppe)(CO)Cl] complex was the most active of the series particularly for the hydrosilylation of 1-phenylpropyne where it gave complete conversion after 20 hours at 65 °C and 2 mol% catalyst. This is in contrast to the PPh₂Me analogue, which was entirely inactive under the same conditions.



Scheme 3.19

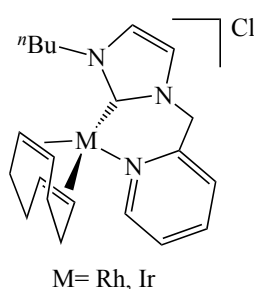
An elegant example of how catalyst regioselectivity can be tuned by the correct choice of ligand was described by Faller *et al.* (Scheme 3.20).⁴⁸ Whereas the dimeric Rh complex [RhCp*Cl]₂ gave almost exclusively the β-Z isomer upon hydrosilylation of phenylacetylene with Ph₃SiH the BINAP (2,2'-bis(diphenylphosphino)-1,1'-binaphthyl) containing complex [RhCp*BINAP](SbF₆)₂ gave almost exclusively the β-E isomer.



Scheme 3.20

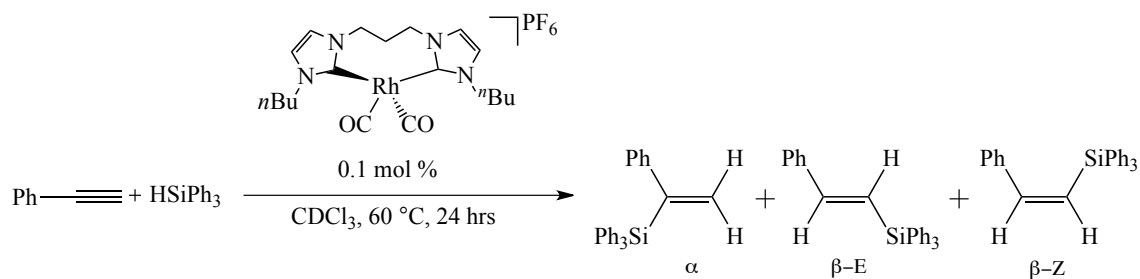
The cationic Ir and Rh complexes containing a mixed donor NHC-pyridyl chelate

(Scheme 3.21) were also investigated as catalysts for the hydrosilylation of phenylacetylene.⁴⁹ The Rh compound (5 mol %) was found to be the more effective catalyst achieving 86% conversion after 24 hours at room temperature, with a surprisingly high regioselectivity for the β -Z product (β -E: β -Z: α = 0:95:5). The analogous Ir compound (5 mol %) on the other hand achieved only 38% conversion over the same time with very poor product selectivity (β -E: β -Z: α = 42:45:13).



Scheme 3.21

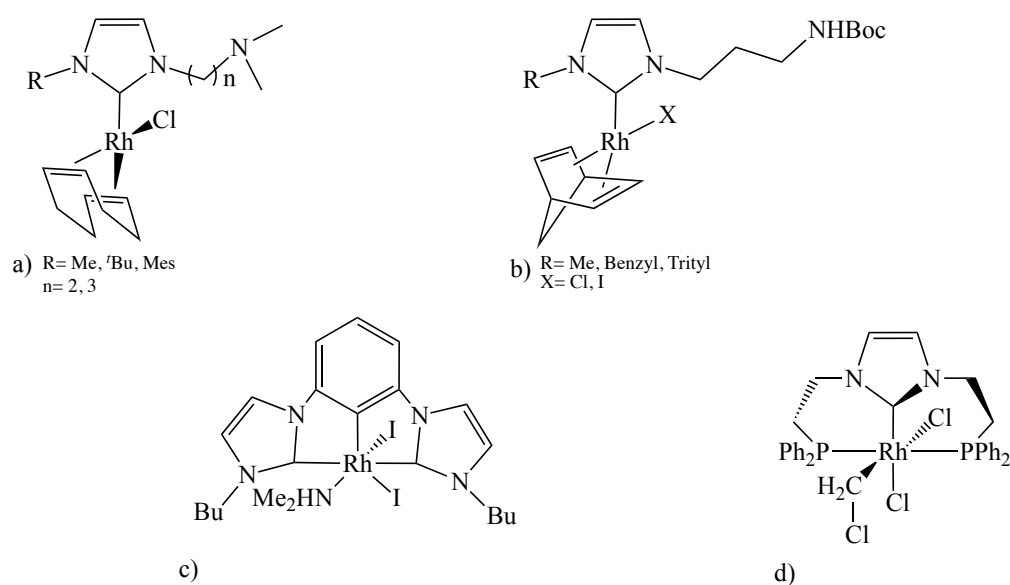
A range of Ir and Rh bis-NHC containing complexes have also been applied as catalysts for the hydrosilylation of both phenylacetylene and 1-hexyne.⁵⁰ The rhodium catalysts were found to be far more effective than the iridium catalysts with CO containing complexes found to be the most effective (Scheme 3.22).



Scheme 3.22

Other catalyst motifs that have been explored include Rh(I) catalysts containing

monodentate NHC ligands with a pendant secondary or tertiary amine substituent (Scheme 3.23 a and b),^{51,52} CCC pincer Rh(III) complex (Scheme 3.23 c)²⁹ and pincer PCP Rh(III) complex (Scheme 3.23 d).⁵³ The PCP containing complex (Scheme 3.23 d) was particularly notable for the prolonged activity of the complex, which allowed catalyst loadings as low as 0.001 mol% to be used, facilitating the quantitative hydrosilylation of phenylacetylene with Me₂PhSiH over 24 hours at room temperature.

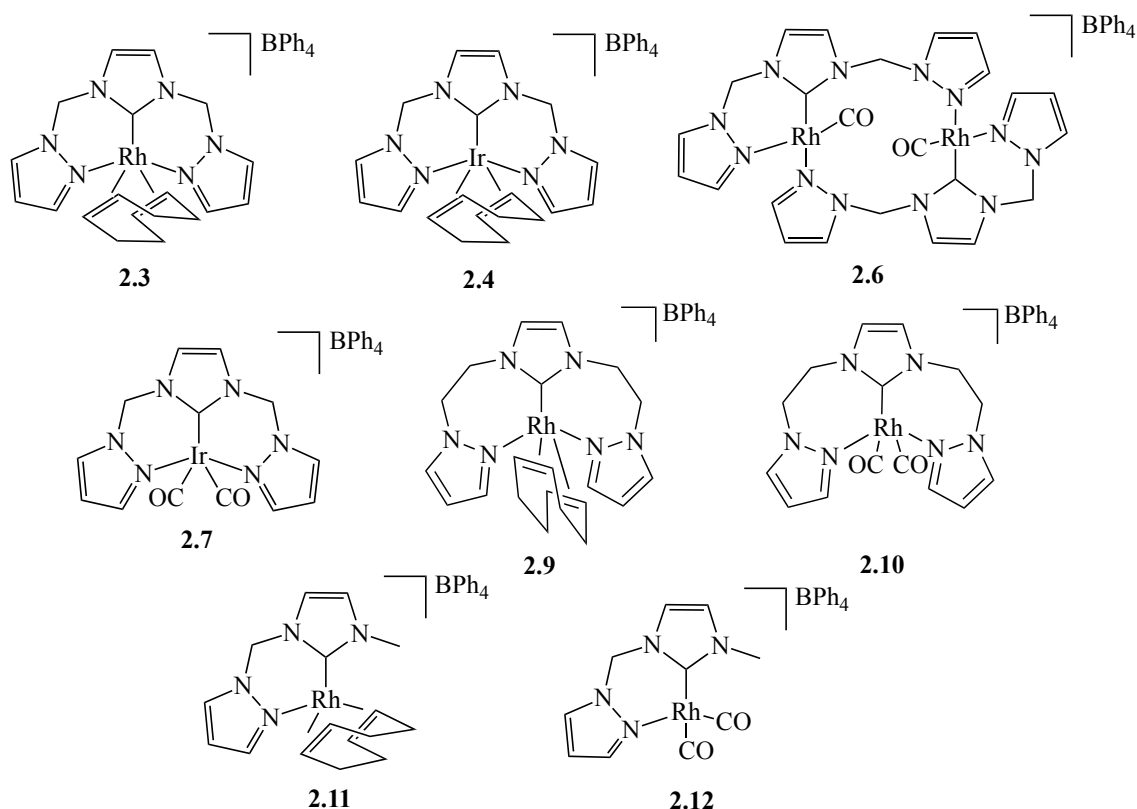


Scheme 3.23

3.1.4 Objectives

The newly synthesised pincer complexes [Rh(NCN^{Me})(COD)]BPh₄ (**2.3**), [Ir(NCN^{Me})(COD)]BPh₄ (**2.4**), [Rh(NCN^{Me})(CO)]₂(BPh₄)₂ (**2.6**), [Ir(NCN^{Me})(CO)₂]BPh₄ (**2.7**), [Rh(NCN^{Et})(COD)]BPh₄ (**2.9**), [Rh(NCN^{Et})(CO)₂]BPh₄ (**2.10**) (Scheme 3.24), which were described in chapter 2 of this thesis, were investigated as catalysts for a number of different organic reactions involving the addition of an X-H bond across an unsaturated CC triple bond. The reactions taken into consideration were: hydroamination, hydroalkoxylation and hydrosilylation. To explore

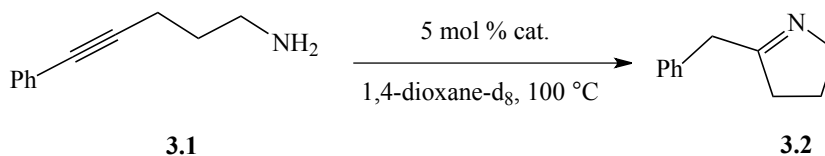
the reactivity of alkynes towards the addition of N-H bonds we investigated the intramolecular hydroamination of 5-phenyl-4-pentyn-1-amine as well as the inter-molecular hydroamination of phenylacetylene with aniline. The reactivity of alkynes towards O-H bond addition was explored by investigating the catalysed cyclisation of 4-pentynoic acid as well as the double hydroalkoxylation of the alkyne diol 2-(5-hydroxypent-1-ynyl)benzyl alcohol. Finally we explored the addition of Si-H bonds to phenylacetylene and 1-phenyl-1-propyne using Et_3SiH . For comparison we also included the previously reported complexes $[\text{Rh}(\text{NC}^{\text{Me}})(\text{COD})]\text{BPh}_4$ (**2.11**) and $[\text{Rh}(\text{NC}^{\text{Me}})(\text{CO})_2]\text{BPh}_4$ (**2.12**) (Scheme 3.24), which contain a bidentate NHC-pyrazolyl ligand, into several of our catalytic studies.



Scheme 3.24

3.2 Results and discussion

3.2.1 Intra-molecular hydroamination of 5-phenyl-4-pentyn-1-amine (3.1) to 2-benzyl-1-pyrroline (3.2)



Scheme 3.25

The six Ir(I) and Rh(I) pincer complexes $[\text{Rh}(\text{NCN}^{\text{Me}})(\text{COD})]\text{BPh}_4$ (**2.3**), $[\text{Ir}(\text{NCN}^{\text{Me}})(\text{COD})]\text{BPh}_4$ (**2.4**), $[\text{Rh}(\text{NCN}^{\text{Me}})(\text{CO})]_2(\text{BPh}_4)_2$ (**2.6**), $[\text{Ir}(\text{NCN}^{\text{Me}})(\text{CO})_2]\text{BPh}_4$ (**2.7**), $[\text{Rh}(\text{NCN}^{\text{Et}})(\text{COD})]\text{BPh}_4$ (**2.9**), $[\text{Rh}(\text{NCN}^{\text{Et}})(\text{CO})_2]\text{BPh}_4$ (**2.10**), and the two chelated Rh(I) complexes $[\text{Rh}(\text{NC}^{\text{Me}})(\text{COD})]\text{BPh}_4$ (**2.11**) and $[\text{Rh}(\text{NC}^{\text{Me}})(\text{CO})_2]\text{BPh}_4$ (**2.12**) were tested as catalysts for the intra-molecular hydroamination of 5-phenyl-4-pentyn-1-amine (**3.1**) to 2-benzyl-1-pyrroline (**3.2**) (Scheme 3.25). The reaction was carried out at 100 °C in dioxane- d_8 using 5 mol% catalyst and the reaction progress was monitored periodically by ^1H NMR spectroscopy. (NB: for the bimetallic catalyst $[(\text{Rh}(\text{NCN}^{\text{Me}})(\text{CO}))_2(\text{BPh}_4)_2]$ (**2.6**) only 2.5 mol% of catalyst was used to maintain a constant Rh loading of 5 mol%). Percent conversions were determined via comparison of the substrate and product integrals. Figure 3.1 shows the percent conversion versus time for the complexes with COD co-ligand **2.3**, **2.4**, **2.9** and **2.11**.

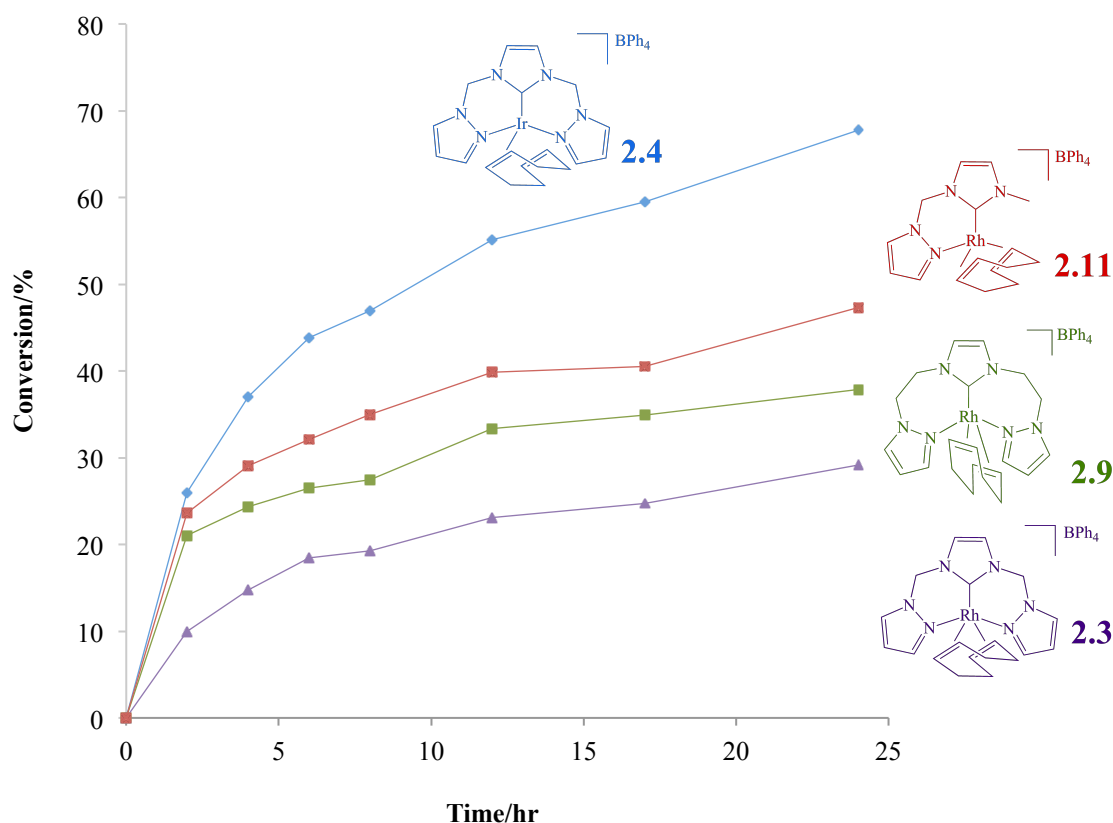


Figure 3.1: Reaction profile for the hydroamination of 5-phenyl-4-pentyn-1-amine (**3.1**) to 2-benzyl-1-pyrroline (**3.2**) in 1,4-dioxane- d_8 at 100 °C using 5 mol % catalyst loading of $[\text{Rh}(\text{NCN}^{\text{Me}})(\text{COD})]\text{BPh}_4$ (**2.3**), $[\text{Ir}(\text{NCN}^{\text{Me}})(\text{COD})]\text{BPh}_4$ (**2.4**), $[\text{Rh}(\text{NCN}^{\text{Et}})(\text{COD})]\text{BPh}_4$ (**2.9**) and $[\text{Rh}(\text{NCN}^{\text{Me}})(\text{COD})]\text{BPh}_4$ (**2.11**).

A broad range of catalytic activities was observed for the complexes with COD co-ligands. The Ir pincer complex **2.4** was the most active catalyst of this series achieving 68% conversion to 2-benzyl-1-pyrroline (**3.2**) after 24 hours. Conversely, the analogous Rh pincer complex **2.3** was the least active catalyst of the series achieving only 29% conversion over the same time. Interestingly, increasing the length of the pincer ligand arm from methyl in complex **2.3**, to ethyl in complex **2.9** results in a significant improvement of catalyst activity with complex **2.9** achieving a final conversion of 38% after 24 hours. In Chapter 2 we demonstrated how increasing the length of the pincer arm appeared to increase the lability of one of the pyrazole donor

groups (section 2.4.2.1, chapter 2). Here we can now see how that increased lability appears to lead to an increase in catalyst activity, presumably via allowing greater access to a vacant coordination site on Rh. This trend is further confirmed when we examine the catalytic activity of the chelated complex **2.11**, which lacks a third donor group. Complex **2.11** achieves a final conversion after 24 hours of 48%, significantly higher than both **2.3** (29%) and **2.9** (38%). The Ir analogues of the ethyl bridged complex **2.9** and the chelate complex **2.11** could not be prepared, therefore an examination of this trend for Ir complexes is precluded.

Figure 3.2 shows the percent conversion versus time for the complexes with CO co-ligands **2.6**, **2.7**, **2.10** and **2.12**. Complexes $[\text{Rh}(\text{NCN}^{\text{Me}})(\text{CO})_2](\text{BPh}_4)_2$ (**2.6**), $[\text{Ir}(\text{NCN}^{\text{Me}})(\text{CO})_2]\text{BPh}_4$ (**2.7**), $[\text{Rh}(\text{NCN}^{\text{Et}})(\text{CO})_2]\text{BPh}_4$ (**2.10**) and $[\text{Rh}(\text{NC}^{\text{Me}})(\text{CO})_2]\text{BPh}_4$ (**2.12**) were generated in situ by displacement of the COD co-ligand under 1 atmosphere of CO from complexes **2.3**, **2.4**, **2.9** and **2.11**, respectively. The reactions were performed under a CO atmosphere in dioxane- d_8 at 100 °C and periodically monitored by ^1H NMR spectroscopy for 24 hours.

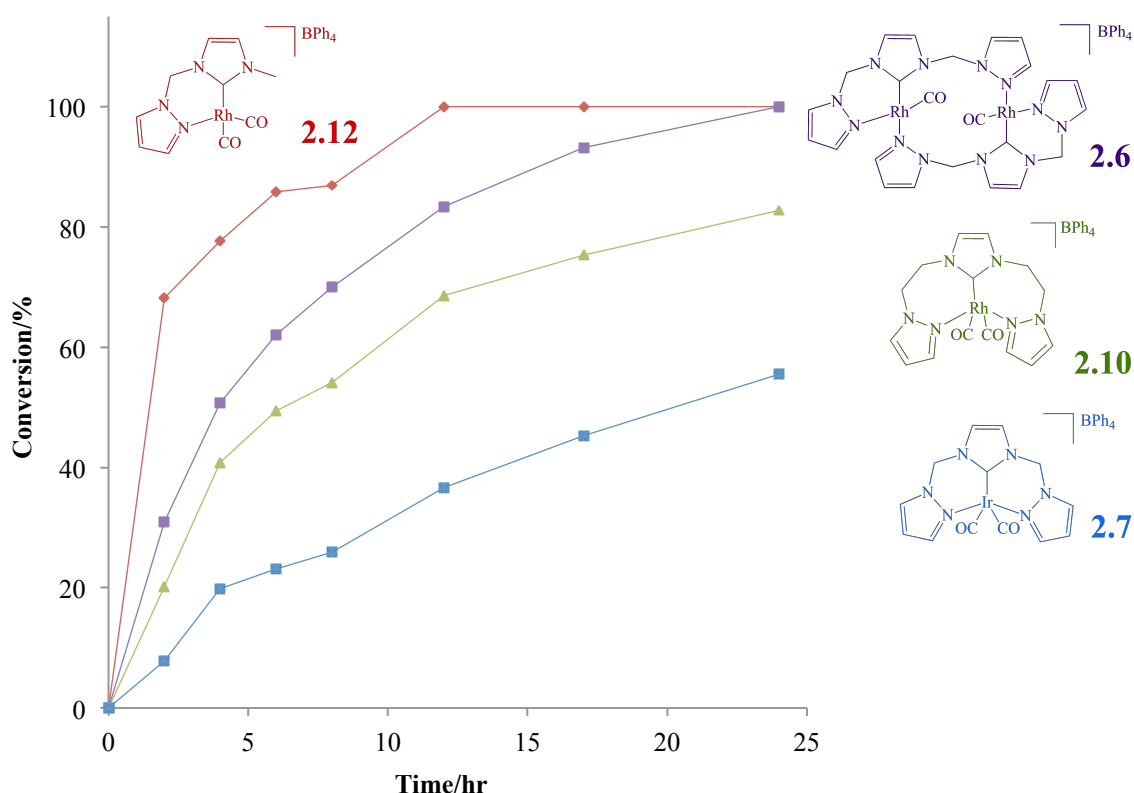
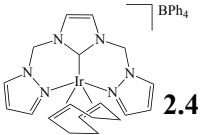
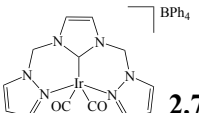
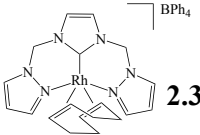
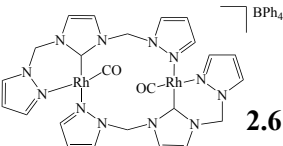
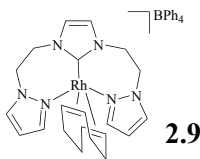
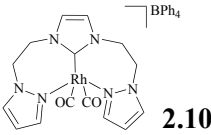
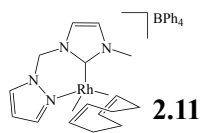
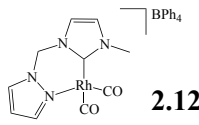


Figure 3.2: Reaction profile for the hydroamination of 5-phenyl-4-pentyn-1-amine (**3.1**) to 2-benzyl-1-pyrroline (**3.2**) in 1,4-dioxane- d_8 at 100 °C using 5 mol% catalyst loading of $[\text{Rh}(\text{NCN}^{\text{Me}})(\text{CO})_2]\text{BPh}_4$ (**2.6**), $[\text{Ir}(\text{NCN}^{\text{Me}})(\text{CO})_2]\text{BPh}_4$ (**2.7**), $[\text{Rh}(\text{NCN}^{\text{Et}})(\text{CO})_2]\text{BPh}_4$ (**2.10**) and $[\text{Rh}(\text{NC}^{\text{Me}})(\text{CO})_2]\text{BPh}_4$ (**2.12**).

The chelated Rh complex $[\text{Rh}(\text{NC}^{\text{Me}})(\text{CO})_2]\text{BPh}_4$ (**2.12**) was the most active catalyst amongst this series achieving >98 % conversion of the substrate 5-phenyl-4-pentyn-1-amine (**3.1**) to 2-benzyl-1-pyrroline (**3.2**) in only 12 hours. Complex **2.12** had a very fast initial rate converting 68% of the substrate in only the first two hours. The Ir complex $[\text{Ir}(\text{NCN}^{\text{Me}})(\text{CO})_2]\text{BPh}_4$ (**2.7**) was the least active catalyst achieving 56 % conversion of 5-phenyl-4-pentyn-1-amine (**3.1**) in 24 hours. This is significantly slower than both rhodium pincer complexes **2.6** and **2.10**, which achieved 98% and 83% conversion, respectively, after 24 hours. Rhodium is therefore a more suitable metal centre for complexes with CO co-ligands.

In order to compare the reactivity of complexes with COD co-ligands versus CO co-ligands, the catalytic performances of the eight catalysts after 12 hours is summarised in Table 3.1.

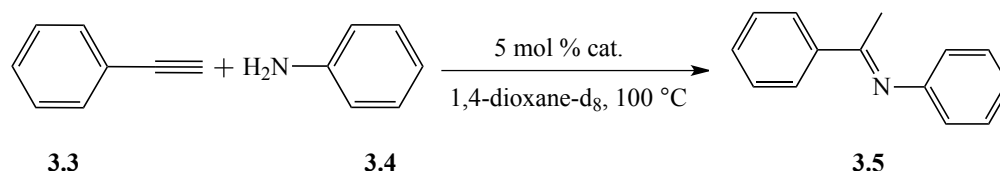
Table 3.1: Catalytic efficiency of $[\text{Rh}(\text{NCN}^{\text{Me}})(\text{COD})]\text{BPh}_4$ (**2.3**), $[\text{Ir}(\text{NCN}^{\text{Me}})(\text{COD})]\text{BPh}_4$ (**2.4**), $[\text{Rh}(\text{NCN}^{\text{Me}})(\text{CO})]_2(\text{BPh}_4)_2$ (**2.6**), $[\text{Ir}(\text{NCN}^{\text{Me}})(\text{CO})_2]\text{BPh}_4$ (**2.7**), $[\text{Rh}(\text{NCN}^{\text{Et}})(\text{COD})]\text{BPh}_4$ (**2.9**), $[\text{Rh}(\text{NCN}^{\text{Et}})(\text{CO})_2]\text{BPh}_4$ (**2.10**), $[\text{Rh}(\text{NCN}^{\text{Me}})(\text{COD})]\text{BPh}_4$ (**2.11**) and $[\text{Rh}(\text{NCN}^{\text{Me}})(\text{CO})_2]\text{BPh}_4$ (**2.12**) for the cyclisation of 5-phenyl-4-pentyn-1-amine (**3.1**).^[a]

Catalyst (COD)	Conversion (24 hrs)	Catalyst (CO)	Conversion (24 hrs)
 2.4	55%	 2.7	37%
 2.3	23%	 2.6	83%
 2.9	33%	 2.10	68%
 2.11	40%	 2.12	>98%

[a] Reaction carried out in 1,4-dioxane-d₈ at 100 °C using 5 mol% catalyst loading.

Among the eight catalysts tested on the intra-molecular hydroamination of 5-phenyl-4-pentyn-1-amine (**3.1**), the chelated complex $[\text{Rh}(\text{NC}^{\text{Me}})(\text{CO})_2]\text{BPh}_4$ (**2.12**) performed best reaching complete conversion after 12 hours. The carbonylated Rh complexes showed higher activity than their COD analogues. While the iridium complex $[\text{Ir}(\text{NCN}^{\text{Me}})(\text{CO})_2]\text{BPh}_4$ (**2.7**) was the worst performing among the carbonylated complexes, its COD analogue $[\text{Ir}(\text{NCN}^{\text{Me}})(\text{COD})]\text{BPh}_4$ (**2.4**) was the fastest among the complexes with COD co-ligand. The chelating coordination of the NC^{Me} ligand in complexes **2.11** and **2.12** proved to be more beneficial than the pincer ligand coordination for the intra-molecular hydroamination of 5-phenyl-4-pentyn-1-amine (**3.1**) for both rhodium complexes with CO and COD co-ligands.

3.2.2 Inter-molecular hydroamination of phenylacetylene (**3.3**) and aniline (**3.4**)



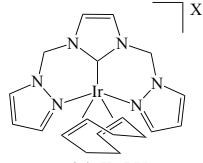
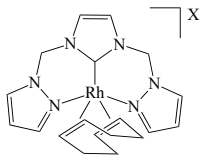
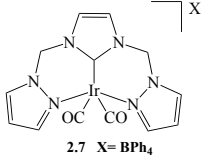
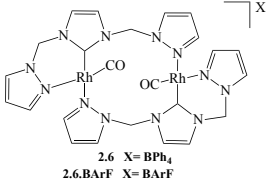
Scheme 3.26

The inter-molecular hydroamination reaction is known to be significantly more challenging than the intra-molecular reaction. To fully explore the efficiency of our pincer complexes for the inter-molecular hydroamination reaction we therefore examined the catalytic activity of both the tetraphenylborate (BPh_4) salt $[\text{Rh}(\text{NCN}^{\text{Me}})(\text{COD})]\text{BPh}_4$ (**2.3**), $[\text{Ir}(\text{NCN}^{\text{Me}})(\text{COD})]\text{BPh}_4$ (**2.4**), $[\text{Rh}(\text{NCN}^{\text{Me}})(\text{CO})]_2(\text{BPh}_4)_2$ (**2.6**), $[\text{Ir}(\text{NCN}^{\text{Me}})(\text{CO})_2]\text{BPh}_4$ (**2.7**), as well as the analogous complexes containing the more weakly coordinating

tetrakis(3,5-trifluoromethylphenyl)borate (BArF) anion: [Rh(NCN^{Me})(COD)]BArF (**2.3.BArF**), [Ir(NCN^{Me})(COD)]BArF (**2.4.BArF**), (Rh(NCN^{Me})(CO))₂(BArF)₂ (**2.6.BArF**), [Ir(NCN^{Me})(CO)₂](BArF) (**2.7.BArF**). Messerle *et al.*⁵⁴ have previously shown that substitution of BPh₄⁻ with BArF leads to a significant enhancement of catalytic rate for Ir and Rh hydroalkoxylation catalysts. The reaction under investigation in this study is the inter-molecular hydroamination of phenylacetylene (**3.3**) and aniline (**3.4**) at 100 °C in dioxane-d₈ using 5 mol% catalyst (Scheme 3.26), with the reaction progress monitored after 24 hours (Table 3.2). The complexes with CO co-ligand **2.6**, **2.7**, **2.6.BArF** and **2.7.BArF** were generated in situ by performing the reaction under 1 atmosphere of CO.

The four BPh₄⁻ complexes **2.3**, **2.4**, **2.6** and **2.7** although quite reactive on the intra-molecular hydroamination of 5-phenyl-4-pentyn-1-amine (**3.1**), barely reacted on the more challenging inter-molecular hydroamination reaction of phenylacetylene (**3.3**) and aniline (**3.4**). Interestingly, the substitution of BPh₄⁻ with BArF did not lead to a consistent enhancement of reaction rate for all catalysts. For the complexes with COD co-ligand the final conversion after 24 hours was either less than (**2.3BArF**= 2%) or approximately equal (**2.4BArF**= 6%) to that achieved with BPh₄⁻ complex **2.3** and **2.4** (7 and 5%, respectively).

Table 3.2: Catalytic efficiency of $[\text{Rh}(\text{NCN}^{\text{Me}})(\text{COD})]\text{BPh}_4$ (**2.3**), $[\text{Ir}(\text{NCN}^{\text{Me}})(\text{COD})]\text{BPh}_4$ (**2.4**), $[\text{Rh}(\text{NCN}^{\text{Me}})(\text{CO})]_2(\text{BPh}_4)_2$ (**2.6**), $[\text{Ir}(\text{NCN}^{\text{Me}})(\text{CO})_2]\text{BPh}_4$ (**2.7**), $[\text{Rh}(\text{NCN}^{\text{Me}})(\text{COD})]\text{BArF}$ (**2.3.BArF**), $[\text{Ir}(\text{NCN}^{\text{Me}})(\text{COD})]\text{BArF}$ (**2.4.BArF**), $[\text{Rh}(\text{NCN}^{\text{Me}})(\text{CO})]_2(\text{BArF})_2$ (**2.6.BArF**) and $[\text{Ir}(\text{NCN}^{\text{Me}})(\text{CO})_2]\text{BArF}$ (**2.7.BArF**) for the addition of phenylacetylene (**3.3**) to aniline (**3.4**).^[a]

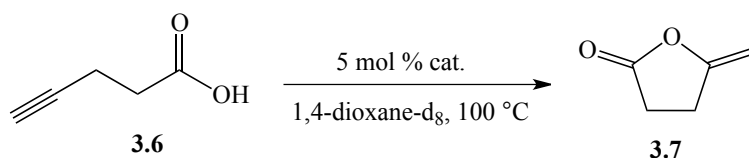
Catalyst	Conversion (24 hrs)	
	X=BPh ₄	X=BArF
 <p>2.4 X= BPh₄ 2.4.BArF X= BArF</p>	5 %	6%
 <p>2.3 X= BPh₄ 2.3.BArF X= BArF</p>	7 %	2%
 <p>2.7 X= BPh₄ 2.7.BArF X= BArF</p>	< 1 %	18%
 <p>2.6 X= BPh₄ 2.6.BArF X= BArF</p>	< 1 %	32%

[a] Reaction carried out in 1,4-dioxane-d₈ at 100 °C using 5 mol% catalyst loading.

For the complexes with CO co-ligands on the other hand a significant improvement of catalyst activity was observed. The complex $[\text{Rh}(\text{NCN}^{\text{Me}})(\text{CO})]_2(\text{BArF})_2$ (**2.6.BArF**) was the most active catalyst of the series reaching 32% conversion in 24 hours. In comparison the complex $[\text{Ir}(\text{NCN}^{\text{Me}})(\text{CO})_2]\text{BArF}$ (**2.7.BArF**) achieved only 18% over 24 hours. While for the CO containing complexes rhodium (**2.6.BArF**) is more active

than iridium (**2.7.BArF**), for the complexes with COD co-ligand the opposite is true with iridium (**2.4.BArF**) more active than rhodium (**2.3.BArF**). These outcomes are consistent with the results obtained on the intra-molecular hydroamination of 5-phenyl-4-pentyn-1-amine (**3.1**).

3.2.3 Hydroalkoxylation of 4-pentynoic acid (**3.6**) to γ -methylene- γ -butyrolactone (**3.7**)



Scheme 3.27

To explore the efficiency of the pincer complexes as catalyst for the addition of O-H bonds to alkynes we first explored the cyclisation of 4-pentynoic acid (**3.6**) to γ -methylene- γ -butyrolactone (**3.7**) (Scheme 3.27). The reaction was performed in THF- d_8 at 80 °C and the progress was monitored periodically by ^1H NMR spectroscopy for 24 hours. Figure 3.3 shows an example of the reaction progress as monitored by ^1H NMR spectroscopy.

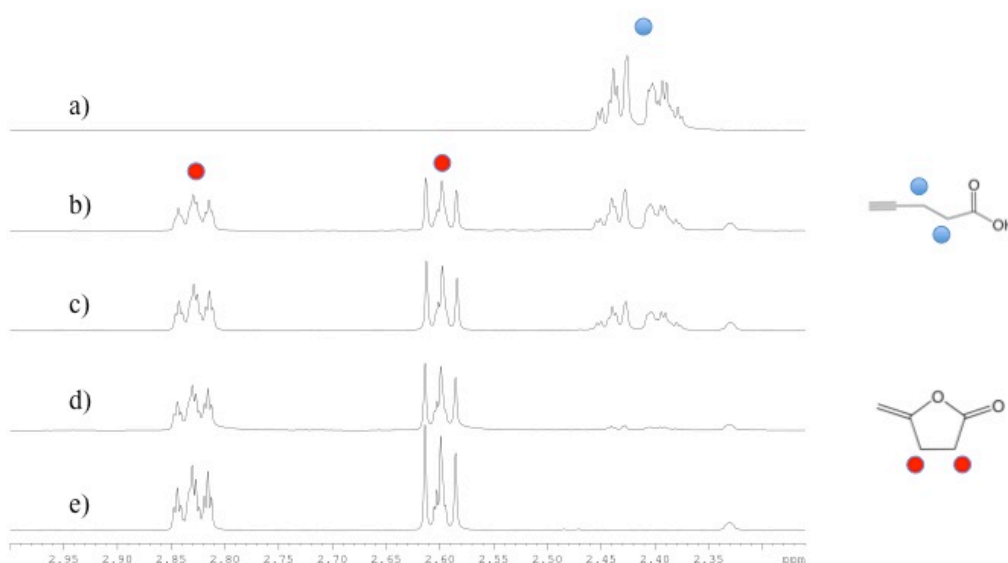


Figure 3.3: Stacked ^1H NMR spectra (THF-d_8 , 600 MHz, 333K) of hydroxylation of 4-pentynoic acid (**3.6**) to γ -methylene- γ -butyrolactone (**3.7**) in THF-d_8 at 80 °C at fixed time intervals: a) $t=0$; b) $t= 4.3$ hrs; c) $t= 5.6$ hrs; d) $t= 12$ hrs; e) $t= 29$ hrs.

The Ir(I) and Rh(I) pincer complexes $[\text{Rh}(\text{NCN}^{\text{Me}})(\text{COD})]\text{BPh}_4$ (**2.3**), $[\text{Ir}(\text{NCN}^{\text{Me}})\text{COD}]\text{BPh}_4$ (**2.4**), $[\text{Rh}(\text{NCN}^{\text{Me}})(\text{CO})]_2(\text{BPh}_4)_2$ (**2.6**), $[\text{Ir}(\text{NCN}^{\text{Me}})(\text{CO})_2]\text{BPh}_4$ (**2.7**), $[\text{Rh}(\text{NCN}^{\text{Et}})(\text{COD})]\text{BPh}_4$ (**2.9**), $[\text{Rh}(\text{NCN}^{\text{Et}})(\text{CO})_2]\text{BPh}_4$ (**2.10**), and the chelated complexes $[\text{Rh}(\text{NC}^{\text{Me}})(\text{COD})]\text{BPh}_4$ (**2.11**) and $[\text{Rh}(\text{NC}^{\text{Me}})(\text{CO})_2]\text{BPh}_4$ (**2.12**) were tested on this reaction. Note, the complexes with CO co-ligand were generated in situ from the corresponding COD containing complexes by performing the reactions under an atmosphere of CO. In Figure 3.4 the reaction profiles for the cyclisation of 4-pentynoic acid (**3.6**) to γ -methylene- γ -butyrolactone (**3.7**) by complexes with COD co-ligand **2.3**, **2.4**, **2.9** and **2.11** are shown.

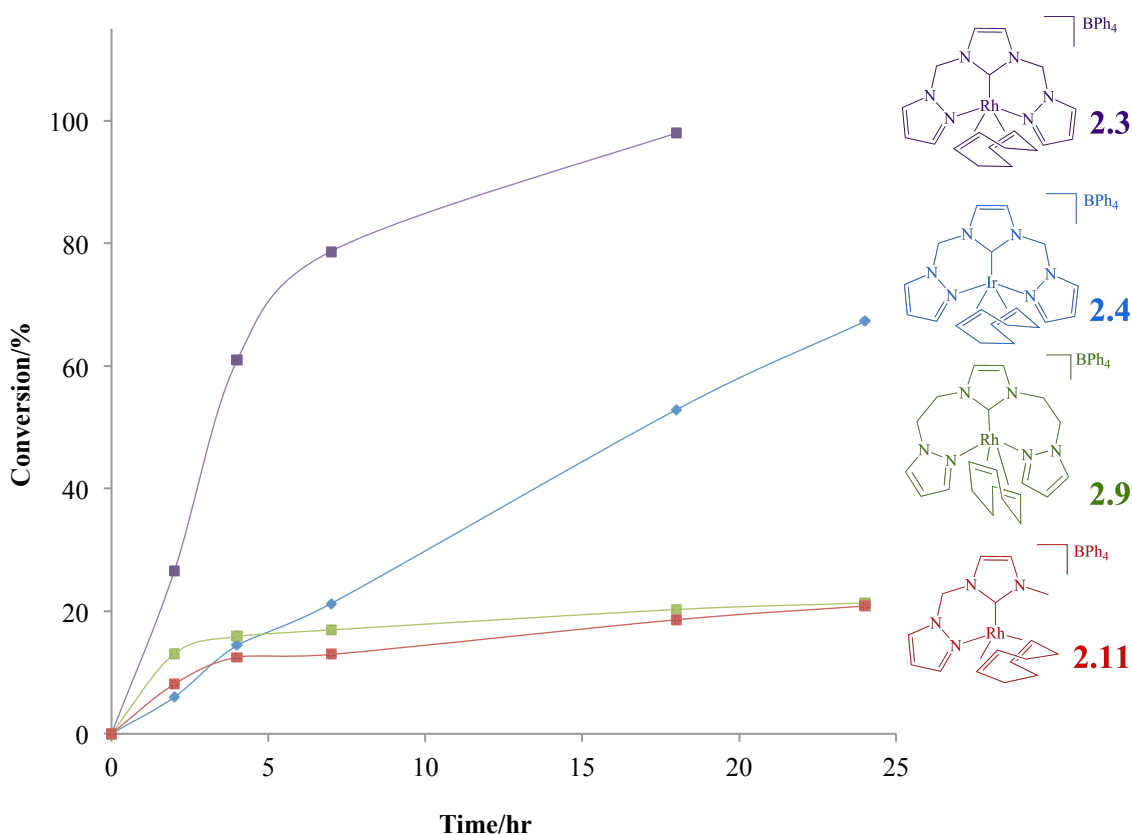


Figure 3.4: Reaction profile for the cyclisation of 4-pentynoic acid (**3.6**) in 1,4-dioxane- d_8 at 100 °C using 5 mol% of $\text{Rh}(\text{NCN}^{\text{Me}})(\text{COD})\text{BPh}_4$ (**2.3**), $[\text{Ir}(\text{NCN}^{\text{Me}})(\text{COD})]\text{BPh}_4$ (**2.4**), $[\text{Rh}(\text{NCN}^{\text{Et}})(\text{COD})]\text{BPh}_4$ (**2.9**) and $[\text{Rh}(\text{NC}^{\text{Me}})(\text{COD})]\text{BPh}_4$ (**2.11**).

$\text{Rh}(\text{NCN}^{\text{Me}})(\text{COD})\text{BPh}_4$ (**2.3**) was found to be the most active catalyst amongst the four COD containing catalysts reaching complete conversion after 18 hours. Both catalysts $[\text{Rh}(\text{NCN}^{\text{Et}})(\text{COD})]\text{BPh}_4$ (**2.9**) and $[\text{Rh}(\text{NC}^{\text{Me}})(\text{COD})]\text{BPh}_4$ (**2.11**) only achieved a maximum conversion of 21 % after 24 hours. Surprisingly by introducing a slight change to the catalysts structure by increasing the length of the pincer ligand arm from methyl in complex **2.3** to ethyl in complex **2.9** leads to a dramatic decrease of the catalyst efficiency. The reaction profile for complex **2.11**, which contains the chelating NHC-pyrazolyl ligand, appears strikingly similar to the catalytic profile of the pincer complex with the ethyl arm **2.9**. This suggests that both catalysts are following a similar reaction pathway with both catalysts deactivating a short time into the reaction. In Chapter 2 we showed how increasing the length of the ligand arm increased the lability

of the second pyrazole donor group. Potentially it is the strongly 3-coordinated κ^3 binding mode of the methyl bridged NCN^{Me} pincer ligand in complex $[\text{Rh}(\text{NCN}^{\text{Me}})(\text{COD})]\text{BPh}_4$ (**2.3**), that stabilizes it against decomposition thereby leading to a much more active catalyst. The analogous Ir complex $[\text{Ir}(\text{NCN}^{\text{Me}})(\text{COD})]\text{BPh}_4$ (**2.4**) was also found to be an effective catalyst for the cyclisation of 4-pentynoic acid (**3.6**), achieving a final conversion of 67 % after 24 hours. This catalyst showed a strikingly different reaction profile compared to the analogous Rh complex **2.3**. For the iridium complex **2.4** the percent conversion increases linearly with time suggesting a zero order dependence on the substrate concentration.

In Figure 3.5 are reported the reaction profiles for the cyclisation of 4-pentynoic acid (**3.6**) to γ -methylene- γ -butyrolactone (**3.7**) by complexes containing a CO co-ligand **2.6**, **2.7**, **2.10** and **2.12**.

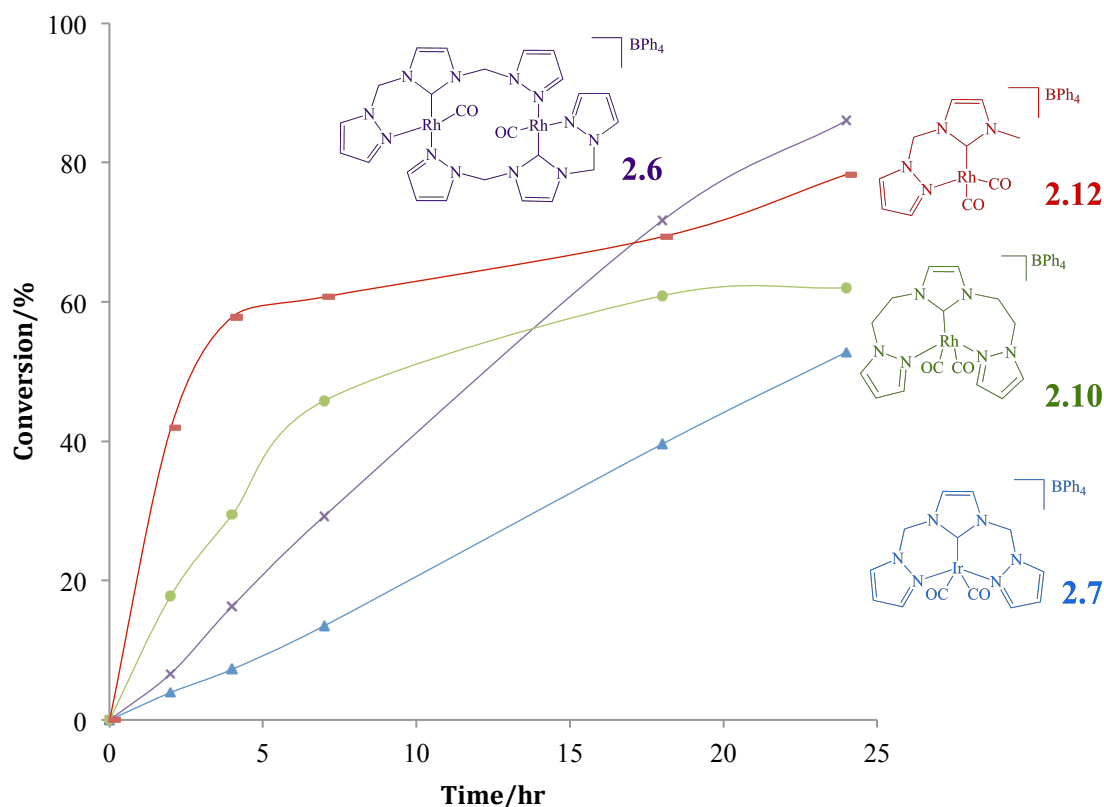


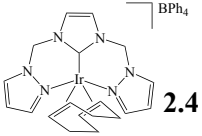
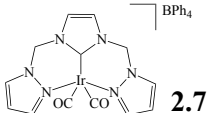
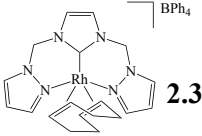
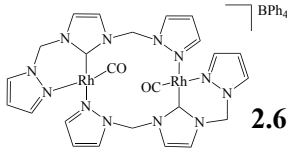
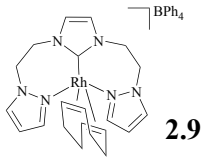
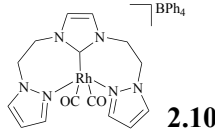
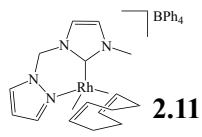
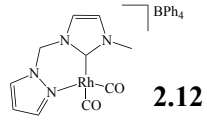
Figure 3.5: Reaction profile for the cyclisation of 4-pentynoic acid (**3.6**) in 1,4-dioxane- d_8 at 100 °C using 5 mol% of $[\text{Rh}(\text{NCN}^{\text{Me}})(\text{CO})_2](\text{BPh}_4)_2$ (**2.6**), $[\text{Ir}(\text{NCN}^{\text{Me}})(\text{CO})_2]\text{BPh}_4$ (**2.7**), $[\text{Rh}(\text{NCN}^{\text{Et}})(\text{CO})_2]\text{BPh}_4$ (**2.10**) and $[\text{Rh}(\text{NC}^{\text{Me}})(\text{CO})_2]\text{BPh}_4$ (**2.12**).

Among the CO containing complexes the bimetallic $[\text{Rh}(\text{NCN}^{\text{Me}})(\text{CO})_2](\text{BPh}_4)_2$ (**2.6**) reached the highest conversion (86%) in 24 hours. $[\text{Ir}(\text{NCN}^{\text{Me}})(\text{CO})_2]\text{BPh}_4$ (**2.7**) was the slowest catalyst achieving 53 % conversion in the same time. Figure 3.5 highlights a difference in the reaction profiles for the four catalysts under investigation here. Both the bimetallic complex **2.6** and the iridium complex **2.7** show a linear increase in conversion versus time. This is in contrast to complex $[\text{Rh}(\text{NC}^{\text{Me}})(\text{CO})_2]\text{BPh}_4$ (**2.12**) which contains a chelating ligand group, where a more conventional sigmoidal reaction profile is observed. The reaction profile of complex $[\text{Rh}(\text{NCN}^{\text{Et}})(\text{CO})_2]\text{BPh}_4$ (**2.10**), which was shown to exhibit a higher lability of one pyrazole donor group, appears to lie somewhere in between these two extremes. Both complexes **2.12** and **2.10** show a very high initial catalytic activity achieving 61 % and 46 % conversion, respectively, within

the first 7 hours of reaction. However this is followed by a rapid deactivation of the catalyst leading to final conversions after 24 hours of only 78 % (**2.12**) and 62 % (**2.10**). In contrast, for complex $[\text{Rh}(\text{NCN}^{\text{Me}})(\text{CO})]_2(\text{BPh}_4)_2$ (**2.6**) despite appearing as a relatively poorer catalyst over shorter time frames (< 7 hours), the activity of the catalyst is maintained over the whole 24 hours leading to the highest total conversion of 86% for the series.

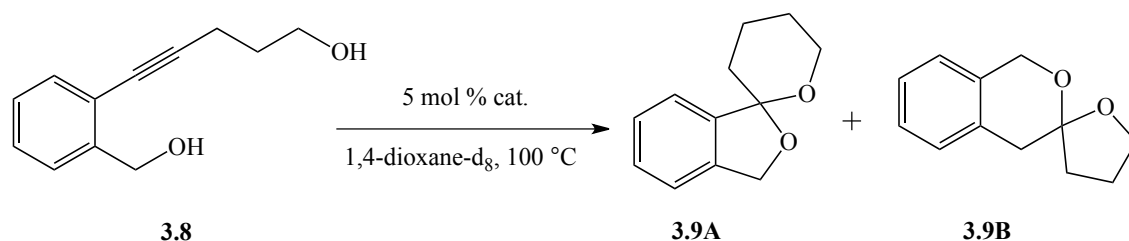
In Table 3.3 are summarised the catalytic conversions of the eight complexes for the cyclisation of 4-pentynoic acid. The most active catalyst of the series was the pincer rhodium complex $[\text{Rh}(\text{NCN}^{\text{Me}})(\text{COD})]\text{BPh}_4$ (**2.3**) containing the COD co-ligand (> 98 % conversion in 24 hours). The corresponding CO containing complex $[\text{Rh}(\text{NCN}^{\text{Me}})(\text{CO})_2](\text{BPh}_4)_2$ (**2.6**) was also highly active (86 % conversion in 24 hours) however a dramatic difference in reaction profile was observed between these two catalysts. The COD containing iridium complex $[\text{Ir}(\text{NCN}^{\text{Me}})(\text{COD})]\text{BPh}_4$ (**2.4**) was also more active than the analogous CO containing complex $[\text{Ir}(\text{NCN}^{\text{Me}})(\text{CO})_2]\text{BPh}_4$ (**2.7**), with conversions of 67 % and 53 %, respectively, after 24 hours. However, this trend was not observed for the remaining COD containing complexes $[\text{Rh}(\text{NCN}^{\text{Et}})(\text{COD})]\text{BPh}_4$ (**2.9**) and $[\text{Rh}(\text{NC}^{\text{Me}})(\text{COD})]\text{BPh}_4$ (**2.11**) due to rapid deactivation of these catalysts during reaction.

Table 3.3: Catalytic efficiency of $[\text{Rh}(\text{NCN}^{\text{Me}})(\text{COD})]\text{BPh}_4$ (**2.3**), $[\text{Ir}(\text{NCN}^{\text{Me}})(\text{COD})]\text{BPh}_4$ (**2.4**), $[\text{Rh}(\text{NCN}^{\text{Me}})(\text{CO})]_2(\text{BPh}_4)_2$ (**2.6**), $[\text{Ir}(\text{NCN}^{\text{Me}})(\text{CO})_2]\text{BPh}_4$ (**2.7**), $[\text{Rh}(\text{NCN}^{\text{Et}})(\text{COD})]\text{BPh}_4$ (**2.9**), $[\text{Rh}(\text{NCN}^{\text{Et}})(\text{CO})_2]\text{BPh}_4$ (**2.10**), $[\text{Rh}(\text{NC}^{\text{Me}})(\text{COD})]\text{BPh}_4$ (**2.11**) and $[\text{Rh}(\text{NC}^{\text{Me}})(\text{CO})_2]\text{BPh}_4$ (**2.12**) for the cyclisation 4-pentynoic acid (**3.6**) to γ -methylene- γ -butyrolactone (**3.7**).^[a]

Catalyst (COD)	Conversion (24 hrs)	Catalyst (CO)	Conversion (24 hrs)
 2.4	67%	 2.7	53%
 2.3	98%	 2.6	86%
 2.9	21%	 2.10	62%
 2.11	21%	 2.12	78%

[a] Reaction carried out in 1,4-dioxane- d_8 at 100 °C using 5 mol% catalyst loading.

3.2.4 Cyclisation of 2-(5-Hydroxypent-1-ynyl)benzyl alcohol (3.8)



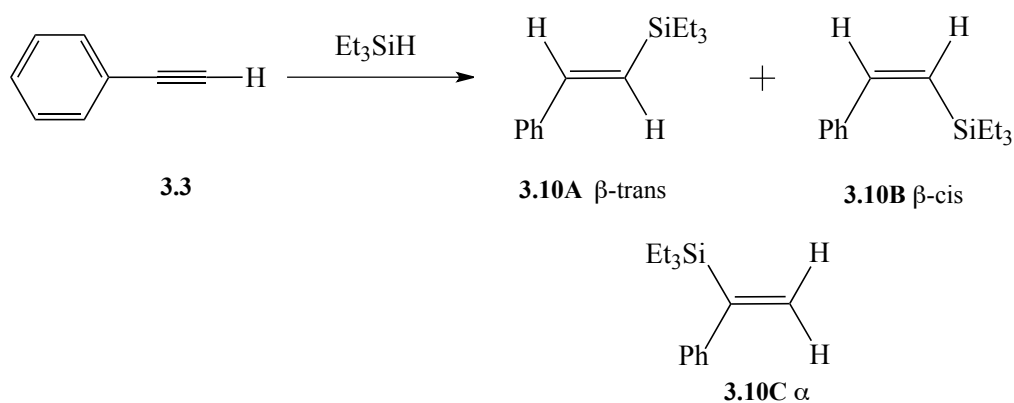
Scheme 3.28

The pincer complexes $[\text{Rh}(\text{NCN}^{\text{Me}})(\text{COD})]\text{BPh}_4$ (**2.3**), $[\text{Ir}(\text{NCN}^{\text{Me}})(\text{COD})]\text{BPh}_4$ (**2.4**), $[\text{Rh}(\text{NCN}^{\text{Me}})(\text{CO})]_2(\text{BPh}_4)_2$ (**2.6**), $[\text{Ir}(\text{NCN}^{\text{Me}})(\text{CO})_2]\text{BPh}_4$ (**2.7**), $[\text{Rh}(\text{NCN}^{\text{Et}})(\text{COD})]\text{BPh}_4$ (**2.9**), $[\text{Rh}(\text{NCN}^{\text{Et}})(\text{CO})_2]\text{BPh}_4$ (**2.10**) and chelated complexes $[\text{Rh}(\text{NC}^{\text{Me}})(\text{COD})]\text{BPh}_4$ (**2.11**) and $[\text{Rh}(\text{NC}^{\text{Me}})(\text{CO})_2]\text{BPh}_4$ (**2.12**) were tested as catalysts for the dihydroalkoxylation of 2-(5-hydroxypent-1-ynyl)benzyl alcohol (**3.8**) (Scheme 3.28). NMR scale solutions of the diol and 5 mol% of the desired catalyst in deuterated 1,4-dioxane were prepared. The reactions were heated at 100 °C, however after 24 hours only a complex mixture of products could be identified. No characteristic peaks due to formation of the desired spiroketal products **3.9A** and **3.9B** were detected at any time during reaction.

3.2.5 Catalysed hydrosilylation of alkynes

The four Ir(I) and Rh(I) pincer complexes $[\text{Rh}(\text{NCN}^{\text{Me}})(\text{COD})]\text{BPh}_4$ (**2.3**), $[\text{Ir}(\text{NCN}^{\text{Me}})(\text{COD})]\text{BPh}_4$ (**2.4**), $[\text{Rh}(\text{NCN}^{\text{Me}})(\text{CO})]_2(\text{BPh}_4)_2$ (**2.6**) and $[\text{Ir}(\text{NCN}^{\text{Me}})(\text{CO})_2]\text{BPh}_4$ (**2.7**), were investigated as catalysts for the hydrosilylation of both terminal and internal alkynes. The alkynes under investigation were phenylacetylene (**3.3**) and 1-phenylpropyne (**3.10**). The reactions were performed in acetone-*d*₆ at 55 °C using Et₃SiH as the reducing agent and 3 mol% catalyst. In situ

carbonylation of $[\text{Rh}(\text{NCN}^{\text{Me}})(\text{COD})]\text{BPh}_4$ (**2.3**) and $[\text{Ir}(\text{NCN}^{\text{Me}})(\text{COD})]\text{BPh}_4$ (**2.4**) was performed to displace the COD co-ligand and generate the complexes with CO co-ligand $[\text{Rh}(\text{NCN}^{\text{Me}})(\text{CO})]_2(\text{BPh}_4)_2$ (**2.6**) and $[\text{Ir}(\text{NCN}^{\text{Me}})(\text{CO})_2]\text{BPh}_4$ (**2.7**) and the catalysis was carried out under 1 atmosphere of CO. The hydrosilylation of phenylacetylene (**3.3**) can lead to three different vinylsilane products β -*cis* (**3.10A**), β -*trans* (**3.10B**) and α (**3.10C**) (Scheme 3.29). The three isomers could be identified due to characteristic signals in their ^1H NMR spectrum (Figure 3.6).



Scheme 3.29

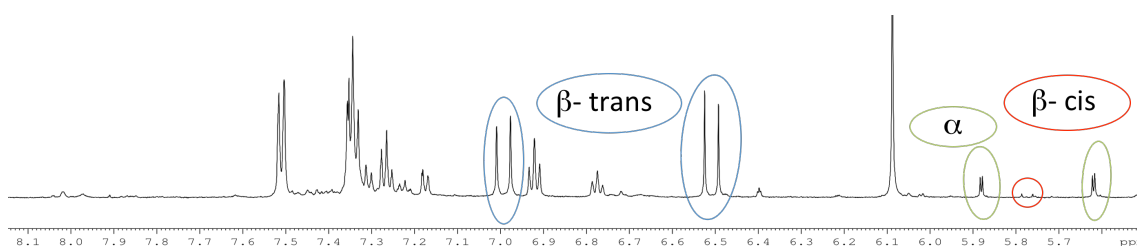


Figure 3.6: ^1H NMR spectrum (acetone- d_6 , 400 MHz, 333K) showing the three vinylsilanes products from the hydrosilylation of phenylacetylene (**3.3**) with triethylsilane using $[\text{Rh}(\text{NCN}^{\text{Me}})(\text{COD})]\text{BPh}_4$ (**2.3**).

In Figure 3.7 are reported the catalytic conversions achieved by complexes $[\text{Rh}(\text{NCN}^{\text{Me}})(\text{COD})]\text{BPh}_4$ (**2.3**), $[\text{Ir}(\text{NCN}^{\text{Me}})(\text{COD})]\text{BPh}_4$ (**2.4**), $[\text{Rh}(\text{NCN}^{\text{Me}})(\text{CO})]_2[\text{BPh}_4]_2$ (**2.6**) and $[\text{Ir}(\text{NCN}^{\text{Me}})(\text{CO})_2]\text{BPh}_4$ (**2.7**) in acetone- d_6 at 55 °C after 24 hours.

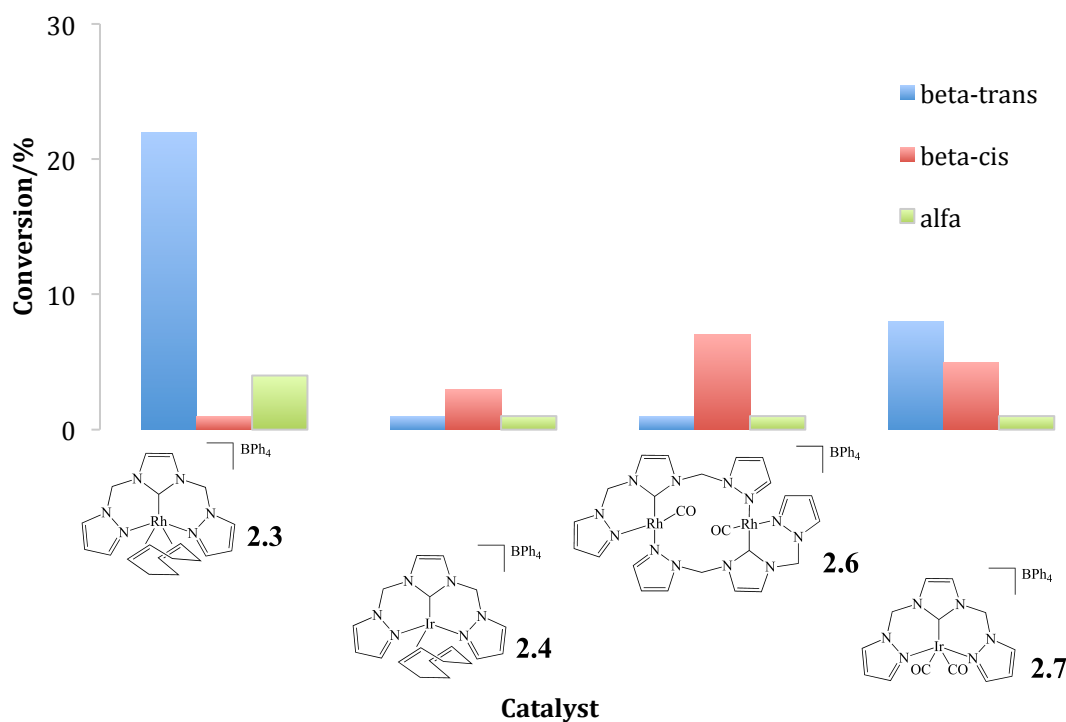
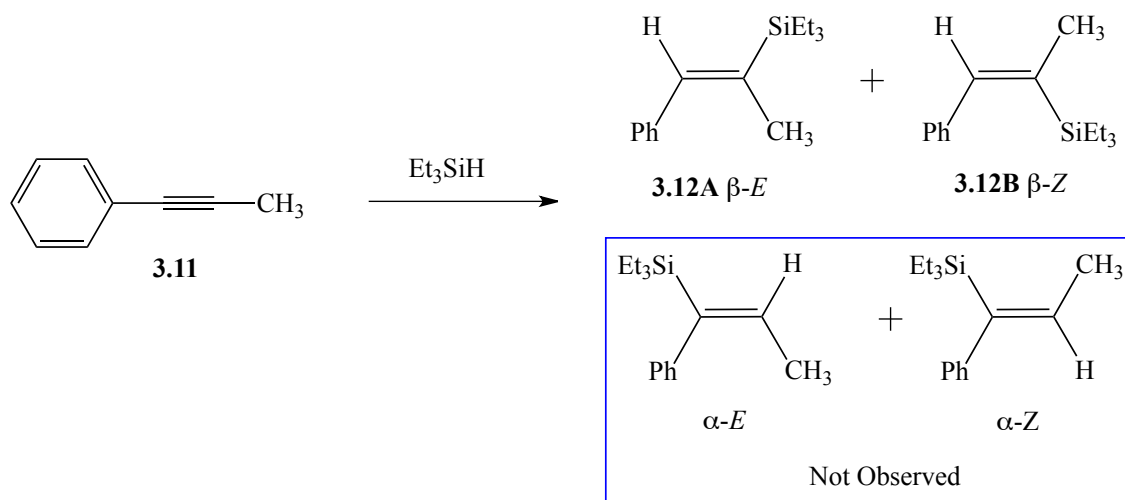


Figure 3.7: Product distribution at 24 hours for the hydrosilylation of phenylacetylene (**3.3**) in acetone- d_6 at 55 °C with 3 mol% of the pincer complexes $[\text{Rh}(\text{NCN}^{\text{Me}})(\text{COD})]\text{BPh}_4$ (**2.3**), $[\text{Ir}(\text{NCN}^{\text{Me}})(\text{COD})]\text{BPh}_4$ (**2.4**), $[\text{Rh}(\text{NCN}^{\text{Me}})(\text{CO})]_2[\text{BPh}_4]_2$ (**2.6**) and $[\text{Ir}(\text{NCN}^{\text{Me}})(\text{CO})_2]\text{BPh}_4$ (**2.7**).

$[\text{Rh}(\text{NCN}^{\text{Me}})(\text{COD})]\text{BPh}_4$ (**2.3**) was the most active complex reaching a total conversion of 31%. The product distribution of β -trans: β -cis: α isomers of 14:3:1 clearly show how complex **2.3** favours the formation of the most thermodynamically stable β -trans product. $[\text{Ir}(\text{NCN}^{\text{Me}})(\text{COD})]\text{BPh}_4$ (**2.4**) proved to be quite inactive with an overall conversion of < 1%. A Rh metal centre is therefore more active than iridium for complexes with COD co-ligands. This outcome is reversed for complexes with CO co-ligands. Complex $[\text{Ir}(\text{NCN}^{\text{Me}})(\text{CO})_2]\text{BPh}_4$ (**2.7**) reached 14 % total conversion with

the major formation of the β -trans product. In comparison the rhodium complex $[\text{Rh}(\text{NCN}^{\text{Me}})(\text{CO})]_2(\text{BPh}_4)_2$ (**2.6**) only reached a poor 9 % conversion in 24 hours. Interestingly, the regioselectivity of the reaction was different when using this bimetallic rhodium compound with only the β -cis isomer being formed. No signs of dehydrogenation or polymerization products were detected by ^1H NMR for all catalytic reactions.^{55,56}

We also wished to investigate the hydrosilylation of non-terminal alkynes, we therefore examined the reaction of 1-phenylpropyne (**3.11**) with Et_3SiH . The hydrosilylation of 1-phenylpropyne (**3.11**) can potentially lead to the formation of four products, two pairs of isomers (*E* or *Z*) obtained from the addition of the Et_3Si to either the phenyl (α) or methyl (β) end of the alkyne (Scheme 3.30). In this study only β -*E* (**3.12A**) and β -*Z* (**3.12B**) isomers were observed.



Scheme 3.30

In Figure 3.8 are reported the catalytic conversions achieved by complexes $[\text{Rh}(\text{NCN}^{\text{Me}})(\text{COD})]\text{BPh}_4$ (**2.3**), $[\text{Ir}(\text{NCN}^{\text{Me}})(\text{COD})]\text{BPh}_4$ (**2.4**),

$[\text{Rh}(\text{NCN}^{\text{Me}})(\text{CO})]_2(\text{BPh}_4)_2$ (**2.6**) and $[\text{Ir}(\text{NCN}^{\text{Me}})(\text{CO})_2]\text{BPh}_4$ (**2.7**) in acetone- d_6 at 55 °C after 24 hours.

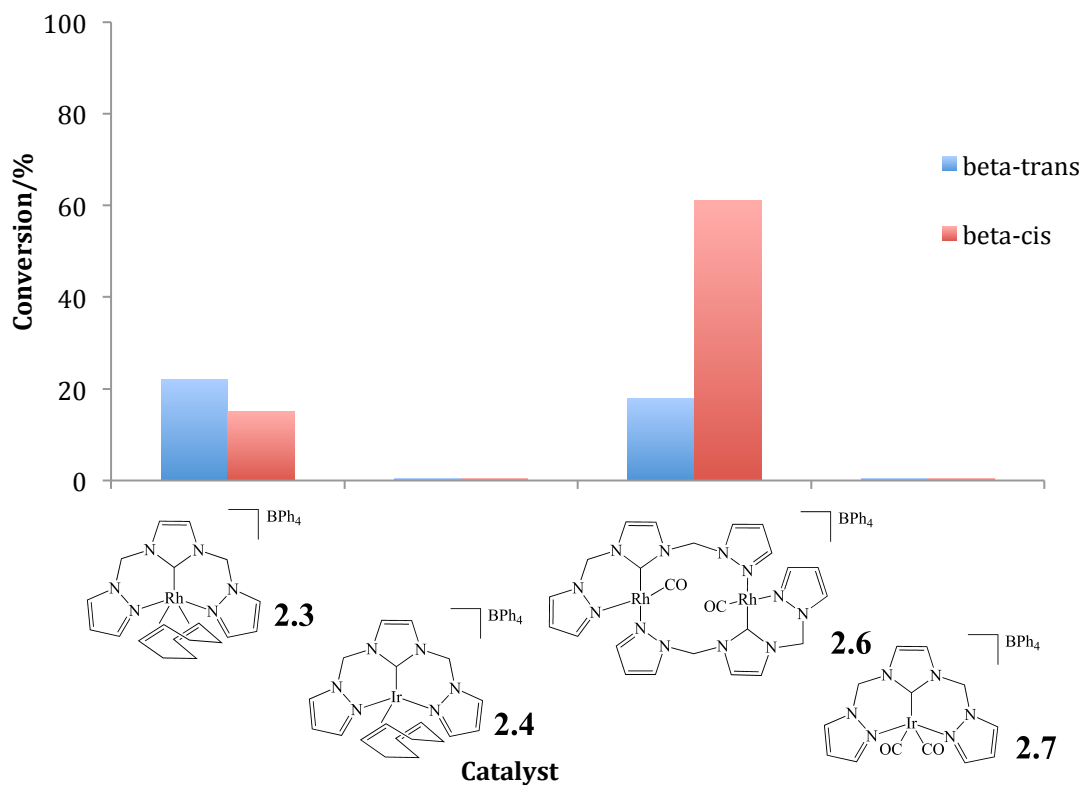


Figure 3.8: Product distribution at 24 hours for the hydrosilylation of 1-phenylpropyne (**3.11**) in acetone- d_6 at 55 °C with 3 mol% of the pincer complexes $[\text{Rh}(\text{NCN}^{\text{Me}})(\text{COD})]\text{BPh}_4$ (**2.3**), $[\text{Ir}(\text{NCN}^{\text{Me}})(\text{COD})]\text{BPh}_4$ (**2.4**), $[\text{Rh}(\text{NCN}^{\text{Me}})(\text{CO})]_2(\text{BPh}_4)_2$ (**2.6**) and $[\text{Ir}(\text{NCN}^{\text{Me}})(\text{CO})_2]\text{BPh}_4$ (**2.7**).

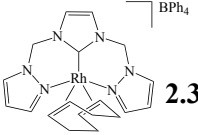
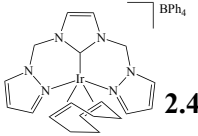
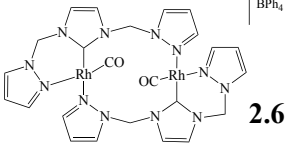
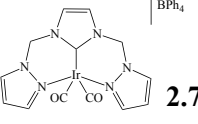
Complex $[\text{Rh}(\text{NCN}^{\text{Me}})(\text{COD})]\text{BPh}_4$ (**2.3**) achieved a total conversion of 37 % with an isomeric distribution of $\beta\text{-Z}:\beta\text{-E} = 1.4:1$. The bimetallic CO containing complex $[\text{Rh}(\text{NCN}^{\text{Me}})(\text{CO})]_2(\text{BPh}_4)_2$ (**2.6**), instead achieved an excellent conversion of 79 % with an inverse isomeric distribution of $\beta\text{-Z}:\beta\text{-E} = 0.3:1$. The iridium complexes $[\text{Ir}(\text{NCN}^{\text{Me}})(\text{COD})]\text{BPh}_4$ (**2.4**) and $[\text{Ir}(\text{NCN}^{\text{Me}})(\text{CO})_2]\text{BPh}_4$ (**2.7**) on the other hand revealed to be entirely inactive catalysts for the transformation of non-terminal alkynes.

A comparison of the maximum conversion achieved for the hydrosilylation of phenylacetylene (**3.3**) and 1-phenylpropyne (**3.11**) with Et_3SiH by the four pincer

complexes $[\text{Rh}(\text{NCN}^{\text{Me}})(\text{COD})\text{BPh}_4]$ (**2.3**), $[\text{Ir}(\text{NCN}^{\text{Me}})(\text{COD})]\text{BPh}_4$ (**2.4**), $[\text{Rh}(\text{NCN}^{\text{Me}})(\text{CO})]_2(\text{BPh}_4)_2$ (**2.6**) and $[\text{Ir}(\text{NCN}^{\text{Me}})(\text{CO})_2]\text{BPh}_4$ (**2.7**) is reported in Table 3.4.

$[\text{Rh}(\text{NCN}^{\text{Me}})(\text{COD})]\text{BPh}_4$ (**2.3**) was the only complex to be active in the hydrosilylation of both phenylacetylene (**3.3**) and 1-phenylpropyne (**3.11**). The most surprising difference is that observed for the bimetallic complex $[\text{Rh}(\text{NCN}^{\text{Me}})(\text{CO})]_2(\text{BPh}_4)_2$ (**2.6**), which showed a very high activity toward the hydrosilylation of 1-phenylpropyne (**3.11**) (79 % conversion in 24 hours), yet was a very poor catalyst for the hydrosilylation of phenylacetylene (**3.3**) (7 % conversion in 24 hours). For both substrates complex **2.6** showed a high regioselectivity toward the β -*E* isomer, which is opposite to that observed using the analogous COD complex **2.3**, where the β -*Z* isomer was preferred. The catalytic activity of the iridium CO containing complex $[\text{Ir}(\text{NCN}^{\text{Me}})(\text{CO})_2]\text{BPh}_4$ (**2.7**) also showed a strong dependence on the identity of the substrate, with moderate conversions achieved for the terminal alkyne phenylacetylene (**3.3**) (23 % in 24 hours), yet no conversion for 1-phenylpropyne (**3.11**). The contrasting reactivity described here suggests that the mechanism through which the hydrosilylation reactions proceed is different for each catalyst.

Table 3.4: Hydrosilylation of phenylacetylene (R= H) (**3.3**) with Et₃SiH and 1-phenylpropyne (R= CH₃) (**3.11**) with Et₃SiH using [Rh(NCN^{Me})(COD)]BPh₄ (**2.3**), [Ir(NCN^{Me})(COD)]BPh₄ (**2.4**), [Rh(NCN^{Me})(CO)]₂(BPh₄)₂ (**2.6**) and [Ir(NCN^{Me})(CO)₂]BPh₄ (**2.7**) is reported in table 3.4.^[a]

Catalyst	Conversion (24 hrs)	
	Phenylacetylene (3.3)	1-Phenylpropyne (3.11)
 2.3	31% (β-trans:β-cis:α=14:3:1)	37% (β-Z:β-E=1.4:1)
 2.4	<1%	<1%
 2.6	7% (β-trans:β-cis:α=0:0:1)	79% (β-Z:β-E =0.3:1)
 2.7	23% (β-trans:β-cis:α=1:0:0)	<1%

[a] Reaction carried in acetone-d₆ at 55 °C using 3 mol% catalyst loading.

3.3 Summary and conclusions

The six Ir(I) and Rh(I) pincer complexes of [Rh(NCN^{Me})(COD)]BPh₄ (**2.3**), [Ir(NCN^{Me})(COD)]BPh₄ (**2.4**), [Rh(NCN^{Me})(CO)]₂(BPh₄)₂ (**2.6**), [Ir(NCN^{Me})(CO)₂]BPh₄ (**2.7**), [Rh(NCN^{Et})(COD)]BPh₄ (**2.9**), [Rh(NCN^{Et})(CO)₂]BPh₄

(**2.10**) and the two analogous chelated complexes $[\text{Rh}(\text{NC}^{\text{Me}})(\text{COD})]\text{BPh}_4$ (**2.11**) and $[\text{Rh}(\text{NC}^{\text{Me}})(\text{CO})_2]\text{BPh}_4$ (**2.12**) were tested as catalysts for a variety of X-H bond addition reactions to alkynes. For the intra-molecular hydroamination of 5-phenyl-4-pentyn-1-amine (**3.1**) the pincer NCN ligand geometry proved to inhibit the activity of the catalysts compared to the bidentate *N,C*- ligand. The opposite was observed for the intra-molecular cyclisation of 4-pentynoic acid (**3.6**), where the pincer motif was found to stabilise the catalysts against deactivation resulting in higher overall conversions. Typically, it was the CO containing catalysts that were the most active for the addition of N-H and O-H bonds to alkynes, with the rhodium complexes of this group more efficient than iridium.

Apart from affecting the relative rates of reaction, the catalyst structure also appeared to have a pronounced impact on the mechanism for the cyclisation of 4-pentynoic acid (**3.6**). For example, a sigmoidal reaction profile was observed with the rhodium complex $[\text{Rh}(\text{NCN}^{\text{Me}})(\text{COD})]\text{BPh}_4$ (**2.3**), however a linear reaction profile was observed with the analogous iridium complex $[\text{Ir}(\text{NCN}^{\text{Me}})(\text{COD})]\text{BPh}_4$ (**2.4**) and rhodium complex with CO co-ligand $[\text{Rh}(\text{NCN}^{\text{Me}})(\text{CO})]_2(\text{BPh}_4)_2$ (**2.6**). Similarly, the divergent substrate dependence and regioselectivities observed during the hydrosilylation of phenylacetylene and 1-phenylpropene suggest that the exact mechanism of the reaction is dependent on the catalysts identity.

The bimetallic rhodium complex $[\text{Rh}(\text{NCN}^{\text{Me}})(\text{CO})]_2(\text{BArF})_2$ (**2.6.BArF**) proved to be particularly advantageous for the inter-molecular hydroamination of aniline and phenylacetylene (**3.3**), where it was found to be the most active catalyst of the series. The analogous BPh_4^- salt $[\text{Rh}(\text{NCN}^{\text{Me}})(\text{CO})]_2(\text{BPh}_4)_2$ (**2.6**) was found to be the most active catalyst for the inter-molecular hydrosilylation of 1-phenylpropyne. Further work is needed to determine whether the bimetallic nature of these complexes is

retained during reaction and how any benefit is obtained from the close arrangement of the two metal centres.

3.4 References

- (1) Bauer, R. C.; Gloaguen, Y.; Lutz, M.; Reek, J. N. H.; de Bruin, B.; van der Vlugt, J. I. *Dalton Trans.* **2011**, 40, 8822.
- (2) Feller, M.; Ben-Ari, E.; Iron, M. A.; Diskin-Posner, Y.; Leituss, G.; Shimon, L. J. W.; Konstantinovski, L.; Milstein, D. *Inorg. Chem.* **2010**, 49, 1615.
- (3) Selander, N.; J. Szabó, K. *Chem. Rev.* **2010**, 111, 2048.
- (4) Leis, W.; Mayer, H. A.; Kaska, W. C. *Coord. Chem. Rev.* **2008**, 252, 1787.
- (5) Pugh, D.; Danopoulos, A. A. *Coord. Chem. Rev.* **2007**, 251, 610.
- (6) Moulton, C. J.; Shaw, B. L. *J. Chem. Soc., Dalton Trans.* **1976**, 1020.
- (7) Ohff, M.; Ohff, A.; van der Boom, M. E.; Milstein, D. *J. Am. Chem. Soc.* **1997**, 119, 11687.
- (8) Bedford, R. B.; Draper, S. M.; Noelle Scully, P.; Welch, S. L. *New J. Chem.* **2000**, 24, 745.
- (9) Singleton, J. T. *Tetrahedron* **2003**, 59, 1837.
- (10) Zhang, J.; Leituss, G.; Ben-David, Y.; Milstein, D. *J. Am. Chem. Soc.* **2005**, 127, 10840.
- (11) Precht, M. H. G.; Wobser, K.; Theyssen, N.; Ben-David, Y.; Milstein, D.; Leitner, W. *Catalysis Science & Technology* **2012**, 2, 2039.
- (12) Gnanaprakasam, B.; Zhang, J.; Milstein, D. *Angew. Chem., Int. Ed. Engl.* **2010**, 49, 1468.
- (13) Khaskin, E.; Iron, M. A.; Shimon, L. J. W.; Zhang, J.; Milstein, D. *J. Am. Chem. Soc.* **2010**, 132, 8542.
- (14) Zhang, J.; Leituss, G.; Ben-David, Y.; Milstein, D. *Angew. Chem., Int. Ed.* **2006**, 45, 1113.

-
- (15) Kohl, S. W.; Weiner Lev; Schwartzburd, L.; Konstantinovski, L.; Shimon, L. J. W.; Yehoshoa, B.-D.; Iron, M. A.; Milstein, D. *Science* **2009**, *324*, 74.
- (16) Lv, K.; Cui, D. *Organometallics* **2010**, *29*, 2987.
- (17) Gibson, V. C.; Spitzmesser, S. K. *Chem. Rev.* **2003**, *103*, 283.
- (18) Gao, W.; Cui, D. *J. Am. Chem. Soc.* **2008**, *130*, 4984.
- (19) Theodore, R. H.; Hollis, T. K.; Edward, J. V. *Organometallics* **2012**, *31*, 3002.
- (20) Liu, F.; S. Goldman, A. *Chem. Commun.* **1999**, 655.
- (21) Choi, J.; MacArthur, A. H.; Brookhart, M.; Goldman, A. S. *Chem. Rev.* **2011**, *111*, 1761.
- (22) Timpa, S. D.; Fafard, C. M.; Herbert, D. E.; Ozerov, O. V. *Dalton Trans.* **2011**, *40*, 5426.
- (23) van der Boom, M. E.; Milstein, D. *Chem. Rev.* **2003**, *103*, 1759.
- (24) Zhao, J.; Goldman, A. S.; Hartwig, J. F. *Science* **2005**, *307*, 1080.
- (25) McLoughlin, M. A.; Flesher, R. J.; Kaska, W. C.; Mayer, H. A. *Organometallics* **1994**, *13*, 3816.
- (26) Morgan, E.; MacLean, D.; McDonald, R.; Turculet, L. *J. Am. Chem. Soc.* **2009**, *131*, 14234.
- (27) Fang, H.; Choe, Y.-K.; Li, Y.; Shimada, S. *Chem. Asian J.* **2011**, *6*, 2512.
- (28) Bauer, E.; Andavan, G.; Hollis, T.; Rubio, R.; Cho, J.; Kuchenbeiser, G.; Helgert, T.; Letko, C.; Tham, F. *Org. Lett.* **2008**, *10*, 1175.
- (29) Andavan, G. T. S.; Bauer, E. B.; Letko, C. S.; Hollis, T. K.; Tham, F. S. *J. Organomet. Chem.* **2005**, *690*, 5938.
- (30) Chianese, A. R.; Shaner, S. E.; Tendler, J. A.; Pudalov, D. M.; Shopov, D. Y.; Kim, D.; Rogers, S. L.; Mo, A. *Organometallics* **2012**, *31*, 7359.

-
- (31) Hartung, C. G.; Tillack, A.; Trauthwein, H.; Beller, M. *J. Org. Chem.* **2001**, *66*, 6339.
- (32) Alonso-Moreno, C.; Carrillo-Hermosilla, F.; Romero-Fernández, J.; Rodríguez, A. M.; Otero, A.; Antiñolo, A. *Adv. Synth. Catal.* **2009**, *351*, 881.
- (33) Sakai, K.; Kochi, T.; Kakiuchi, F. *Org. Lett.* **2011**, *13*, 3928.
- (34) Burling, S.; Field, L. D.; Messerle, B. A.; Turner, P. *Organometallics* **2004**, *23*, 1714.
- (35) Field, L. D.; Messerle, B. A.; Vuong, K. Q.; Turner, P. *Organometallics* **2005**, *24*, 4241.
- (36) Field, L. D.; Messerle, B. A.; Vuong, K. Q.; Turner, P.; Failes, T. *Organometallics* **2007**, *26*, 2058.
- (37) Julian, L. D.; Hartwig, J. F. *J. Am. Chem. Soc.* **2010**, *132*, 13813.
- (38) Rung-Yi, L.; Surekha, K.; Akito, H.; Fumiyuki, O.; Yi-Hong, L.; Shie-Ming, P.; Shiuh-Tzung, L. *Organometallics* **2007**, *26*, 1062.
- (39) Gray, K.; Page, M. J.; Wagler, J.; Messerle, B. A. *Organometallics* **2012**, *31*, 6270.
- (40) Li, X.; Chianese, A. R.; Vogel, T.; Crabtree, R. H. *Org. Lett.* **2005**, *7*, 5437.
- (41) Elgafi, S.; Field, L. D.; Messerle, B. A. *J. Organomet. Chem.* **2000**, *607*, 97.
- (42) Man, B. Y. W.; Bhadbhade, M.; Messerle, B. A. *New J. Chem.* **2011**, *35*, 1730.
- (43) Ho, J. H. H.; Black, D. S. C.; Messerle, B. A.; Clegg, J. K.; Turner, P. *Organometallics* **2006**, *25*, 5800.
- (44) Chan, D. M. T.; Marder, T. B.; Milstein, D.; Taylor, N. J. *J. Am. Chem. Soc.* **1987**, *109*, 6385.
- (45) Geier, M. J.; Vogels, C. M.; Decken, A.; Westcott, S. A. *Eur. J. Inorg. Chem.* **2010**, *2010*, 4602.

-
- (46) Ho, J. H. H.; Choy, S. W. S.; Macgregor, S. A.; Messerle, B. A. *Organometallics* **2011**, *30*, 5978.
- (47) Field, L. D.; Ward, A. J. *J. Organomet. Chem.* **2003**, *681*, 91.
- (48) Faller, J. W.; D'Alliessi, D. G. *Organometallics* **2002**, *21*, 1743.
- (49) Mas-Marzá, E.; Sanaú, M.; Peris, E. *Inorg. Chem.* **2005**, *44*, 9961.
- (50) Viciano, M.; Mas-Marzá, E.; Sanaú, M.; Peris, E. *Organometallics* **2006**, *25*, 3063.
- (51) Jiménez, M. V.; Pérez-Torrente, J. J.; Bartolomé, M. I.; Gierz, V.; Lahoz, F. J.; Oro, L. A. *Organometallics* **2007**, *27*, 224.
- (52) Busetto, L.; Cassani, M. C.; Femoni, C.; Mancinelli, M.; Mazzanti, A.; Mazzoni, R.; Solinas, G. *Organometallics* **2011**, *30*, 5258.
- (53) Zeng, J. Y.; Hsieh, M.-H.; Lee, H. M. *J. Organomet. Chem.* **2005**, *690*, 5662.
- (54) Dabb, S. L.; Ho, J. H. H.; Hodgson, R.; Messerle, B. A.; Wagler, J. *Dalton Trans.* **2009**, 634.
- (55) Jun, C.-H.; Crabtree, R. H. *J. Organomet. Chem.* **1993**, *447*, 177.
- (56) Kishimoto, Y.; Eckerle, P.; Miyatake, T.; Ikariya, T.; Noyori, R. *J. Am. Chem. Soc.* **1994**, *116*, 12131.

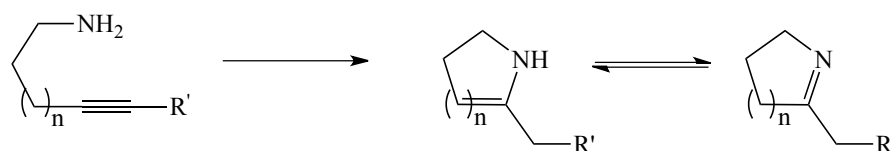
Inter-molecular
Hydroamination

4.1 Introduction

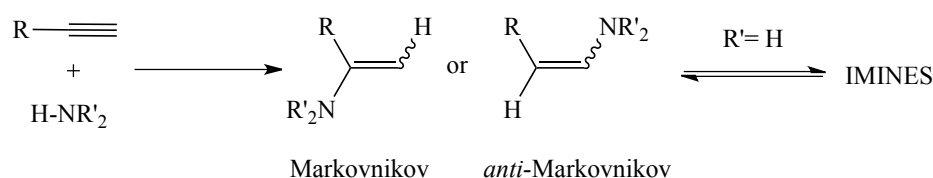
4.1.1 The inter-molecular hydroamination of alkynes

Amines, enamines and imines are important chemical intermediates in the synthesis of natural compounds, pharmacological agents, fine chemicals, agrochemicals, dyes and many other valuable molecules.¹ An important route to the synthesis of these compounds is hydroamination, which leads to the synthesis of *N*-containing compounds through the addition of an N-H bond across an unsaturated CC bond. During this process no side product formation occurs, making it a very atom efficient and environmentally attractive method. Hydroamination can occur either intra-molecularly (Scheme 4.1 a) or inter-molecularly (Scheme 4.1 b) and use either primary or secondary amines. For the hydroamination of alkynes with primary amines the resulting enamines often tautomerise to give the more stable imines as the final product. Both Markovnikov and anti-Markovnikov regioisomers are also possible.²

a) INTRA-MOLECULAR HYDROAMINATION



b) INTER-MOLECULAR HYDROAMINATION



Scheme 4.1

The alkyne π -bonds are approximately 70 kJ mol^{-1} weaker than a π -bond of a typical

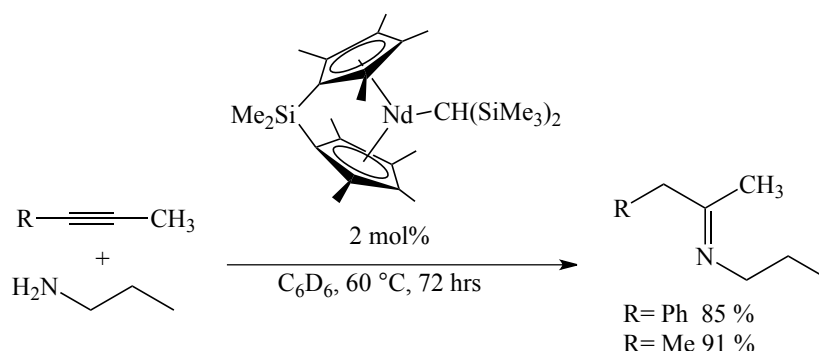
alkene, they are less sterically hindered and have more nucleophilic sp-hybridized C-atoms.¹ Although the hydroamination of alkynes is slightly exothermic² there are a few factors that hamper the success of this reaction. Firstly, hydroamination is characterised by a high reaction barrier due to the electrostatic repulsion between the nitrogen electron lone pair and the electron rich π -bond. At the same time, the use of high reaction temperatures disfavors the formation of products due to the negative entropy of the reaction. Finally, the [2+2] cycloaddition of N-H across the C-C bond is orbital-forbidden under thermal conditions because of the high-energy difference between the $\pi(\text{CC})$ and $\sigma(\text{NH})$ bond energy. A catalyst is therefore necessary in order to lower the energy barrier enough for the reaction to proceed.

The much higher entropic penalty of bringing two separate molecules together during the inter-molecular hydroamination reaction significantly increases the difficulty of this process compared to the intra-molecular hydroamination reaction. One of the current challenges in this field is therefore the development of catalysts that can effectively facilitate the inter-molecular hydroamination of alkynes.

4.1.2 Inter-molecular hydroamination catalysts

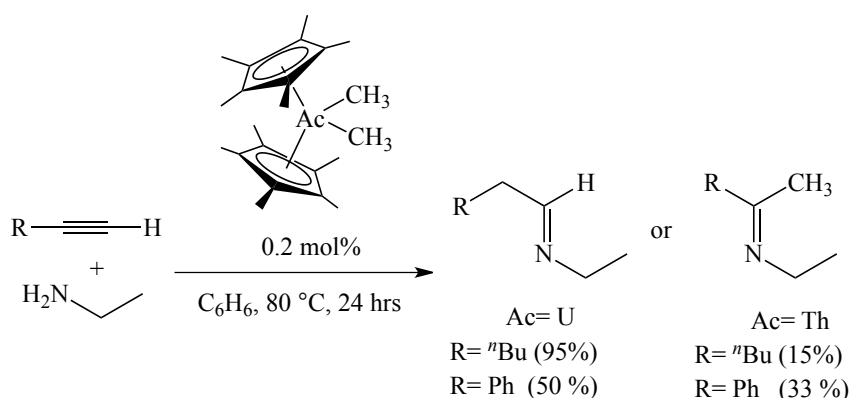
4.1.2.1 Lanthanide and actinide complexes

The first organolanthanide catalysts that were used for the hydroamination of alkynes were reported in 1996 by Tobin Marks *et al.*³ Catalysts of the general formula $(\text{Me}_2\text{SiCp}^\#)_2\text{LnCH}(\text{SiMe}_3)_2$ ($\text{Cp}^\# = \eta^5\text{-C}_5\text{Me}_4$, Ln = Sm, Lu, Nd) were used to promote the inter-molecular hydroamination of internal alkynes using primary aliphatic amines (Scheme 4.2). The reactions proceeded at 60 °C, yielding up to 91 % of the imine products, but a much extended reaction time of 3 days was required.



Scheme 4.2

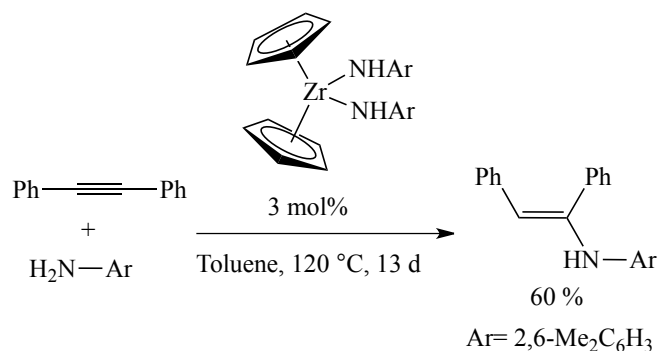
Eisen *et al.* have also used similar actinide based complexes of the type $\text{Cp}^*_2\text{AcMe}_2$ ($\text{Cp}^* = \eta^5\text{-C}_5\text{Me}_5$, $\text{Ac} = \text{U}, \text{Th}$) to promote the hydroamination of terminal alkynes.⁴ The uranium catalyst was reported to be very efficient for the hydroamination of aliphatic alkynes reaching up to 95 % conversion of 1-hexyne in 24 hours at 80 °C and only 0.2 mol% catalyst loading (Scheme 4.3). The catalyst was much less efficient for the hydroamination of phenylacetylene (50 % conversion, 24 hours). When thorium was used as the catalyst the alternative Markovnikov regioisomers were exclusively formed, however much lower yields were obtained.



Scheme 4.3

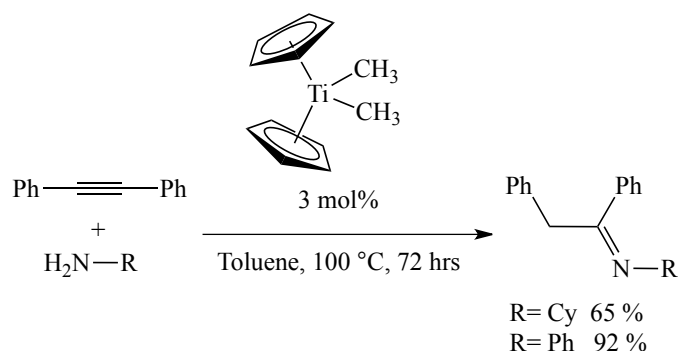
4.1.2.2 Early Transition Metal Complexes

The first group IV metal catalysts that promoted the inter-molecular hydroamination of alkynes were reported in 1992 by Bergman *et al.*⁵ They found the zirconium(IV) bisamide complex $\text{Cp}_2\text{Zr}(\text{NHAr})_2$ ($\text{Cp} = \eta^5\text{-C}_5\text{H}_5$, $\text{Ar} = 2,6\text{-dimethylphenyl}$) catalyzed the inter-molecular addition of 2,6-dimethylaniline to internal alkynes at 120 °C and 3 mol% catalyst (Scheme 4.4). Under these conditions the hydroamination of diphenylacetylene gave the enamine product over exceptionally long reaction times (60 % after 13 days).



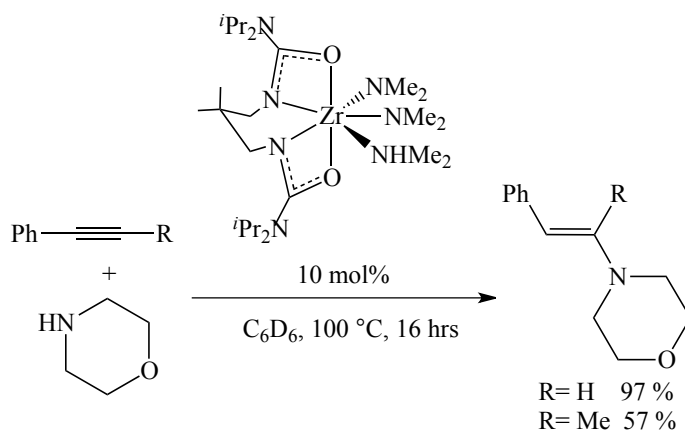
Scheme 4.4

In comparison, the structurally related titanium(IV) complex Cp_2TiMe_2 was shown to be a far more active and general catalyst for the inter-molecular hydroamination of internal alkynes with both aliphatic and aromatic amines. For example, the hydroamination of diphenylacetylene at 100 °C for 72 hours using 3 mol% Cp_2TiMe_2 gave good conversions in the case of both cyclohexylamine (65 %) and aniline (92 %) as substrates (Scheme 4.5).⁶



Scheme 4.5

More recently a zirconium ureate complex was reported by Schafer *et al.* to be an efficient catalyst for the hydroamination of alkynes using secondary amines (Scheme 4.6).⁷ These reactions were performed at 100 °C for 16 hours with quite high catalyst loadings of 10 mol%. Under such conditions the efficiency of conversion to the corresponding enamine product was found to be much higher in the case of phenylacetylene (97 %) than in case of to the internal alkyne 1-phenyl-1-propyne (57 %).

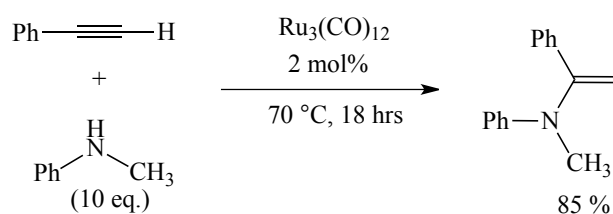


Scheme 4.6

4.1.2.3 Late Transition Metal Complexes

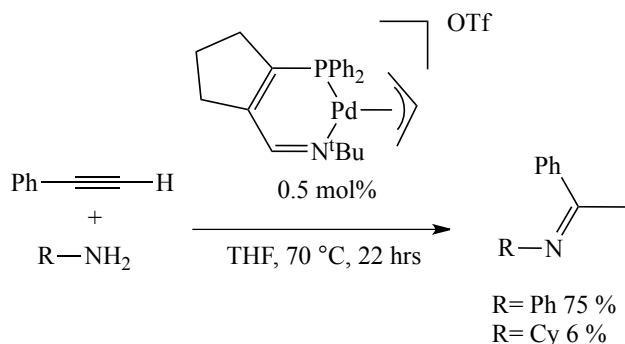
Among catalysts of the late transition metals, those of $\text{Ru}^{8,9,10}$ and $\text{Pd}^{11,12}$ are those

most commonly investigated for the inter-molecular hydroamination reaction. The first example of a Ru catalysed inter-molecular hydroamination reaction was published in 1999 using $\text{Ru}_3(\text{CO})_{12}$.⁸ The hydroamination of phenylacetylene and *N*-methylaniline was carried out in sealed glass tubes using 2 mol% of $\text{Ru}_3(\text{CO})_{12}$ catalyst at 70 °C for 18 hours in the absence of a solvent (Scheme 4.7). High conversions were achieved (85 %), however a ten-fold excess of amine was necessary for the reaction to proceed. The formation of an (amido)ruthenium hydride complex was proposed as the active inter-mediate for this reaction.¹⁰



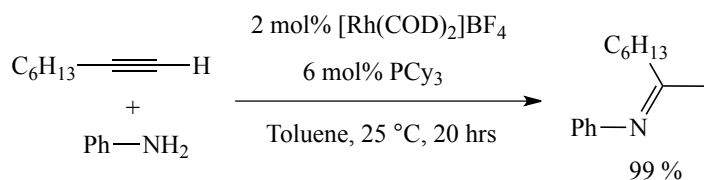
Scheme 4.7

A palladium allyl complex containing a phosphine-imine chelate has recently been demonstrated to catalyse the hydroamination of phenylacetylene using a variety of amines (Scheme 4.8).¹² The reaction was performed using only 0.5 mol% catalyst at 70 °C for 22 hours. When aniline was used, high conversions were achieved (75 %), however cyclohexylamine gave very poor conversions (6 %).



Scheme 4.8

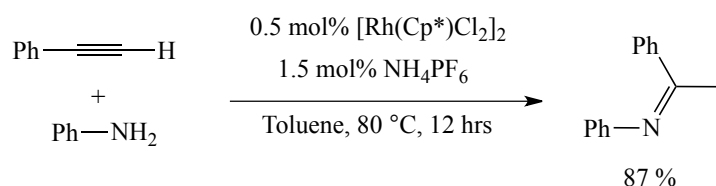
A number of rhodium catalysts for the inter-molecular hydroamination reaction have been reported.¹³⁻¹⁵ In 2001 Beller *et al.* reported the application of the commercially available complex $[\text{Rh}(\text{COD})_2]\text{BF}_4$ (COD= 1,5-cyclooctadiene) in combination with the phosphine ligand PCy_3 as an exceptionally efficient catalyst for the inter-molecular hydroamination of terminal aliphatic alkynes and primary aromatic amines.¹⁶ For example, when 2 mol% Rh and 6 mol% PCy_3 were combined with 1-octyne and aniline, then quantitative conversion of the substrates was achieved after 20 hours at room temperature (Scheme 4.9). The substrate scope of this reaction however was very limited. The combination of aniline and phenylacetylene gave less than 10 % conversion under the same conditions, while 1-octyne was entirely unreactive towards aliphatic amines.



Scheme 4.9

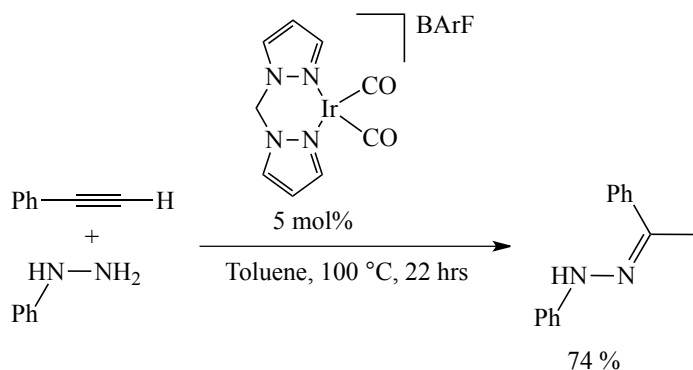
Just recently Leong *et al.* reported that the Rh(III) complex $[\text{Cp}^*\text{RhCl}_2]_2$, in

combination with a halide abstracting reagent, was able to successfully catalyze the inter-molecular hydroamination of aromatic alkynes and amines.¹⁵ The hydroamination of phenylacetylene with aniline achieved 87 % conversion using 0.5 mol% Rh and 1.5 mol% NH_4PF_6 at 80 °C after 12 hours (Scheme 4.10). The catalyst system was also able to tolerate a wide range of electron withdrawing and donating substituents on both substrates.



Scheme 4.10

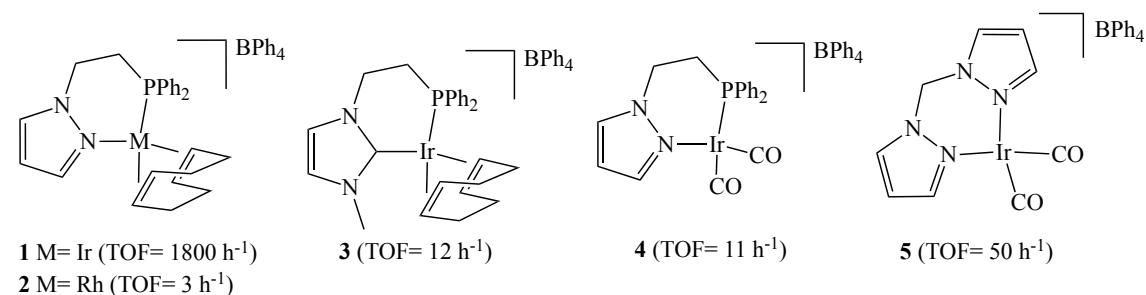
Very few examples of iridium catalyzed inter-molecular hydroamination of alkynes have been reported in the literature.¹⁶ An interesting example reported by Messerle *et al.* involved the addition of phenylhydrazine to phenylacetylene.¹⁷ This reaction was performed at 100 °C using 5 mol% of the bis(pyrazolyl)methane (bpm) complex $[\text{Ir}(\text{bpm})(\text{CO})_2]\text{BArF}$ (BArF = tetrakis(3,5-trifluoromethylphenyl)borate), and resulted in 74 % conversion after 22 hours (Scheme 4.11).



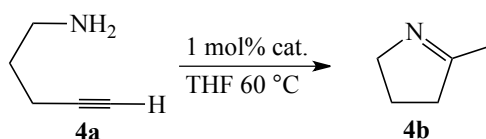
Scheme 4.11

4.1.3 Ir(I) and Rh(I) Intra-molecular Hydroamination Catalysts

Messerle *et al.* have developed a series of Ir(I) and Rh(I) catalysts featuring a selection of bidentate ligands containing nitrogen, phosphorus and *N*-heterocyclic carbene donor groups with COD and CO co-ligands (Scheme 4.12 a).¹⁸⁻²⁰ These complexes were shown to efficiently catalyse the intra-molecular hydroamination reaction. The most efficient catalyst of this series was found to be the iridium COD complex **1** which contains a pyrazolyl-phosphine (PyP) chelate.¹⁸ This catalyst effected the hydroamination of 4-pentyn-1-amine (**4a**) to 2-methyl-1-pyrroline (**4b**) (Scheme 4.12 b) within 30 minute at 60 °C and 1.4 mol% catalyst loading (turnover frequency, TOF= 1800 h⁻¹).



a)



b)

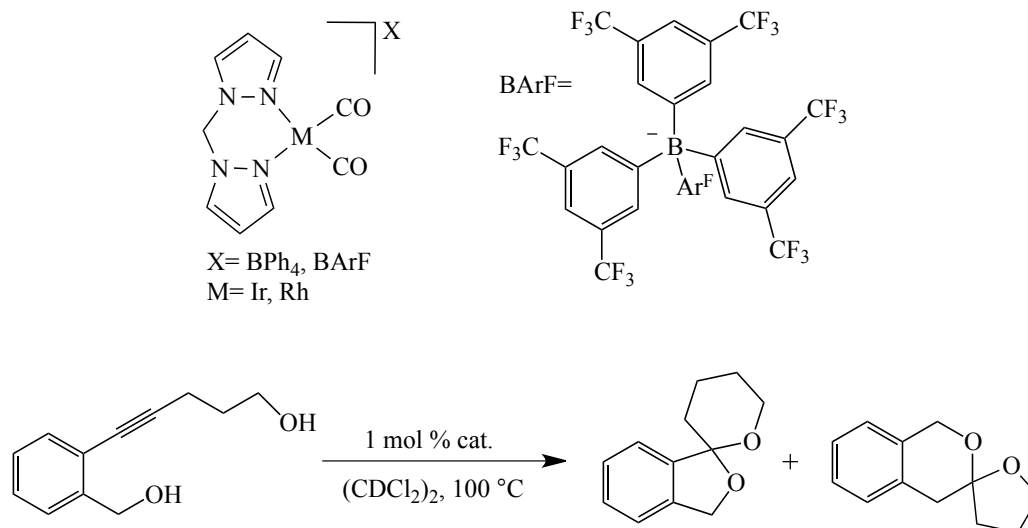
Scheme 4.12

The investigation of related catalysts all gave lower conversions for the same reaction. For example substitution of the pyrazolyl-phosphine ligand in **1** for an *N*-heterocyclic carbene (NHC)-phosphine chelate (complex **3**) drastically reduced the efficiency of the

catalyst (TOF= 12 h⁻¹).²⁰ Similarly for the analogous rhodium complex with the PyP ligand **2** (TOF= 3 h⁻¹) and Ir complex with carbonyl co-ligands **4** (TOF= 11 h⁻¹).¹⁸ Typically it was found that Rh(I) and Ir(I) complexes with carbonyl co-ligands were more active catalysts compared to the related systems with COD co-ligand. For example the iridium bis(pyrazolyl)methane (bpm) complex **5** was also a very efficient catalyst for the hydroamination of 4-pentyn-1-amine achieving complete conversion within 2.2 hours at 60 °C and 1.4 mol% catalyst (TOF= 50 h⁻¹).¹⁹

4.1.4 Counter ion effects on Ir(I) and Rh(I) catalysts

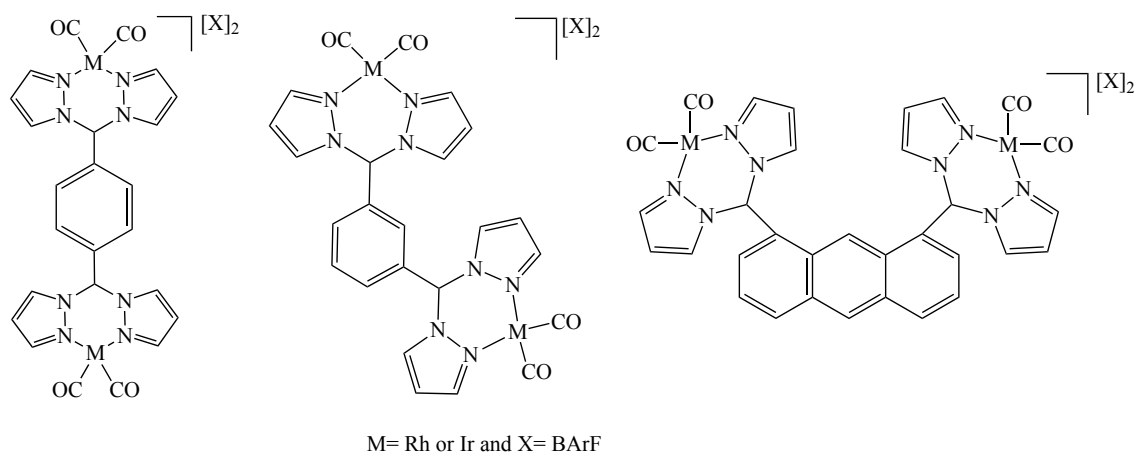
The nature of the counter ion in homogenous transition metal catalysts is well known to have a significant impact on catalyst efficiency. Weakly coordinating anions, such as tetrakis(3,5-trifluoromethylphenyl)borate (BArF), can lead to much improved catalyst activity. This is due to an extremely poor affinity of the anion for vacant coordination sites on the metal, which are therefore more available for reaction. The BArF anion is also more stable than BPh₄⁻ towards B-Ar bond cleavage, which improves catalyst stability (see Section 1.7, Chapter 1). In 2010 Messerle *et al.* investigated the catalytic activity of Rh(I) and Ir(I) complexes of the type [M(bpm)(CO)₂]X (where X= BPh₄⁻ or BArF) for the dihydroalkoxylation of 2-(5-hydroxypent-1-ynyl)benzyl alcohol (Scheme 4.13).²¹ They found that substitution of the BPh₄⁻ counter ion for BArF led to a massive increase in reaction rate for both iridium and rhodium systems. For example, the BArF catalyst [Rh(bpm)(CO)₂]BArF achieved complete conversion of the substrate after 0.22 hours (TOF= 961 h⁻¹) compared to a reaction time of 21 hours (TOF= 90 h⁻¹) for the BPh₄⁻ catalyst [Rh(bpm)(CO)₂]BPh₄ under identical conditions.



Scheme 4.13

4.1.5 Bimetallic Ir(I) and Rh(I) Catalysts

The use of bimetallic complexes in homogeneous catalysis has been shown on many occasions to yield catalysts of very high efficiency. The activity of the bimetallic catalysts is often several orders of magnitude greater than the sum of the corresponding monometallic catalysts. This phenomenon is known as intermetallic ‘cooperativity’. Very recently Messerle *et al.* reported the synthesis of a bimetallic system where two Ir(I) or Rh(I) bis(pyrazolyl)methane complexes were immobilized onto a shared aromatic scaffold (Scheme 4.14).²² These complexes were shown to be very active for the dihydroalkoxylation of a range of alkynediol substrates to yield spiroketals. The bimetallic catalysts were shown to be much more active than the two monometallic counterparts with the catalyst cooperativity increasing as the metal-metal separation decreased. The application of these bimetallic systems towards related catalytic transformations has yet to be investigated.



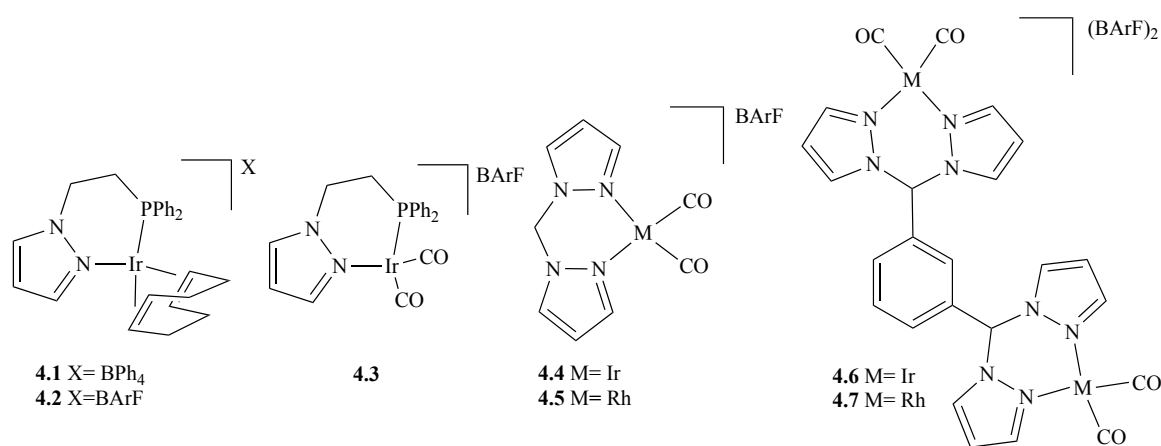
Scheme 4.14

4.1.6 Objectives

The aim of this work was to identify a catalytic system that would be highly active for the inter-molecular hydroamination of alkynes. A series of Ir(I) and Rh(I) complexes were tested and the influence of the ligands, coligands and counter ions investigated, as well as a bimetallic catalyst motif. The catalysts under investigation are shown in Scheme 4.15, with key areas of investigation described below:

- A series of catalysts will be investigated for their ability to catalyse the inter-molecular hydroamination of terminal alkynes with primary amines. To explore the substrate scope of these catalysts both aromatic and aliphatic substituents on both substrates will be examined.
- Optimisation of catalytic reactions will be explored by investigating influence of solvent and temperature on the efficiency of these reactions.
- The influence of counter ion on catalyst activity will be investigated by comparing catalysts containing the tetraphenylborate (BPh_4^-) anion with catalysts containing the more weakly coordinating *tetrakis*(3,5-trifluoromethylphenyl)borate (BArF) anion.

- The effect of the catalyst co-ligand on the efficiency of the catalyst will be explored by investigating both 1,5-cyclooctadiene (COD) and the strongly π -basic carbon monoxide (CO) co-ligands.
- The chelating ligand group will be varied from the mixed *P,N*-donor ligand 1-[2-(diphenylphosphino)ethyl]pyrazole (PyP) to the more weakly coordinating *N,N*-donor ligand *bis*(1-pyrazolyl)methane (bpm).
- How the identity of the metal centre impacts the catalytic activity of the complex will be explored by testing both Rh(I) and Ir(I) complexes.
- The catalytic efficiency of two bimetallic Ir(I) and Rh(I) complexes will be investigated in order to assess whether cooperative enhancement of the catalyst activity can be achieved for inter-molecular hydroamination.

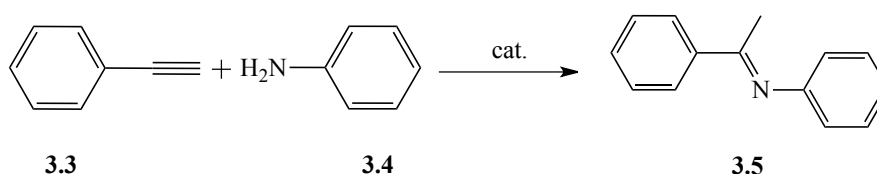


Scheme 4.15

4.2 Results and discussion

4.2.1 Hydroamination of phenylacetylene (3.3) and aniline (3.4)

4.2.1.1 Catalysts with *P,N*-donor ligand: [Ir(PyP)(COD)]BPh₄ (4.1), [Ir(PyP)(COD)]BArF (4.2) and [Ir(PyP)(CO)]BArF (4.3)



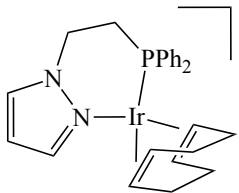
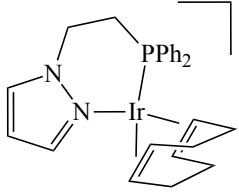
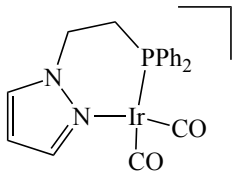
Scheme 4.16

The reaction of phenylacetylene with aniline (Scheme 4.16) was carried out on a small scale in deuterated solvents within NMR tubes sealed under a N₂ atmosphere. A catalyst loading of 3 mol% was used and reaction conversions were determined by acquisition of the ¹H NMR spectrum of the solution and comparison of the substrate and product integrals with the integral of an internal standard (1,3,5-trimethoxybenzene) of known quantity. The results for the hydroamination of phenylacetylene (3.3) and aniline (3.4) using catalysts [Ir(PyP)(COD)]BPh₄ (4.1), [Ir(PyP)(COD)]BArF (4.2) and [Ir(PyP)(CO)]BArF (4.3) are summarized in Table 4.1.

The first catalyst to be investigated was the tetraphenylborate salt [Ir(PyP)(COD)]BPh₄ (4.1). The reaction was performed at 100 °C in a variety of solvents TCE-d₂, toluene-d₈ and 1,4-dioxane-d₈ and after 24 hours no product formation was detected. However, the ¹H NMR spectrum of the reaction solution revealed no trace of the phenylacetylene (3.3) starting material either and a broad lump in the aromatic region of the spectrum suggested the phenylacetylene (3.3) had oligomerized. The oligomerisation/polymerization of phenylacetylene (3.3) is

commonly observed under such vigorous reaction conditions when the rate of hydroamination is comparatively slow.²³⁻²⁵

Table 4.1: Comparison of the catalytic activity of [Ir(PyP)(COD)]BPh₄ (**4.1**), [Ir(PyP)(COD)]BArF₄ (**4.2**) and [Ir(PyP)(CO)₂]BArF₄ (**4.3**) for the inter-molecular hydroamination of phenylacetylene (**3.3**) and aniline (**3.4**).^[a]

Entry	Catalyst	Solvent	Conversion (%)	
			(1.5 hrs)	(25 hrs)
1	 4.1	TCE-d ₂ (100 °C)	-	<1
2		Tol-d ₈ (100°C)	-	<1
3		1,4-dioxane-d ₈ (100°C)	-	<1
4	 4.2	C ₆ D ₆ (60 °C)	-	26
5		CDCl ₃ (60 °C)	-	13
6		TCE-d ₂ (60 °C)	-	18
7	 4.3	C ₆ D ₆ (60 °C)	29	>98
8		CDCl ₃ (60 °C)	36	80
9		TCE-d ₂ (60°C)	56	81
10		Tol-d ₈ (100°C)	53	>98
11		TCE-d ₂ (100°C)	45	67

[a] 3 mol% catalyst loading used;

The ineffectual result for this catalyst was surprising considering its very high activity for the intra-molecular hydroamination reaction. For example, complete conversion of 4-pentyn-1-amine (**4a**) to 2-methyl-1-pyroline (**4b**) (Scheme 4.12b) was achieved within 30 minutes using 1.4 mol% of [Ir(PyP)(COD)]BPh₄ (**4.1**) at 60 °C.¹⁸

Substitution of the BPh₄⁻ anion in [Ir(PyP)(COD)]BPh₄ (**4.1**) with the *tetrakis*(3,5-trifluoromethylphenyl)borate (BArF) anion in [Ir(PyP)(COD)]BArF (**4.2**) resulted in a much improved catalyst activity. The hydroamination of phenylacetylene (**3.3**) and aniline (**3.4**) was performed at 60 °C in three different solvents: C₆D₆, CDCl₃ and TCE-d₂. The highest conversion was achieved in the non-chlorinated solvent C₆D₆ with 26 % conversion to the *E-N*-(1-phenylethylidene)benzeneamine imine (**3.5**) after 25 hours. Both CDCl₃ and TCE-d₂ gave considerably lower conversions, 18 % and 13% respectively.

Substitution of the COD co-ligand in [Ir(PyP)(COD)]BArF (**4.2**) with the more π -acid carbonyl ligands in [Ir(PyP)(CO)₂]BArF (**4.3**) also led to a dramatic improvement in the catalysts activity. At 60 °C catalyst **4.3** was able to reach complete conversion of the substrates (>98 %) to the desired imine (**3.5**) within 25 hours in C₆D₆. The catalyst performed less well in chlorinated solvents TCE-d₂ (81 %) and CDCl₃ (80 %). Although, the initial reaction rate after 1.5 hours was higher in TCE-d₂ (56 %) and CDCl₃ (36 %) compared to C₆D₆ (29 %).

To see if [Ir(PyP)(CO)₂]BArF (**4.3**) could tolerate harsher reaction conditions the catalysis was also performed at 100 °C. Complete conversion to product was still observed after 25 hours in toluene and an elevated initial reaction rate after 1.5 hours was recorded; 53 % conversion (100 °C) versus 29 % conversion (60 °C). For the chlorinated solvent TCE-d₂, the catalysts performed worse at 100 °C compared to 60 °C with a total conversion of only 67 % achieved after 25 hours. This result suggests

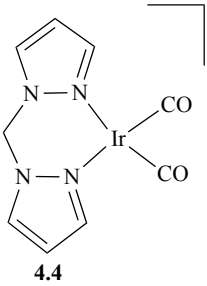
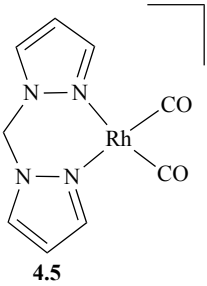
that the catalyst is decomposing in TCE-d₂, a process that is accelerated at higher reaction temperatures. This would also account for the higher initial rates for [Ir(PyP)(CO)₂]BArF (**4.3**) in CDCl₃ and TCE-d₂ at 60 °C despite a lower final conversion compared to the reaction in C₆D₆.

The much higher reactivity of the catalyst with CO co-ligand [Ir(PyP)(CO)₂]BArF (**4.3**) compared to the catalyst with COD co-ligand [Ir(PyP)(COD)]BArF (**4.2**) is in contrast to the results obtained using the analogous BPh₄⁻ salts [Ir(PyP)(CO)₂]BPh₄ (**4**) (see section 4.1.3) and [Ir(PyP)(COD)]BPh₄ (**4.1**) for the intra-molecular hydroamination of 4-pentyn-1-amine. In this case [Ir(PyP)(CO)₂]BPh₄ (**4**) was found to be extremely unreactive (TOF= 11 h⁻¹) compared to [Ir(PyP)(COD)]BPh₄ (**4.1**, TOF= 1800 h⁻¹).¹⁸

4.2.1.2 Catalysts with *N,N*-donor ligands: [Ir(bpm)(CO)₂]BArF (**4.4**) and [Rh(bpm)(CO)₂]BArF (**4.5**)

The hydroamination of phenylacetylene (**3.3**) and aniline (**3.4**) using [Ir(bpm)(CO)₂]BArF (**4.4**) and [Rh(bpm)(CO)₂]BArF (**4.5**) was performed using 3 mol% catalyst at 100 °C in toluene-d₈, TCE-d₂ and 1,4-dioxane-d₈. Product conversions were determined after 24 hours and are summarized in Table 4.2.

Table 4.2: Comparison of the catalytic activity of [Ir(bpm)(CO)₂]BArF (**4.4**) and [Rh(bpm)(CO)₂]BArF (**4.5**) for the inter-molecular hydroamination of phenylacetylene (**3.3**) and aniline (**3.4**).^[a]

Entry	Catalyst	Solvent	Conversion (%) (24 hrs)
1	 4.4	Toluene-d ₈	94
2		TCE-d ₂	85 (50%/0.4h)
3		1,4-dioxane-d ₈	61
4	 4.5	Toluene-d ₈	22
5		TCE-d ₂	10
6		1,4-dioxane-d ₈	21

[a] Reaction performed at 100 °C using 3 mol% catalyst loading

The iridium catalyst [Ir(bpm)(CO)₂]BArF (**4.4**) achieved the highest conversion in toluene-d₈ (94 %), which was significantly more efficient than the reaction in TCE-d₂ (85 %) and 1,4-dioxane-d₈ (61 %). The reaction in TCE-d₂ gave a very fast initial reaction rate with 50 % conversion obtained after only 0.4 hours, however a further 23.6 hours was required to obtain another 30 % conversion, indicating that the complex may be decomposing in this solvent. A similar result was described above for the PyP containing complexes **4.2** and **4.3**.

The rhodium complex [Rh(bpm)(CO)₂]BArF (**4.5**) was shown to be a much poorer catalyst than its iridium analogue **4.4**. Complex **4.5** only achieved a maximum

conversion of 22 % in toluene-d₈, 21 % in dioxane-d₈ and a very poor 10 % in TCE-d₂. These results are comparable with the outcomes obtained for the intra-molecular hydroamination of 4-pentyn-1-amine (**4a**) (Scheme 4.12) using the BPh₄⁻ catalysts [Ir(bpm)(CO)₂]BPh₄ (**5**) and [Rh(bpm)(CO)₂]BPh₄ (**6**).¹⁹ For the iridium complex **6** complete conversion of 4-pentyn-1-amine (**4a**) to 2-methyl-1-pyroline (**4b**) was achieved after 2.2 hours at 60 °C using 1.5 mol% catalyst, whereas the rhodium complex **5** managed only 90 % conversion after 12 hours.

The highest conversion achieved using [Ir(bpm)(CO)₂]BArF (**4.4**) (94%, 24 hours) is comparable to that obtained with the PyP containing catalyst [Ir(PyP)(CO)₂]BArF (**4.3**) (98%, 25 hours). Variation of the *P,N*-donor ligand in **4.3** to a *N,N*-donor ligand in **4.4** therefore has little impact on the catalysts efficiency.

4.2.1.3 Bimetallic catalysts: (μ-L)[Ir(CO)₂]₂(BArF)₂ (**4.6**) and (μ-L)[Rh(CO)₂]₂(BArF)₂ (**4.7**)

The catalytic efficiency of the bimetallic catalysts (μ-L)[Ir(CO)₂]₂(BArF)₂ (**4.6**) and (μ-L)[Rh(CO)₂]₂(BArF)₂ (**4.7**) for the hydroamination of phenylacetylene (**3.3**) and aniline (**3.4**) was performed at 100 °C in TCE-d₂ or toluene-d₈. For comparison to the monometallic catalysts described above only 1.5 mol% of the bimetallic complexes were used to give a total metal loading of 3 mol%. The reactions were performed in NMR tubes that were heated inside the NMR spectrometer with product conversions determined by periodic acquisition of the solutions ¹H NMR spectrum. The resulting time-course plots are shown in Figure 4.1.

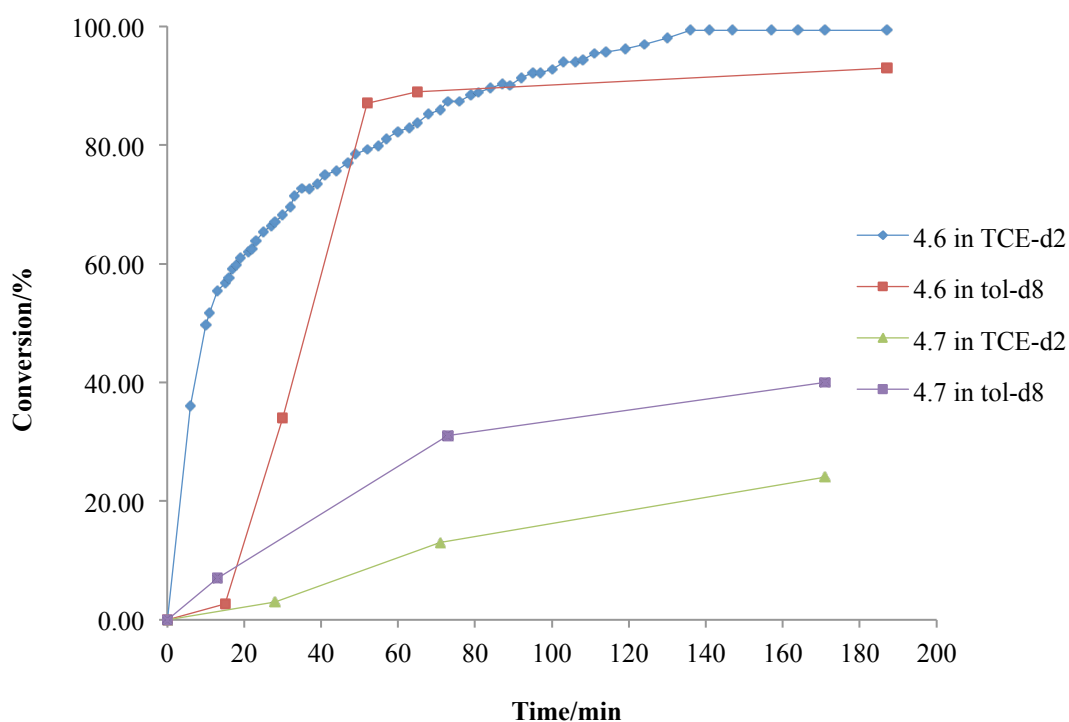


Figure 4.1: Reaction profile of the inter-molecular hydroamination of phenylacetylene (**3.3**) and aniline (**3.4**) into *E-N*-(1-phenylethylidene)benzeneamine (**3.5**) catalysed by 1.5 mol% of complexes $(\mu\text{-L})[\text{Ir}(\text{CO})_2]_2(\text{BArF})_2$ (**4.6**) and $(\mu\text{-L})[\text{Rh}(\text{CO})_2]_2(\text{BArF})_2$ (**4.7**) at 100 °C in TCE-d₂ and toluene-d₈.

The bimetallic iridium complex $(\mu\text{-L})[\text{Ir}(\text{CO})_2]_2(\text{BArF})_2$ (**4.6**) proved to be the fastest catalyst reaching >98 % conversion in TCE-d₂ and 93 % conversion in toluene-d₈ after just 3 hours. Note, for the reaction performed in toluene-d₈ a short delay of approximately 20 minutes was observed before the catalyst began to convert substrate to product. This is suspected to be the result of poor solubility of the isolated complex in this solvent, however during reaction the complex color is taken up into solution. This is in contrast to TCE-d₂ where the bimetallic complex is entirely soluble.

For the corresponding bimetallic rhodium complex $(\mu\text{-L})[\text{Rh}(\text{CO})_2]_2(\text{BArF})_2$ (**4.7**) much lower catalytic activities were achieved with product conversions after 3 hours of 40 % and 25 % in TCE-d₂ and toluene-d₈, respectively. A similar effect of solvent was observed here where TCE-d₂ gave immediate conversion to product

compared to a short induction period observed in toluene- d_8 .

A comparison of the activity of the bimetallic iridium catalyst $(\mu\text{-L})[\text{Ir}(\text{CO})_2]_2(\text{BArF})_2$ (**4.6**) with the fastest monometallic catalysts $[\text{Ir}(\text{PyP})(\text{CO})_2]\text{BArF}$ (**4.3**) and $[\text{Ir}(\text{bpm})(\text{CO})_2]\text{BArF}$ (**4.4**) in TCE- d_2 is shown in Figure 4.2. Similar reaction profiles are observed for all three catalysts with a rapid initial reaction rate followed by a prolonged climb to higher conversions. The bimetallic catalyst can be seen to maintain a higher activity across both regimes, which results in complete conversion of the substrate over short reaction times.

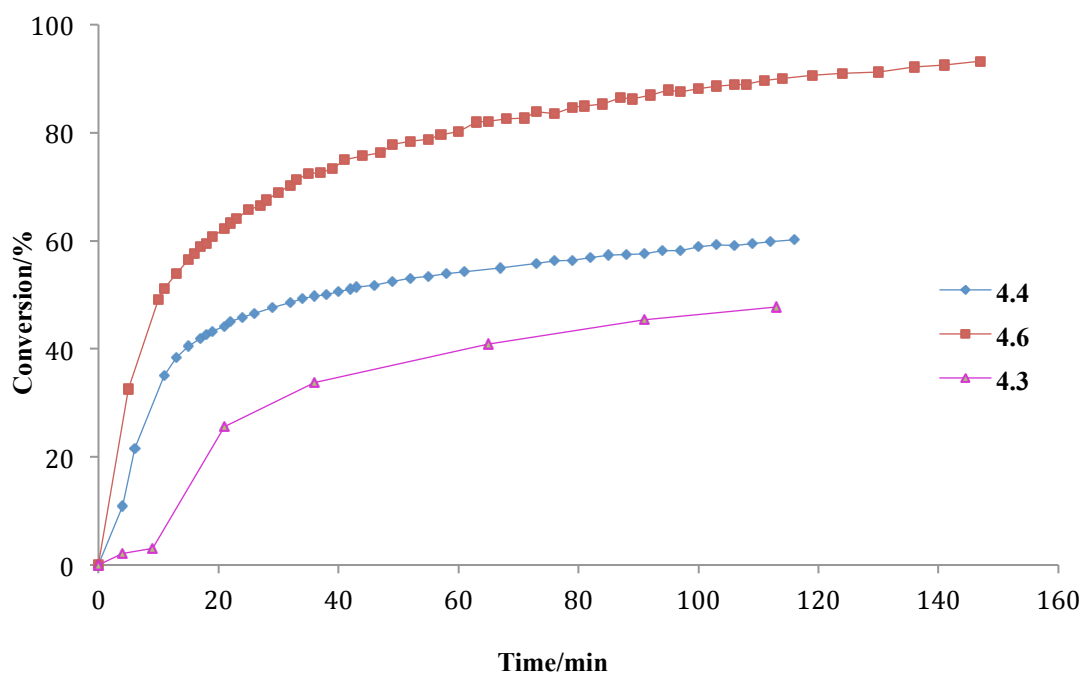
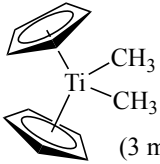
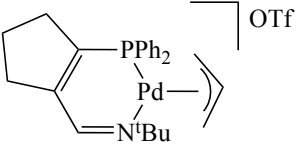
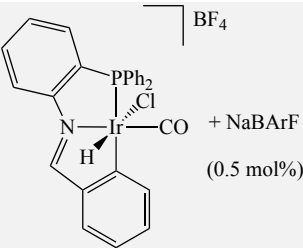
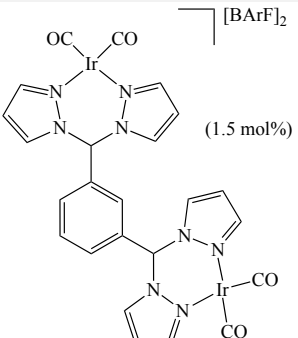


Figure 4.2 Reaction profile of the inter-molecular hydroamination of phenylacetylene (**3.3**) and aniline (**3.4**) into *E-N*-(1-phenylethylidene)benzeneamine (**3.5**) catalysed by 3.0 mol% metal loading $[\text{Ir}(\text{PyP})(\text{COD})]\text{BPh}_4$ (**4.1**), $[\text{Ir}(\text{bpm})(\text{CO})_2]\text{BArF}_4$ (**4.4**) and $(\mu\text{-L})[\text{Ir}(\text{CO})_2]_2(\text{BArF})_2$ (**4.6**) at 100 °C in TCE- d_2 .

In comparison to other hydroamination catalysts investigated for the reaction of phenylacetylene (**3.3**) with aniline (**3.4**) the bimetallic catalyst $(\mu\text{-L})[\text{Ir}(\text{CO})_2]_2(\text{BArF})_2$ (**4.6**) is among the fastest reported to date. The efficiency of the other catalysts that were

tested for this reaction is summarized in Table 4.3. As can be seen, for most catalysts only partial conversions are achieved over prolonged reaction times at elevated temperatures. The only catalyst which approaches the efficiency of $(\mu\text{-L})[\text{Ir}(\text{CO})_2]_2(\text{BArF})_2$ (**4.6**) is an iridium(III) hydride complex (entry 7).

Table 4.3: Comparison of the catalytic efficiency of $(\mu\text{-L})[\text{Ir}(\text{CO})_2]_2(\text{BArF})_2$ (**4.6**) with literature precedents for the inter-molecular hydroamination of phenylacetylene (**3.3**) and aniline (**3.4**) into *E-N*-(1-phenylethylidene)benzeneamine (**3.5**).

Entry	Catalyst	Temperature (solvent)	Reaction Time	Conversion
1 ²⁶	$\text{Ti}(\text{OAc})_3$ (2 mol%)	60 °C (neat)	7 h	57 %
2 ²⁷	 (3 mol%)	180 W microwave (toluene)	2 h	67 %
3 ⁹	$\text{Ru}_3(\text{CO})_{12} / \text{NH}_4\text{PF}_6$ (0.1 mol%)	100 °C (neat)	12 h	84 %
4 ¹²	 (0.5 mol%)	70 °C (THF)	22 h	75 %
5 ¹³	$[\text{Rh}(\text{COD})_2]\text{BF}_4 / \text{PCy}_3$ (2 mol%)	25 °C (toluene)	20 h	10 %
6 ¹⁵	$[\text{Rh}(\text{Cp}^*)\text{Cl}_2]_2 / \text{NH}_4\text{PF}_6$ (0.5 mol%)	80 °C (toluene)	12 h	87 %
7 ¹⁶	 (0.5 mol%) + NaBArF	110 °C (toluene)	12 h	100 %
8	 (1.5 mol%)	100 °C (TCE)	3 h	100 %

4.2.2 Hydroamination of aliphatic substrates with aniline

To investigate whether the catalysts described in this work can be applied to substrates containing aliphatic substituents we included 1-heptyne and 1-hexylamine into our reaction schemes.

Initial investigations looked at using $[\text{Ir}(\text{bpm})(\text{CO})_2]\text{BArF}$ (**4.4**), $[\text{Rh}(\text{bpm})(\text{CO})_2]\text{BArF}$ (**4.5**) and $(\mu\text{-L})[\text{Ir}(\text{CO})_2]_2(\text{BArF})_2$ (**4.6**) as catalysts for the hydroamination of 1-heptyne (**4.8**) and aniline (**3.3**) at 100 °C in toluene- d_8 using 3 mol% metal loading (Table 4.4). Interestingly two isomeric products were formed from this reaction depending on whether the phenyl group of the imine was located *trans* (*Z*) (**4.9**) or *cis* (*E*) (**4.10**) to the C_5H_{11} alkyl chain. The fastest catalyst of the series was the bimetallic complex $(\mu\text{-L})[\text{Ir}(\text{CO})_2]_2(\text{BArF})_2$ (**4.6**) which achieved 67 % conversion after 19 hours, more than twice as efficient than the analogous monometallic complex $[\text{Ir}(\text{bpm})(\text{CO})_2]\text{BArF}$ (**4.4**) (28 % conversion after 24 hours). The regioselectivity of both catalysts was similar (*Z:E* = 2:1) with the less sterically hindered *Z* (**4.9**) isomer favored. The rhodium catalyst $[\text{Rh}(\text{bpm})(\text{CO})_2]\text{BArF}$ (**4.5**) was found to be almost entirely unreactive towards 1-heptyne (**4.8**) giving less than 5 % conversion after 24 hours.

In comparison to the hydroamination of phenylacetylene (**3.3**) and aniline (**3.4**) it is immediately apparent that aliphatic alkynes are considerably less reactive than aromatic alkynes using these catalysts.

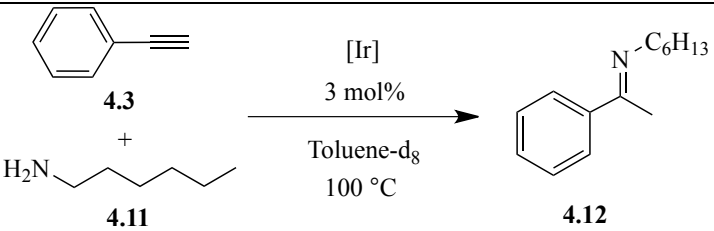
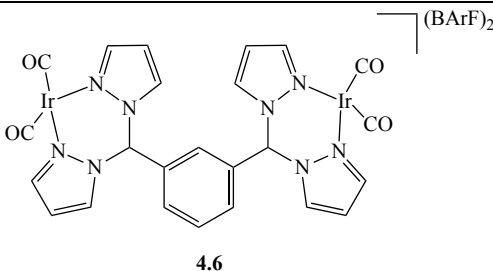
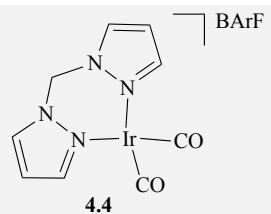
Table 4.4: Comparison of the catalytic activity of $[\text{Ir}(\text{bpm})(\text{CO})_2]\text{BArF}$ (**4.4**), $[\text{Rh}(\text{bpm})(\text{CO})_2]\text{BArF}$ (**4.5**) and $(\mu\text{-L})[\text{Ir}(\text{CO})_2]_2(\text{BArF})_2$ (**4.6**) for the inter-molecular hydroamination of aniline (**3.4**) and 1-heptyne (**4.8**).

Entry	Catalyst	Conversion (time)
1 ^[c]	 4.6	67 % (19 hrs) Z:E = 44:23
2	 4.4	28 % (24 hrs) Z:E = 19:9
3	 4.5	<5 % (24 hrs)

The influence of varying the amine substituent was investigated next. The hydroamination of phenylacetylene (**3.3**) and 1-hexylamine (**4.11**) was performed with the monometallic catalyst $[\text{Ir}(\text{bpm})(\text{CO})_2]\text{BArF}$ (**4.4**) and bimetallic catalyst $(\mu\text{-L})[\text{Ir}(\text{CO})_2]_2(\text{BArF})_2$ (**4.6**) at 100 °C and 3 mol% metal loading (Table 4.5). In this case only the *Z* isomer was detected. After 19 hours the bimetallic catalyst **4.6**

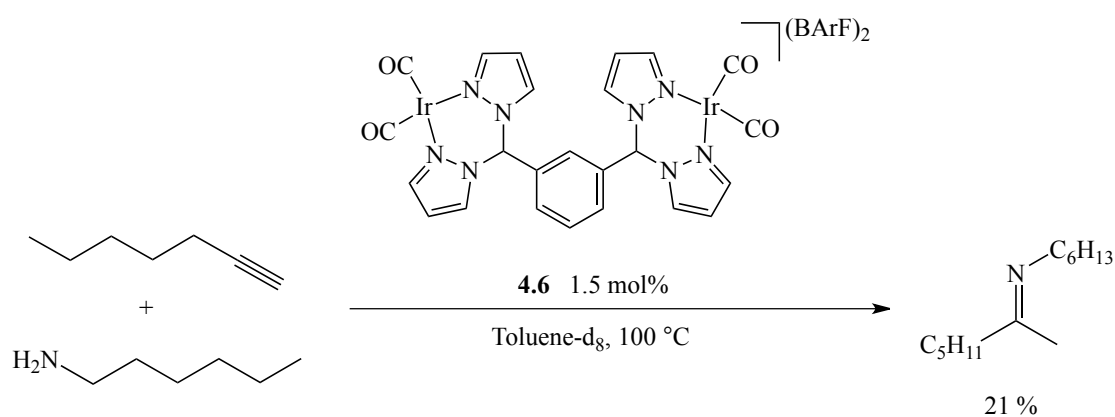
achieved 26 % conversion, compared to 18 % conversion after 24 hours for the monometallic catalyst **4.4**. These conversions are considerably lower than what was obtained for the hydroamination of both phenylacetylene (**3.3**) and 1-heptyne (**4.8**) with aniline (**3.4**) suggesting that the nature of the amine substituent has the greatest impact on the reactions efficiency.

Table 4.5: Comparison of the catalytic activity of $[\text{Ir}(\text{bpm})(\text{CO})_2]\text{BArF}$ (**4.4**), and $(\mu\text{-L})[\text{Ir}(\text{CO})_2]_2(\text{BArF})_2$ (**4.6**) complexes for the inter-molecular hydroamination of phenylacetylene (**3.3**) and 1-hexylamine (**4.11**).

		
Entry	Catalyst	Conversion (time)
1	 4.6	26 % (19 hrs)
2	 4.4	18 % (24 hrs)

Finally, the combination of both aliphatic substrates was investigated. The hydroamination of 1-heptyne (**4.8**) and 1-hexylamine was performed with only the

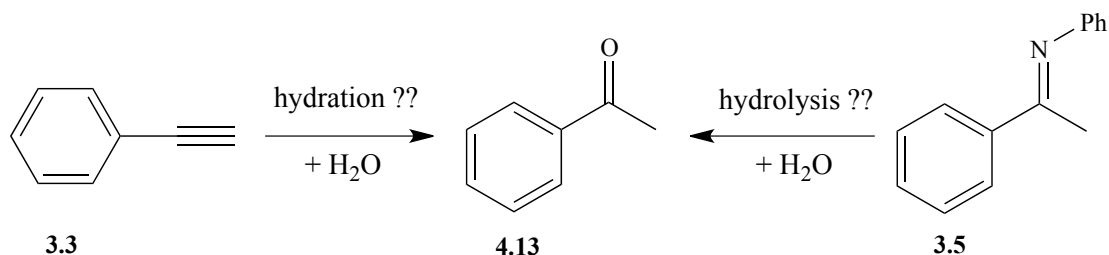
most active catalyst of the series, $(\mu\text{-L})[\text{Ir}(\text{CO})_2]_2(\text{BArF})_2$ (**4.6**), at 100 °C and 3 mol% metal loading (Scheme 4.16). After 19 hours 21 % conversion was achieved with only a single isomer (*Z*) observed from this reaction. Surprisingly, despite combining the two most difficult substrates the efficiency of this reaction was comparable to the hydroamination of phenylacetylene (**3.3**) with 1-hexylamine (**4.11**). Possibly it is the nature of the amine substituent only, which limits the efficiency of this reaction.



Scheme 4.16

4.2.3 Investigation of Imine Hydrolysis

For many of the catalytic reactions performed above involving the hydroamination of aniline and phenylacetylene (**3.3**) the formation of the desired imine product was accompanied by the formation of a small amount of acetophenone (**4.13**) side product. To determine whether the acetophenone (**4.13**) originated from the hydrolysis of the imine product or the catalyzed hydration of phenylacetylene (**3.3**) (Scheme 4.17) the following investigations were performed.



Scheme 4.17

First, the hydration of phenylacetylene (**3.3**) was attempted by combining substrate **3.3**, the bimetallic catalyst $(\mu\text{-L})[\text{Ir}(\text{CO})_2]_2(\text{BArF})_2$ (**4.6**) (1.5 mol%) and a drop of deionized H_2O in TCE-d_2 and heating the solution at $100\text{ }^\circ\text{C}$ for 24 hours. Under these conditions no acetophenone (**4.13**) was detected. Secondly the rate of imine hydrolysis was investigated by combining *E-N*-(1-phenylethylidene)benzeneamine (**3.5**) with a drop of H_2O in TCE-d_2 . After 19 hours at $100\text{ }^\circ\text{C}$ 53 % conversion to acetophenone (**4.13**) was observed indicating that the hydrolysis reaction proceeds at an appreciable rate under the conditions employed during catalysis.

Finally, the hydroamination of phenylacetylene (**3.3**) and aniline (**3.4**) using $(\mu\text{-L})[\text{Ir}(\text{CO})_2]_2(\text{BArF})_2$ (**4.6**) (1.5 mol%) was performed in TCE-d_2 at $100\text{ }^\circ\text{C}$ and monitored over prolonged reaction times. The time course plot shown in Figure 4.3 shows the conversion to both imine (**3.5**) and acetophenone (**4.13**) products. Initially the imine product **3.5** is the major constituent, however, as time proceeds **3.5** is consumed and the concentration of acetophenone (**4.13**) increases. This clearly demonstrates that the acetophenone originates from hydrolysis of the imine. For this reason the sum of both acetophenone (**4.13**) and imine (**3.5**) products were included in the total percent conversions reported for all hydroamination reactions.

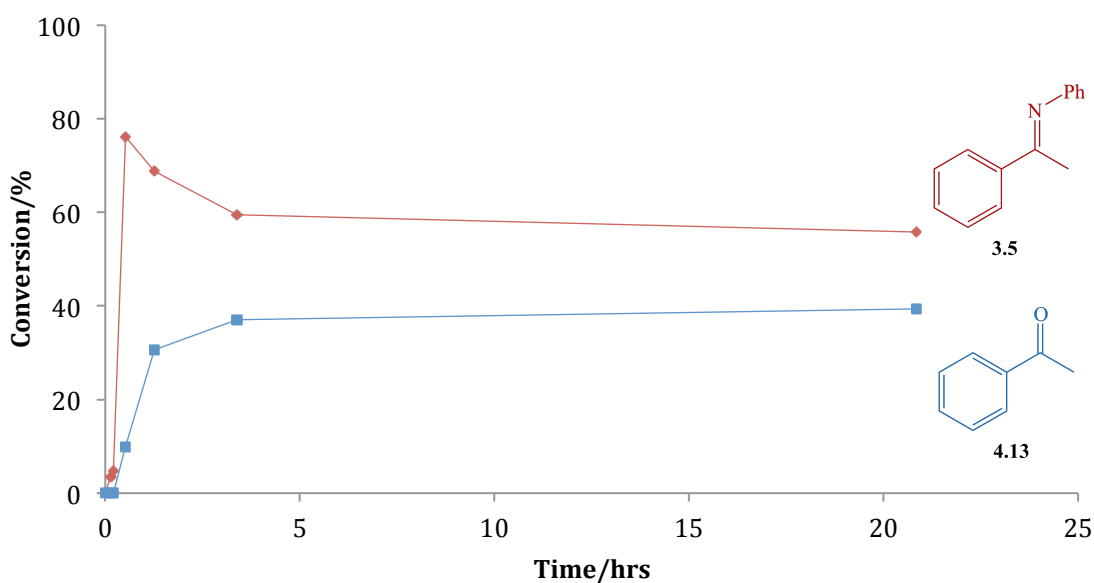


Figure 4.3: Inter-molecular hydroamination of phenylacetylene (**3.3**) and aniline (**3.4**) into *E-N*-(1-phenylethylidene)benzeneamine (**3.5**) and acetophenone (**4.13**) with addition of deionized H₂O performed in TCE-d₂ at 100 °C using 1.5 mol % of (μ-L)[Ir(CO)₂]₂(BARF)₂ (**4.6**).

4.3 Summary and Conclusions

A series of Ir(I) and Rh(I) catalysts were investigated for the inter-molecular hydroamination reaction. The influence of counter ion, ligand groups, solvent and temperature on the efficiency of the catalysts was investigated allowing the following conclusions to be made:

- The more weakly coordinating BARF counter ion resulted in much higher catalytic activities compared to BPh₄⁻;
- CO co-ligands furnished far more efficient catalysts compared to COD co-ligands;
- Unexpectedly, the substitution of *P,N*-donor ligands for *N,N*-donor ligands had little impact on the catalyst activity;
- The use of a bimetallic complex structure significantly increased the efficiency

of the catalyst in comparison to analogous monometallic structures;

- Halogenated solvents tended to be unsuitable for the reaction of monometallic complexes due to catalyst deactivation, however the higher solubility of the bimetallic catalysts in these solvents proved advantageous;
- Aliphatic substrates gave much lower conversions for all catalysts.
- The formation of acetophenone was determined to be a product of imine hydrolysis due to the presence of adventitious water in the reaction mixture.

4.4 References

- (1) Severin, R.; Doye, S. *Chem. Soc. Rev.* **2007**, *36*, 1407.
- (2) Pohlki, F.; Doye, S. *Chem. Soc. Rev.* **2003**, *32*, 104.
- (3) Li, Y.; Marks, T. J. *Organometallics* **1996**, *15*, 3770.
- (4) Haskel, A.; Straub, T.; Eisen, M. S. *Organometallics* **1996**, *15*, 3773.
- (5) Walsh, P. J.; Baranger, A. M.; Bergman, R. G. *J. Am. Chem. Soc.* **1992**, *114*, 1708.
- (6) Haak, E.; Bytschkov, I.; Doye, S. *Angew. Chem., Int. Ed.* **1999**, *38*, 3389.
- (7) Leitch, D.; Payne, P.; Dunbar, C.; Schafer, L. *J. Am. Chem. Soc.* **2009**, *131*, 18246.
- (8) Uchimaru, Y. *Chem. Commun.* **1999**, 1133.
- (9) Tokunaga, M.; Eckert, M.; Wakatsuki, Y. *Angew. Chem., Int. Ed.* **1999**, *38*, 3222.
- (10) Tokunaga, M.; Ota, M.; Haga, M.-a.; Wakatsuki, Y. *Tetrahedron Lett.* **2001**, *42*, 3865.
- (11) Kadota, I.; Shibuya, A.; Lutete, L. M.; Yamamoto, Y. *J. Org. Chem.* **1999**, *64*, 4570.
- (12) Shaffer, A. R.; Schmidt, J. A. R. *Organometallics* **2008**, *27*, 1259.
- (13) Hartung, C.; Tillack, A.; Trauthwein, H.; Beller, M. *J. Org. Chem.* **2001**, *66*, 6339.
- (14) Alonso-Moreno, C.; Carrillo-Hermosilla, F.; Romero-Fernández, J.; Rodríguez, A. M.; Otero, A.; Antiñolo, A. *Adv. Synth. Catal.* **2009**, *351*, 881.
- (15) Kumaran, E.; Leong, W. K. *Organometallics* **2012**, *31*, 1068.
- (16) Rung-Yi, L.; Surekha, K.; Akito, H.; Fumiyuki, O.; Yi-Hong, L.; Shie-Ming, P.; Shiuh-Tzung, L. *Organometallics* **2007**, *26*, 1062.

-
- (17) Dabb, S. L.; Messerle, B. A. *Dalton Trans.* **2008**, 0, 6368.
- (18) Field, L. D.; Messerle, B. A.; Vuong, K. Q.; Turner, P.; Failes, T. *Organometallics* **2007**, 26, 2058.
- (19) Burling, S.; Field, L. D.; Messerle, B. A.; Turner, P. *Organometallics* **2004**, 23, 1714.
- (20) Field, L. D.; Messerle, B. A.; Vuong, K. Q.; Turner, P. *Organometallics* **2005**, 24, 4241.
- (21) Ho, J. H. H.; Hodgson, R.; Wagler, J.; Messerle, B. A. *Dalton Trans.* **2010**, 39, 4062.
- (22) Ho, J. H. H.; Choy, S. W. S.; Macgregor, S. A.; Messerle, B. A. *Organometallics* **2011**, 30, 5978.
- (23) Hartung, C.; Tillack, A.; Trauthwein, H.; Beller, M. *J. Org. Chem.* **2001**, 66, 6339.
- (24) Jiménez, M. V.; Pérez-Torrente, J. J.; Bartolomé, M. I.; Gierz, V.; Lahoz, F. J.; Oro, L. A. *Organometallics* **2007**, 27, 224.
- (25) Mori, A.; Takahisa, E.; Yamamura, Y.; Kato, T.; Mudalige, A. P.; Kajiro, H.; Hirabayashi, K.; Nishihara, Y.; Hiyama, T. *Organometallics*, **2004**, 23, 1755.
- (26) Barluenga, J.; Aznar, F. *Synthesis* **1977**, 3, 195.
- (27) Bytschkov, I.; Doye, S. *Eur. J. Org. Chem.* **2001**, 2001, 4411.

Summary and Conclusions

5.1 Summary and Conclusions

The coordination and catalytic chemistry of a series of Ir and Rh complexes was investigated with the aim of facilitating X-H (X= Si, O and N) bond addition across an alkyne C≡C triple bond. Towards this end the following achievements were made:

Synthesis of NCN pincer complexes

Two new pincer ligand precursors; bis(methylpyrazolyl)imidazolium tetraphenylborate $\text{NCN}^{\text{Me}}\cdot\text{HBPh}_4$ (**2.1**) and bis(ethylpyrazolyl)imidazolium tetraphenylborate $\text{NCN}^{\text{Et}}\cdot\text{HBPh}_4$ (**2.2**) were synthesised. These ligands were coordinated to Rh(I) and Ir(I) metal centres to yield the following complexes: $[\text{Rh}(\text{NCN}^{\text{Me}})(\text{COD})]\text{BPh}_4$ (**2.3**), $[\text{Ir}(\text{NCN}^{\text{Me}})(\text{COD})]\text{BPh}_4$ (**2.4**), $[\text{Ir}(\text{NCN}^{\text{Me}})_2(\text{COD})]\text{BPh}_4$ (**2.5**), $[\text{Rh}(\text{NCN}^{\text{Me}})\text{CO}]_2(\text{BPh}_4)_2$ (**2.6**), $[\text{Ir}(\text{NCN}^{\text{Me}})(\text{CO})_2]\text{BPh}_4$ (**2.7**), $[\text{Ir}(\text{NCN}^{\text{Et}})_2(\text{COD})]\text{BPh}_4$ (**2.8**), $[\text{Rh}(\text{NCN}^{\text{Et}})(\text{COD})]\text{BPh}_4$ (**2.9**), $[\text{Rh}(\text{NCN}^{\text{Et}})(\text{CO})_2]\text{BPh}_4$ (**2.10**), $[\text{Ir}(\text{NCN}^{\text{Me}})(\text{PPh}_3)_2(\text{CO})]\text{BPh}_4$ (**2.1V**) and $[\text{Ir}(\text{NCN}^{\text{Et}})(\text{PPh}_3)_2(\text{CO})]\text{BPh}_4$ (**2.2V**).

The length of the alkyl chain (methyl or ethyl) linking the NHC and pyrazole donor groups in NCN^{Me} and NCN^{Et} was found to have a pronounced impact on their coordination properties. Typically the longer ethyl linker of NCN^{Et} led to a higher lability of the pyrazole donor groups. For example the NCN^{Et} pincer ligand was observed to bind in a bidentate (κ^2) coordination mode in $[\text{Rh}(\text{NCN}^{\text{Et}})(\text{COD})]\text{BPh}_4$ (**2.9**) and monodentate (κ^1) in $[\text{Ir}(\text{NCN}^{\text{Et}})_2(\text{COD})]\text{BPh}_4$ (**2.8**). In comparison a facial tridentate (κ^3) coordination mode was observed for the analogous NCN^{Me} containing complexes $[\text{Rh}(\text{NCN}^{\text{Me}})(\text{COD})]\text{BPh}_4$ (**2.3**) and $[\text{Ir}(\text{NCN}^{\text{Me}})(\text{COD})]\text{BPh}_4$ (**2.4**).

An unusual bimetallic complex $[\text{Rh}(\text{NCN}^{\text{Me}})\text{CO}]_2(\text{BPh}_4)_2$ (**2.6**) was also prepared which was shown to have a relatively short Rh-Rh distance of 3.341 Å.

Catalysed C-X bond formation using complexes with NCN pincer ligand

The new pincer complexes $[\text{Rh}(\text{NCN}^{\text{Me}})(\text{COD})]\text{BPh}_4$ (**2.3**), $[\text{Ir}(\text{NCN}^{\text{Me}})(\text{COD})]\text{BPh}_4$ (**2.4**), $[\text{Rh}(\text{NCN}^{\text{Me}})\text{CO}]_2(\text{BPh}_4)_2$ (**2.6**), $[\text{Ir}(\text{NCN}^{\text{Me}})(\text{CO})_2]\text{BPh}_4$ (**2.7**), $[\text{Rh}(\text{NCN}^{\text{Et}})(\text{COD})]\text{BPh}_4$ (**2.9**) and $[\text{Rh}(\text{NCN}^{\text{Et}})(\text{CO})_2]\text{BPh}_4$ (**2.10**) were investigated as catalysts for the hydroamination, hydroalkoxylation and hydrosilylation of alkynes. Their reactivity was compared with two analogous complexes $[\text{Rh}(\text{NC}^{\text{Me}})\text{COD}]\text{BPh}_4$ (**2.11**) and $[\text{Rh}(\text{NC}^{\text{Me}})(\text{CO})_2]\text{BPh}_4$ (**2.12**) containing an NHC-pyrazolyl chelate (NC^{Me}). Overall the Rh complexes showed to have a higher catalytic activity compared to the analogous Ir complexes. Complexes with CO co-ligands were also found to be more active than COD containing complexes for the addition of N-H and O-H bonds to alkynes.

Compared to the complexes **2.11** and **2.12** with *N,C*- bidentate ligands, the pincer ligand geometry was responsible for a decrease in catalyst activity for the intramolecular hydroamination of 5-phenyl-4-pentyn-1-amine (**3.1**). On the contrary, pincer ligands appeared to stabilise the catalyst against deactivation during the cyclisation of 4-pentynoic acid (**3.6**), resulting in higher catalytic activities. For the hydrosilylation of phenylacetylene (**3.3**) and 1-phenylpropyne (**3.10**) small changes in catalyst structure resulted in vastly different substrate dependencies and product regioselectivities.

Catalysed inter-molecular hydroamination

A series of Ir(I) and Rh(I) catalysts were investigated for the intermolecular hydroamination of terminal alkynes with primary amines. The influence of the metal centre, counterion, ligand groups, solvent and temperature on the catalyst efficiency was evaluated. It was observed that catalyst activity was strongly dependent on the nature of

the counter ion with complexes containing the weakly coordinating BArF anion found to be much more effective than complexes containing BPh₄. In general catalysts containing CO coligands were more beneficial than those containing COD, with iridium catalysts significantly more active than rhodium. Surprisingly the nature of the chelating ligand group, either bis(pyrazolyl)methane (bpm) or 1-[2-(diphenylphosphino)ethyl]pyrazole (PyP), had little impact on the activity of the catalyst.

The bimetallic system (μ -L)[Ir(CO)₂]₂(BArF)₂ (**4.6**) was found to be much more efficient than any monometallic catalyst. This was particularly true for the hydroamination of phenylacetylene (**3.3**) and aniline (**3.4**) for which it is one of the most efficient catalysts known.

Experimental

PART 1: E.1 GENERAL PROCEDURE

E.1.1 General consideration

All manipulations of metal complexes and air sensitive reagents were carried out using standard Schlenk techniques¹ or in a nitrogen or argon filled glove box. For the purposes of air sensitive manipulations and in the preparation of metal complexes, solvents were dried and distilled under an atmosphere of nitrogen or argon using standard procedures and stored under nitrogen or argon in glass ampoules, each fitted with a Youngs[®] Teflon valve prior to use. Tetrahydrofuran (thf), diethyl ether, *n*-pentane, and toluene were distilled from sodium-benzophenoneketyl. Dichloromethane (dcm) was distilled from calcium hydride. Methanol was distilled from dimethoxymagnesium. Dimethyl sulfoxide (dmsO) was dried over molecular sieves (4 Å) and degassed via three freeze-pump-thaw cycles prior to use.²

The bulk compressed gases nitrogen (>99.5 %), argon (>99.5 %), carbon monoxide (>99.5 %) were obtained from British Oxygen Company (BOC Gases) or Linde Gas Pty. Ltd. ¹³C-Labelled carbon monoxide (>99 %) was obtained from Cambridge Isotopes Laboratories.

Except where specified, chemicals were purchased from either Aldrich Chemical Company Inc. or Alfa Aesar Inc. and used as received. The metal halide salts RhCl₃·xH₂O and IrCl₃·xH₂O were purchased from Precious Metals Online PMO P/L and used without further purification. The metal precursors [Ir(μ-Cl)(COD)]₂,³ [Rh(μ-Cl)(COD)]₂,⁴ and [Ir(PPh₃)₂(CO)Cl]⁵ were synthesized using reported methods. The metal complexes [Ir(bpm)(CO)₂]BArF,⁶ [Rh(bpm)(CO)₂]BArF,⁶ (μ-L)[Ir(CO)₂]₂(BArF)₂,⁷ (μ-L)[Rh(CO)₂]₂(BArF)₂,⁷ [Ir(PyP)(COD)]BPh₄,⁸

$[\text{Ir}(\text{PyP})(\text{COD})]\text{BArF}_4$ ⁶ and $[\text{Ir}(\text{PyP})(\text{CO})_2]\text{BArF}_4$ ⁶ were prepared using the reported method. The metal complexes $[\text{Rh}(\text{NCN}^{\text{Me}})(\text{COD})]\text{BArF}$, $[\text{Ir}(\text{NCN}^{\text{Me}})(\text{COD})]\text{BArF}$, $(\text{Rh}(\text{NCN}^{\text{Me}})(\text{CO}))_2(\text{BArF})_2$, $[\text{Ir}(\text{NCN}^{\text{Me}})(\text{CO})_2]\text{BArF}$, $[\text{Rh}(\text{NC}^{\text{Me}})(\text{COD})]\text{BPh}_4$ and $[\text{Rh}(\text{NC}^{\text{Me}})(\text{CO})_2]\text{BPh}_4$ were kindly provided by Dr. Michael J. Page.

E.1.2 NMR spectroscopy

Air sensitive NMR samples were prepared either in a nitrogen or argon filled glove box or on a high vacuum line by vacuum transfer of solvent into an NMR tube fitted with a concentric Teflon valve (Youngs[®]). Deuterated solvents for NMR purposes were obtained from Cambridge Isotopes Laboratories (CIL), except for CDCl_3 which was purchased from either CIL or Aldrich Chemical Company Inc. Deuterated solvents used with air sensitive compounds were degassed via three freeze-pump-thaw cycles and were vacuum distilled from suitable drying reagents immediately prior to use or the solvents were handled exclusively under a nitrogen or argon atmosphere.

The ^1H , ^{13}C and ^{31}P NMR spectra were recorded on Bruker DPX300 (with an automatic sample changer), DPX300, DMX500, DMX400 and DMX600 spectrometers, operating at 300.13, 300.17, 400.23, 500.13 and 600.13 MHz (^1H); 75.49, 75.48, 100.64, 125.76 and 150.90 MHz (^{13}C); 161.98 and 242.94 MHz (^{31}P). The spectra were recorded at 298 K unless otherwise specified. Chemical shifts (δ) are quoted in ppm. ^1H NMR and ^{13}C NMR chemical shifts were referenced internally to residual solvent resonances. Uncertainties in chemical shifts are typically ± 0.01 ppm for ^1H and ± 0.05 ppm for ^{13}C . Coupling constants (J) are given in Hz and have an uncertainty of ± 0.05 Hz for ^1H - ^1H and ^1H - ^{31}P and ± 0.5 Hz for ^{13}C - ^{103}Rh couplings. The following abbreviations are used in reporting the multiplicity of NMR resonances: s, singlet; d, doublet; t, triplet; q, quartet; p, pentet; m, multiplet; br, broad. The following two-dimensional NMR

techniques were routinely used for the assignment of organic and organometallic compounds: COSY (**C**ORrelation spectroscop**Y**), NOESY (**N**uclear **O**verhauser **E**ffect Spectroscop**Y**), HSQC (**H**eteronuclear **S**ingle **Q**uantum **C**oherence) and HMBC (**H**eteronuclear **M**ultiple **B**ond **C**orrelation). NMR data were processed using standard Bruker software (Topspin) version 3.1.

E.1.3 Other characterisation techniques

IR spectra were recorded using an ATI Mattson *Genesis Series* F.T.I.R. spectrometer or an Avatar 370 FTIR spectrometer.

Elemental analyses were carried out at the Campbell Microanalytical Laboratory, the University of Otago, New Zealand and the Elemental Analysis Unit, The Research School of Chemistry, the Australian National University.

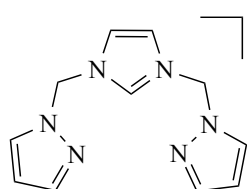
Single crystal X-ray analysis was performed by Dr Mohan Bhadbhade at the Mark Wainwright Analytical Centre, University of New South Wales, Sydney. X-ray diffraction data were measured using a Bruker kappa APEXII CCD Area Detector Diffractometer using Mo K(alpha) radiation. The structures were solved with the use of SIR92 and refined using SHELXL-97 software package.

High resolution mass spectra were acquired at the Bioanalytical Mass Spectrometry Facility (BMSF), the University of New South Wales, Australia. The ESI-MS spectra were obtained using a Micromass ZQ mass spectrometer. In reporting mass spectral data, M is defined as the molecular weight of the compound of interest. Alternatively, in the case of cationic compounds M is defined as the molecular weight of the cationic fragments.

PART 2: EXPERIMENTAL FOR CHAPTER 2

E.2.1 Synthesis of NCN ligands

E.2.1.1 Synthesis of $\text{NCN}^{\text{Me}}\cdot\text{HBPh}_4$ (2.1)



2.1

1-Hydroxy methyl pyrazole (1.6 g, 16.3 mmol) was dissolved in 70 ml of chloroform and an excess of SOCl_2 (5 ml, 68.5 mmol) was added drop-wise. The solution was refluxed overnight. The solvent was then reduced to dryness, the crude residue of 1-chloromethylpyrazole was suspended in dry toluene (70 ml), trimethylsilyl imidazole (1.2 ml, 8.2 mmol) added and left stirring overnight at reflux. The toluene was removed *via* cannula leaving a brown sticky solid behind. The residue was redissolved in dry and degassed methanol (160 ml) to which NaBPh_4 (2.8g, 8.2 mmol) was added, resulting in the product as white precipitate which was filtered and washed with methanol (70 ml).

Yield: 1.89 g, 42 %.

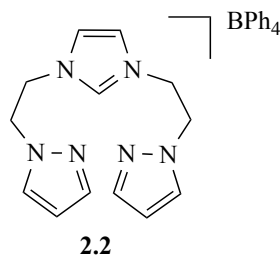
^1H NMR (400 MHz, $\text{dms}\text{-d}_6$) δ 9.62 (t, $^4J = 1.5$ Hz, 1H, Im H^2), 8.10 (d, $^3J = 2.4$ Hz, 2H, Pz H^5), 7.84 (d, $^3J = 1.4$ Hz, 2H, Im $\text{H}^{4/5}$), 7.65 (d, $^3J = 1.3$ Hz, 2H, Pz H^3), 7.20 (m, 8H, *o*- BPh_4), 6.94 (t, $^3J = 7.3$ Hz, 8H, *m*- BPh_4), 6.78 (t, $^3J = 7.2$ Hz, 4H, *p*- BPh_4), 6.58 (s, 4H, CH_2), 6.40 (t, $^3J = 2.0$ Hz, 2H, Pz H^4) ppm.

$^{13}\text{C}\{^1\text{H}\}$ NMR (100 MHz, $\text{dms}\text{-d}_6$) δ 163.4 (q, $^1J(\text{B-C}) = 49.7$ Hz, *i*- C of BPh_4), 141.8 (Pz C^3), 136.9 (Im C^2), 135.6 (*o*- C of BPh_4), 131.7 (Pz C^5), 125.3 (*m*- C of BPh_4), 122.4 (Im $\text{C}^{4/5}$), 121.6 (*p*- C of BPh_4), 107.2 (Pz C^4), 61.6 (CH_2) ppm.

ESI-MS (MeOH) m/z : 229.12 (100 %) [M- BPh₄⁻]

Anal. Found: C, 76.34; H, 6.16; N, 15.07; Anal. Calc: C, 76.64; H, 6.06; N, 15.32.

E.2.1.2 Synthesis of NCN^{Et}.HBPh₄ (2.2)



BPh₄ Bromoethyl pyrazole was degassed *via* three freeze-pump-thaw cycles prior to use. Trimethylsilyl imidazole was dried over molecular 4 Å sieves and also degassed. Two molar equivalents of bromoethyl pyrazole (3.2 g, 18.3 mmol) were dissolved in

dry and degassed toluene (70 ml) to which trimethylsilyl imidazole (1.3 g, 9.1 mmol) was then added. The mixture was refluxed overnight. The toluene was removed *via* cannula leaving a brown sticky solid behind. The crude product was redissolved in dry and degassed methanol (100 ml) to which NaBPh₄ (3.1 g, 9.1 mmol) was added and stirred for 30 min. The resulting white precipitate was filtrated and washed with methanol (10 ml).

Yield: 3.8g, 72%.

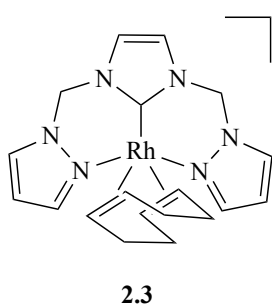
¹H (400 MHz, dms_o-d₆) δ 8.72 (t, ⁴*J* = 1.4 Hz, 1H, Im **H**²), 7.54 (d, ³*J* = 2.0 Hz, 2H, Pz **H**⁵), 7.47 (d, ³*J* = 1.3 Hz, 2H, Pz **H**³), 7.41 (d, ³*J* = 1.4 Hz, 2H, Im **H**^{4/5}), 7.19 (m, 8H, *o*-BPh₄), 6.93 (t, ³*J* = 7.4 Hz, 8H, *m*-BPh₄), 6.79 (t, ³*J* = 7.2 Hz, 4H, *p*-BPh₄), 6.23 (t, ³*J* = 2.0 Hz, 2H, Pz **H**⁴), 4.55 (m, 8H, CH₂) ppm.

¹³C {¹H} NMR (100 MHz, dms_o-d₆) δ 163.4 (q, ¹*J*(B-C) = 49.3 Hz, *i*-C of BPh₄), 139.7 (Pz **C**³), 136.7 (Im **C**²), 135.5 (*o*-C of BPh₄), 130.6 (Pz **C**⁵), 125.3 (*m*-C of BPh₄), 122.5 (Im **C**^{4/5}), 121.5 (s, *p*-C of BPh₄), 105.7 (s, Pz **C**⁴), 50.4 (CH₂), 49.04 (CH₂) ppm.

Anal. Found: C, 77.46; H, 6.54; N, 14.37; Anal. Calc.: C, 77.08; H, 6.47; N, 14.58.

E.2.2 Synthesis of Rh and Ir COD containing complexes with $\text{NCN}^{\text{Me}}\cdot\text{HBPh}_4$ (2.1)

E.2.2.1 Synthesis of $[\text{Rh}(\text{NCN}^{\text{Me}})(\text{COD})]\text{BPh}_4$ (2.3)



The imidazolium ligand precursor $\text{NCN}^{\text{Me}}\cdot\text{HBPh}_4$ (2.1) (0.175 g, 0.32 mmol), $[\text{Rh}(\mu\text{-Cl})(\text{COD})]_2$ metal complex (0.093 g, 0.16 mmol) and NaOEt (0.11 g, 1.6 mmol) were suspended in dry and degassed thf (30 ml) and the mixture was stirred for 2 hrs at room temperature. The solvent was then removed under vacuum and the crude product was redissolved in dcm (20 ml). After stirring for 30 min, the resulting cloudy yellow solution was filtered and pentane (15 ml) was added to precipitate the product as a yellow powder which was then filtered and dried under vacuum. X-ray quality crystals were obtained by layering a dcm solution of (2.3) with pentane.

Yield: 0.187 g, 77%.

^1H (400 MHz, $\text{dms}\text{-d}_6$) δ 8.00 (m, 4H, Pz $\text{H}^{3/5}$), 7.44 (s, 2H, Im $\text{H}^{4/5}$), 7.17 (m, 8H, *o*-BPh₄), 6.92 (t, $^3J = 7.4$ Hz, 8H, *m*-BPh₄), 6.78 (t, $^3J = 7.2$ Hz, 4H, *p*-BPh₄), 6.63 (br s, 2H, NCH₂), 6.38 (t, $^3J = 2.1$ Hz, 2H, Pz H^4), 6.36 (br s, 2H, NCH₂), 5.19 (br s, 2H, CH of COD), 3.11 (br s, 2H, CH of COD), 2.40 (br s, 2H, CH₂ of COD), 2.16 (br s, 2H, CH₂ of COD), 2.00 (br s, 4H, CH₂ of COD) ppm.

$^{13}\text{C}\{^1\text{H}\}$ NMR (100 MHz, $\text{dms}\text{-d}_6$) δ 184.0 (d, $^1J(\text{Rh-C}) = 43.7$ Im C²), 163.4 (q, $^1J(\text{B-C}) = 49.4$ Hz, *i*-C of BPh₄), 142.1 (Pz C^{3 or 5}), 135.5 (*o*-C of BPh₄), 132.2 (Pz C^{3 or 5}),

125.3 (*m*- C of BPh₄), 122.0 (Im C^{4/5}), 121.5 (*p*- C of BPh₄), 106.8 (Pz C⁴), 103.3 (CH of COD) 62.5 (NCH₂), 51.7 (d, ¹*J* (Rh-C)= 16.2, CH of COD), 34.0 (CH₂ of COD), 28.2 (CH₂ of COD) ppm.

ESI-MS (MeOH), *m/z*: 439.11 (100 %) [M- BPh₄⁻]

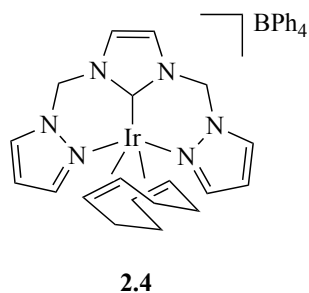
E.2.2.2 Reaction of NCN^{Me} (2.1) with [Ir(μ-Cl)(COD)]₂

Reaction of NCN^{Me}.HBPh₄ (**2.1**) with [Ir(μ-Cl)(COD)]₂ gave two distinct products: a) [Ir(NCN^{Me})(COD)]BPh₄ (**2.4**) and b) [Ir(NCN^{Me})₂(COD)]BPh₄ (**2.5**).

The imidazolium ligand precursor NCN^{Me}.HBPh₄ (**2.1**) (0.31 g, 0.56 mmol), [Ir(μ-Cl)(COD)]₂ (0.19 g, 0.28 mmol) and NaOEt (0.095 g, 1.4 mmol) were suspended in dry and degassed methanol (30 ml) and the mixture stirred for 2 hrs at room temperature. A pale yellow precipitate was filtered from an orange solution. The precipitate was redissolved in thf (20 ml), filtered and the product **2.4** was recrystallised by addition of diethyl ether (10 ml). Reduction of the orange filtrate to dryness and recrystallization of the residue from dcm/pentane gave **2.5** as an orange solid. X-ray quality crystals of both complexes were obtained by layering dcm solutions of the complexes with pentane.

[Ir(NCN^{Me})(COD)]BPh₄ (**2.4**): Yield: 0.21 g, 46%.

[Ir(NCN^{Me})₂(COD)]BPh₄ (**2.5**): Yield: 0.072 g, 12%.

a) [Ir(NCN^{Me})(COD)]BPh₄ (2.4)

¹H NMR (400 MHz, dms_o-d₆) δ 8.06 (d, ³*J* = 2.3 Hz, 4H, Pz **H**^{3/5}), 7.46 (s, 2H, Im **H**^{4/5}), 7.17 (m, 8H, *o*- BPh₄), 6.92 (t, ³*J* = 7.4 Hz, 8H, *m*- BPh₄), 6.78 (t, ³*J* = 7.2 Hz, 8H, *p*- BPh₄), 6.66 (d, ²*J* = 13.4 Hz, 2H, NCH₂), 6.48 (t, ³*J* = 2.2 Hz, 2H, Pz **H**⁴), 6.18 (d, ²*J* = 13.4 Hz, 2H, NCH₂), 2.13 (br s, 4H, CH₂ of COD), 1.82 (br s, 4H, CH₂ of COD) ppm.

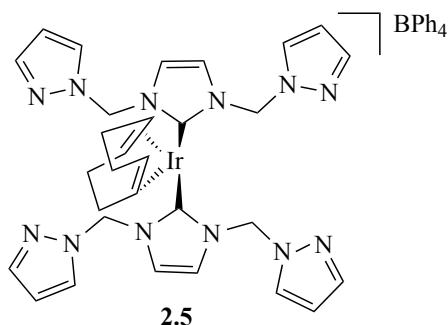
¹³C {¹H} NMR (100 MHz, dms_o-d₆) δ 163.4 (q, ¹*J* (B-C) = 51.38 Hz, *i*- C of BPh₄), 142.5 (Pz **C**^{3 or 5}), 135.5 (*o*- C of BPh₄), 132.6 (Pz **C**^{3 or 5}), 125.3 (*m*- C of BPh₄), 121.5 (*p*- C of BPh₄ and Im **C**^{4/5}), 107.3 (Pz **C**⁴), 62.9 (NCH₂), 32.7 (br s, CH₂ of COD) ppm.

The **CH** and **CH** of COD are not visible in either ¹H NMR or ¹³C {¹H} NMR at room temperature. These signals appeared at 248K.

¹H (400 MHz, acetone-d₆, 248K) δ 4.98 (br s, 2H, **CH** of COD), 2.76 (br s, 2H, **CH** of COD) ppm.

Anal. Found: C, 60.65; H, 5.66; N, 9.67; Anal. Calc.: C, 60.84; H, 5.34; N, 9.90.

ESI-MS (MeOH), *m/z*: 529.17 (100 %) [M- BPh₄].

b) $[\text{Ir}(\text{NCN}^{\text{Me}})_2(\text{COD})]\text{BPh}_4$ (**2.5**)

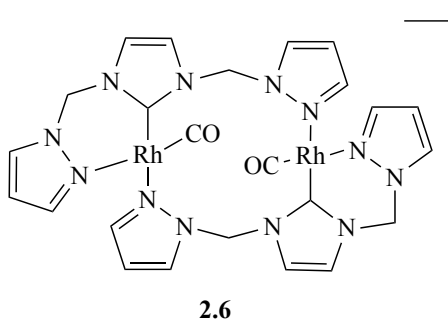
^1H (400 MHz, $\text{dms}\text{-d}_6$) δ 8.06 (d, $^3J = 2.2$ Hz, 4H, Pz H^3 or 5), 7.62 (d, $^3J = 1.5$, 4H, Pz H^3 or 5), 7.18 (m, 8H, *o*- BPh₄), 7.17 (s, 4H, Im $\text{H}^{4/5}$), 6.92 (t, $^3J = 7.4$ Hz, 12H, *m*- BPh₄ and NCH₂), 6.79 (t, $^3J = 7.1$ Hz, 8H, *p*- BPh₄), 6.51 (d, $^2J = 13.4$ Hz, 4H, NCH₂), 6.41 (t, $^3J = 2.0$ Hz, 4H, Pz H^4), 4.37 (br s, 4H, CH of COD), 2.42 (br s, 4H, CH₂ of COD), 1.96 (br s, 4H, CH₂ of COD) ppm.

$^{13}\text{C}\{^1\text{H}\}$ NMR (100 MHz, $\text{dms}\text{-d}_6$) δ 163.4 (q, $^1J(\text{B-C}) = 49.2$ Hz, *i*- C of BPh₄), 141.3 (Pz C^3 or 5), 135.5 (*o*- C of BPh₄), 132.0 (Pz C^3 or 5), 125.3 (q, $^3J(\text{B-C}) = 2.6$ Hz, *m*- C of BPh₄), 121.5 (*p*- C of BPh₄), 122.0 (Im $\text{C}^{3/5}$), 106.8 (Pz C^4), 103.3 (CH of COD) 62.5 (NCH₂), 51.7 (CH of COD), 34.0 (CH₂ of COD), 28.2 (CH₂ of COD) ppm.

ESI-MS (MeOH), m/z : 758.28 (100 %) $[\text{M} - \text{BPh}_4]^-$.

E.2.3 Synthesis of Rh and Ir CO containing complexes with $\text{NCN}^{\text{Me}} \cdot \text{HBPh}_4$ (**2.1**)

E.2.3.1 Synthesis of $[\text{Rh}(\text{NCN}^{\text{Me}})(\text{CO})]_2(\text{BPh}_4)_2$ (**2.6**)



$[\text{Rh}(\text{NCN}^{\text{Me}})(\text{COD})]\text{BPh}_4$ **2.3** (0.100 g, 0.132 mmol) was dissolved in dry and degassed thf. The solution was degassed via two freeze-pump-thaw cycles and then treated under an atmosphere of carbon

monoxide using a balloon until the bimetallic **2.6** complex precipitated leaving a clear solution. The solid product was filtered and washed with pentane. X-ray quality crystals were grown by layering pentane over an acetone solution of the complex.

Yield: 0.051 g, 57%

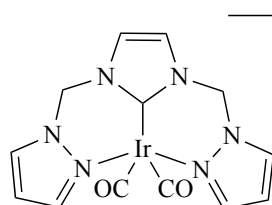
^1H NMR (400 MHz, $\text{dms}\text{-d}_6$) δ 8.76 (d, $^3J = 2.5$ Hz, 2H, Pz $\text{H}^{3'}$ or $5'$), 7.93 (d, $^3J = 1.9$, 2H, Pz $\text{H}^{3'}$ or $5'$), 7.81 (d, $^3J = 2.3$ Hz, 2H, Pz H^5), 7.76 (d, $^3J = 1.9$, 2H, Im H^4), 7.68 (d, $^3J = 2.0$, 2H, Im $\text{H}^{4'}$), 7.28 (d, $^2J = 13.8$ Hz, 2H, NCH^{a}), 7.17 (m, 16H, *o*-BPh₄), 6.92 (t, $^3J = 7.4$ Hz, 18H, *m*-BPh₄ and NCH^{b}), 6.78 (t, $^3J = 7.5$ Hz, 8H, *p*-BPh₄), 6.67 (t, $^3J = 2.4$ Hz, 2H, Pz $\text{H}^{4'}$), 6.62 (d, $^2J = 13.8$ Hz, 2H, NCH^{b}), 6.42 (d, $^2J = 13.5$ Hz, 2H, NCH^{a}), 5.70 (t, $^3J = 2.4$ Hz, 2H, Pz H^4), 4.55 (d, $^3J = 2.0$ Hz, 2H, Pz H^3) ppm.

$^{13}\text{C}\{^1\text{H}\}$ NMR (100 MHz, $\text{dms}\text{-d}_6$) δ 163.4 (q, $^1J(\text{B-C}) = 49.0$ Hz, *i*-C of BPh₄), 146.8 (Pz C^5 or 3), 140.1 (Pz C^5 or 3), 136.0 (Pz C^5 or 3), 135.6 (*o*-C of BPh₄), 133.0 (Pz C^5 or 3), 125.3 (*m*-C of BPh₄), 124.7 (Im C^4 or 5), 121.5 (*p*-C of BPh₄), 120.1 (Im C^4 or 5), 108.8 (Pz C^4), 107.0 (Pz C^4) 63.4 (NCH_2), 62.5 (NCH_2) ppm.

$^{13}\text{C}\{^1\text{H}\}$ NMR (150 MHz, acetone-d_6 , 193K) δ 189.2 (d, $^1J(\text{Rh-C}) = 78.0$, CO) ppm.

IR (KBr disc): ν 1998 (br s, CO) cm^{-1} .

E.2.3.2 Synthesis of $[\text{Ir}(\text{NCN}^{\text{Me}})(\text{CO})_2]\text{BPh}_4$ (**2.7**)



The following reaction was carried out *in situ* as the product proved to be unstable in the absence of a CO

atmosphere. In a Young's[®] NMR tube, [Ir(NCN^{Me})(COD)]BPh₄ (**2.4**) (50 mg, 58.9 μ mol) was dissolved in dry and degassed thf-d₈. The content of the Young's[®] NMR tube then was exposed to an atmosphere of CO for 10 minutes to give a bright yellow solution.

¹H NMR (600 MHz, thf-d₈) δ 7.84 (d, ³J= 1.5 Hz, 2H, Pz **H**³), 7.63 (d, ³J= 2.2, 2H, Pz **H**⁵), 7.37 (m, 8H, *o*- BPh₄), 7.02 (s, 2H, Im **H**^{4/5}), 6.88 (t, ³J= 7.6 Hz, 8H, *m*- BPh₄), 6.75 (t, ³J= 7.1 Hz, 4H, *p*- BPh₄), 6.41 (t, ³J= 2.4 Hz, 2H, Pz **H**⁴), 5.87 (br s, 4H, NCH₂) ppm.

¹³C{¹H} NMR (150 MHz, thf-d₈) δ 165.1 (q, ¹J(B-C)= 49.0 Hz, *i*- C of BPh₄), 145.4 (Pz **C**³), 137.4 (*o*- C of BPh₄), 133.9 (Pz **C**⁵), 126.0 (d, ³J(B-C)= 4.0 Hz, *m*- C of BPh₄), 123.2 (Im **C**^{4/5}), 121.2 (*p*- C of BPh₄), 108.6 (Pz **C**⁴), 64.2 (NCH₂) ppm.

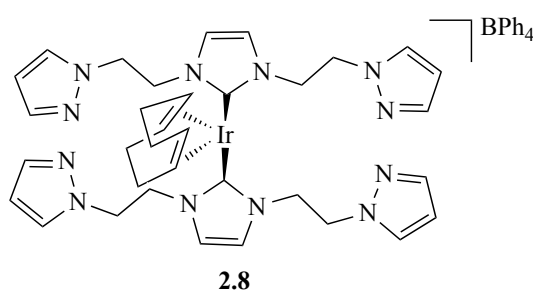
¹H NMR (600 MHz, thf-d₈, 193K) δ 5.90 (d, ²J= 13.1 Hz, 2H, NCH₂), 5.79 (d, ²J= 13.1 Hz, 2H, NCH₂) ppm.

¹³C{¹H} NMR (150 MHz, thf-d₈, 193K) δ 181.7 (br s, CO)

IR (thf): ν 2081 (s, CO), 2013 (s, CO) cm⁻¹.

E.2.4 Synthesis of Ir and Rh COD containing complexes with $\text{NCN}^{\text{Et}}\cdot\text{HBPh}_4$ (2.2)

E.2.4.1. Synthesis of $[\text{Ir}(\text{NCN}^{\text{Et}})_2(\text{COD})]\text{BPh}_4$ (2.8)



An excess of NaOEt (0.088 g, 1.3 mmol), $[\text{Ir}(\mu\text{-Cl})(\text{COD})]_2$ (0.094 g, 0.14 mmol) and $\text{NCN}^{\text{Et}}\cdot\text{HBPh}_4$ (**2.2**) (0.310, 0.54 mmol) were suspended in thf and stirred for 1 hr at room temperature. Filtered and the product

precipitated by addition of diethyl ether. The product was further purified by recrystallization with thf/diethyl ether. X-ray quality crystals were grown by layering a dcm solution of (**2.8**) with pentane.

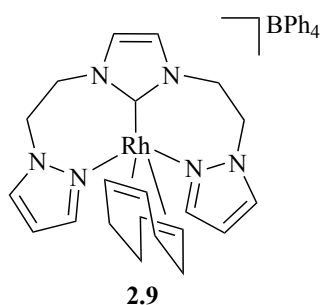
Yield: 0.026 g, 16%;

^1H NMR (400 MHz, $\text{dms}\text{-d}_6$) δ 7.48 (d, $^3J = 2.0$ Hz, 4H, Pz H^5), 7.45 (d, $^3J = 1.6$, 4H, Pz H^3), 7.41 (s, 4H, Im $\text{H}^{4/5}$), 7.17 (m, 8H, *o*- BPh₄), 6.92 (t, $^3J = 7.4$ Hz, 8H, *m*- BPh₄), 6.78 (t, $^3J = 7.1$ Hz, 4H, *p*- BPh₄), 6.21 (t, $^3J = 2.0$ Hz, 4H, Pz H^4), 4.88 (m, 4H, NCH₂), 4.62 (m, 8H, NCH₂), 4.32 (m, 4H, NCH₂), 2.86 (br s, 4H, CH of COD), 2.02 (br s, 4H, CH₂ of COD), 1.60 (m, 4H, CH₂ of COD) ppm.

$^{13}\text{C}\{^1\text{H}\}$ NMR (100 MHz, $\text{dms}\text{-d}_6$) δ 164.4 (q, $^1J(\text{B-C}) = 50.9$ Hz, *i*- C of BPh₄), 139.4 (Pz C^3), 135.5 (*o*- C of BPh₄), 130.3 (Pz C^5), 125.3 (*m*- C of BPh₄), 121.5 (*p*- C of BPh₄), 121.0 (Im $\text{C}^{4/5}$), 105.6 (Pz C^4), 75.6 (CH of COD) 50.4 (NCH₂), 49.9 (NCH₂) 30.8 (CH₂ of COD) ppm.

ESI-MS (MeOH), m/z : 813.34 (100 %) $[\text{M} - \text{BPh}_4]^-$.

E.2.4.2 Synthesis of [Rh(NCN^{Et})(COD)]BPh₄ (**2.9**)



An excess of NaOEt (0.071 g, 1.1 mmol), [Rh(μ -Cl)(COD)]₂ (0.101 g, 0.17 mmol) and the imidazolium ligand precursor NCN^{Et}.HBPh₄ (**2.2**) (0.200 g, 0.35 mmol) were suspended in dry and degassed acetone and stirred at room temperature for 1 hr. The mixture was filtered and the product **2.9** precipitated by addition of pentane. X-ray quality crystals were grown by layering a dcm solution of **2.9** with pentane.

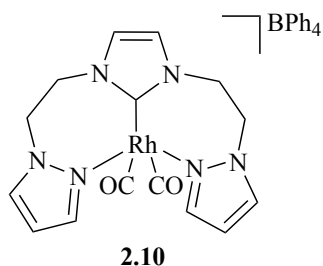
Yield: 0.0993 g, 37%;

¹H NMR (400 MHz, acetone-d₆) δ 7.49 (m, 4H, Pz **H**^{3/5}), 7.35 (m, 8H, *o*- BPh₄), 7.11 (s, 2H, Im **H**^{4/5}), 6.92 (t, ³*J*= 7.4 Hz, 8H, *m*- BPh₄), 6.78 (t, ³*J*= 7.1 Hz, 4H, *p*- BPh₄), 6.23 (t, ³*J*= 2.1 Hz, 2H, Pz **H**⁴), 5.32 (m, 2H, CH₂), 4.67 (m, 6H, CH₂) 3.82 (br s, 2H, CH of COD), 2.46 (br s, 2H, CH₂ of COD), 2.07 (br s, 2H, CH₂ of COD) ppm

¹³C{¹H} NMR (100 MHz, acetone-d₆) δ 181.9 (Im **C**²), 163.9 (q, ¹*J*(B-C)= 50.9 Hz, *i*- C of BPh₄), 139.5 (Pz **C**^{3 or 5}), δ 136.0 (*o*- C of BPh₄), 130.0 (Pz **C**^{3 or 5}), 125.0 (*m*-C of BPh₄), 121.4 (Im **C**^{4/5}), 121.2 (*p*- C of BPh₄), 105.5 (Pz **C**⁴), 89.5 (CH of COD) 50.9 (CH₂), 50.7 (CH₂) 30.2 (CH₂ of COD), 28.8 (CH₂ of COD) ppm.

ESI-MS (MeOH), *m/z*: 467.14 (100 %) [M- BPh₄].

E.2.4.3 Synthesis of $[\text{Rh}(\text{NCN}^{\text{Et}})(\text{CO})_2]\text{BPh}_4$ (**2.10**)



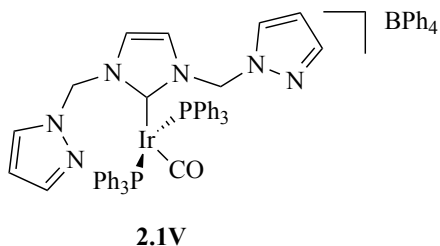
The following reaction was carried out *in situ* as the product proved to be unstable in the absence of a CO atmosphere. In a Young's[®] NMR tube, $[\text{Rh}(\text{NCN}^{\text{Et}})(\text{COD})]\text{BPh}_4$ (**2.9**) (0.050 g, 0.063 mmol) was dissolved in dry and degassed acetone- d_6 . The content of the Young's[®] NMR tube then was exposed to an atmosphere of CO and left reacting for 10 minutes to give a yellow solution. The solution was frozen and the atmosphere replenished with CO to ensure complete displacement of the COD co-ligand with CO.

^1H NMR (500 MHz, acetone- d_6) δ 7.65 (m, 4H, Pz $\text{H}^{3/5}$), 7.35 (m, 8H, *o*- BPh₄), 7.17 (s, 2H, Im $\text{H}^{4/5}$), 6.92 (t, $^3J = 7.4$ Hz, 8H, *m*- BPh₄), 6.78 (t, $^3J = 7.1$ Hz, 4H, *p*- BPh₄), 6.35 (t, $^3J = 2.2$ Hz, 2H, Pz H^4), 5.10 (br s, 4H, CH₂), 4.78 (t, $^3J = 5.7$ Hz, 4H, CH₂) ppm.

IR (thf): ν 2098 (s, CO), 2034 (s, CO) cm^{-1} .

E.2.5 Synthesis of $\text{Ir}(\text{PPh}_3)_2(\text{CO})$ complexes with $\text{NCN}^{\text{Me}}.\text{HBPh}_4$ (**2.1**) and $\text{NCN}^{\text{Et}}.\text{HBPh}_4$ (**2.2**)

E.2.5.1 Synthesis of $[\text{Ir}(\text{NCN}^{\text{Me}})(\text{PPh}_3)_2(\text{CO})]\text{BPh}_4$ (**2.1V**)



The imidazolium ligand precursor $\text{NCN}^{\text{Me}}.\text{HBPh}_4$ (**2.1**) (0.070 g, 0.13 mmol), Vaska's complex $[\text{Ir}(\text{PPh}_3)_2\text{COCl}]$ (0.101 g, 0.13 mmol) and NaOEt (0.030 g, 0.4 mmol) were suspended in dry and

degassed methanol (25 ml). The reaction was refluxed overnight. The resulting yellow precipitate was filtrated and recrystallized from thf/pentane. X-ray quality crystals were grown by layering a thf solution of **2.1V** with pentane.

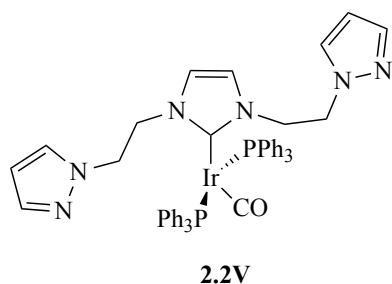
Yield: 0.042 g, 33%;

^1H NMR (400 MHz, thf- d_8) δ 7.58-7.33 (m, 32H, PPh_3 and Pz $\text{H}^{5 \text{ or } 3}$), 7.28 (m, 8H, *o*- BPh_4), 7.06 (d, $^3J = 2.0$ Hz, 2H, Pz $\text{H}^{5 \text{ or } 3}$), 6.82 (t, $^3J = 7.6$ Hz, 8H, *m*- BPh_4), 6.68 (t, $^3J = 7.2$ Hz, 4H, *p*- BPh_4), 6.14 (br s, 2H, Pz H^4), 5.42 (br s, 2H, Im $\text{H}^{4/5}$) ppm.

$^{31}\text{P}\{^1\text{H}\}$ NMR (161.98 MHz, thf- d_6): 17.37 ppm;

ESI-MS (MeOH), m/z : 973.25 (100 %) $[\text{M} - \text{BPh}_4]^-$

E.2.5.2 Synthesis of $[\text{Ir}(\text{NCN}^{\text{Et}})(\text{PPh}_3)_2(\text{CO})]\text{BPh}_4$ (**2.2V**)



BPh_4 The imidazolium ligand salt $\text{NCN}^{\text{Et}} \cdot \text{HBPh}_4$ (**2.2**) (0.104 g, 0.18 mmol), Vaska's complex $[\text{Ir}(\text{PPh}_3)_2(\text{CO})\text{Cl}]$ (0.14 g, 0.18 mmol) and NaOEt (0.068 g, 1

mmol) were suspended in dry and degassed methanol (25 ml). The reaction was left stirring overnight at reflux. The resulting yellow precipitate was filtered and recrystallized from thf/pentane. X-ray quality crystals were grown by layering a thf solution of **2.2V** with pentane

Yield: 0.069 g, 29%;

^1H NMR (400 MHz, thf-d_8) δ 7.52-7.37 (m, 32H, PPh_3 and Pz H^3), 7.28 (m, 8H, *o*- BPh_4), 6.99 (d, $^3J = 2.0$ Hz, 2H, Pz H^5), 6.82 (t, $^3J = 7.6$ Hz, 8H, *m*- BPh_4), 6.68 (t, $^3J = 7.2$ Hz, 4H, *p*- BPh_4), 6.14 (t, $^3J = 1.8$ Hz, 2H, Pz H^4), 6.11 (s, 2H, Im $\text{H}^{4/5}$), 3.81 (t, $^3J = 7.1$ Hz, 2H, NCH_2), 3.40 (t, $^3J = 7.1$ Hz, 2H, NCH_2) ppm.

$^{13}\text{C}\{^1\text{H}\}$ NMR (100 MHz, thf-d_6) δ 176.7 (CO), 165.2 (q, $^1J(\text{B-C}) = 48.8$ Hz, *i*-C of BPh_4), 140.3 (Pz C^3), 137.2 (*o*-C of BPh_4), 134.9 (t, $^3J = 5.8$ Hz, *o*, *m*, *p*-C of PPh_3), 132.8 (t, $^1J(\text{P-C}) = 27.2$ Hz, *i*-C of PPh_3), 132.3 (PPh_3), 130.4 (Pz C^5), 129.9 (t, $^1J = 4.6$ Hz, PPh_3), 125.8 (*m*-C of BPh_4), 123.8 (Im $\text{C}^{4/5}$), 121.9 (*p*-C of BPh_4), 106.5 (Pz C^4), 50.8 (NCH_2), 50.0 (NCH_2) ppm.

$^{31}\text{P}\{^1\text{H}\}$ NMR (161.98 MHz, thf-d_6): 21.84 ppm;

IR (thf) $\nu = 2002$ (s, CO) cm^{-1} ;

ESI-MS (MeOH), m/z : 1001.29 (100 %) $[\text{M-BPh}_4^-]$.

PART 3: EXPERIMENTAL FOR CHAPTER 3

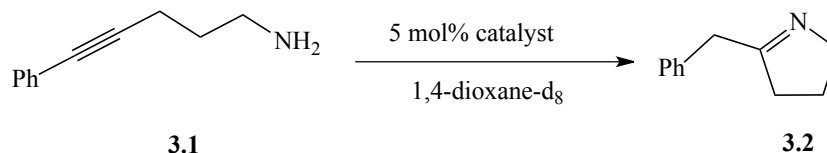
E.3.1 Iridium(I) and Rhodium(I) Catalysed reactions

All metal complex catalyzed reactions were performed on a small scale in NMR tubes fitted with a Young's[®] concentric Teflon valve. The NMR samples were prepared either in a nitrogen or argon filled glove box. Substrates were purchased from Sigma Aldrich, dried over the appropriate drying agent and distilled prior to use. Aniline, phenylacetylene and *n*-hexylamine were dried over CaH₂ and 1-heptyne over activated 4 Å molecular sieves. Deuterated solvents were purchased from Cambridge Isotope Labs and, with the exception of 1,1,2,2-tetrachloroethane, dried before use. ¹H NMR spectra were recorded on Bruker Avance III 400 or Avance III 500 spectrometers. All spectra were recorded at 298K, unless otherwise stated. The temperature in the NMR magnet was calibrated using an Omega Microprocessor Thermometer (Model HH23). ¹H NMR chemical shifts are referenced to internal solvent chemical shifts.

E.3.1.2 General procedure

Conversion of substrate to product was determined by integration of the product resonances relative to the substrate resonances in the ¹H NMR spectrum. For intermolecular hydroaminations, 1,3,5-trimethoxybenzene was used as an internal standard. The catalyst μmol value reported here refers to a number of moles of metal centres and not of the complex. Complexes with CO co-ligand were prepared *in situ* in Young's[®] NMR tubes and the catalysis were performed under 1 atmosphere of CO .

E.3.1.3 Intra-molecular hydroamination of 5-phenyl-4-pentyn-1-amine (3.1) to 2-methyl-1-pyrroline (3.2)



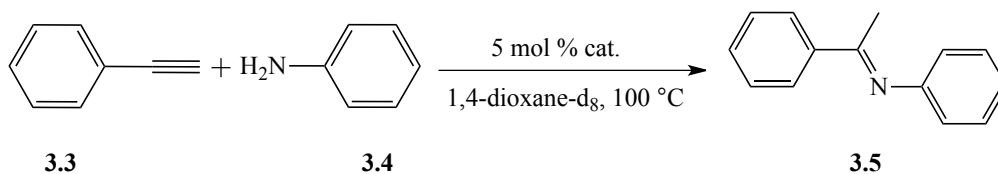
0.6 ml of A stock solution (0.6 mL) in deuterated 1,4-dioxane- d_8 of 5-phenyl-4-pentyn-1-amine (0.15 M) was added to 2.5 μmol of catalyst in a Young's[®] NMR tube. The final catalyst concentration was 5 mol%. The tubes were then heated at 100 °C in a oil bath and the solution periodically monitored by ^1H NMR. The identification of the product was confirmed by comparison with the product ^1H NMR resonances reported in the literature.⁹

Table E.1: Quantity of catalysts and substrates used for the intra-molecular hydroamination of 5-phenyl-4-pentyn-1-amine (**3.1**) to 2- benzyl-1-pyrroline (**3.2**) in dioxane- d_8 at 100 °C using pincer complexes with BPh_4 counter ion.

Catalyst	Mass of cat. (mg)	Stock sol. (ml) ^c	Mol (%)
$[\text{Rh}(\text{NCN}^{\text{Me}})\text{COD}]\text{BPh}_4$ (2.3)	4.9	5.2	5.0
$[\text{Ir}(\text{NCN}^{\text{Me}})\text{COD}]\text{BPh}_4$ (2.4)	5.1	4.8	5.0
$[\text{Rh}(\text{NCN}^{\text{Et}})(\text{COD})]\text{BPh}_4$ (2.9)	4.8	4.9	5.0
$[\text{Rh}(\text{NC}^{\text{Me}})(\text{COD})]\text{BPh}_4$ (2.11)	4.2	4.9	5.0
$[\text{Rh}(\text{NCN}^{\text{Me}})(\text{CO})_2][\text{BPh}_4]_2$ (2.6) ^{a,b}	4.6 ^b	4.9	5.0
$[\text{Ir}(\text{NCN}^{\text{Me}})(\text{CO})_2]\text{BPh}_4$ (2.7) ^{a,b}	5.1 ^b	4.8	5.0
$[\text{Rh}(\text{NCN}^{\text{Et}})(\text{CO})_2]\text{BPh}_4$ (2.10) ^{a,b}	4.9 ^b	5.0	5.0
$[\text{Rh}(\text{NC}^{\text{Me}})(\text{CO})_2]\text{BPh}_4$ (2.12) ^{a,b}	4.2 ^b	4.9	5.0

a) complexes prepared *in situ*; b) mass refers to the analogous complex with COD co-ligand;

c) M= 0.24 mol/L.

E.3.1.4 Inter-molecular hydroamination of phenylacetylene (3.3) and aniline (3.4)

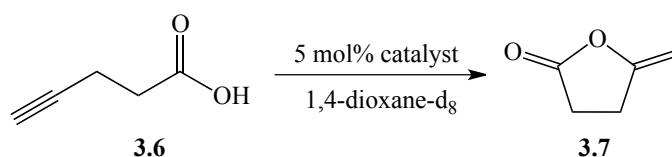
0.6 ml of a stock solution of aniline (**3.4**, 0.15 M), phenylacetylene (**3.3**, 0.13 M) and internal standard (0.04 M) in deuterated 1,4-dioxane-d₈ was added to 2.5 μmol of catalyst in a Young's[®] NMR tube to reach a final concentration of 5 mol%. The tubes were then heated at 100 °C in an oil bath and the solution periodically monitored by ¹H NMR. The identification of the product was confirmed by comparison with the product ¹H NMR resonances reported in the literature.⁹

Table E.2: Quantity of catalysts and substrates used for the inter-molecular hydroamination of phenylacetylene (**3.3**) and aniline (**3.4**) into *E-N*-(1-phenylethylidene)benzeneamine imine (**3.5**) in dioxane at 100 °C using pincer complexes.

Catalyst	Mass of cat. (mg)	Stock sol. (ml) ^c	Mol (%)
[Rh(NCN ^{Me})(COD)]BPh ₄ (2.3)	4.7	5.0	5.0
[Ir(NCN ^{Me})(COD)]BPh ₄ (2.4)	5.1	4.8	5.0
(Rh(NCN ^{Me})(CO)) ₂ (BPh ₄) ₂ (2.6) ^{a,b}	4.7 ^b	5.0	5.0
[Ir(NCN ^{Me})(CO) ₂]BPh ₄ (2.7) ^{a,b}	5.2 ^b	4.8	5.0
[Rh(NCN ^{Me})(COD)]BArF (2.3.BArF)	8.0	5.1	5.0
[Ir(NCN ^{Me})(COD)]BArF (2.4.BArF)	8.6	5.1	5.0
(Rh(NCN ^{Me})(CO)) ₂ (BArF) ₂ (2.6.BArF) ^{a,b}	8.0 ^b	5.1	5.0
[Ir(NCN ^{Me})(CO) ₂]BArF (2.7.BArF) ^{a,b}	8.5 ^b	5.1	5.0

a) complexes prepared *in situ*; b) mass calculated based on the molecular weight of the analogous complex with COD co-ligand; c) M= 0.25 mol/L.

E.3.1.5 Catalysed hydroxylation of 4-pentynoic acid (**3.6**)



0.5 ml of a stock solution of 5-pentynoic acid (**3.6**) (0.25 M) in deuterated 1,4-dioxane-d₈ was added to 6.0 μmol of catalyst in a Young's[®] NMR tube to reach a final concentration of 5 mol%. The tubes were then heated at 100 °C in an oil bath and

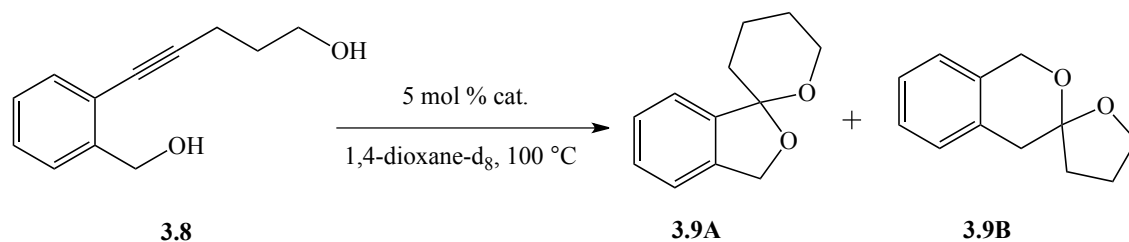
the solution periodically monitored by ^1H NMR. The γ -methylene- γ -butyrolactone (**3.7**) product was identified by comparison with ^1H NMR from the literature.¹⁰

Table E.3: Quantity of catalysts and substrates used for the hydroalkoxylation 4-pentynoic acid (**3.6**) to γ -methylene- γ -butyrolactone (**3.7**) 100 °C using pincer complexes with BPh_4^- counter ion.

Catalyst	Mass of cat. (mg)	Stock sol. (ml) ^c	Mol (%)
$[\text{Rh}(\text{NCN}^{\text{Me}})\text{COD}]\text{BPh}_4$ (2.3)	4.7	5.2	5.0
$[\text{Ir}(\text{NCN}^{\text{Me}})\text{COD}]\text{BPh}_4$ (2.4)	5.0	4.9	5.0
$[\text{Rh}(\text{NCN}^{\text{Et}})(\text{COD})]\text{BPh}_4$ (2.9)	4.8	5.1	5.0
$[\text{Rh}(\text{NC}^{\text{Me}})(\text{COD})]\text{BPh}_4$ (2.11)	4.3	5.2	5.0
$[\text{Rh}(\text{NCN}^{\text{Me}})(\text{CO})_2]\text{BPh}_4$ (2.6) ^{a,b}	4.9	5.4	5.0
$[\text{Ir}(\text{NCN}^{\text{Me}})(\text{CO})_2]\text{BPh}_4$ (2.7) ^{a,b}	5.1	5.0	5.0
$[\text{Rh}(\text{NCN}^{\text{Et}})(\text{CO})_2]\text{BPh}_4$ (2.10) ^{a,b}	4.7	5.0	5.0
$[\text{Rh}(\text{NC}^{\text{Me}})(\text{CO})_2]\text{BPh}_4$ (2.12) ^{a,b}	4.3	5.2	5.0

a) complexes prepared *in situ*; b) mass calculated based on the molecular weight of the analogous complex with COD co-ligand; c) M= 0.25 mol/L.

E.3.1.6 Catalysed dihydroalkoxylation of 2-(5-Hydroxypent-1-ynyl)benzyl alcohol (3.8)



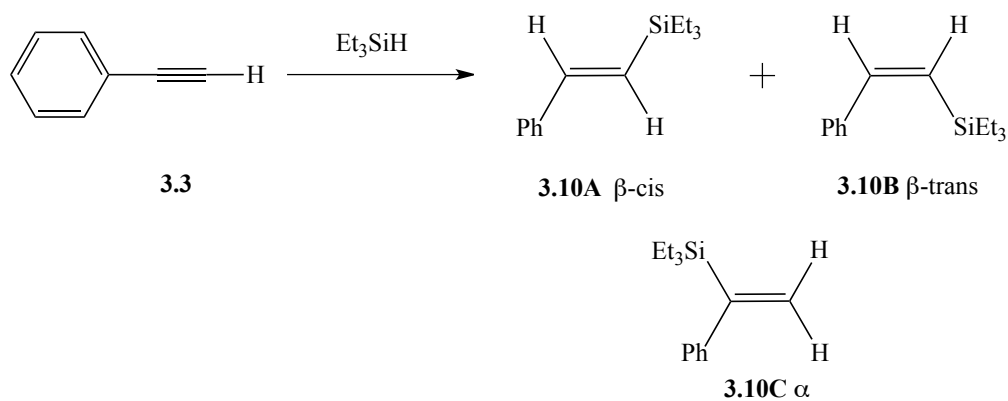
0.45 ml of a stock solution of 2-(5-Hydroxypent-1-ynyl)benzyl alcohol (**3.8**) (0.28 M) in deuterated 1,4-dioxane- d_8 was added to 6.0 μmol of catalyst in a Young's[®] NMR tube to reach a final concentration of 5 mol%. The tubes were then heated at 100°C in an oil bath and the solution periodically monitored by ^1H NMR. The 5,6- (**3.9A**) and 6,5- (**3.9B**) spiroketal products were indentified by comparison with ^1H NMR from the literature.^{11,12}

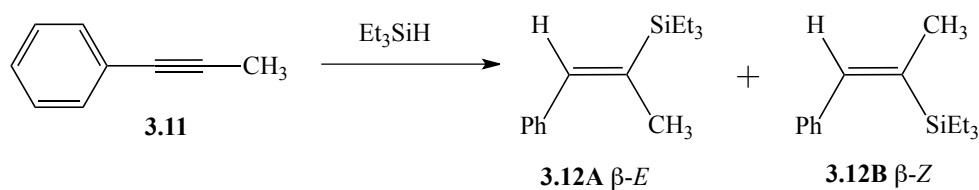
Table E.4: Quantity of catalysts and substrates used for the dihydroalkoxylation of 2-(5-Hydroxypent-1-ynyl)benzyl alcohol (**3.8**) into 5,6- (**3.9A**) and 6,5- (**3.9B**) spiroketals in dioxane- d_8 at 100 °C using pincer complexes with BPh_4^- counter ion.

Catalyst	Mass of cat. (mg)	Stock sol. (ml) ^c	Mol (%)
$[Rh(NCN^{Me})COD]BPh_4$ (2.3)	4.9	4.6	5.0
$[Ir(NCN^{Me})COD]BPh_4$ (2.4)	5.2	4.4	5.0
$[Rh(NCN^{Et})(COD)]BPh_4$ (2.9)	4.9	4.4	5.0
$[Rh(NC^{Me})(COD)]BPh_4$ (2.11)	4.2	4.4	5.0
$[Rh(NCN^{Me})(CO)]_2[BPh_4]_2$ (2.6) ^{a,b}	4.9 ^b	4.6	5.0
$[Ir(NCN^{Me})(CO)]_2[BPh_4]_2$ (2.7) ^{a,b}	5.2 ^b	4.4	5.0
$[Rh(NCN^{Et})(CO)]_2[BPh_4]_2$ (2.10) ^{a,b}	4.9 ^b	4.4	5.0
$[Rh(NC^{Me})(CO)]_2[BPh_4]_2$ (2.12) ^{a,b}	4.4 ^b	4.6	5.0

a) complexes prepared *in situ*; b) mass calculated based on the molecular weight of the analogous complex with COD co-ligand; c) M= 0.28 mol/L.

E.3.1.7 Catalysed hydrosilylation of alkynes





An aliquot of the desired alkyne (83 μmol) and Et_3SiH (91 μmol) was added to a solution of catalyst (2.3 μmol , 3 mol%) in acetone- d_6 (0.6 mL) in a Young's[®] NMR tube. The tubes were then heated at 55 °C in a sand bath and the progress of the reaction periodically monitored by ^1H NMR. The vinylsilane products were indentified by comparison with ^1H NMR data reported in the literature.¹³

Table E.5: Quantity of catalysts and substrates used for the hydrosilylation of phenylacetylene (**3.3**) and Et_3SiH in acetone- d_6 at 60 °C using pincer complexes with BPh_4^- counter ion.

Catalyst	Mass of cat. (mg)	Mass of 3.3 (mg)	Mass of Et_3SiH (mg)	Mol (%)
$[\text{Rh}(\text{NCN}^{\text{Me}})\text{COD}]\text{BPh}_4$ (2.3)	1.9	8.5	9.7	3.0
$[\text{Ir}(\text{NCN}^{\text{Me}})\text{COD}]\text{BPh}_4$ (2.4)	2	8.8	9.6	3.0
$[\text{Rh}(\text{NCN}^{\text{Me}})(\text{CO})_2][\text{BPh}_4]_2$ (2.6) ^{a,b}	1.8 ^b	8.3	9.9	3.0
$[\text{Ir}(\text{NCN}^{\text{Me}})(\text{CO})_2]\text{BPh}_4$ (2.7) ^{a,b}	2.1 ^b	8.9	9.7	3.0

a) complexes prepared *in situ*; b) mass calculated based on the molecular weight of the analogous complex with COD co-ligand;

Table E.6: Quantity of catalysts and substrates used for the hydrosilylation of 1-phenylpropyne (**3.11**) and Et₃SiH in acetone-d₆ at 60 °C using pincer complexes with BPh₄[−] counter ion.

Catalyst	Mass of cat. (mg)	Mass of 3.11 (mg)	Mass of Et ₃ SiH (mg)	Mol (%)
[Rh(NCN ^{Me})COD]BPh ₄ (2.3)	1.8	9.7	9.7	2.9
[Ir(NCN ^{Me})COD]BPh ₄ (2.4)	2.1	9.5	9.6	2.8
[Rh(NCN ^{Me})(CO)] ₂ [BPh ₄] ₂ (2.6) ^{a,b}	2.0 ^b	10.4	9.9	2.9
[Ir(NCN ^{Me})(CO)] ₂ BPh ₄ (2.7) ^{a,b}	2.1 ^b	9.4	9.7	2.8

a) complexes prepared *in situ*; b) mass calculated based on the molecular weight of the analogous complex with COD co-ligand;

E.3.2 Crystallographic Data

Crystallographic data for the solid state structures of $[\text{Rh}(\text{NCN}^{\text{Me}})(\text{COD})]\text{BPh}_4$ (**2.3**), $[\text{Ir}(\text{NCN}^{\text{Me}})(\text{COD})]\text{BPh}_4$ (**2.4**), $[\text{Ir}(\text{k}^1\text{-NCN}^{\text{Me}})_2(\text{COD})]\text{BPh}_4$ (**2.5**), $[\text{Rh}(\mu\text{-NCN}^{\text{Me}}\text{CO})_2(\text{BPh}_4)_2]$ (**2.6**), $\text{Rh}(\text{NCN}^{\text{Et}})(\text{COD})]\text{BPh}_4$ (**2.9**) and $[\text{Ir}(\text{NCN}^{\text{Me}})(\text{PPh}_3)_2(\text{CO})]\text{BPh}_4$ (**2.1V**).

$[\text{Rh}(\text{NCN}^{\text{Me}})(\text{COD})]\text{BPh}_4$ (**2.3**)

Crystal data	
Chemical formula	$\text{C}_{43}\text{H}_{44}\text{BN}_6\text{Rh}$
M_r	845.46
Crystal system, space group	Monoclinic, $P2_1/n$
Temperature (K)	156
a, b, c (Å)	17.425 (3), 11.8512 (16), 21.719 (3)
β (°)	108.686 (5)
V (Å ³)	4248.8 (11)
Z	4
Radiation type	Mo $K\alpha$
μ (mm ⁻¹)	0.57
Crystal size (mm)	$0.33 \times 0.30 \times 0.09$
Data collection	
Diffractometer	Bruker kappa APEXII CCD Diffractometer
Absorption correction	Multi-scan <i>SADABS</i> (Bruker, 2001)
T_{\min}, T_{\max}	0.837, 0.950
No. of measured, independent and observed $[I > 2s(I)]$ reflections	29496, 7459, 6533
R_{int}	0.032
$(\sin \theta/\lambda)_{\text{max}}$ (Å ⁻¹)	0.595

Refinement	
$R[F^2 > 2s(F^2)], wR(F^2), S$	0.038, 0.119, 1.04
No. of reflections	7459
No. of parameters	533
No. of restraints	0
H-atom treatment	H-atom parameters constrained
$\Delta_{\text{max}}, \Delta_{\text{min}} (\text{e } \text{\AA}^{-3})$	0.86, -0.47

[Ir(NCN^{Me})(COD)]BPh₄ (2.4)

Crystal data	
Chemical formula	C ₄₃ H ₄₄ BIrN ₆
<i>M</i> _r	917.94
Crystal system, space group	Monoclinic, <i>P</i> 2 ₁ / <i>c</i>
Temperature (K)	163
<i>a</i> , <i>b</i> , <i>c</i> (Å)	11.8066 (4), 9.6104 (3), 35.9142 (11)
β (°)	95.944 (2)
<i>V</i> (Å ³)	4053.1 (2)
<i>Z</i>	4
Radiation type	Mo <i>K</i> α
μ (mm ⁻¹)	3.34
Crystal size (mm)	0.17 × 0.13 × 0.05
Data collection	
Diffractometer	Bruker kappa APEXII CCD Diffractometer
Absorption correction	Multi-scan <i>SADABS</i> (Bruker, 2001)
<i>T</i> _{min} , <i>T</i> _{max}	0.599, 0.840
No. of measured, independent and observed [<i>I</i> > 2 <i>s</i> (<i>I</i>)] reflections	27051, 7108, 5974
<i>R</i> _{int}	0.037
(sin θ/λ) _{max} (Å ⁻¹)	0.595
Refinement	
<i>R</i> [<i>F</i> ² > 2 <i>s</i> (<i>F</i> ²)], <i>wR</i> (<i>F</i> ²), <i>S</i>	0.028, 0.059, 1.05
No. of reflections	7108
No. of parameters	505
No. of restraints	0
H-atom treatment	H-atom parameters constrained
Δ _{max} , Δ _{min} (e Å ⁻³)	0.77, -1.11

[Ir(κ^1 -NCN^{Me})₂(COD)]BPh₄ (2.5)

Crystal data	
Chemical formula	C ₅₅ H ₅₆ BIrN ₁₂
M_r	1155.00
Crystal system, space group	Triclinic, $P\bar{1}$
Temperature (K)	293
a, b, c (Å)	10.3367 (3), 12.8201 (4), 19.6142 (7)
α, β, γ (°)	92.847 (1), 102.154 (2), 94.312 (1)
V (Å ³)	2528.05 (14)
Z	2
Radiation type	Mo $K\alpha$
μ (mm ⁻¹)	2.80
Crystal size (mm)	0.36 × 0.29 × 0.21
Data collection	
Diffractometer	Bruker kappa APEXII CCD Diffractometer
Absorption correction	Multi-scan <i>SADABS</i> (Bruker, 2001)
T_{\min}, T_{\max}	0.432, 0.591
No. of measured, independent and observed [$I > 2\sigma(I)$] reflections	35831, 8907, 8566
R_{int}	0.027
$(\sin \theta/\lambda)_{\text{max}}$ (Å ⁻¹)	0.595
Refinement	
$R[F^2 > 2\sigma(F^2)], wR(F^2), S$	0.025, 0.066, 1.05
No. of reflections	8907
No. of parameters	641
No. of restraints	0

H-atom treatment	H-atom parameters constrained
$\Delta_{\text{max}}, \Delta_{\text{min}}$ (e Å ⁻³)	1.21, -1.56

[Rh(μ -NCN^{Me})CO]₂(BPh₄)₂ (2.6)

Crystal data	
Chemical formula	C ₇₂ H ₆₄ B ₂ N ₁₂ O ₂ Rh ₂
<i>M</i> _r	707.44
Crystal system, space group	Monoclinic, <i>P</i> 2 ₁ / <i>n</i>
Temperature (K)	150
<i>a</i> , <i>b</i> , <i>c</i> (Å)	12.6272 (4), 26.3368 (8), 22.9366 (7)
β (°)	91.129 (1)
<i>V</i> (Å ³)	7626.3 (4)
<i>Z</i>	8
Radiation type	Mo <i>K</i> α
μ (mm ⁻¹)	0.48
Crystal size (mm)	0.13 × 0.09 × 0.07
Data collection	
Diffractometer	Bruker kappa APEXII CCD Diffractometer
Absorption correction	Multi-scan <i>SADABS</i> (Bruker, 2001)
<i>T</i> _{min} , <i>T</i> _{max}	0.939, 0.968
No. of measured, independent and observed [<i>I</i> > 2 <i>s</i> (<i>I</i>)] reflections	80179, 13379, 6866
<i>R</i> _{int}	0.115
(sin θ/λ) _{max} (Å ⁻¹)	0.595
Refinement	
<i>R</i> [<i>F</i> ² > 2 <i>s</i> (<i>F</i> ²)], <i>wR</i> (<i>F</i> ²), <i>S</i>	0.065, 0.194, 1.03
No. of reflections	13379
No. of parameters	884
No. of restraints	39
H-atom treatment	H-atom parameters constrained
Δ _{max} , Δ _{min} (e Å ⁻³)	0.75, -0.46

Rh(NCN^{Et})(COD)]BPh₄ (2.9)

Crystal data	
Chemical formula	C ₄₅ H ₄₈ BN ₆ Rh
<i>M</i> _r	786.61
Crystal system, space group	Monoclinic, <i>P</i> 2 ₁
Temperature (K)	180
<i>a</i> , <i>b</i> , <i>c</i> (Å)	11.6656 (3), 11.3435 (3), 14.6475 (4)
β (°)	97.391 (1)
<i>V</i> (Å ³)	1922.18 (9)
<i>Z</i>	2
Radiation type	Mo <i>K</i> α
μ (mm ⁻¹)	0.49
Crystal size (mm)	0.36 × 0.17 × 0.09
Data collection	
Diffractometer	Bruker kappa APEXII CCD Diffractometer
Absorption correction	Multi-scan <i>SADABS</i> (Bruker, 2001)
<i>T</i> _{min} , <i>T</i> _{max}	0.846, 0.960
No. of measured, independent and observed [<i>I</i> > 2 <i>s</i> (<i>I</i>)] reflections	14078, 6146, 5963
<i>R</i> _{int}	0.026
(sin θ/λ) _{max} (Å ⁻¹)	0.595
Refinement	
<i>R</i> [<i>F</i> ² > 2 <i>s</i> (<i>F</i> ²)], <i>wR</i> (<i>F</i> ²), <i>S</i>	0.021, 0.055, 1.04
No. of reflections	6146
No. of parameters	478
No. of restraints	1
H-atom treatment	H-atom parameters constrained
Δ _{max} , Δ _{min} (e Å ⁻³)	0.33, -0.22

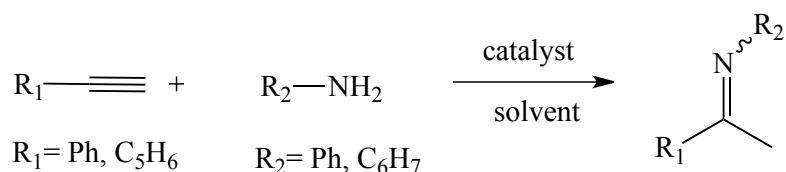
Absolute structure	Flack H D (1983), Acta Cryst. A39, 876-881
Flack parameter	-0.017 (16)

[Ir(NCN^{Me})(PPh₃)₂(CO)BPh₄ (2.1V)]

Crystal data	
Chemical formula	C ₇₂ H ₆₂ BIrN ₆ OP ₂
<i>M</i> _r	1232.75
Crystal system, space group	?, ?
Temperature (K)	293
<i>a</i> , <i>b</i> , <i>c</i> (Å)	13.4663 (3), 13.9568 (4), 17.4852 (4)
α, β, γ (°)	88.321 (1), 88.690 (1), 68.105 (1)
<i>V</i> (Å ³)	3047.68 (13)
<i>Z</i>	2
Radiation type	Mo <i>K</i> α
μ (mm ⁻¹)	2.29
Crystal size (mm)	0.36 × 0.17 × 0.09
Data collection	
Diffractometer	Bruker kappa APEXII CCD Diffractometer
Absorption correction	—
No. of measured, independent and observed [<i>I</i> > 2 <i>s</i> (<i>I</i>)] reflections	66139, 10696, 10056
<i>R</i> _{int}	0.028
(sin θ/λ) _{max} (Å ⁻¹)	0.595
Refinement	
<i>R</i> [<i>F</i> ² > 2 <i>s</i> (<i>F</i> ²)], <i>wR</i> (<i>F</i> ²), <i>S</i>	0.018, 0.044, 1.96
No. of reflections	10696
No. of parameters	748
No. of restraints	0
H-atom treatment	H atoms treated by a mixture of independent and constrained refinement
Δ _{max} , Δ _{min} (e Å ⁻³)	0.54, -0.39

PART 4: EXPERIMENTAL FOR CHAPTER 4

E.4.1 Inter-molecular hydroamination catalysis of terminal alkynes with amines



Terminal alkyne (86 μmol) and 1.2 molar excess of amine (104 μmol) were added to a solution of catalyst (2.3 μmol , 3 mol%) in a selected deuterated solvent (0.6 mL). The tubes were heated at either 60 °C or 100 °C using a sand or oil bath and the reaction progress periodically monitored by ^1H NMR. The imine products were indentified by comparison with ^1H NMR data reported in the literature.¹⁴

Table E.7: Catalysed conversion of aniline (**3.4**) and 1-heptyne (**4.8**) in toluene- d_8 at 100 °C using bimetallic complexes with *N,N*- bidentate ligands.

Catalyst	Mass of cat. (mg)	Mass of 3.4 (mg)	Mass of 4.8 (mg)	Mol (%)
[Ir(bpm)(CO) ₂](BArF) (4.4)	3.4	10.1	8.7	3
[Rh(bpm)(CO) ₂](BArF) (4.5)	3.1	10.2	8.7	2.9
(μ -L)[Ir(CO) ₂] ₂ (BArF) ₂ (4.6) ^a	3.5	9.8	8.5	2.9

a) mol% calculated on the number of metal centres.

Table E.8: Catalysed conversion of phenylacetylene (**3.3**) and 1-hexylamine (**4.11**) in toluene-d₈ at 100 °C using bimetallic complexes with *N,N*- bidentate ligands.

Catalyst	Mass of cat. (mg)	Mass of 3.3 (mg)	Mass of 4.11 (mg)	Mol (%)
[Ir(bpm)(CO) ₂](BArF) (4.4)	3.4	9.1	10.7	3.0
(μ-L)[Ir(CO) ₂] ₂ (BArF) ₂ (4.6) ^a	3.5	8.8	10.4	3.0

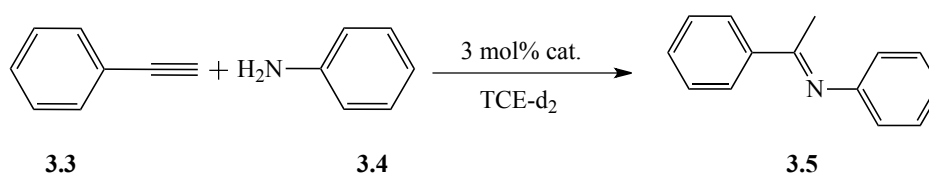
a) mol% calculated on the number of metal centres.

Table E.9: Catalysed conversion of 1-heptyne (**4.8**) and 1-hexylamine (**4.11**) in toluene-d₈ at 100 °C using bimetallic complex (μ-L)[Ir(CO)₂]₂(BArF)₂ (**4.6**).

Catalyst	Mass of cat. (mg)	Mass of 4.8 (mg)	Mass of 4.11 (mg)	Mol (%)
(μ-L)[Ir(CO) ₂] ₂ (BArF) ₂ (4.6) ^a	3.5	8.4	10.6	3.0

a) mol% calculated on the number of metal centres.

E.4.2 Inter-molecular hydroamination of phenylacetylene (**3.3**) and aniline (**3.4**)



0.6 ml of a stock solution of phenylacetylene (**3.3**, 0.13 M), aniline (**3.4**, 0.15 M), internal standard (0.04 M) in TCE-d₂ was added to 2.4 μmol of catalyst in a Young's[®] NMR tube to reach a final concentration of 3 mol%. The tubes were then heated at 100 °C in an oil bath and the solution periodically monitored by ¹H NMR. The identification

of the product was confirmed by comparison with the product ^1H NMR resonances reported in the literature.⁹

Table E.10: Quantity of catalysts and substrates used for the inter-molecular hydroamination of phenylacetylene (**3.3**) and aniline (**3.4**) into *E-N*-(1-phenylethylidene)benzeneamine imine (**3.5**) at 100 °C using Ir(I) complexes with *P,N*- and *N,N*- bidentate ligands in various solvents.

Catalyst	Solvent	Mass of cat. (mg)	Mass of 3.3 (mg)	Mass of 3.4 (mg)	Mol (%)
[Ir(PyP)(COD)]BPh ₄ (4.1)	TCE-d ₂	6.3	23.8	26.0	3.0
[Ir(PyP)(COD)]BPh ₄ (4.1)	Tol-d ₈	6.3	23.8	26.0	3.0
[Ir(PyP)(COD)]BPh ₄ (4.1)	1,4-Dioxane-d ₈	6.3	23.8	26.0	3.0
[Ir(PyP)(COD)]BArF (4.2)	TCE-d ₂	10.1	23.8	26.0	3.0
[Ir(PyP)(COD)]BArF (4.2)	Tol-d ₈	10.1	23.8	26.0	3.0
[Ir(PyP)(COD)]BArF (4.2)	1,4-Dioxane-d ₈	10.1	23.8	26.0	3.0
[Ir(PyP)(CO) ₂]BArF (4.3)	TCE-d ₂	9.4	23.8	26.0	3.0
[Ir(PyP)(CO) ₂]BArF (4.3)	Tol-d ₈	9.4	23.8	26.0	3.0
[Ir(PyP)(CO) ₂]BArF (4.3)	1,4-Dioxane-d ₈	9.4	23.8	26.0	3.0

Table E.11: Quantity of catalysts and substrates used for the inter-molecular hydroamination of phenylacetylene (**3.3**) and aniline (**3.4**) into *E-N*-(1-phenylethylidene)benzeneamine imine (**3.5**) at 100 °C using complexes with *N,N*-bidentate ligands in various solvents.

Catalyst	Solvent	Mass of cat. (mg)	Mass of 3.3 (mg)	Mass of 3.4 (mg)	Mol (%)
[Ir(bpm)(CO) ₂]BArF (4.4)	TCE-d ₂	8.9	23.8	26.0	3.0
[Ir(bpm)(CO) ₂]BArF (4.4)	Tol-d ₈	8.9	23.8	26.0	3.0
[Ir(bpm)(CO) ₂]BArF (4.4)	1,4-Dioxane-d ₈	8.9	23.8	26.0	3.0
[Rh(bpm)(CO) ₂]BArF (4.5)	TCE-d ₂	8.2	23.8	26.0	3.0
[Rh(bpm)(CO) ₂]BArF (4.5)	Tol-d ₈	8.2	23.8	26.0	3.0
[Rh(bpm)(CO) ₂]BArF (4.5)	1,4-Dioxane-d ₈	8.2	23.8	26.0	3.0

Table E.12: Quantity of catalysts and substrates used for the inter-molecular hydroamination of phenylacetylene (**3.3**) and aniline (**3.4**) into *E-N*-(1-phenylethylidene)benzeneamine imine (**3.5**) at 100 °C using bimetallic complexes with *N,N*- bidentate ligands.

Catalyst	Solvent	Mass of cat. (mg) ^a	Mass of 3.3 (mg)	Mass of 3.4 (mg)	Mol (%)
(μ -L)[Ir(CO) ₂] ₂ (BArF) ₂ (4.6)	TCE-d ₂	3.1	4.1	4.5	3.0
(μ -L)[Ir(CO) ₂] ₂ (BArF) ₂ (4.6)	Tol-d ₈	3.1	4.1	4.5	3.0
(μ -L)[Rh(CO) ₂] ₂ (BArF) ₂ (4.7)	TCE-d ₂	3.0	4.1	4.5	3.0
(μ -L)[Rh(CO) ₂] ₂ (BArF) ₂ (4.7)	Tol-d ₈	3.0	4.1	4.5	3.0

a) mol% calculated on the number of metal centres.

Table E.13: Quantity of catalysts and substrates used for the inter-molecular hydroamination of phenylacetylene (**3.3**) and aniline (**3.4**) into *E-N*-(1-phenylethylidene)benzeneamine imine (**3.5**) in TCE-d₂ at 100 °C using complexes with *P,N*- and *N,N*- bidentate ligands.

Catalyst	Mass of cat. (mg)	Stock sol ^a (ml)	Mol (%)
[Ir(PyP)(CO) ₂]BArF (4.3)	3.3	6.4	3.0
[Ir(bpm)(CO) ₂]BArF (4.4)	3.1	6.4	3.0
(μ -L)[Ir(CO) ₂] ₂ (BArF) ₂ (4.6) ^b	3.1	6.2	3.0

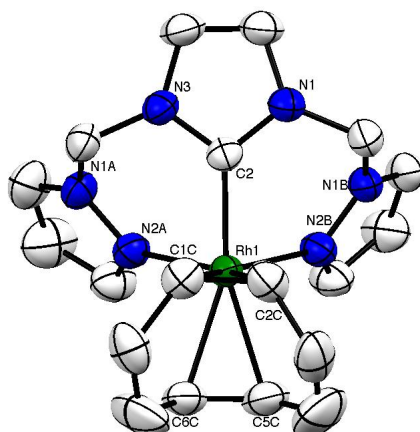
a) M= 0.13 mol/L; b) mol% calculated on the number of metal centres.

E.5 References

- (1) Shriver, D. F.; Drezzdon, M. A. *The Manipulation of Air Sensitive Compounds*, 2nd ed; John Wiley & Sons: New York, **1986**.
- (2) Armarego, W. L. F.; Chai, C. L. L. *Purification of Laboratory Chemicals*, 6th ed; Elsevier Inc., **2003**.
- (3) Choudhury, J.; Podder, S.; Roy, S. *J. Am. Chem. Soc.* **2005**, 127, 6162.
- (4) Giordano, G.; Crabtree, R. H.; Heintz, R. M.; Forster, D.; Morris, D. E. In *Inorg. Synth.*; John Wiley & Sons, Inc., **2007**, 88.
- (5) Vaska, L.; DiLuzio, J. W. *J. Am. Chem. Soc.* **1961**, 83, 2784.
- (6) Dabb, S. L.; Ho, J. H. H.; Hodgson, R.; Messerle, B. A.; Wagler, J. *Dalton Trans.* **2009**, 0, 634.
- (7) Ho, J. H. H.; Choy, S. W. S.; Macgregor, S. A.; Messerle, B. A. *Organometallics* **2011**, 30, 5978.
- (8) Field, L. D.; Messerle, B. A.; Vuong, K. Q.; Turner, P.; Failes, T. *Organometallics* **2007**, 26, 2058.
- (9) Yanwu, L.; Tobin, J. M. *J. Am. Chem. Soc.* **1996**, 118.
- (10) Elgafi, S.; Field, L. D.; Messerle, B. A. *J. Organomet. Chem.* **2000**, 607, 97.
- (11) Fugami, K.; Hagiwara, N.; Okeda, T.; Kosugi, M. *Chem. Lett.* **1998**, 27, 81.
- (12) Elsley, D. A.; MacLeod, D.; Miller, J. A.; Quayle, P.; Davies, G. M. *Tetrahedron Lett.* **1992**, 33, 409.
- (13) Esteruelas, M. A.; Oliván, M.; Oro, L. A.; Tolosa, J. *J. Organomet. Chem.* **1995**, 487, 143.
- (14) Samec, J. S. M.; Bäckvall, J.-E. *Chem. Eur. J.* **2002**, 8, 2955.

Appendix

[Rh(NCN^{Me})(COD)]BPh₄ (2.3)

**Table 1. Experimental details**

Crystal data			
Chemical formula	C ₄₃ H ₄₄ BN ₆ Rh		
<i>M</i> _r	845.46		
Crystal system, space group	Monoclinic, <i>P</i> 2 ₁ / <i>n</i>		
Temperature (K)	156		
<i>a</i> , <i>b</i> , <i>c</i> (Å)	17.425 (3), 11.8512 (16), 21.719 (3)		
<i>b</i> (°)	108.686 (5)		
<i>V</i> (Å ³)	4248.8 (11)		
<i>Z</i>	4		
Radiation type	Mo <i>K</i> α		
<i>m</i> (mm ^{−1})	0.57		
Crystal size (mm)	0.33 × 0.30 × 0.09		
Data collection			
Diffractometer	Bruker kappa APEXII CCD Diffractometer		
Absorption correction	Multi-scan		

	<i>SADABS</i> (Bruker, 2001)
T_{\min}, T_{\max}	0.837, 0.950
No. of measured, independent and observed [$I > 2s(I)$] reflections	29496, 7459, 6533
R_{int}	0.032
$(\sin \theta/\lambda)_{\max}$ (\AA^{-1})	0.595
Refinement	
$R[F^2 > 2s(F^2)], wR(F^2), S$	0.038, 0.119, 1.04
No. of reflections	7459
No. of parameters	533
No. of restraints	0
H-atom treatment	H-atom parameters constrained
$D\rho_{\max}, D\rho_{\min}$ (e \AA^{-3})	0.86, -0.47

Computer programs: *APEX2* (Bruker, 2007), *SHELXS-97* (Sheldrick, 2008), *SHELXL-97* (Sheldrick, 2008), *SHELXTL-Plus* (Sheldrick, 2008).

Table 2. Selected geometric parameters (\AA , $^\circ$)

Rh1—N2B	2.267 (2)	C4B—H4B	0.9500
Rh1—N2A	2.270 (2)	C4B—C5B	1.362 (5)
Rh1—C1C	2.097 (3)	C4A—H4A	0.9500
Rh1—C2C	2.097 (3)	C4A—C5A	1.372 (6)
Rh1—C2	1.982 (3)	C4—H4	0.9500
Rh1—C5C	2.270 (3)	C4—C5	1.340 (5)
Rh1—C6C	2.273 (3)	C5C—H5C	0.9500
N1B—N2B	1.363 (4)	C5C—C6C	1.365 (5)
N1B—C5B	1.350 (4)	C5B—H5B	0.9500

N1A—N2A	1.367 (4)	C5A—H5A	0.9500
N1A—C5A	1.351 (5)	C5—H5	0.9500
N1—C2	1.351 (4)	C6C—H6C	0.9500
N1—C5	1.391 (4)	C6C—C7C	1.501 (6)
N1—C6B	1.464 (4)	C6B—N1B	1.451 (4)
N2B—C3B	1.330 (4)	C6B—H6B1	0.9900
N2A—C3A	1.342 (4)	C6B—H6B2	0.9900
N3—C4	1.393 (4)	C6A—N1A	1.458 (4)
N3—C6A	1.453 (4)	C6A—H6A1	0.9900
Cl1E—Cl2E	0.753 (15)	C6A—H6A2	0.9900
Cl1E—Cl3E	0.579 (16)	C7C—H7C1	0.9900
Cl1E—Cl4E	0.611 (13)	C7C—H7C2	0.9900
Cl1E—Cl5E	0.504 (16)	C7C—C8C	1.452 (6)
Cl1E—Cl6E	0.744 (17)	C8C—H8C1	0.9900
Cl1E—C1E ⁱ	1.97 (4)	C8C—H8C2	0.9900
Cl2E—Cl3E	1.10 (2)	C11D—C12D	1.389 (5)
Cl2E—Cl4E	0.733 (16)	C11D—C16D	1.381 (5)
Cl2E—Cl5E	1.00 (2)	C12D—H12D	0.9500
Cl2E—Cl6E	0.833 (18)	C12D—C13D	1.399 (5)
Cl2E—C1E ⁱ	1.70 (4)	C13D—H13D	0.9500
Cl3E—Cl4E	1.04 (2)	C13D—C14D	1.362 (6)
Cl3E—Cl5E	0.65 (2)	C14D—H14D	0.9500
Cl3E—Cl6E	0.568 (19)	C14D—C15D	1.369 (5)
Cl3E—C1E ⁱ	2.03 (4)	C15D—H15D	0.9500
Cl4E—Cl5E	0.53 (2)	C15D—C16D	1.400 (4)
Cl4E—Cl6E	1.17 (2)	C16D—H16D	0.9500

C14E—C1E ⁱ	1.54 (4)	C21D—C22D	1.400 (4)
C15E—C16E	1.00 (2)	C21D—C26D	1.404 (4)
C15E—C1E ⁱ	1.65 (4)	C22D—H22D	0.9500
C16E—C1E ⁱ	2.03 (4)	C22D—C23D	1.384 (4)
C1E—C11E	1.79 (4)	C23D—H23D	0.9500
C1E—C11E ⁱ	1.97 (4)	C23D—C24D	1.387 (5)
C1E—C12E	1.60 (4)	C24D—H24D	0.9500
C1E—C12E ⁱ	1.70 (4)	C24D—C25D	1.371 (5)
C1E—C13E	1.48 (4)	C25D—H25D	0.9500
C1E—C14E ⁱ	1.53 (4)	C25D—C26D	1.392 (5)
C1E—C14E	1.93 (4)	C26D—H26D	0.9500
C1E—C15E ⁱ	1.65 (4)	C31D—C32D	1.402 (4)
C1E—C15E	1.77 (4)	C31D—C36D	1.394 (4)
C1E—C16E	1.20 (4)	C32D—H32D	0.9500
C1E—C16E ⁱ	2.03 (4)	C32D—C33D	1.397 (5)
C1E—C1E ⁱ	1.80 (7)	C33D—H33D	0.9500
C1D—H1D1	0.9900	C33D—C34D	1.374 (6)
C1D—H1D2	0.9900	C34D—H34D	0.9500
C1D—C11D	1.766 (8)	C34D—C35D	1.372 (6)
C1D—C11'	1.685 (10)	C35D—H35D	0.9500
C1D—C12D	1.659 (9)	C35D—C36D	1.405 (5)
C1D—C12'	1.827 (12)	C36D—H36D	0.9500
C1C—H1C	0.9500	C41D—C42D	1.378 (5)
C1C—C2C	1.439 (5)	C41D—C46D	1.411 (5)
C1C—C8C	1.504 (5)	C42D—H42D	0.9500
C2C—H2C	0.9500	C42D—C43D	1.406 (6)

C2C—C3C	1.527 (5)	C43D—H43D	0.9500
C2—N3	1.348 (4)	C43D—C44D	1.388 (9)
C3C—H3C1	0.9900	C44D—H44D	0.9500
C3C—H3C2	0.9900	C44D—C45D	1.364 (8)
C3C—C4C	1.507 (8)	C45D—H45D	0.9500
C3B—H3B	0.9500	C45D—C46D	1.391 (6)
C3B—C4B	1.397 (5)	C46D—H46D	0.9500
C3A—H3A	0.9500	B1D—C11D	1.659 (4)
C3A—C4A	1.405 (5)	B1D—C21D	1.643 (4)
C4C—H4C1	0.9900	B1D—C31D	1.656 (4)
C4C—H4C2	0.9900	B1D—C41D	1.653 (4)
C4C—C5C	1.466 (7)		
Cl2D—C1D—Cl1'	112.4 (6)	C43D—C42D—H42D	18.1
Cl2D—C1D—Cl1D	109.2 (5)	C44D—C43D—C42D	119.1 (5)
Cl1'—C1D—Cl1D	11.6 (4)	C44D—C43D—H43D	120.5
Cl2D—C1D—Cl2'	12.2 (8)	C42D—C43D—H43D	120.5
Cl1'—C1D—Cl2'	119.5 (6)	C45D—C44D—C43D	119.3 (4)
Cl1D—C1D—Cl2'	114.1 (5)	C45D—C44D—H44D	120.3
Cl2D—C1D—H1D1	109.8	C43D—C44D—H44D	120.3
Cl1'—C1D—H1D1	98.5	C44D—C45D—C46D	120.4 (5)
Cl1D—C1D—H1D1	109.8	C44D—C45D—H45D	119.8
Cl2'—C1D—H1D1	116.2	C46D—C45D—H45D	119.8
Cl2D—C1D—H1D2	109.8	C45D—C46D—C41D	122.9 (5)
Cl1'—C1D—H1D2	117.2	C45D—C46D—H46D	118.6
Cl1D—C1D—H1D2	109.8	C41D—C46D—H46D	118.6

Cl2'—C1D—H1D2	97.7	Cl6E—C1E—Cl3E	21.4 (12)
H1D1—C1D—H1D2	108.3	Cl6E—C1E—Cl4E ⁱ	153 (3)
C2—Rh1—C2C	93.65 (12)	Cl3E—C1E—Cl4E ⁱ	141 (3)
C2—Rh1—C1C	91.76 (13)	Cl6E—C1E—Cl2E	30.6 (13)
C2C—Rh1—C1C	40.14 (13)	Cl3E—C1E—Cl2E	41.7 (13)
C2—Rh1—N2B	82.29 (10)	Cl4E ⁱ —C1E—Cl2E	126 (3)
C2C—Rh1—N2B	116.12 (12)	Cl6E—C1E—Cl5E ⁱ	140 (3)
C1C—Rh1—N2B	155.39 (12)	Cl3E—C1E—Cl5E ⁱ	137 (3)
C2—Rh1—N2A	82.03 (10)	Cl4E ⁱ —C1E—Cl5E ⁱ	18.7 (8)
C2C—Rh1—N2A	154.06 (12)	Cl2E—C1E—Cl5E ⁱ	110 (2)
C1C—Rh1—N2A	114.15 (12)	Cl6E—C1E—Cl2E ⁱ	133 (3)
N2B—Rh1—N2A	88.77 (10)	Cl3E—C1E—Cl2E ⁱ	116 (3)
C2—Rh1—C5C	163.49 (13)	Cl4E ⁱ —C1E—Cl2E ⁱ	25.5 (9)
C2C—Rh1—C5C	80.42 (15)	Cl2E—C1E—Cl2E ⁱ	114 (2)
C1C—Rh1—C5C	93.44 (14)	Cl5E ⁱ —C1E—Cl2E ⁱ	34.7 (10)
N2B—Rh1—C5C	86.50 (12)	Cl6E—C1E—Cl5E	32.7 (14)
N2A—Rh1—C5C	109.91 (13)	Cl3E—C1E—Cl5E	20.7 (9)
C2—Rh1—C6C	161.45 (13)	Cl4E ⁱ —C1E—Cl5E	123 (2)
C2C—Rh1—C6C	90.93 (13)	Cl2E—C1E—Cl5E	34.2 (11)
C1C—Rh1—C6C	80.25 (13)	Cl5E ⁱ —C1E—Cl5E	117 (2)
N2B—Rh1—C6C	111.66 (11)	Cl2E ⁱ —C1E—Cl5E	100 (2)
N2A—Rh1—C6C	86.00 (11)	Cl6E—C1E—Cl1E	17.3 (11)
C5C—Rh1—C6C	34.98 (13)	Cl3E—C1E—Cl1E	17.1 (8)
C2—N1—C5	111.0 (3)	Cl4E ⁱ —C1E—Cl1E	137 (2)
C2—N1—C6B	119.3 (2)	Cl2E—C1E—Cl1E	24.8 (8)
C5—N1—C6B	127.8 (3)	Cl5E ⁱ —C1E—Cl1E	126 (2)

N3—C2—N1	104.9 (2)	Cl2E ⁱ —C1E—Cl1E	116 (2)
N3—C2—Rh1	126.3 (2)	Cl5E—C1E—Cl1E	16.2 (6)
N1—C2—Rh1	127.4 (2)	Cl6E—C1E—C1E ⁱ	83 (3)
C2—N3—C4	110.7 (3)	Cl3E—C1E—C1E ⁱ	76 (3)
C2—N3—C6A	119.9 (3)	Cl4E ⁱ —C1E—C1E ⁱ	70 (2)
C4—N3—C6A	127.9 (3)	Cl2E—C1E—C1E ⁱ	60 (2)
C5—C4—N3	107.0 (3)	Cl5E ⁱ —C1E—C1E ⁱ	61 (2)
C5—C4—H4	126.5	Cl2E ⁱ —C1E—C1E ⁱ	54 (2)
N3—C4—H4	126.5	Cl5E—C1E—C1E ⁱ	55 (2)
C4—C5—N1	106.4 (3)	Cl1E—C1E—C1E ⁱ	66 (2)
C4—C5—H5	126.8	Cl6E—C1E—Cl4E	34.5 (14)
N1—C5—H5	126.8	Cl3E—C1E—Cl4E	32.3 (11)
N3—C6A—N1A	110.1 (3)	Cl4E ⁱ —C1E—Cl4E	119 (2)
N3—C6A—H6A1	109.6	Cl2E—C1E—Cl4E	21.4 (8)
N1A—C6A—H6A1	109.6	Cl5E ⁱ —C1E—Cl4E	108 (2)
N3—C6A—H6A2	109.6	Cl2E ⁱ —C1E—Cl4E	100.0 (19)
N1A—C6A—H6A2	109.6	Cl5E—C1E—Cl4E	15.7 (7)
H6A1—C6A—H6A2	108.2	Cl1E—C1E—Cl4E	18.4 (6)
C5A—N1A—N2A	111.2 (3)	C1E ⁱ —C1E—Cl4E	48.4 (19)
C5A—N1A—C6A	129.3 (3)	Cl6E—C1E—Cl1E ⁱ	139 (3)
N2A—N1A—C6A	119.4 (2)	Cl3E—C1E—Cl1E ⁱ	131 (2)
C3A—N2A—N1A	105.0 (3)	Cl4E ⁱ —C1E—Cl1E ⁱ	14.3 (7)
C3A—N2A—Rh1	135.8 (2)	Cl2E—C1E—Cl1E ⁱ	112 (2)
N1A—N2A—Rh1	119.03 (19)	Cl5E ⁱ —C1E—Cl1E ⁱ	12.6 (7)
N2A—C3A—C4A	111.0 (4)	Cl2E ⁱ —C1E—Cl1E ⁱ	22.2 (7)
N2A—C3A—H3A	124.5	Cl5E—C1E—Cl1E ⁱ	111 (2)

C4A—C3A—H3A	124.5	Cl1E—C1E—Cl1E ⁱ	123 (2)
C5A—C4A—C3A	105.0 (3)	C1E ⁱ —C1E—Cl1E ⁱ	57 (2)
C5A—C4A—H4A	127.5	Cl4E—C1E—Cl1E ⁱ	105.0 (17)
C3A—C4A—H4A	127.5	Cl6E—C1E—Cl6E ⁱ	119 (3)
N1A—C5A—C4A	107.8 (3)	Cl3E—C1E—Cl6E ⁱ	109 (2)
N1A—C5A—H5A	126.1	Cl4E ⁱ —C1E—Cl6E ⁱ	34.7 (11)
C4A—C5A—H5A	126.1	Cl2E—C1E—Cl6E ⁱ	93.5 (19)
N1B—C6B—N1	109.1 (3)	Cl5E ⁱ —C1E—Cl6E ⁱ	29.2 (10)
N1B—C6B—H6B1	109.9	Cl2E ⁱ —C1E—Cl6E ⁱ	23.7 (8)
N1—C6B—H6B1	109.9	Cl5E—C1E—Cl6E ⁱ	89.5 (17)
N1B—C6B—H6B2	109.9	Cl1E—C1E—Cl6E ⁱ	102.0 (18)
N1—C6B—H6B2	109.9	C1E ⁱ —C1E—Cl6E ⁱ	35.7 (17)
H6B1—C6B—H6B2	108.3	Cl4E—C1E—Cl6E ⁱ	84.1 (15)
C5B—N1B—N2B	111.3 (3)	Cl1E ⁱ —C1E—Cl6E ⁱ	21.4 (7)
C5B—N1B—C6B	128.9 (3)	Cl5E—Cl1E—Cl3E	73 (3)
N2B—N1B—C6B	119.7 (2)	Cl5E—Cl1E—Cl4E	56 (3)
C3B—N2B—N1B	104.7 (3)	Cl3E—Cl1E—Cl4E	123 (3)
C3B—N2B—Rh1	134.6 (2)	Cl5E—Cl1E—Cl6E	105 (3)
N1B—N2B—Rh1	119.34 (19)	Cl3E—Cl1E—Cl6E	49 (2)
N2B—C3B—C4B	111.3 (3)	Cl4E—Cl1E—Cl6E	118 (2)
N2B—C3B—H3B	124.3	Cl5E—Cl1E—Cl2E	104 (3)
C4B—C3B—H3B	124.3	Cl3E—Cl1E—Cl2E	111 (2)
C5B—C4B—C3B	105.2 (3)	Cl4E—Cl1E—Cl2E	64.0 (17)
C5B—C4B—H4B	127.4	Cl6E—Cl1E—Cl2E	67.6 (16)
C3B—C4B—H4B	127.4	Cl5E—Cl1E—C1E	79 (3)
N1B—C5B—C4B	107.4 (3)	Cl3E—Cl1E—C1E	49 (2)

N1B—C5B—H5B	126.3	Cl4E—Cl1E—C1E	93.8 (19)
C4B—C5B—H5B	126.3	Cl6E—Cl1E—C1E	28.5 (17)
C2C—C1C—C8C	124.5 (3)	Cl2E—Cl1E—C1E	62.9 (18)
C2C—C1C—Rh1	69.91 (18)	Cl5E—Cl1E—C1E ⁱ	46 (3)
C8C—C1C—Rh1	113.6 (2)	Cl3E—Cl1E—C1E ⁱ	88 (2)
C2C—C1C—H1C	117.8	Cl4E—Cl1E—C1E ⁱ	38.2 (17)
C8C—C1C—H1C	117.8	Cl6E—Cl1E—C1E ⁱ	84.2 (17)
Rh1—C1C—H1C	86.5	Cl2E—Cl1E—C1E ⁱ	58.5 (17)
C1C—C2C—C3C	123.5 (3)	C1E—Cl1E—C1E ⁱ	57 (2)
C1C—C2C—Rh1	69.95 (18)	Cl4E—Cl2E—Cl1E	48.5 (14)
C3C—C2C—Rh1	115.2 (3)	Cl4E—Cl2E—Cl6E	96 (2)
C1C—C2C—H2C	118.3	Cl1E—Cl2E—Cl6E	55.7 (16)
C3C—C2C—H2C	118.3	Cl4E—Cl2E—Cl5E	30.9 (16)
Rh1—C2C—H2C	85.0	Cl1E—Cl2E—Cl5E	29.2 (13)
C4C—C3C—C2C	113.8 (4)	Cl6E—Cl2E—Cl5E	65.2 (19)
C4C—C3C—H3C1	108.8	Cl4E—Cl2E—Cl3E	65.9 (19)
C2C—C3C—H3C1	108.8	Cl1E—Cl2E—Cl3E	29.4 (12)
C4C—C3C—H3C2	108.8	Cl6E—Cl2E—Cl3E	30.3 (14)
C2C—C3C—H3C2	108.8	Cl5E—Cl2E—Cl3E	35.5 (12)
H3C1—C3C—H3C2	107.7	Cl4E—Cl2E—C1E	106 (2)
C5C—C4C—C3C	117.7 (4)	Cl1E—Cl2E—C1E	92 (2)
C5C—C4C—H4C1	107.9	Cl6E—Cl2E—C1E	46.9 (19)
C3C—C4C—H4C1	107.9	Cl5E—Cl2E—C1E	82 (2)
C5C—C4C—H4C2	107.9	Cl3E—Cl2E—C1E	63.3 (18)
C3C—C4C—H4C2	107.9	Cl4E—Cl2E—C1E ⁱ	64.5 (19)
H4C1—C4C—H4C2	107.2	Cl1E—Cl2E—C1E ⁱ	99.3 (19)

C6C—C5C—C4C	126.3 (5)	Cl6E—Cl2E—C1E ⁱ	101 (2)
C6C—C5C—Rh1	72.61 (19)	Cl5E—Cl2E—C1E ⁱ	70.1 (18)
C4C—C5C—Rh1	108.8 (3)	Cl3E—Cl2E—C1E ⁱ	90.4 (18)
C6C—C5C—H5C	116.9	C1E—Cl2E—C1E ⁱ	66 (2)
C4C—C5C—H5C	116.9	Cl6E—Cl3E—Cl1E	81 (3)
Rh1—C5C—H5C	88.5	Cl6E—Cl3E—Cl5E	110 (4)
C5C—C6C—C7C	122.1 (4)	Cl1E—Cl3E—Cl5E	48.0 (18)
C5C—C6C—Rh1	72.4 (2)	Cl6E—Cl3E—Cl4E	87 (3)
C7C—C6C—Rh1	109.0 (2)	Cl1E—Cl3E—Cl4E	29.5 (15)
C5C—C6C—H6C	119.0	Cl5E—Cl3E—Cl4E	24.8 (19)
C7C—C6C—H6C	119.0	Cl6E—Cl3E—Cl2E	48 (2)
Rh1—C6C—H6C	88.6	Cl1E—Cl3E—Cl2E	39.7 (15)
C8C—C7C—C6C	117.2 (3)	Cl5E—Cl3E—Cl2E	64 (2)
C8C—C7C—H7C1	108.0	Cl4E—Cl3E—Cl2E	39.8 (11)
C6C—C7C—H7C1	108.0	Cl6E—Cl3E—C1E	50 (3)
C8C—C7C—H7C2	108.0	Cl1E—Cl3E—C1E	114 (3)
C6C—C7C—H7C2	108.0	Cl5E—Cl3E—C1E	106 (3)
H7C1—C7C—H7C2	107.2	Cl4E—Cl3E—C1E	98.6 (18)
C7C—C8C—C1C	115.8 (3)	Cl2E—Cl3E—C1E	75 (2)
C7C—C8C—H8C1	108.3	Cl6E—Cl3E—C1E ⁱ	82 (3)
C1C—C8C—H8C1	108.3	Cl1E—Cl3E—C1E ⁱ	75 (2)
C7C—C8C—H8C2	108.3	Cl5E—Cl3E—C1E ⁱ	47 (2)
C1C—C8C—H8C2	108.3	Cl4E—Cl3E—C1E ⁱ	47.6 (15)
H8C1—C8C—H8C2	107.4	Cl2E—Cl3E—C1E ⁱ	56.8 (15)
C21D—B1D—C41D	111.5 (2)	C1E—Cl3E—C1E ⁱ	59 (2)
C21D—B1D—C31D	104.5 (2)	Cl5E—Cl4E—Cl1E	52 (2)

C41D—B1D—C31D	113.0 (3)	Cl5E—Cl4E—Cl2E	104 (3)
C21D—B1D—C11D	112.1 (2)	Cl1E—Cl4E—Cl2E	67.4 (19)
C41D—B1D—C11D	104.7 (2)	Cl5E—Cl4E—Cl3E	31 (2)
C31D—B1D—C11D	111.3 (2)	Cl1E—Cl4E—Cl3E	27.8 (13)
C16D—C11D—C12D	114.4 (3)	Cl2E—Cl4E—Cl3E	74.3 (19)
C16D—C11D—B1D	125.2 (3)	Cl5E—Cl4E—Cl6E	59 (3)
C12D—C11D—B1D	120.4 (3)	Cl1E—Cl4E—Cl6E	34.2 (13)
C11D—C12D—C13D	122.8 (4)	Cl2E—Cl4E—Cl6E	45.3 (15)
C11D—C12D—H12D	118.6	Cl3E—Cl4E—Cl6E	29.1 (10)
C13D—C12D—H12D	118.6	Cl5E—Cl4E—ClE ⁱ	94 (3)
C14D—C13D—C12D	120.6 (3)	Cl1E—Cl4E—ClE ⁱ	128 (2)
C14D—C13D—H13D	119.7	Cl2E—Cl4E—ClE ⁱ	90 (2)
C12D—C13D—H13D	119.7	Cl3E—Cl4E—ClE ⁱ	102.3 (19)
C13D—C14D—C15D	118.9 (3)	Cl6E—Cl4E—ClE ⁱ	96.6 (17)
C13D—C14D—H14D	120.5	Cl5E—Cl4E—ClE	64 (3)
C15D—C14D—H14D	120.5	Cl1E—Cl4E—ClE	67.8 (17)
C14D—C15D—C16D	119.5 (3)	Cl2E—Cl4E—ClE	52.6 (19)
C14D—C15D—H15D	120.2	Cl3E—Cl4E—ClE	49.1 (15)
C16D—C15D—H15D	120.2	Cl6E—Cl4E—ClE	35.5 (13)
C11D—C16D—C15D	123.8 (3)	ClE ⁱ —Cl4E—ClE	61 (2)
C11D—C16D—H16D	118.1	Cl1E—Cl5E—Cl4E	72 (3)
C15D—C16D—H16D	118.1	Cl1E—Cl5E—Cl3E	59 (3)
C22D—C21D—C26D	115.2 (3)	Cl4E—Cl5E—Cl3E	124 (4)
C22D—C21D—B1D	121.3 (2)	Cl1E—Cl5E—Cl6E	46 (2)
C26D—C21D—B1D	123.3 (3)	Cl4E—Cl5E—Cl6E	94 (3)
C23D—C22D—C21D	122.9 (3)	Cl3E—Cl5E—Cl6E	32.3 (18)

C23D—C22D—H22D	118.6	Cl1E—Cl5E—Cl2E	47 (2)
C21D—C22D—H22D	118.6	Cl4E—Cl5E—Cl2E	45 (2)
C22D—C23D—C24D	120.1 (3)	Cl3E—Cl5E—Cl2E	81 (2)
C22D—C23D—H23D	120.0	Cl6E—Cl5E—Cl2E	49.2 (13)
C24D—C23D—H23D	120.0	Cl1E—Cl5E—Cl1E ⁱ	122 (3)
C25D—C24D—C23D	118.9 (3)	Cl4E—Cl5E—Cl1E ⁱ	68 (3)
C25D—C24D—H24D	120.5	Cl3E—Cl5E—Cl1E ⁱ	117 (3)
C23D—C24D—H24D	120.5	Cl6E—Cl5E—Cl1E ⁱ	96.8 (19)
C24D—C25D—C26D	120.6 (3)	Cl2E—Cl5E—Cl1E ⁱ	75.1 (19)
C24D—C25D—H25D	119.7	Cl1E—Cl5E—Cl1E	85 (3)
C26D—C25D—H25D	119.7	Cl4E—Cl5E—Cl1E	100 (3)
C25D—C26D—C21D	122.2 (3)	Cl3E—Cl5E—Cl1E	54 (2)
C25D—C26D—H26D	118.9	Cl6E—Cl5E—Cl1E	40.3 (15)
C21D—C26D—H26D	118.9	Cl2E—Cl5E—Cl1E	63.7 (19)
C36D—C31D—C32D	114.5 (3)	Cl1E ⁱ —Cl5E—Cl1E	63 (2)
C36D—C31D—B1D	121.9 (3)	Cl3E—Cl6E—Cl1E	50 (2)
C32D—C31D—B1D	123.2 (3)	Cl3E—Cl6E—Cl2E	102 (3)
C33D—C32D—C31D	123.4 (3)	Cl1E—Cl6E—Cl2E	56.7 (16)
C33D—C32D—H32D	118.3	Cl3E—Cl6E—Cl5E	38 (2)
C31D—C32D—H32D	118.3	Cl1E—Cl6E—Cl5E	29.2 (12)
C34D—C33D—C32D	120.0 (4)	Cl2E—Cl6E—Cl5E	65.6 (19)
C34D—C33D—H33D	120.0	Cl3E—Cl6E—Cl4E	64 (3)
C32D—C33D—H33D	120.0	Cl1E—Cl6E—Cl4E	27.5 (11)
C35D—C34D—C33D	118.8 (4)	Cl2E—Cl6E—Cl4E	38.7 (12)
C35D—C34D—H34D	120.6	Cl5E—Cl6E—Cl4E	27.0 (12)
C33D—C34D—H34D	120.6	Cl3E—Cl6E—Cl1E	109 (3)

C34D—C35D—C36D	120.7 (4)	Cl1E—Cl6E—C1E	134 (3)
C34D—C35D—H35D	119.7	Cl2E—Cl6E—C1E	103 (3)
C36D—C35D—H35D	119.7	Cl5E—Cl6E—C1E	107 (2)
C31D—C36D—C35D	122.6 (3)	Cl4E—Cl6E—C1E	110 (2)
C31D—C36D—H36D	118.7	Cl3E—Cl6E—C1E ⁱ	82 (3)
C35D—C36D—H36D	118.7	Cl1E—Cl6E—C1E ⁱ	74.5 (16)
C42D—C41D—C46D	114.6 (3)	Cl2E—Cl6E—C1E ⁱ	55.2 (17)
C42D—C41D—B1D	124.9 (3)	Cl5E—Cl6E—C1E ⁱ	54.0 (16)
C46D—C41D—B1D	120.4 (3)	Cl4E—Cl6E—C1E ⁱ	48.6 (13)
C41D—C42D—C43D	123.7 (5)	C1E—Cl6E—C1E ⁱ	61 (3)
C41D—C42D—H42D	118.1		

Symmetry code(s): (i) $-x+1, -y, -z+2$.

[Ir(NCN^{Me})(COD)]BPh₄ (2.4)

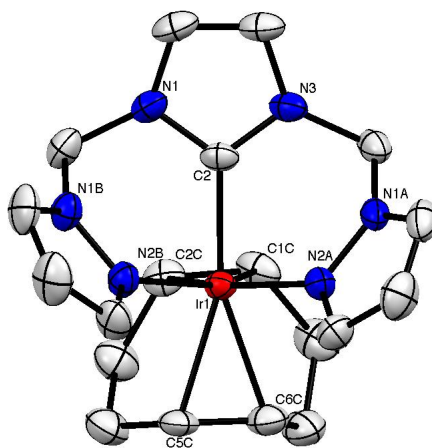


Table 1. Experimental details

Crystal data	
Chemical formula	C ₄₃ H ₄₄ BIrN ₆

M_r	917.94
Crystal system, space group	Monoclinic, $P2_1/c$
Temperature (K)	163
a, b, c (Å)	11.8066 (4), 9.6104 (3), 35.9142 (11)
β (°)	95.944 (2)
V (Å ³)	4053.1 (2)
Z	4
Radiation type	Mo $K\alpha$
μ (mm ⁻¹)	3.34
Crystal size (mm)	$0.17 \times 0.13 \times 0.05$
Data collection	
Diffractometer	Bruker kappa APEXII CCD Diffractionmeter
Absorption correction	Multi-scan <i>SADABS</i> (Bruker, 2001)
T_{\min}, T_{\max}	0.599, 0.840
No. of measured, independent and observed [$I > 2s(I)$] reflections	27051, 7108, 5974
R_{int}	0.037
$(\sin \theta/\lambda)_{\max}$ (Å ⁻¹)	0.595
Refinement	
$R[F^2 > 2s(F^2)], wR(F^2), S$	0.028, 0.059, 1.05
No. of reflections	7108
No. of parameters	505
No. of restraints	0
H-atom treatment	H-atom parameters constrained
$D\rho_{\max}, D\rho_{\min}$ (e Å ⁻³)	0.77, -1.11

Computer programs: *APEX2* (Bruker, 2007), *SHELXS-97* (Sheldrick, 2008), *SHELXL-97* (Sheldrick, 2008), *SHELXTL-Plus* (Sheldrick, 2008).

Table 2. Selected geometric parameters (Å, °)

Ir1—C2	1.995 (4)	B1D—C31D	1.659 (5)
Ir1—C2C	2.093 (4)	C11D—C16D	1.399 (5)
Ir1—C1C	2.093 (4)	C11D—C12D	1.404 (5)
Ir1—N2A	2.194 (3)	C12D—C13D	1.385 (5)
Ir1—C5C	2.210 (4)	C12D—H12D	0.9500
Ir1—C6C	2.233 (4)	C13D—C14D	1.389 (5)
Ir1—N2B	2.247 (3)	C13D—H13D	0.9500
N1—C2	1.354 (5)	C14D—C15D	1.367 (6)
N1—C5	1.391 (5)	C14D—H14D	0.9500
N1—C6B	1.456 (5)	C15D—C16D	1.389 (5)
C2—N3	1.345 (5)	C15D—H15D	0.9500
N3—C4	1.388 (5)	C16D—H16D	0.9500
N3—C6A	1.454 (5)	C21D—C22D	1.398 (5)
C4—C5	1.324 (6)	C21D—C26D	1.413 (5)
C4—H4	0.9500	C22D—C23D	1.390 (5)
C5—H5	0.9500	C22D—H22D	0.9500
C6A—N1A	1.446 (5)	C23D—C24D	1.380 (6)
C6A—H6A1	0.9900	C23D—H23D	0.9500
C6A—H6A2	0.9900	C24D—C25D	1.384 (6)
N1A—C5A	1.339 (5)	C24D—H24D	0.9500
N1A—N2A	1.364 (4)	C25D—C26D	1.383 (5)

N2A—C3A	1.325 (5)	C25D—H25D	0.9500
C3A—C4A	1.384 (6)	C26D—H26D	0.9500
C3A—H3A	0.9500	C31D—C32D	1.394 (5)
C4A—C5A	1.359 (6)	C31D—C36D	1.403 (5)
C4A—H4A	0.9500	C32D—C33D	1.392 (5)
C5A—H5A	0.9500	C32D—H32D	0.9500
C6B—N1B	1.448 (5)	C33D—C34D	1.377 (6)
C6B—H6B1	0.9900	C33D—H33D	0.9500
C6B—H6B2	0.9900	C34D—C35D	1.372 (6)
N1B—C5B	1.331 (5)	C34D—H34D	0.9500
N1B—N2B	1.363 (4)	C35D—C36D	1.384 (5)
N2B—C3B	1.331 (5)	C35D—H35D	0.9500
C3B—C4B	1.385 (6)	C36D—H36D	0.9500
C3B—H3B	0.9500	C41D—C46D	1.391 (5)
C4B—C5B	1.360 (6)	C41D—C42D	1.401 (5)
C4B—H4B	0.9500	C42D—C43D	1.381 (5)
C5B—H5B	0.9500	C42D—H42D	0.9500
C1C—C2C	1.463 (6)	C43D—C44D	1.380 (6)
C1C—C8C	1.508 (6)	C43D—H43D	0.9500
C1C—H1C	0.9500	C44D—C45D	1.371 (6)
C2C—C3C	1.527 (6)	C44D—H44D	0.9500
C2C—H2C	0.9500	C45D—C46D	1.388 (5)
C3C—C4C	1.512 (6)	C45D—H45D	0.9500
C3C—H3C1	0.9900	C46D—H46D	0.9500
C3C—H3C2	0.9900	O1E—C4E	1.409 (6)
C4C—C5C	1.510 (6)	O1E—C1E	1.430 (5)

C4C—H4C1	0.9900	C1E—C2E	1.485 (7)
C4C—H4C2	0.9900	C1E—H1E1	0.9900
C5C—C6C	1.394 (6)	C1E—H1E2	0.9900
C6C—C7C	1.515 (6)	C2E—C3E	1.518 (7)
C7C—C8C	1.521 (6)	C2E—H2E1	0.9900
C7C—H7C1	0.9900	C2E—H2E2	0.9900
C7C—H7C2	0.9900	C3E—C4E	1.479 (7)
C8C—H8C1	0.9900	C3E—H3E1	0.9900
C8C—H8C2	0.9900	C3E—H3E2	0.9900
B1D—C41D	1.638 (5)	C4E—H4E1	0.9900
B1D—C21D	1.646 (6)	C4E—H4E2	0.9900
B1D—C11D	1.648 (5)		
C2—Irl—C2C	94.82 (15)	C8C—C7C—H7C2	109.0
C2—Irl—C1C	92.04 (15)	H7C1—C7C—H7C2	107.8
C2C—Irl—C1C	40.91 (16)	C1C—C8C—C7C	113.1 (4)
C2—Irl—N2A	82.94 (13)	C1C—C8C—H8C1	109.0
C2C—Irl—N2A	159.95 (14)	C7C—C8C—H8C1	109.0
C1C—Irl—N2A	119.09 (15)	C1C—C8C—H8C2	109.0
C2—Irl—C5C	162.33 (16)	C7C—C8C—H8C2	109.0
C2C—Irl—C5C	81.63 (16)	H8C1—C8C—H8C2	107.8
C1C—Irl—C5C	96.34 (16)	C41D—B1D—C21D	109.4 (3)
N2A—Irl—C5C	106.21 (14)	C41D—B1D—C11D	108.4 (3)
C2—Irl—C6C	161.10 (16)	C21D—B1D—C11D	107.2 (3)
C2C—Irl—C6C	89.66 (16)	C41D—B1D—C31D	107.5 (3)
C1C—Irl—C6C	79.39 (16)	C21D—B1D—C31D	113.5 (3)

N2A—Ir1—C6C	86.57 (14)	C11D—B1D—C31D	110.8 (3)
C5C—Ir1—C6C	36.57 (15)	C16D—C11D—C12D	114.8 (3)
C2—Ir1—N2B	80.60 (13)	C16D—C11D—B1D	121.1 (3)
C2C—Ir1—N2B	113.72 (14)	C12D—C11D—B1D	124.0 (3)
C1C—Ir1—N2B	153.28 (15)	C13D—C12D—C11D	123.1 (4)
N2A—Ir1—N2B	85.68 (12)	C13D—C12D—H12D	118.5
C5C—Ir1—N2B	84.99 (14)	C11D—C12D—H12D	118.5
C6C—Ir1—N2B	114.30 (14)	C12D—C13D—C14D	119.9 (4)
C2—N1—C5	110.4 (3)	C12D—C13D—H13D	120.0
C2—N1—C6B	118.3 (3)	C14D—C13D—H13D	120.0
C5—N1—C6B	128.3 (3)	C15D—C14D—C13D	118.7 (4)
N3—C2—N1	104.7 (3)	C15D—C14D—H14D	120.7
N3—C2—Ir1	126.6 (3)	C13D—C14D—H14D	120.7
N1—C2—Ir1	127.0 (3)	C14D—C15D—C16D	121.0 (4)
C2—N3—C4	110.9 (3)	C14D—C15D—H15D	119.5
C2—N3—C6A	119.3 (3)	C16D—C15D—H15D	119.5
C4—N3—C6A	128.4 (3)	C15D—C16D—C11D	122.5 (4)
C5—C4—N3	107.0 (4)	C15D—C16D—H16D	118.8
C5—C4—H4	126.5	C11D—C16D—H16D	118.8
N3—C4—H4	126.5	C22D—C21D—C26D	114.1 (4)
C4—C5—N1	107.0 (4)	C22D—C21D—B1D	124.1 (3)
C4—C5—H5	126.5	C26D—C21D—B1D	121.7 (3)
N1—C5—H5	126.5	C23D—C22D—C21D	122.9 (4)
N1A—C6A—N3	109.5 (3)	C23D—C22D—H22D	118.6
N1A—C6A—H6A1	109.8	C21D—C22D—H22D	118.6
N3—C6A—H6A1	109.8	C24D—C23D—C22D	120.8 (4)

N1A—C6A—H6A2	109.8	C24D—C23D—H23D	119.6
N3—C6A—H6A2	109.8	C22D—C23D—H23D	119.6
H6A1—C6A—H6A2	108.2	C23D—C24D—C25D	118.7 (4)
C5A—N1A—N2A	111.1 (3)	C23D—C24D—H24D	120.7
C5A—N1A—C6A	129.4 (3)	C25D—C24D—H24D	120.7
N2A—N1A—C6A	119.6 (3)	C26D—C25D—C24D	119.8 (4)
C3A—N2A—N1A	104.6 (3)	C26D—C25D—H25D	120.1
C3A—N2A—Irl	134.0 (3)	C24D—C25D—H25D	120.1
N1A—N2A—Irl	120.7 (2)	C25D—C26D—C21D	123.7 (4)
N2A—C3A—C4A	111.4 (4)	C25D—C26D—H26D	118.2
N2A—C3A—H3A	124.3	C21D—C26D—H26D	118.2
C4A—C3A—H3A	124.3	C32D—C31D—C36D	114.3 (3)
C5A—C4A—C3A	105.3 (4)	C32D—C31D—B1D	126.3 (3)
C5A—C4A—H4A	127.4	C36D—C31D—B1D	119.5 (3)
C3A—C4A—H4A	127.4	C33D—C32D—C31D	123.0 (4)
N1A—C5A—C4A	107.6 (4)	C33D—C32D—H32D	118.5
N1A—C5A—H5A	126.2	C31D—C32D—H32D	118.5
C4A—C5A—H5A	126.2	C34D—C33D—C32D	120.4 (4)
N1B—C6B—N1	109.0 (3)	C34D—C33D—H33D	119.8
N1B—C6B—H6B1	109.9	C32D—C33D—H33D	119.8
N1—C6B—H6B1	109.9	C35D—C34D—C33D	118.7 (4)
N1B—C6B—H6B2	109.9	C35D—C34D—H34D	120.7
N1—C6B—H6B2	109.9	C33D—C34D—H34D	120.7
H6B1—C6B—H6B2	108.3	C34D—C35D—C36D	120.3 (4)
C5B—N1B—N2B	112.0 (3)	C34D—C35D—H35D	119.8
C5B—N1B—C6B	128.6 (4)	C36D—C35D—H35D	119.8

N2B—N1B—C6B	119.1 (3)	C35D—C36D—C31D	123.4 (4)
C3B—N2B—N1B	103.9 (3)	C35D—C36D—H36D	118.3
C3B—N2B—Irl	135.1 (3)	C31D—C36D—H36D	118.3
N1B—N2B—Irl	119.8 (2)	C46D—C41D—C42D	114.5 (3)
N2B—C3B—C4B	111.5 (4)	C46D—C41D—B1D	125.2 (3)
N2B—C3B—H3B	124.3	C42D—C41D—B1D	120.2 (3)
C4B—C3B—H3B	124.3	C43D—C42D—C41D	123.5 (4)
C5B—C4B—C3B	105.3 (4)	C43D—C42D—H42D	118.3
C5B—C4B—H4B	127.3	C41D—C42D—H42D	118.3
C3B—C4B—H4B	127.3	C44D—C43D—C42D	119.4 (4)
N1B—C5B—C4B	107.2 (4)	C44D—C43D—H43D	120.3
N1B—C5B—H5B	126.4	C42D—C43D—H43D	120.3
C4B—C5B—H5B	126.4	C45D—C44D—C43D	119.5 (4)
C2C—C1C—C8C	123.6 (4)	C45D—C44D—H44D	120.3
C2C—C1C—Irl	69.5 (2)	C43D—C44D—H44D	120.3
C8C—C1C—Irl	115.6 (3)	C44D—C45D—C46D	120.0 (4)
C2C—C1C—H1C	118.2	C44D—C45D—H45D	120.0
C8C—C1C—H1C	118.2	C46D—C45D—H45D	120.0
Irl—C1C—H1C	85.0	C45D—C46D—C41D	123.1 (4)
C1C—C2C—C3C	121.8 (4)	C45D—C46D—H46D	118.5
C1C—C2C—Irl	69.6 (2)	C41D—C46D—H46D	118.5
C3C—C2C—Irl	114.4 (3)	C4E—O1E—C1E	105.6 (4)
C1C—C2C—H2C	119.1	O1E—C1E—C2E	105.0 (4)
C3C—C2C—H2C	119.1	O1E—C1E—H1E1	110.7
Irl—C2C—H2C	86.2	C2E—C1E—H1E1	110.7
C4C—C3C—C2C	112.8 (4)	O1E—C1E—H1E2	110.7

C4C—C3C—H3C1	109.0	C2E—C1E—H1E2	110.7
C2C—C3C—H3C1	109.0	H1E1—C1E—H1E2	108.8
C4C—C3C—H3C2	109.0	C1E—C2E—C3E	102.7 (4)
C2C—C3C—H3C2	109.0	C1E—C2E—H2E1	111.2
H3C1—C3C—H3C2	107.8	C3E—C2E—H2E1	111.2
C3C—C4C—C5C	114.3 (4)	C1E—C2E—H2E2	111.2
C3C—C4C—H4C1	108.7	C3E—C2E—H2E2	111.2
C5C—C4C—H4C1	108.7	H2E1—C2E—H2E2	109.1
C3C—C4C—H4C2	108.7	C4E—C3E—C2E	104.7 (4)
C5C—C4C—H4C2	108.7	C4E—C3E—H3E1	110.8
H4C1—C4C—H4C2	107.6	C2E—C3E—H3E1	110.8
C6C—C5C—C4C	125.0 (4)	C4E—C3E—H3E2	110.8
C6C—C5C—Irl	72.6 (2)	C2E—C3E—H3E2	110.8
C4C—C5C—Irl	107.8 (3)	H3E1—C3E—H3E2	108.9
C5C—C6C—C7C	123.0 (4)	O1E—C4E—C3E	108.3 (4)
C5C—C6C—Irl	70.8 (2)	O1E—C4E—H4E1	110.0
C7C—C6C—Irl	112.9 (3)	C3E—C4E—H4E1	110.0
C6C—C7C—C8C	112.8 (3)	O1E—C4E—H4E2	110.0
C6C—C7C—H7C1	109.0	C3E—C4E—H4E2	110.0
C8C—C7C—H7C1	109.0	H4E1—C4E—H4E2	108.4
C6C—C7C—H7C2	109.0		
C5—N1—C2—N3	-2.0 (4)	C5C—Irl—C2C—C3C	6.7 (3)
C6B—N1—C2—N3	-164.0 (3)	C6C—Irl—C2C—C3C	42.5 (3)
C5—N1—C2—Irl	163.5 (3)	N2B—Irl—C2C—C3C	-74.0 (3)
C6B—N1—C2—Irl	1.5 (5)	C1C—C2C—C3C—C4C	89.7 (5)

C2C—Ir1—C2—N3	-124.9 (3)	Ir1—C2C—C3C—C4C	9.5 (5)
C1C—Ir1—C2—N3	-84.0 (3)	C2C—C3C—C4C—C5C	-29.0 (6)
N2A—Ir1—C2—N3	35.1 (3)	C3C—C4C—C5C—C6C	-47.9 (6)
C5C—Ir1—C2—N3	157.6 (4)	C3C—C4C—C5C—Ir1	33.1 (5)
C6C—Ir1—C2—N3	-21.7 (7)	C2—Ir1—C5C—C6C	-179.6 (4)
N2B—Ir1—C2—N3	121.8 (3)	C2C—Ir1—C5C—C6C	100.8 (3)
C2C—Ir1—C2—N1	72.6 (3)	C1C—Ir1—C5C—C6C	62.6 (3)
C1C—Ir1—C2—N1	113.5 (3)	N2A—Ir1—C5C—C6C	-60.2 (3)
N2A—Ir1—C2—N1	-127.4 (3)	N2B—Ir1—C5C—C6C	-144.3 (3)
C5C—Ir1—C2—N1	-4.9 (7)	C2—Ir1—C5C—C4C	58.3 (6)
C6C—Ir1—C2—N1	175.8 (4)	C2C—Ir1—C5C—C4C	-21.2 (3)
N2B—Ir1—C2—N1	-40.7 (3)	C1C—Ir1—C5C—C4C	-59.5 (3)
N1—C2—N3—C4	1.7 (4)	N2A—Ir1—C5C—C4C	177.7 (3)
Ir1—C2—N3—C4	-163.9 (3)	C6C—Ir1—C5C—C4C	-122.1 (4)
N1—C2—N3—C6A	169.2 (3)	N2B—Ir1—C5C—C4C	93.7 (3)
Ir1—C2—N3—C6A	3.6 (5)	C4C—C5C—C6C—C7C	-5.5 (6)
C2—N3—C4—C5	-0.7 (5)	Ir1—C5C—C6C—C7C	-105.4 (4)
C6A—N3—C4—C5	-166.7 (4)	C4C—C5C—C6C—Ir1	99.9 (4)
N3—C4—C5—N1	-0.6 (5)	C2—Ir1—C6C—C5C	179.6 (4)
C2—N1—C5—C4	1.7 (5)	C2C—Ir1—C6C—C5C	-76.3 (3)
C6B—N1—C5—C4	161.3 (4)	C1C—Ir1—C6C—C5C	-116.2 (3)
C2—N3—C6A—N1A	-60.4 (5)	N2A—Ir1—C6C—C5C	123.4 (3)
C4—N3—C6A—N1A	104.6 (4)	N2B—Ir1—C6C—C5C	39.7 (3)
N3—C6A—N1A—C5A	-119.2 (4)	C2—Ir1—C6C—C7C	-61.7 (6)
N3—C6A—N1A—N2A	60.1 (4)	C2C—Ir1—C6C—C7C	42.3 (3)
C5A—N1A—N2A—	0.1 (4)	C1C—Ir1—C6C—C7C	2.5 (3)

C3A			
C6A—N1A—N2A—C3A	-179.3 (3)	N2A—Irl—C6C—C7C	-118.0 (3)
C5A—N1A—N2A—Irl	172.1 (2)	C5C—Irl—C6C—C7C	118.7 (4)
C6A—N1A—N2A—Irl	-7.4 (4)	N2B—Irl—C6C—C7C	158.3 (3)
C2—Irl—N2A—C3A	136.4 (4)	C5C—C6C—C7C—C8C	92.9 (5)
C2C—Irl—N2A—C3A	-138.9 (4)	Irl—C6C—C7C—C8C	11.5 (5)
C1C—Irl—N2A—C3A	-135.2 (4)	C2C—C1C—C8C—C7C	-53.5 (6)
C5C—Irl—N2A—C3A	-28.1 (4)	Irl—C1C—C8C—C7C	28.1 (5)
C6C—Irl—N2A—C3A	-59.3 (4)	C6C—C7C—C8C—C1C	-25.0 (6)
N2B—Irl—N2A—C3A	55.4 (4)	C41D—B1D—C11D—C16D	-85.0 (4)
C2—Irl—N2A—N1A	-32.7 (3)	C21D—B1D—C11D—C16D	33.0 (4)
C2C—Irl—N2A—N1A	52.0 (5)	C31D—B1D—C11D—C16D	157.3 (3)
C1C—Irl—N2A—N1A	55.7 (3)	C41D—B1D—C11D—C12D	91.5 (4)
C5C—Irl—N2A—N1A	162.7 (3)	C21D—B1D—C11D—C12D	-150.5 (3)
C6C—Irl—N2A—N1A	131.5 (3)	C31D—B1D—C11D—C12D	-26.2 (5)
N2B—Irl—N2A—N1A	-113.8 (3)	C16D—C11D—C12D—C13D	0.0 (5)
N1A—N2A—C3A—C4A	-0.4 (4)	B1D—C11D—C12D—C13D	-176.7 (3)
Irl—N2A—C3A—C4A	-170.7 (3)	C11D—C12D—C13D—C14D	-0.9 (6)
N2A—C3A—C4A—C5A	0.4 (5)	C12D—C13D—C14D—C15D	1.5 (6)
N2A—N1A—C5A—C4A	0.1 (5)	C13D—C14D—C15D—C16D	-1.2 (6)
C6A—N1A—C5A—C4A	179.5 (4)	C14D—C15D—C16D—C11D	0.3 (6)
C3A—C4A—C5A—	-0.3 (5)	C12D—C11D—C16D—C15D	0.3 (5)

N1A			
C2—N1—C6B—N1B	60.3 (4)	B1D—C11D—C16D—C15D	177.1 (3)
C5—N1—C6B—N1B	-97.9 (4)	C41D—B1D—C21D—C22D	5.7 (5)
N1—C6B—N1B—C5B	112.5 (4)	C11D—B1D—C21D—C22D	-111.6 (4)
N1—C6B—N1B—N2B	-61.1 (4)	C31D—B1D—C21D—C22D	125.7 (4)
C5B—N1B—N2B—C3B	0.2 (4)	C41D—B1D—C21D—C26D	-178.0 (3)
C6B—N1B—N2B—C3B	174.8 (3)	C11D—B1D—C21D—C26D	64.7 (4)
C5B—N1B—N2B—Irl	-169.1 (3)	C31D—B1D—C21D—C26D	-58.0 (4)
C6B—N1B—N2B—Irl	5.5 (4)	C26D—C21D—C22D—C23D	1.8 (5)
C2—Irl—N2B—C3B	-128.6 (4)	B1D—C21D—C22D—C23D	178.4 (3)
C2C—Irl—N2B—C3B	140.2 (4)	C21D—C22D—C23D—C24D	1.1 (6)
C1C—Irl—N2B—C3B	155.8 (4)	C22D—C23D—C24D—C25D	-2.3 (6)
N2A—Irl—N2B—C3B	-45.1 (4)	C23D—C24D—C25D—C26D	0.5 (6)
C5C—Irl—N2B—C3B	61.6 (4)	C24D—C25D—C26D—C21D	2.7 (6)
C6C—Irl—N2B—C3B	39.2 (4)	C22D—C21D—C26D—C25D	-3.7 (5)
C2—Irl—N2B—N1B	36.6 (3)	B1D—C21D—C26D—C25D	179.7 (3)
C2C—Irl—N2B—N1B	-54.6 (3)	C41D—B1D—C31D—C32D	143.9 (3)
C1C—Irl—N2B—N1B	-39.0 (5)	C21D—B1D—C31D—C32D	22.8 (5)
N2A—Irl—N2B—N1B	120.1 (3)	C11D—B1D—C31D—C32D	-97.8 (4)
C5C—Irl—N2B—N1B	-133.1 (3)	C41D—B1D—C31D—C36D	-36.9 (5)
C6C—Irl—N2B—N1B	-155.6 (3)	C21D—B1D—C31D—C36D	-158.0 (3)
N1B—N2B—C3B—C4B	0.2 (5)	C11D—B1D—C31D—C36D	81.4 (4)
Irl—N2B—C3B—C4B	167.0 (3)	C36D—C31D—C32D—C33D	-0.6 (5)
N2B—C3B—C4B—C5B	-0.5 (5)	B1D—C31D—C32D—C33D	178.7 (4)
N2B—N1B—C5B—C4B	-0.6 (5)	C31D—C32D—C33D—C34D	0.8 (6)
C6B—N1B—C5B—C4B	-174.5 (4)	C32D—C33D—C34D—C35D	-0.8 (6)

C3B—C4B—C5B—N1B	0.7 (5)	C33D—C34D—C35D—C36D	0.5 (7)
C2—Irl—C1C—C2C	-95.0 (2)	C34D—C35D—C36D—C31D	-0.3 (7)
N2A—Irl—C1C—C2C	-178.1 (2)	C32D—C31D—C36D—C35D	0.3 (6)
C5C—Irl—C1C—C2C	69.4 (2)	B1D—C31D—C36D—C35D	-179.0 (4)
C6C—Irl—C1C—C2C	102.0 (2)	C21D—B1D—C41D—C46D	-116.0 (4)
N2B—Irl—C1C—C2C	-22.0 (4)	C11D—B1D—C41D—C46D	0.6 (5)
C2—Irl—C1C—C8C	146.5 (3)	C31D—B1D—C41D—C46D	120.4 (4)
C2C—Irl—C1C—C8C	-118.5 (4)	C21D—B1D—C41D—C42D	64.9 (4)
N2A—Irl—C1C—C8C	63.5 (4)	C11D—B1D—C41D—C42D	-178.5 (3)
C5C—Irl—C1C—C8C	-49.1 (3)	C31D—B1D—C41D—C42D	-58.7 (4)
C6C—Irl—C1C—C8C	-16.5 (3)	C46D—C41D—C42D—C43D	1.9 (6)
N2B—Irl—C1C—C8C	-140.5 (3)	B1D—C41D—C42D—C43D	-178.9 (4)
C8C—C1C—C2C—C3C	1.1 (6)	C41D—C42D—C43D—C44D	-1.3 (6)
Irl—C1C—C2C—C3C	-106.7 (4)	C42D—C43D—C44D—C45D	-0.3 (6)
C8C—C1C—C2C—Irl	107.8 (4)	C43D—C44D—C45D—C46D	1.1 (6)
C2—Irl—C2C—C1C	87.5 (2)	C44D—C45D—C46D—C41D	-0.4 (6)
N2A—Irl—C2C—C1C	4.9 (5)	C42D—C41D—C46D—C45D	-1.1 (5)
C5C—Irl—C2C—C1C	-109.9 (2)	B1D—C41D—C46D—C45D	179.8 (4)
C6C—Irl—C2C—C1C	-74.1 (2)	C4E—O1E—C1E—C2E	-37.8 (5)
N2B—Irl—C2C—C1C	169.4 (2)	O1E—C1E—C2E—C3E	33.4 (5)
C2—Irl—C2C—C3C	-155.9 (3)	C1E—C2E—C3E—C4E	-17.2 (6)
C1C—Irl—C2C—C3C	116.6 (4)	C1E—O1E—C4E—C3E	26.5 (6)
N2A—Irl—C2C—C3C	121.5 (4)	C2E—C3E—C4E—O1E	-5.1 (7)

[Ir(κ^1 -NCN^{Me})₂(COD)]BPh₄ (2.5)

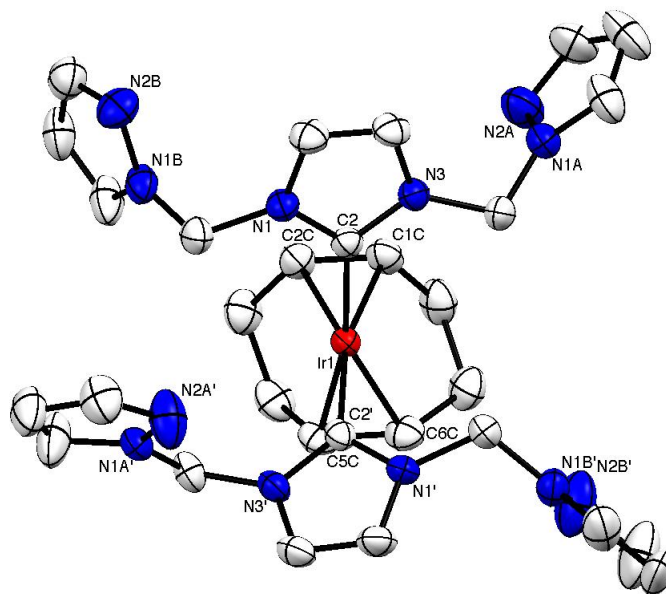


Table 1. Experimental details

Crystal data	
Chemical formula	C ₅₅ H ₅₆ BIrN ₁₂
<i>M</i> _r	1155.00
Crystal system, space group	Triclinic, <i>P</i> [−] 1
Temperature (K)	293
<i>a</i> , <i>b</i> , <i>c</i> (Å)	10.3367 (3), 12.8201 (4), 19.6142 (7)
α, β, γ (°)	92.847 (1), 102.154 (2), 94.312 (1)
<i>V</i> (Å ³)	2528.05 (14)
<i>Z</i>	2
Radiation type	Mo <i>K</i> α
μ (mm ^{−1})	2.80
Crystal size (mm)	0.36 × 0.29 × 0.21
Data collection	
Diffractometer	Bruker kappa APEXII CCD

	Diffractometer
Absorption correction	Multi-scan <i>SADABS</i> (Bruker, 2001)
T_{\min}, T_{\max}	0.432, 0.591
No. of measured, independent and observed [$I > 2\sigma(I)$] reflections	35831, 8907, 8566
R_{int}	0.027
$(\sin \theta/\lambda)_{\max}$ (\AA^{-1})	0.595
Refinement	
$R[F^2 > 2\sigma(F^2)], wR(F^2), S$	0.025, 0.066, 1.05
No. of reflections	8907
No. of parameters	641
No. of restraints	0
H-atom treatment	H-atom parameters constrained
$\Delta_{\max}, \Delta_{\min}$ (e \AA^{-3})	1.21, -1.56

Computer programs: *APEX2* (Bruker, 2007), *SHELXS-97* (Sheldrick, 2008), *SHELXL-97* (Sheldrick, 2008), *SHELXTL-Plus* (Sheldrick, 2008).

Table 2. Selected geometric parameters (\AA , $^\circ$)

Ir1—C2'	2.046 (3)	C4C—C5C	1.527 (5)
Ir1—C2	2.048 (3)	C4C—H4C1	0.9700
Ir1—C6C	2.179 (3)	C4C—H4C2	0.9700
Ir1—C2C	2.180 (3)	C5C—C6C	1.399 (5)
Ir1—C5C	2.210 (3)	C6C—C7C	1.506 (5)
Ir1—C1C	2.213 (3)	C7C—C8C	1.530 (5)
N1—C2	1.359 (4)	C7C—H7C1	0.9700
N1—C5	1.385 (4)	C7C—H7C2	0.9700

N1—C6B	1.459 (4)	C8C—H8C1	0.9700
C2—N3	1.358 (4)	C8C—H8C2	0.9700
N3—C4	1.383 (4)	B1D—C41D	1.647 (4)
N3—C6A	1.462 (4)	B1D—C31D	1.649 (4)
C4—C5	1.329 (5)	B1D—C11D	1.649 (4)
C4—H4	0.9300	B1D—C21D	1.650 (4)
C5—H5	0.9300	C11D—C12D	1.395 (5)
C6A—N1A	1.438 (4)	C11D—C16D	1.402 (5)
C6A—H6A1	0.9700	C12D—C13D	1.396 (5)
C6A—H6A2	0.9700	C12D—H12D	0.9300
N1A—C5A	1.341 (5)	C13D—C14D	1.385 (7)
N1A—N2A	1.356 (4)	C13D—H13D	0.9300
N2A—C3A	1.319 (5)	C14D—C15D	1.369 (7)
C3A—C4A	1.390 (7)	C14D—H14D	0.9300
C3A—H3A	0.9300	C15D—C16D	1.391 (5)
C4A—C5A	1.357 (7)	C15D—H15D	0.9300
C4A—H4A	0.9300	C16D—H16D	0.9300
C5A—H5A	0.9300	C21D—C26D	1.398 (4)
C6B—N1B	1.439 (5)	C21D—C22D	1.405 (4)
C6B—H6B1	0.9700	C22D—C23D	1.388 (5)
C6B—H6B2	0.9700	C22D—H22D	0.9300
N1B—C5B	1.345 (5)	C23D—C24D	1.375 (5)
N1B—N2B	1.352 (4)	C23D—H23D	0.9300
N2B—C3B	1.328 (5)	C24D—C25D	1.379 (5)
C3B—C4B	1.380 (6)	C24D—H24D	0.9300
C3B—H3B	0.9300	C25D—C26D	1.390 (5)

C4B—C5B	1.358 (6)	C25D—H25D	0.9300
C4B—H4B	0.9300	C26D—H26D	0.9300
C5B—H5B	0.9300	C31D—C36D	1.398 (4)
N1'—C2'	1.356 (4)	C31D—C32D	1.406 (4)
N1'—C5'	1.387 (4)	C32D—C33D	1.386 (5)
N1'—C6B'	1.456 (4)	C32D—H32D	0.9300
C2'—N3'	1.362 (4)	C33D—C34D	1.381 (5)
N3'—C4'	1.378 (4)	C33D—H33D	0.9300
N3'—C6A'	1.444 (4)	C34D—C35D	1.378 (5)
C4'—C5'	1.328 (5)	C34D—H34D	0.9300
C4'—H4'	0.9300	C35D—C36D	1.386 (5)
C5'—H5'	0.9300	C35D—H35D	0.9300
C6A'—N1A'	1.461 (4)	C36D—H36D	0.9300
C6A'—H6A3	0.9700	C41D—C42D	1.396 (5)
C6A'—H6A4	0.9700	C41D—C46D	1.396 (5)
N1A'—C5A'	1.329 (5)	C42D—C43D	1.391 (5)
N1A'—N2A'	1.334 (4)	C42D—H42D	0.9300
N2A'—C3A'	1.328 (5)	C43D—C44D	1.374 (6)
C3A'—C4A'	1.365 (6)	C43D—H43D	0.9300
C3A'—H3A'	0.9300	C44D—C45D	1.380 (6)
C4A'—C5A'	1.359 (6)	C44D—H44D	0.9300
C4A'—H4A'	0.9300	C45D—C46D	1.387 (5)
C5A'—H5A'	0.9300	C45D—H45D	0.9300
C6B'—N1B'	1.426 (4)	C46D—H46D	0.9300
C6B'—H6B3	0.9700	C1E—C12'	1.348 (15)
C6B'—H6B4	0.9700	C1E—C1E'	1.60 (2)

N1B'—C5B'	1.341 (5)	C1E—Cl2E	1.729 (16)
N1B'—N2B'	1.342 (5)	C1E—Cl1E	1.743 (15)
N2B'—C3B'	1.305 (7)	C1E—Cl4E	1.82 (2)
C3B'—C4B'	1.356 (8)	C1E—Cl3E	1.982 (16)
C3B'—H3B'	0.9300	Cl1E—Cl3E	0.578 (6)
C4B'—C5B'	1.370 (7)	Cl1E—Cl4E	1.192 (17)
C4B'—H4B'	0.9300	Cl1E—C1E'	1.811 (18)
C5B'—H5B'	0.9300	Cl2E—Cl2'	0.957 (6)
C1C—C2C	1.404 (5)	Cl2E—C1E'	1.332 (18)
C1C—C8C	1.518 (5)	Cl2'—C1E'	1.810 (18)
C2C—C3C	1.509 (5)	C1E'—Cl3E	1.535 (19)
C3C—C4C	1.516 (6)	C1E'—Cl4E	1.56 (2)
C3C—H3C1	0.9700	Cl3E—Cl4E	1.194 (17)
C3C—H3C2	0.9700	Cl4E—Cl4E ⁱ	1.93 (3)
C2'—Ir1—C2	97.11 (12)	C8C—C7C—H7C1	108.7
C2'—Ir1—C6C	87.02 (13)	C6C—C7C—H7C2	108.7
C2—Ir1—C6C	153.43 (14)	C8C—C7C—H7C2	108.7
C2'—Ir1—C2C	155.63 (13)	H7C1—C7C—H7C2	107.6
C2—Ir1—C2C	90.39 (13)	C1C—C8C—C7C	112.9 (3)
C6C—Ir1—C2C	96.58 (14)	C1C—C8C—H8C1	109.0
C2'—Ir1—C5C	88.14 (13)	C7C—C8C—H8C1	109.0
C2—Ir1—C5C	168.01 (13)	C1C—C8C—H8C2	109.0
C6C—Ir1—C5C	37.16 (14)	C7C—C8C—H8C2	109.0
C2C—Ir1—C5C	80.63 (13)	H8C1—C8C—H8C2	107.8
C2'—Ir1—C1C	164.58 (13)	C41D—B1D—C31D	110.3 (2)

C2—Ir1—C1C	89.44 (13)	C41D—B1D—C11D	109.7 (2)
C6C—Ir1—C1C	81.03 (14)	C31D—B1D—C11D	111.1 (2)
C2C—Ir1—C1C	37.26 (13)	C41D—B1D—C21D	109.4 (2)
C5C—Ir1—C1C	88.18 (13)	C31D—B1D—C21D	109.1 (2)
C2—N1—C5	111.4 (3)	C11D—B1D—C21D	107.2 (2)
C2—N1—C6B	124.9 (3)	C12D—C11D—C16D	115.0 (3)
C5—N1—C6B	123.7 (3)	C12D—C11D—B1D	123.7 (3)
N3—C2—N1	103.3 (3)	C16D—C11D—B1D	121.2 (3)
N3—C2—Ir1	127.2 (2)	C11D—C12D—C13D	122.5 (4)
N1—C2—Ir1	129.3 (2)	C11D—C12D—H12D	118.8
C2—N3—C4	111.7 (3)	C13D—C12D—H12D	118.8
C2—N3—C6A	124.0 (3)	C14D—C13D—C12D	120.3 (4)
C4—N3—C6A	124.1 (3)	C14D—C13D—H13D	119.9
C5—C4—N3	106.7 (3)	C12D—C13D—H13D	119.9
C5—C4—H4	126.7	C15D—C14D—C13D	118.9 (4)
N3—C4—H4	126.7	C15D—C14D—H14D	120.5
C4—C5—N1	107.0 (3)	C13D—C14D—H14D	120.5
C4—C5—H5	126.5	C14D—C15D—C16D	120.2 (4)
N1—C5—H5	126.5	C14D—C15D—H15D	119.9
N1A—C6A—N3	112.5 (3)	C16D—C15D—H15D	119.9
N1A—C6A—H6A1	109.1	C15D—C16D—C11D	123.0 (4)
N3—C6A—H6A1	109.1	C15D—C16D—H16D	118.5
N1A—C6A—H6A2	109.1	C11D—C16D—H16D	118.5
N3—C6A—H6A2	109.1	C26D—C21D—C22D	115.2 (3)
H6A1—C6A—H6A2	107.8	C26D—C21D—B1D	123.6 (3)
C5A—N1A—N2A	112.4 (3)	C22D—C21D—B1D	120.9 (3)

C5A—N1A—C6A	127.4 (3)	C23D—C22D—C21D	122.2 (3)
N2A—N1A—C6A	120.2 (3)	C23D—C22D—H22D	118.9
C3A—N2A—N1A	104.0 (4)	C21D—C22D—H22D	118.9
N2A—C3A—C4A	111.7 (4)	C24D—C23D—C22D	120.7 (3)
N2A—C3A—H3A	124.1	C24D—C23D—H23D	119.7
C4A—C3A—H3A	124.1	C22D—C23D—H23D	119.7
C5A—C4A—C3A	105.5 (4)	C23D—C24D—C25D	119.1 (3)
C5A—C4A—H4A	127.3	C23D—C24D—H24D	120.4
C3A—C4A—H4A	127.3	C25D—C24D—H24D	120.4
N1A—C5A—C4A	106.4 (4)	C24D—C25D—C26D	119.9 (3)
N1A—C5A—H5A	126.8	C24D—C25D—H25D	120.1
C4A—C5A—H5A	126.8	C26D—C25D—H25D	120.1
N1B—C6B—N1	112.7 (3)	C25D—C26D—C21D	122.9 (3)
N1B—C6B—H6B1	109.1	C25D—C26D—H26D	118.5
N1—C6B—H6B1	109.1	C21D—C26D—H26D	118.5
N1B—C6B—H6B2	109.1	C36D—C31D—C32D	114.5 (3)
N1—C6B—H6B2	109.1	C36D—C31D—B1D	123.5 (3)
H6B1—C6B—H6B2	107.8	C32D—C31D—B1D	122.0 (3)
C5B—N1B—N2B	111.1 (3)	C33D—C32D—C31D	123.0 (3)
C5B—N1B—C6B	129.0 (3)	C33D—C32D—H32D	118.5
N2B—N1B—C6B	119.9 (3)	C31D—C32D—H32D	118.5
C3B—N2B—N1B	104.4 (3)	C34D—C33D—C32D	120.3 (3)
N2B—C3B—C4B	112.2 (4)	C34D—C33D—H33D	119.8
N2B—C3B—H3B	123.9	C32D—C33D—H33D	119.8
C4B—C3B—H3B	123.9	C35D—C34D—C33D	118.6 (3)
C5B—C4B—C3B	104.5 (4)	C35D—C34D—H34D	120.7

C5B—C4B—H4B	127.7	C33D—C34D—H34D	120.7
C3B—C4B—H4B	127.7	C34D—C35D—C36D	120.4 (3)
N1B—C5B—C4B	107.8 (4)	C34D—C35D—H35D	119.8
N1B—C5B—H5B	126.1	C36D—C35D—H35D	119.8
C4B—C5B—H5B	126.1	C35D—C36D—C31D	123.1 (3)
C2'—N1'—C5'	111.6 (3)	C35D—C36D—H36D	118.5
C2'—N1'—C6B'	124.0 (3)	C31D—C36D—H36D	118.5
C5'—N1'—C6B'	124.0 (3)	C42D—C41D—C46D	114.5 (3)
N1'—C2'—N3'	102.9 (3)	C42D—C41D—B1D	122.9 (3)
N1'—C2'—Ir1	128.8 (2)	C46D—C41D—B1D	122.5 (3)
N3'—C2'—Ir1	127.2 (2)	C43D—C42D—C41D	123.2 (3)
C2'—N3'—C4'	111.9 (3)	C43D—C42D—H42D	118.4
C2'—N3'—C6A'	124.5 (3)	C41D—C42D—H42D	118.4
C4'—N3'—C6A'	123.5 (3)	C44D—C43D—C42D	120.0 (4)
C5'—C4'—N3'	106.8 (3)	C44D—C43D—H43D	120.0
C5'—C4'—H4'	126.6	C42D—C43D—H43D	120.0
N3'—C4'—H4'	126.6	C43D—C44D—C45D	119.0 (3)
C4'—C5'—N1'	106.8 (3)	C43D—C44D—H44D	120.5
C4'—C5'—H5'	126.6	C45D—C44D—H44D	120.5
N1'—C5'—H5'	126.6	C44D—C45D—C46D	119.9 (4)
N3'—C6A'—N1A'	110.6 (3)	C44D—C45D—H45D	120.0
N3'—C6A'—H6A3	109.5	C46D—C45D—H45D	120.0
N1A'—C6A'—H6A3	109.5	C45D—C46D—C41D	123.3 (3)
N3'—C6A'—H6A4	109.5	C45D—C46D—H46D	118.4
N1A'—C6A'—H6A4	109.5	C41D—C46D—H46D	118.4
H6A3—C6A'—H6A4	108.1	Cl2'—C1E—C1E'	75.3 (10)

C5A'—N1A'—N2A'	111.8 (3)	Cl2'—C1E—Cl2E	33.4 (4)
C5A'—N1A'—C6A'	125.5 (3)	C1E'—C1E—Cl2E	47.0 (8)
N2A'—N1A'—C6A'	122.7 (3)	Cl2'—C1E—Cl1E	133.9 (11)
C3A'—N2A'—N1A'	104.2 (3)	C1E'—C1E—Cl1E	65.5 (9)
N2A'—C3A'—C4A'	112.1 (4)	Cl2E—C1E—Cl1E	112.4 (8)
N2A'—C3A'—H3A'	124.0	Cl2'—C1E—Cl4E	126.2 (12)
C4A'—C3A'—H3A'	124.0	C1E'—C1E—Cl4E	53.9 (9)
C5A'—C4A'—C3A'	104.4 (4)	Cl2E—C1E—Cl4E	93.1 (9)
C5A'—C4A'—H4A'	127.8	Cl1E—C1E—Cl4E	39.1 (6)
C3A'—C4A'—H4A'	127.8	Cl2'—C1E—Cl3E	119.0 (10)
N1A'—C5A'—C4A'	107.5 (4)	C1E'—C1E—Cl3E	49.4 (8)
N1A'—C5A'—H5A'	126.2	Cl2E—C1E—Cl3E	96.2 (7)
C4A'—C5A'—H5A'	126.2	Cl1E—C1E—Cl3E	16.3 (2)
N1B'—C6B'—N1'	113.6 (3)	Cl4E—C1E—Cl3E	36.3 (6)
N1B'—C6B'—H6B3	108.8	Cl3E—Cl1E—Cl4E	76.2 (11)
N1'—C6B'—H6B3	108.8	Cl3E—Cl1E—C1E	106.0 (10)
N1B'—C6B'—H6B4	108.8	Cl4E—Cl1E—C1E	73.8 (9)
N1'—C6B'—H6B4	108.8	Cl3E—Cl1E—C1E'	53.1 (9)
H6B3—C6B'—H6B4	107.7	Cl4E—Cl1E—C1E'	58.2 (9)
C5B'—N1B'—N2B'	111.8 (3)	C1E—Cl1E—C1E'	53.3 (7)
C5B'—N1B'—C6B'	128.7 (3)	Cl2'—Cl2E—C1E'	103.3 (9)
N2B'—N1B'—C6B'	119.5 (3)	Cl2'—Cl2E—C1E	50.9 (6)
C3B'—N2B'—N1B'	104.7 (4)	C1E'—Cl2E—C1E	61.3 (9)
N2B'—C3B'—C4B'	112.2 (5)	Cl2E—Cl2'—C1E	95.7 (8)
N2B'—C3B'—H3B'	123.9	Cl2E—Cl2'—C1E'	45.8 (7)
C4B'—C3B'—H3B'	123.9	C1E—Cl2'—C1E'	58.6 (8)

C3B'—C4B'—C5B'	105.6 (4)	Cl2E—C1E'—Cl3E	149.4 (14)
C3B'—C4B'—H4B'	127.2	Cl2E—C1E'—Cl4E	125.8 (15)
C5B'—C4B'—H4B'	127.2	Cl3E—C1E'—Cl4E	45.4 (8)
N1B'—C5B'—C4B'	105.6 (4)	Cl2E—C1E'—C1E	71.7 (10)
N1B'—C5B'—H5B'	127.2	Cl3E—C1E'—C1E	78.5 (10)
C4B'—C5B'—H5B'	127.2	Cl4E—C1E'—C1E	70.3 (11)
C2C—C1C—C8C	124.1 (3)	Cl2E—C1E'—Cl2'	31.0 (5)
C2C—C1C—Irl	70.11 (19)	Cl3E—C1E'—Cl2'	119.1 (11)
C8C—C1C—Irl	111.5 (2)	Cl4E—C1E'—Cl2'	114.1 (12)
C1C—C2C—C3C	125.1 (3)	C1E—C1E'—Cl2'	46.1 (7)
C1C—C2C—Irl	72.63 (19)	Cl2E—C1E'—Cl1E	132.7 (12)
C3C—C2C—Irl	109.3 (2)	Cl3E—C1E'—Cl1E	17.5 (3)
C2C—C3C—C4C	114.2 (3)	Cl4E—C1E'—Cl1E	40.6 (8)
C2C—C3C—H3C1	108.7	C1E—C1E'—Cl1E	61.2 (8)
C4C—C3C—H3C1	108.7	Cl2'—C1E'—Cl1E	103.7 (9)
C2C—C3C—H3C2	108.7	Cl1E—Cl3E—Cl4E	75.8 (11)
C4C—C3C—H3C2	108.7	Cl1E—Cl3E—C1E'	109.3 (11)
H3C1—C3C—H3C2	107.6	Cl4E—Cl3E—C1E'	68.3 (10)
C3C—C4C—C5C	112.8 (3)	Cl1E—Cl3E—C1E	57.7 (9)
C3C—C4C—H4C1	109.0	Cl4E—Cl3E—C1E	64.3 (9)
C5C—C4C—H4C1	109.0	C1E'—Cl3E—C1E	52.1 (8)
C3C—C4C—H4C2	109.0	Cl1E—Cl4E—Cl3E	28.0 (5)
C5C—C4C—H4C2	109.0	Cl1E—Cl4E—C1E'	81.2 (12)
H4C1—C4C—H4C2	107.8	Cl3E—Cl4E—C1E'	66.3 (11)
C6C—C5C—C4C	124.1 (3)	Cl1E—Cl4E—C1E	67.2 (9)
C6C—C5C—Irl	70.25 (19)	Cl3E—Cl4E—C1E	79.4 (10)

C4C—C5C—Ir1	111.9 (2)	C1E'—Cl4E—C1E	55.8 (9)
C5C—C6C—C7C	125.6 (3)	Cl1E—Cl4E—Cl4E ⁱ	138.2 (18)
C5C—C6C—Ir1	72.6 (2)	Cl3E—Cl4E—Cl4E ⁱ	133.3 (17)
C7C—C6C—Ir1	108.6 (2)	C1E'—Cl4E—Cl4E ⁱ	133.3 (17)
C6C—C7C—C8C	114.1 (3)	C1E—Cl4E—Cl4E ⁱ	147.0 (16)
C6C—C7C—H7C1	108.7		
C5—N1—C2—N3	-0.5 (4)	C32D—C33D— C34D—C35D	-0.3 (6)
C6B—N1—C2—N3	-177.6 (3)	C33D—C34D— C35D—C36D	0.8 (6)
C5—N1—C2—Ir1	-176.0 (2)	C34D—C35D— C36D—C31D	-0.7 (6)
C6B—N1—C2—Ir1	6.9 (5)	C32D—C31D— C36D—C35D	0.0 (5)
C2'—Ir1—C2—N3	104.7 (3)	B1D—C31D— C36D—C35D	-177.2 (3)
C6C—Ir1—C2—N3	7.1 (5)	C31D—B1D— C41D—C42D	-110.5 (3)
C2C—Ir1—C2—N3	-98.5 (3)	C11D—B1D— C41D—C42D	12.2 (4)
C5C—Ir1—C2—N3	-139.8 (5)	C21D—B1D— C41D—C42D	129.5 (3)
C1C—Ir1—C2—N3	-61.3 (3)	C31D—B1D— C41D—C46D	68.7 (4)
C2'—Ir1—C2—N1	-80.7 (3)	C11D—B1D— C41D—C46D	-168.6 (3)
C6C—Ir1—C2—N1	-178.3 (3)	C21D—B1D—	-51.3 (4)

		C41D—C46D	
C2C—Ir1—C2—N1	76.0 (3)	C46D—C41D— C42D—C43D	-1.6 (5)
C5C—Ir1—C2—N1	34.7 (7)	B1D—C41D— C42D—C43D	177.6 (3)
C1C—Ir1—C2—N1	113.3 (3)	C41D—C42D— C43D—C44D	-0.9 (6)
N1—C2—N3—C4	0.9 (3)	C42D—C43D— C44D—C45D	2.0 (6)
Ir1—C2—N3—C4	176.5 (2)	C43D—C44D— C45D—C46D	-0.6 (7)
N1—C2—N3—C6A	175.5 (3)	C44D—C45D— C46D—C41D	-2.1 (6)
Ir1—C2—N3—C6A	-8.8 (4)	C42D—C41D— C46D—C45D	3.1 (5)
C2—N3—C4—C5	-0.9 (4)	B1D—C41D— C46D—C45D	-176.1 (3)
C6A—N3—C4—C5	-175.6 (3)	Cl2'—C1E—Cl1E— Cl3E	26.7 (18)
N3—C4—C5—N1	0.6 (4)	C1E'—C1E—Cl1E— Cl3E	-7.8 (12)
C2—N1—C5—C4	-0.1 (4)	Cl2E—C1E—Cl1E— Cl3E	-4.5 (13)
C6B—N1—C5—C4	177.1 (3)	Cl4E—C1E—Cl1E— Cl3E	-70.0 (12)
C2—N3—C6A—N1A	134.3 (3)	Cl2'—C1E—Cl1E— Cl4E	96.7 (17)
C4—N3—C6A—N1A	-51.7 (4)	C1E'—C1E—Cl1E— Cl4E	62.2 (11)

N3—C6A—N1A— C5A	110.2 (4)	Cl2E—C1E—Cl1E— Cl4E	65.5 (12)
N3—C6A—N1A— N2A	-70.3 (4)	Cl3E—C1E—Cl1E— Cl4E	70.0 (12)
C5A—N1A—N2A— C3A	-0.4 (5)	Cl2'—C1E—Cl1E— C1E'	34.5 (13)
C6A—N1A—N2A— C3A	180.0 (3)	Cl2E—C1E—Cl1E— C1E'	3.4 (8)
N1A—N2A—C3A— C4A	-0.1 (5)	Cl4E—C1E—Cl1E— C1E'	-62.2 (11)
N2A—C3A—C4A— C5A	0.6 (6)	Cl3E—C1E—Cl1E— C1E'	7.8 (12)
N2A—N1A—C5A— C4A	0.8 (5)	C1E'—C1E—Cl2E— Cl2'	141.6 (12)
C6A—N1A—C5A— C4A	-179.6 (4)	Cl1E—C1E—Cl2E— Cl2'	137.4 (11)
C3A—C4A—C5A— N1A	-0.8 (6)	Cl4E—C1E—Cl2E— Cl2'	172.4 (11)
C2—N1—C6B—N1B	-107.7 (4)	Cl3E—C1E—Cl2E— Cl2'	136.1 (9)
C5—N1—C6B—N1B	75.6 (4)	Cl2'—C1E—Cl2E— C1E'	-141.6 (12)
N1—C6B—N1B— C5B	107.0 (4)	Cl1E—C1E—Cl2E— C1E'	-4.2 (10)
N1—C6B—N1B— N2B	-73.7 (4)	Cl4E—C1E—Cl2E— C1E'	30.9 (11)
C5B—N1B—N2B— C3B	0.1 (4)	Cl3E—C1E—Cl2E— C1E'	-5.4 (9)
C6B—N1B—N2B—	-179.3 (3)	C1E'—Cl2E—Cl2'—	34.1 (11)

C3B		C1E	
N1B—N2B—C3B— C4B	-0.3 (4)	C1E—C12E—C12'— C1E'	-34.1 (11)
N2B—C3B—C4B— C5B	0.3 (5)	C1E'—C1E—C12'— C12E	-28.0 (9)
N2B—N1B—C5B— C4B	0.1 (5)	C11E—C1E—C12'— C12E	-60.3 (14)
C6B—N1B—C5B— C4B	179.4 (3)	C14E—C1E—C12'— C12E	-9.4 (14)
C3B—C4B—C5B— N1B	-0.2 (5)	C13E—C1E—C12'— C12E	-52.0 (10)
C5'—N1'—C2'—N3'	0.4 (4)	C12E—C1E—C12'— C1E'	28.0 (9)
C6B'—N1'—C2'—N3'	-172.5 (3)	C11E—C1E—C12'— C1E'	-32.2 (12)
C5'—N1'—C2'—Ir1	-168.6 (2)	C14E—C1E—C12'— C1E'	18.7 (12)
C6B'—N1'—C2'—Ir1	18.5 (5)	C13E—C1E—C12'— C1E'	-23.9 (9)
C2—Ir1—C2'—N1'	-82.5 (3)	C12'—C12E—C1E'— C13E	-16 (3)
C6C—Ir1—C2'—N1'	71.1 (3)	C1E—C12E—C1E'— C13E	14 (2)
C2C—Ir1—C2'—N1'	170.5 (3)	C12'—C12E—C1E'— C14E	-77.2 (17)
C5C—Ir1—C2'—N1'	108.3 (3)	C1E—C12E—C1E'— C14E	-47.4 (15)
C1C—Ir1—C2'—N1'	32.0 (6)	C12'—C12E—C1E'— C1E	-29.7 (9)

C2—Irl—C2'—N3'	111.0 (3)	C1E—Cl2E—C1E'— Cl2'	29.7 (9)
C6C—Irl—C2'—N3'	-95.4 (3)	Cl2'—Cl2E—C1E'— Cl1E	-24.7 (18)
C2C—Irl—C2'—N3'	4.0 (5)	C1E—Cl2E—C1E'— Cl1E	5.1 (12)
C5C—Irl—C2'—N3'	-58.2 (3)	Cl2'—C1E—C1E'— Cl2E	20.7 (6)
C1C—Irl—C2'—N3'	-134.5 (4)	Cl1E—C1E—C1E'— Cl2E	175.8 (10)
N1'—C2'—N3'—C4'	-0.3 (4)	Cl4E—C1E—C1E'— Cl2E	-140.6 (13)
Irl—C2'—N3'—C4'	168.9 (2)	Cl3E—C1E—C1E'— Cl2E	172.9 (12)
N1'—C2'—N3'—C6A'	174.8 (3)	Cl2'—C1E—C1E'— Cl3E	-152.1 (9)
Irl—C2'—N3'—C6A'	-15.9 (5)	Cl2E—C1E—C1E'— Cl3E	-172.9 (12)
C2'—N3'—C4'—C5'	0.2 (4)	Cl1E—C1E—C1E'— Cl3E	2.9 (4)
C6A'—N3'—C4'—C5'	-175.0 (3)	Cl4E—C1E—C1E'— Cl3E	46.5 (8)
N3'—C4'—C5'—N1'	0.0 (4)	Cl2'—C1E—C1E'— Cl4E	161.3 (12)
C2'—N1'—C5'—C4'	-0.2 (4)	Cl2E—C1E—C1E'— Cl4E	140.6 (13)
C6B'—N1'—C5'—C4'	172.6 (3)	Cl1E—C1E—C1E'— Cl4E	-43.6 (8)
C2'—N3'—C6A'—	-105.3 (4)	Cl3E—C1E—C1E'—	-46.5 (8)

N1A'		Cl4E	
C4'—N3'—C6A'— N1A'	69.3 (4)	Cl2E—C1E—C1E'— Cl2'	-20.7 (7)
N3'—C6A'—N1A'— C5A'	-166.9 (4)	Cl1E—C1E—C1E'— Cl2'	155.0 (9)
N3'—C6A'—N1A'— N2A'	12.8 (5)	Cl4E—C1E—C1E'— Cl2'	-161.3 (12)
C5A'—N1A'—N2A'— C3A'	0.1 (5)	Cl3E—C1E—C1E'— Cl2'	152.1 (10)
C6A'—N1A'—N2A'— C3A'	-179.6 (3)	Cl2'—C1E—C1E'— Cl1E	-155.0 (9)
N1A'—N2A'—C3A'— C4A'	-0.2 (5)	Cl2E—C1E—C1E'— Cl1E	-175.8 (10)
N2A'—C3A'—C4A'— C5A'	0.2 (6)	Cl4E—C1E—C1E'— Cl1E	43.6 (8)
N2A'—N1A'—C5A'— C4A'	0.1 (6)	Cl3E—C1E—C1E'— Cl1E	-2.9 (4)
C6A'—N1A'—C5A'— C4A'	179.8 (4)	C1E—Cl2'—C1E'— Cl2E	-139.2 (13)
C3A'—C4A'—C5A'— N1A'	-0.2 (6)	Cl2E—Cl2'—C1E'— Cl3E	170.8 (17)
C2'—N1'—C6B'— N1B'	-131.9 (3)	C1E—Cl2'—C1E'— Cl3E	31.6 (11)
C5'—N1'—C6B'— N1B'	56.1 (5)	Cl2E—Cl2'—C1E'— Cl4E	119.9 (16)
N1'—C6B'—N1B'— C5B'	-102.0 (4)	C1E—Cl2'—C1E'— Cl4E	-19.3 (12)
N1'—C6B'—N1B'— N2B'	79.2 (5)	Cl2E—Cl2'—C1E'— C1E	139.2 (13)

C5B'—N1B'—N2B'— C3B'	0.5 (6)	Cl2E—Cl2'—C1E'— C11E	161.6 (14)
C6B'—N1B'—N2B'— C3B'	179.5 (4)	C1E—Cl2'—C1E'— C11E	22.4 (9)
N1B'—N2B'—C3B'— C4B'	0.3 (7)	Cl3E—C11E—C1E'— Cl2E	165 (2)
N2B'—C3B'—C4B'— C5B'	-0.9 (7)	Cl4E—C11E—C1E'— Cl2E	-98 (2)
N2B'—N1B'—C5B'— C4B'	-1.0 (5)	C1E—C11E—C1E'— Cl2E	-5.5 (13)
C6B'—N1B'—C5B'— C4B'	-179.9 (4)	Cl4E—C11E—C1E'— Cl3E	96.5 (14)
C3B'—C4B'—C5B'— N1B'	1.1 (6)	C1E—C11E—C1E'— Cl3E	-170.6 (14)
C2'—Ir1—C1C—C2C	153.2 (4)	Cl3E—C11E—C1E'— Cl4E	-96.5 (14)
C2—Ir1—C1C—C2C	-91.4 (2)	C1E—C11E—C1E'— Cl4E	92.9 (13)
C6C—Irl—C1C— C2C	113.5 (2)	Cl3E—C11E—C1E'— C1E	170.6 (14)
C5C—Irl—C1C— C2C	76.9 (2)	Cl4E—C11E—C1E'— C1E	-92.9 (13)
C2'—Ir1—C1C—C8C	33.2 (6)	Cl3E—C11E—C1E'— Cl2'	152.3 (14)
C2—Ir1—C1C—C8C	148.7 (3)	Cl4E—C11E—C1E'— Cl2'	-111.2 (14)
C6C—Irl—C1C— C8C	-6.4 (3)	C1E—C11E—C1E'— Cl2'	-18.3 (7)
C2C—Irl—C1C—	-119.9 (4)	C1E—C11E—Cl3E—	68.3 (10)

C8C		Cl4E	
C5C—Irl—C1C— C8C	-43.1 (3)	C1E'—Cl1E—Cl3E— Cl4E	60.4 (11)
C8C—C1C—C2C— C3C	1.4 (5)	Cl4E—Cl1E—Cl3E— C1E'	-60.4 (11)
Irl—C1C—C2C— C3C	-101.7 (3)	C1E—Cl1E—Cl3E— C1E'	7.9 (12)
C8C—C1C—C2C— Irl	103.1 (3)	Cl4E—Cl1E—Cl3E— C1E	-68.3 (10)
C2'—Irl—C2C—C1C	-163.1 (3)	C1E'—Cl1E—Cl3E— C1E	-7.9 (12)
C2—Irl—C2C—C1C	88.6 (2)	Cl2E—C1E'—Cl3E— Cl1E	-22 (3)
C6C—Irl—C2C— C1C	-65.7 (2)	Cl4E—C1E'—Cl3E— Cl1E	65.2 (13)
C5C—Irl—C2C— C1C	-99.4 (2)	C1E—C1E'—Cl3E— Cl1E	-8.4 (13)
C2'—Irl—C2C—C3C	-41.1 (4)	Cl2'—C1E'—Cl3E— Cl1E	-31.1 (16)
C2—Irl—C2C—C3C	-149.5 (3)	Cl2E—C1E'—Cl3E— Cl4E	-87 (3)
C6C—Irl—C2C— C3C	56.2 (3)	C1E—C1E'—Cl3E— Cl4E	-73.6 (12)
C5C—Irl—C2C— C3C	22.5 (3)	Cl2'—C1E'—Cl3E— Cl4E	-96.3 (14)
C1C—Irl—C2C— C3C	122.0 (4)	Cl1E—C1E'—Cl3E— Cl4E	-65.2 (13)
C1C—C2C—C3C— C4C	44.8 (5)	Cl2E—C1E'—Cl3E— C1E	-13 (2)

Ir1—C2C—C3C— C4C	-37.1 (4)	Cl4E—C1E'—Cl3E— C1E	73.6 (12)
C2C—C3C—C4C— C5C	33.3 (5)	Cl2'—C1E'—Cl3E— C1E	-22.7 (8)
C3C—C4C—C5C— C6C	-93.0 (4)	Cl1E—C1E'—Cl3E— C1E	8.4 (13)
C3C—C4C—C5C— Ir1	-12.6 (4)	Cl2'—C1E—Cl3E— Cl1E	-158.3 (15)
C2'—Ir1—C5C—C6C	-87.5 (2)	C1E'—C1E—Cl3E— Cl1E	170.6 (14)
C2—Ir1—C5C—C6C	156.2 (5)	Cl2E—C1E—Cl3E— Cl1E	175.8 (12)
C2C—Ir1—C5C— C6C	114.2 (2)	Cl4E—C1E—Cl3E— Cl1E	88.9 (13)
C1C—Ir1—C5C— C6C	77.5 (2)	Cl2'—C1E—Cl3E— Cl4E	112.8 (15)
C2'—Ir1—C5C—C4C	152.7 (3)	C1E'—C1E—Cl3E— Cl4E	81.6 (13)
C2—Ir1—C5C—C4C	36.4 (7)	Cl2E—C1E—Cl3E— Cl4E	86.9 (12)
C6C—Ir1—C5C— C4C	-119.8 (4)	Cl1E—C1E—Cl3E— Cl4E	-88.9 (13)
C2C—Ir1—C5C— C4C	-5.6 (3)	Cl2'—C1E—Cl3E— C1E'	31.1 (11)
C1C—Ir1—C5C— C4C	-42.3 (3)	Cl2E—C1E—Cl3E— C1E'	5.2 (9)
C4C—C5C—C6C— C7C	2.9 (6)	Cl1E—C1E—Cl3E— C1E'	-170.6 (14)
Ir1—C5C—C6C—	-100.7 (4)	Cl4E—C1E—Cl3E—	-81.6 (13)

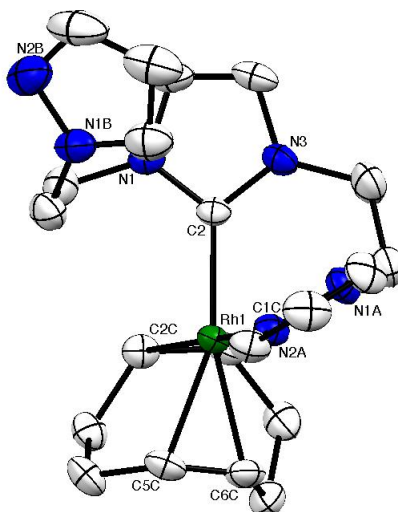
C7C		C1E'	
C4C—C5C—C6C— Ir1	103.7 (3)	C1E—Cl1E—Cl4E— Cl3E	-111.5 (10)
C2'—Ir1—C6C—C5C	90.9 (2)	C1E'—Cl1E—Cl4E— Cl3E	-54.9 (11)
C2—Ir1—C6C—C5C	-169.2 (2)	Cl3E—Cl1E—Cl4E— C1E'	54.9 (11)
C2C—Irl—C6C— C5C	-64.9 (2)	C1E—Cl1E—Cl4E— C1E'	-56.6 (9)
C1C—Irl—C6C— C5C	-98.9 (2)	Cl3E—Cl1E—Cl4E— C1E	111.5 (10)
C2'—Ir1—C6C—C7C	-146.6 (3)	C1E'—Cl1E—Cl4E— C1E	56.6 (9)
C2—Irl—C6C—C7C	-46.7 (4)	Cl3E—Cl1E—Cl4E— Cl4E ⁱ	-95 (3)
C2C—Irl—C6C— C7C	57.6 (3)	C1E—Cl1E—Cl4E— Cl4E ⁱ	153 (3)
C5C—Irl—C6C— C7C	122.5 (4)	C1E'—Cl1E—Cl4E— Cl4E ⁱ	-150 (3)
C1C—Irl—C6C— C7C	23.6 (3)	C1E'—Cl3E—Cl4E— Cl1E	117.9 (12)
C5C—C6C—C7C— C8C	43.3 (5)	C1E—Cl3E—Cl4E— Cl1E	60.7 (10)
Ir1—C6C—C7C— C8C	-38.2 (4)	Cl1E—Cl3E—Cl4E— C1E'	-117.9 (12)
C2C—C1C—C8C— C7C	-92.2 (4)	C1E—Cl3E—Cl4E— C1E'	-57.2 (9)
Ir1—C1C—C8C— C7C	-12.2 (4)	Cl1E—Cl3E—Cl4E— C1E	-60.7 (10)

C6C—C7C—C8C— C1C	34.0 (5)	C1E'—Cl3E—Cl4E— C1E	57.2 (9)
C41D—B1D— C11D—C12D	-97.2 (3)	Cl1E—Cl3E—Cl4E— Cl4E ⁱ	114 (3)
C31D—B1D— C11D—C12D	25.0 (4)	C1E'—Cl3E—Cl4E— Cl4E ⁱ	-128 (3)
C21D—B1D— C11D—C12D	144.1 (3)	C1E—Cl3E—Cl4E— Cl4E ⁱ	175 (3)
C41D—B1D— C11D—C16D	79.9 (4)	Cl2E—C1E'—Cl4E— Cl1E	116.3 (17)
C31D—B1D— C11D—C16D	-157.9 (3)	Cl3E—C1E'—Cl4E— Cl1E	-24.8 (5)
C21D—B1D— C11D—C16D	-38.8 (4)	C1E—C1E'—Cl4E— Cl1E	68.3 (10)
C16D—C11D— C12D—C13D	2.2 (5)	Cl2'—C1E'—Cl4E— Cl1E	82.9 (13)
B1D—C11D— C12D—C13D	179.4 (3)	Cl2E—C1E'—Cl4E— Cl3E	141.1 (17)
C11D—C12D— C13D—C14D	-1.5 (6)	C1E—C1E'—Cl4E— Cl3E	93.2 (11)
C12D—C13D— C14D—C15D	-0.4 (6)	Cl2'—C1E'—Cl4E— Cl3E	107.8 (13)
C13D—C14D— C15D—C16D	1.5 (7)	Cl1E—C1E'—Cl4E— Cl3E	24.8 (5)
C14D—C15D— C16D—C11D	-0.8 (7)	Cl2E—C1E'—Cl4E— C1E	48.0 (15)
C12D—C11D— C16D—C15D	-1.0 (6)	Cl3E—C1E'—Cl4E— C1E	-93.2 (11)
B1D—C11D—	-178.4 (4)	Cl2'—C1E'—Cl4E—	14.6 (9)

C16D—C15D		C1E	
C41D—B1D— C21D—C26D	154.1 (3)	C11E—C1E'—C14E— C1E	-68.3 (10)
C31D—B1D— C21D—C26D	33.4 (4)	C12E—C1E'—C14E— C14E ⁱ	-91 (3)
C11D—B1D— C21D—C26D	-87.0 (3)	C13E—C1E'—C14E— C14E ⁱ	128 (3)
C41D—B1D— C21D—C22D	-32.7 (4)	C1E—C1E'—C14E— C14E ⁱ	-139 (2)
C31D—B1D— C21D—C22D	-153.5 (3)	C12'—C1E'—C14E— C14E ⁱ	-124 (2)
C11D—B1D— C21D—C22D	86.1 (3)	C11E—C1E'—C14E— C14E ⁱ	153 (3)
C26D—C21D— C22D—C23D	2.3 (5)	C12'—C1E—C14E— C11E	-117.4 (14)
B1D—C21D— C22D—C23D	-171.4 (3)	C1E'—C1E—C14E— C11E	-94.9 (13)
C21D—C22D— C23D—C24D	-1.3 (5)	C12E—C1E—C14E— C11E	-122.6 (10)
C22D—C23D— C24D—C25D	-0.7 (5)	C13E—C1E—C14E— C11E	-26.4 (5)
C23D—C24D— C25D—C26D	1.7 (5)	C12'—C1E—C14E— C13E	-91.0 (15)
C24D—C25D— C26D—C21D	-0.6 (5)	C1E'—C1E—C14E— C13E	-68.5 (12)
C22D—C21D— C26D—C25D	-1.3 (5)	C12E—C1E—C14E— C13E	-96.2 (10)
B1D—C21D— C26D—C25D	172.2 (3)	C11E—C1E—C14E— C13E	26.4 (5)

C41D—B1D— C31D—C36D	-20.3 (4)	Cl2'—C1E—Cl4E— C1E'	-22.6 (14)
C11D—B1D— C31D—C36D	-142.2 (3)	Cl2E—C1E—Cl4E— C1E'	-27.7 (10)
C21D—B1D— C31D—C36D	99.9 (3)	Cl1E—C1E—Cl4E— C1E'	94.9 (13)
C41D—B1D— C31D—C32D	162.6 (3)	Cl3E—C1E—Cl4E— C1E'	68.5 (12)
C11D—B1D— C31D—C32D	40.8 (4)	Cl2'—C1E—Cl4E— Cl4E ⁱ	96 (3)
C21D—B1D— C31D—C32D	-77.2 (3)	C1E'—C1E—Cl4E— Cl4E ⁱ	118 (3)
C36D—C31D— C32D—C33D	0.5 (5)	Cl2E—C1E—Cl4E— Cl4E ⁱ	91 (3)
B1D—C31D— C32D—C33D	177.9 (3)	Cl1E—C1E—Cl4E— Cl4E ⁱ	-147 (3)
C31D—C32D— C33D—C34D	-0.4 (5)	Cl3E—C1E—Cl4E— Cl4E ⁱ	-173 (4)

Symmetry code(s): (i) $-x+1, -y+1, -z+1$.

Rh(NCN^{Et})(COD)]BPh₄ (2.9)**Table 1. Experimental details**

Crystal data	
Chemical formula	C ₄₅ H ₄₈ BN ₆ Rh
<i>M</i> _r	786.61
Crystal system, space group	Monoclinic, <i>P</i> 2 ₁
Temperature (K)	180
<i>a</i> , <i>b</i> , <i>c</i> (Å)	11.6656 (3), 11.3435 (3), 14.6475 (4)
<i>b</i> (°)	97.391 (1)
<i>V</i> (Å ³)	1922.18 (9)
<i>Z</i>	2
Radiation type	Mo <i>K</i> α
<i>m</i> (mm ⁻¹)	0.49
Crystal size (mm)	0.36 × 0.17 × 0.09
Data collection	
Diffractometer	Bruker kappa APEXII CCD Diffractometer

Absorption correction	Multi-scan <i>SADABS</i> (Bruker, 2001)
T_{\min}, T_{\max}	0.846, 0.960
No. of measured, independent and observed [$I > 2s(I)$] reflections	14078, 6146, 5963
R_{int}	0.026
$(\sin \theta / \lambda)_{\text{max}}$ (\AA^{-1})	0.595
Refinement	
$R[F^2 > 2s(F^2)], wR(F^2), S$	0.021, 0.055, 1.04
No. of reflections	6146
No. of parameters	478
No. of restraints	1
H-atom treatment	H-atom parameters constrained
$D\rho_{\text{max}}, D\rho_{\text{min}}$ (e \AA^{-3})	0.33, -0.22
Absolute structure	Flack H D (1983), <i>Acta Cryst.</i> A39, 876-881
Flack parameter	-0.017 (16)

Computer programs: *APEX2* (Bruker, 2007), *SHELXS-97* (Sheldrick, 2008), *SHELXL-97* (Sheldrick, 2008), *SHELXTL-Plus* (Sheldrick, 2008).

Table 2. Selected geometric parameters (\AA , $^\circ$)

Rh1—C2	2.037 (2)	C6C—C7C	1.526 (4)
Rh1—N2A	2.089 (2)	C6C—H6C	0.9500
Rh1—C1C	2.122 (2)	C7C—C8C	1.530 (4)
Rh1—C2C	2.159 (2)	C7C—H7C1	0.9900

Rh1—C5C	2.179 (2)	C7C—H7C2	0.9900
Rh1—C6C	2.213 (3)	C8C—H8C1	0.9900
N1—C2	1.361 (3)	C8C—H8C2	0.9900
N1—C5	1.388 (3)	B1—C21D	1.643 (4)
N1—C7B	1.456 (4)	B1—C31D	1.655 (4)
C2—N3	1.350 (3)	B1—C41D	1.658 (3)
N3—C4	1.390 (3)	B1—C11D	1.667 (3)
N3—C7A	1.460 (4)	C11D—C12D	1.395 (4)
C4—C5	1.326 (4)	C11D—C16D	1.397 (4)
C4—H4	0.9500	C12D—C13D	1.391 (4)
C5—H5	0.9500	C12D—H12D	0.9500
N1A—C5A	1.343 (3)	C13D—C14D	1.371 (4)
N1A—N2A	1.352 (3)	C13D—H13D	0.9500
N1A—C6A	1.466 (3)	C14D—C15D	1.376 (4)
N2A—C3A	1.341 (3)	C14D—H14D	0.9500
C3A—C4A	1.377 (4)	C15D—C16D	1.389 (4)
C3A—H3A	0.9500	C15D—H15D	0.9500
C4A—C5A	1.370 (4)	C16D—H16D	0.9500
C4A—H4A	0.9500	C21D—C22D	1.392 (4)
C5A—H5A	0.9500	C21D—C26D	1.413 (4)
C6A—C7A	1.502 (4)	C22D—C23D	1.387 (4)
C6A—H6A1	0.9900	C22D—H22D	0.9500
C6A—H6A2	0.9900	C23D—C24D	1.383 (4)
C7A—H7A1	0.9900	C23D—H23D	0.9500
C7A—H7A2	0.9900	C24D—C25D	1.381 (4)
N1B—C5B	1.333 (4)	C24D—H24D	0.9500

N1B—N2B	1.347 (3)	C25D—C26D	1.382 (4)
N1B—C6B	1.458 (4)	C25D—H25D	0.9500
N2B—C3B	1.340 (5)	C26D—H26D	0.9500
C3B—C4B	1.377 (5)	C31D—C32D	1.399 (4)
C3B—H3B	0.9500	C31D—C36D	1.411 (4)
C4B—C5B	1.366 (4)	C32D—C33D	1.382 (4)
C4B—H4B	0.9500	C32D—H32D	0.9500
C5B—H5B	0.9500	C33D—C34D	1.370 (5)
C6B—C7B	1.519 (4)	C33D—H33D	0.9500
C6B—H6B1	0.9900	C34D—C35D	1.376 (4)
C6B—H6B2	0.9900	C34D—H34D	0.9500
C7B—H7B1	0.9900	C35D—C36D	1.383 (4)
C7B—H7B2	0.9900	C35D—H35D	0.9500
C1C—C2C	1.389 (4)	C36D—H36D	0.9500
C1C—C8C	1.501 (4)	C41D—C46D	1.393 (4)
C1C—H1C	0.9500	C41D—C42D	1.392 (4)
C2C—C3C	1.519 (3)	C42D—C43D	1.396 (4)
C2C—H2C	0.9500	C42D—H42D	0.9500
C3C—C4C	1.521 (4)	C43D—C44D	1.379 (5)
C3C—H3C1	0.9900	C43D—H43D	0.9500
C3C—H3C2	0.9900	C44D—C45D	1.368 (4)
C4C—C5C	1.516 (4)	C44D—H44D	0.9500
C4C—H4C1	0.9900	C45D—C46D	1.390 (4)
C4C—H4C2	0.9900	C45D—H45D	0.9500
C5C—C6C	1.358 (4)	C46D—H46D	0.9500
C5C—H5C	0.9500		

C2—Rh1—N2A	85.37 (8)	C3C—C4C— H4C2	108.8
C2—Rh1—C1C	94.44 (9)	H4C1—C4C— H4C2	107.7
N2A—Rh1—C1C	147.90 (9)	C6C—C5C—C4C	126.0 (3)
C2—Rh1—C2C	95.82 (9)	C6C—C5C—Rh1	73.38 (15)
N2A—Rh1—C2C	174.11 (8)	C4C—C5C—Rh1	108.06 (17)
C1C—Rh1—C2C	37.86 (9)	C6C—C5C—H5C	117.0
C2—Rh1—C5C	157.65 (10)	C4C—C5C—H5C	117.0
N2A—Rh1—C5C	94.76 (9)	Rh1—C5C—H5C	88.5
C1C—Rh1—C5C	97.08 (9)	C5C—C6C—C7C	123.8 (3)
C2C—Rh1—C5C	81.94 (9)	C5C—C6C—Rh1	70.62 (15)
C2—Rh1—C6C	166.05 (10)	C7C—C6C—Rh1	110.75 (19)
N2A—Rh1—C6C	90.68 (9)	C5C—C6C—H6C	118.1
C1C—Rh1—C6C	81.84 (10)	C7C—C6C—H6C	118.1
C2C—Rh1—C6C	89.48 (10)	Rh1—C6C—H6C	88.6
C5C—Rh1—C6C	36.00 (11)	C6C—C7C—C8C	111.0 (3)
C2—N1—C5	111.0 (2)	C6C—C7C— H7C1	109.4
C2—N1—C7B	124.9 (2)	C8C—C7C— H7C1	109.4
C5—N1—C7B	122.8 (2)	C6C—C7C— H7C2	109.4
N3—C2—N1	104.0 (2)	C8C—C7C— H7C2	109.4
N3—C2—Rh1	128.20 (18)	H7C1—C7C—	108.0

		H7C2	
N1—C2—Rh1	127.43 (18)	C1C—C8C—C7C	114.6 (2)
C2—N3—C4	111.1 (2)	C1C—C8C— H8C1	108.6
C2—N3—C7A	127.2 (2)	C7C—C8C— H8C1	108.6
C4—N3—C7A	121.6 (2)	C1C—C8C— H8C2	108.6
C5—C4—N3	107.1 (2)	C7C—C8C— H8C2	108.6
C5—C4—H4	126.5	H8C1—C8C— H8C2	107.6
N3—C4—H4	126.5	C21D—B1— C31D	110.34 (18)
C4—C5—N1	106.8 (2)	C21D—B1— C41D	109.2 (2)
C4—C5—H5	126.6	C31D—B1— C41D	109.4 (2)
N1—C5—H5	126.6	C21D—B1— C11D	109.4 (2)
C5A—N1A—N2A	110.8 (2)	C31D—B1— C11D	111.3 (2)
C5A—N1A—C6A	130.4 (2)	C41D—B1— C11D	107.18 (17)
N2A—N1A—C6A	118.5 (2)	C12D—C11D— C16D	113.9 (2)
C3A—N2A—N1A	105.6 (2)	C12D—C11D— B1	123.3 (3)
C3A—N2A—Rh1	135.83 (18)	C16D—C11D—	122.7 (2)

		B1	
N1A—N2A—Rh1	117.44 (15)	C13D—C12D— C11D	123.1 (2)
N2A—C3A—C4A	110.5 (2)	C13D—C12D— H12D	118.4
N2A—C3A—H3A	124.8	C11D—C12D— H12D	118.4
C4A—C3A—H3A	124.8	C14D—C13D— C12D	120.6 (2)
C5A—C4A—C3A	105.7 (2)	C14D—C13D— H13D	119.7
C5A—C4A—H4A	127.2	C12D—C13D— H13D	119.7
C3A—C4A—H4A	127.2	C13D—C14D— C15D	118.6 (2)
N1A—C5A—C4A	107.4 (2)	C13D—C14D— H14D	120.7
N1A—C5A—H5A	126.3	C15D—C14D— H14D	120.7
C4A—C5A—H5A	126.3	C14D—C15D— C16D	119.9 (2)
N1A—C6A—C7A	115.6 (2)	C14D—C15D— H15D	120.0
N1A—C6A— H6A1	108.4	C16D—C15D— H15D	120.0
C7A—C6A— H6A1	108.4	C15D—C16D— C11D	123.7 (2)
N1A—C6A— H6A2	108.4	C15D—C16D— H16D	118.1

C7A—C6A— H6A2	108.4	C11D—C16D— H16D	118.1
H6A1—C6A— H6A2	107.4	C22D—C21D— C26D	114.5 (2)
N3—C7A—C6A	114.8 (2)	C22D—C21D— B1	124.0 (2)
N3—C7A—H7A1	108.6	C26D—C21D— B1	121.5 (2)
C6A—C7A— H7A1	108.6	C23D—C22D— C21D	123.4 (2)
N3—C7A—H7A2	108.6	C23D—C22D— H22D	118.3
C6A—C7A— H7A2	108.6	C21D—C22D— H22D	118.3
H7A1—C7A— H7A2	107.5	C24D—C23D— C22D	120.1 (3)
C5B—N1B—N2B	112.4 (3)	C24D—C23D— H23D	120.0
C5B—N1B—C6B	127.2 (3)	C22D—C23D— H23D	120.0
N2B—N1B—C6B	119.8 (3)	C25D—C24D— C23D	118.7 (2)
C3B—N2B—N1B	102.8 (3)	C25D—C24D— H24D	120.6
N2B—C3B—C4B	113.3 (3)	C23D—C24D— H24D	120.6
N2B—C3B—H3B	123.4	C24D—C25D— C26D	120.4 (2)
C4B—C3B—H3B	123.4	C24D—C25D—	119.8

		H25D	
C5B—C4B—C3B	103.6 (3)	C26D—C25D— H25D	119.8
C5B—C4B—H4B	128.2	C25D—C26D— C21D	122.9 (2)
C3B—C4B—H4B	128.2	C25D—C26D— H26D	118.6
N1B—C5B—C4B	107.9 (3)	C21D—C26D— H26D	118.6
N1B—C5B—H5B	126.0	C32D—C31D— C36D	113.2 (2)
C4B—C5B—H5B	126.0	C32D—C31D— B1	123.6 (2)
N1B—C6B—C7B	111.9 (2)	C36D—C31D— B1	123.1 (2)
N1B—C6B— H6B1	109.2	C33D—C32D— C31D	123.5 (3)
C7B—C6B— H6B1	109.2	C33D—C32D— H32D	118.2
N1B—C6B— H6B2	109.2	C31D—C32D— H32D	118.2
C7B—C6B— H6B2	109.2	C34D—C33D— C32D	120.9 (3)
H6B1—C6B— H6B2	107.9	C34D—C33D— H33D	119.6
N1—C7B—C6B	111.2 (2)	C32D—C33D— H33D	119.6
N1—C7B—H7B1	109.4	C33D—C34D— C35D	118.4 (3)

C6B—C7B— H7B1	109.4	C33D—C34D— H34D	120.8
N1—C7B—H7B2	109.4	C35D—C34D— H34D	120.8
C6B—C7B— H7B2	109.4	C34D—C35D— C36D	120.2 (3)
H7B1—C7B— H7B2	108.0	C34D—C35D— H35D	119.9
C2C—C1C—C8C	127.0 (2)	C36D—C35D— H35D	119.9
C2C—C1C—Rh1	72.52 (13)	C35D—C36D— C31D	123.7 (3)
C8C—C1C—Rh1	108.35 (17)	C35D—C36D— H36D	118.1
C2C—C1C—H1C	116.5	C31D—C36D— H36D	118.1
C8C—C1C—H1C	116.5	C46D—C41D— C42D	115.2 (2)
Rh1—C1C—H1C	89.1	C46D—C41D— B1	119.6 (2)
C1C—C2C—C3C	124.0 (2)	C42D—C41D— B1	125.1 (2)
C1C—C2C—Rh1	69.62 (14)	C41D—C42D— C43D	122.7 (3)
C3C—C2C—Rh1	111.97 (15)	C41D—C42D— H42D	118.7
C1C—C2C—H2C	118.0	C43D—C42D— H42D	118.7
C3C—C2C—H2C	118.0	C44D—C43D—	120.1 (3)

		C42D	
Rh1—C2C—H2C	88.4	C44D—C43D— H43D	120.0
C2C—C3C—C4C	113.6 (2)	C42D—C43D— H43D	120.0
C2C—C3C— H3C1	108.8	C45D—C44D— C43D	118.8 (3)
C4C—C3C— H3C1	108.8	C45D—C44D— H44D	120.6
C2C—C3C— H3C2	108.8	C43D—C44D— H44D	120.6
C4C—C3C— H3C2	108.8	C44D—C45D— C46D	120.6 (3)
H3C1—C3C— H3C2	107.7	C44D—C45D— H45D	119.7
C5C—C4C—C3C	113.7 (2)	C46D—C45D— H45D	119.7
C5C—C4C— H4C1	108.8	C45D—C46D— C41D	122.7 (3)
C3C—C4C— H4C1	108.8	C45D—C46D— H46D	118.7
C5C—C4C— H4C2	108.8	C41D—C46D— H46D	118.7
C5—N1—C2—N3	-0.2 (3)	C3C—C4C— C5C—C6C	-46.3 (4)
C7B—N1—C2— N3	-167.7 (2)	C3C—C4C— C5C—Rh1	35.9 (3)
C5—N1—C2—	172.88 (17)	C2—Rh1—C5C—	-174.0 (2)

Rh1		C6C	
C7B—N1—C2— Rh1	5.4 (4)	N2A—Rh1— C5C—C6C	-84.58 (17)
N2A—Rh1—C2— N3	60.3 (2)	C1C—Rh1— C5C—C6C	65.53 (18)
C1C—Rh1—C2— N3	-87.5 (2)	C2C—Rh1— C5C—C6C	100.33 (17)
C2C—Rh1—C2— N3	-125.5 (2)	C2—Rh1—C5C— C4C	62.8 (3)
C5C—Rh1—C2— N3	151.6 (2)	N2A—Rh1— C5C—C4C	152.22 (18)
C6C—Rh1—C2— N3	-13.6 (5)	C1C—Rh1— C5C—C4C	-57.7 (2)
N2A—Rh1—C2— N1	-111.1 (2)	C2C—Rh1— C5C—C4C	-22.87 (18)
C1C—Rh1—C2— N1	101.1 (2)	C6C—Rh1— C5C—C4C	-123.2 (3)
C2C—Rh1—C2— N1	63.1 (2)	C4C—C5C— C6C—C7C	-2.0 (4)
C5C—Rh1—C2— N1	-19.8 (4)	Rh1—C5C— C6C—C7C	-102.5 (3)
C6C—Rh1—C2— N1	175.0 (3)	C4C—C5C— C6C—Rh1	100.5 (3)
N1—C2—N3—C4	-0.5 (3)	C2—Rh1—C6C— C5C	170.5 (4)
Rh1—C2—N3— C4	-173.52 (17)	N2A—Rh1— C6C—C5C	97.18 (17)
N1—C2—N3— C7A	177.2 (2)	C1C—Rh1— C6C—C5C	-114.15 (18)

Rh1—C2—N3—C7A	4.2 (4)	C2C—Rh1—C6C—C5C	-76.93 (17)
C2—N3—C4—C5	1.1 (3)	C2—Rh1—C6C—C7C	-69.7 (5)
C7A—N3—C4—C5	-176.8 (2)	N2A—Rh1—C6C—C7C	-143.0 (2)
N3—C4—C5—N1	-1.1 (3)	C1C—Rh1—C6C—C7C	5.7 (2)
C2—N1—C5—C4	0.8 (3)	C2C—Rh1—C6C—C7C	42.9 (2)
C7B—N1—C5—C4	168.7 (2)	C5C—Rh1—C6C—C7C	119.8 (3)
C5A—N1A—N2A—C3A	-0.4 (3)	C5C—C6C—C7C—C8C	94.1 (3)
C6A—N1A—N2A—C3A	173.5 (2)	Rh1—C6C—C7C—C8C	14.1 (3)
C5A—N1A—N2A—Rh1	169.58 (18)	C2C—C1C—C8C—C7C	-40.7 (4)
C6A—N1A—N2A—Rh1	-16.6 (3)	Rh1—C1C—C8C—C7C	40.9 (3)
C2—Rh1—N2A—C3A	109.9 (2)	C6C—C7C—C8C—C1C	-36.8 (4)
C1C—Rh1—N2A—C3A	-159.2 (2)	C21D—B1—C11D—C12D	13.1 (3)
C2C—Rh1—N2A—C3A	8.0 (9)	C31D—B1—C11D—C12D	135.2 (3)
C5C—Rh1—N2A—C3A	-47.7 (2)	C41D—B1—C11D—C12D	-105.2 (3)
C6C—Rh1—	-83.5 (2)	C21D—B1—	-170.6 (2)

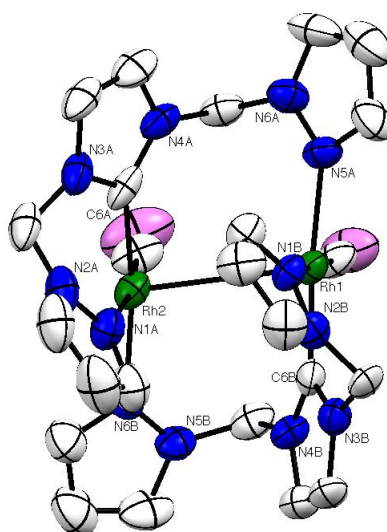
N2A—C3A		C11D—C16D	
C2—Rh1—N2A— N1A	-56.17 (17)	C31D—B1— C11D—C16D	-48.4 (3)
C1C—Rh1— N2A—N1A	34.8 (3)	C41D—B1— C11D—C16D	71.2 (3)
C2C—Rh1— N2A—N1A	-158.1 (7)	C16D—C11D— C12D—C13D	1.7 (4)
C5C—Rh1— N2A—N1A	146.26 (17)	B1—C11D— C12D—C13D	178.4 (2)
C6C—Rh1— N2A—N1A	110.44 (18)	C11D—C12D— C13D—C14D	-0.3 (4)
N1A—N2A— C3A—C4A	0.4 (3)	C12D—C13D— C14D—C15D	-0.8 (4)
Rh1—N2A— C3A—C4A	-166.72 (19)	C13D—C14D— C15D—C16D	0.3 (4)
N2A—C3A— C4A—C5A	-0.3 (3)	C14D—C15D— C16D—C11D	1.3 (4)
N2A—N1A— C5A—C4A	0.2 (3)	C12D—C11D— C16D—C15D	-2.2 (4)
C6A—N1A— C5A—C4A	-172.7 (3)	B1—C11D— C16D—C15D	-178.9 (2)
C3A—C4A— C5A—N1A	0.1 (3)	C31D—B1— C21D—C22D	114.9 (3)
C5A—N1A— C6A—C7A	-92.6 (4)	C41D—B1— C21D—C22D	-5.3 (3)
N2A—N1A— C6A—C7A	94.9 (3)	C11D—B1— C21D—C22D	-122.4 (3)
C2—N3—C7A— C6A	-30.8 (4)	C31D—B1— C21D—C26D	-67.0 (3)

C4—N3—C7A— C6A	146.7 (3)	C41D—B1— C21D—C26D	172.7 (2)
N1A—C6A— C7A—N3	-42.4 (4)	C11D—B1— C21D—C26D	55.7 (3)
C5B—N1B— N2B—C3B	-1.2 (3)	C26D—C21D— C22D—C23D	0.5 (4)
C6B—N1B— N2B—C3B	-173.6 (2)	B1—C21D— C22D—C23D	178.7 (3)
N1B—N2B— C3B—C4B	1.2 (3)	C21D—C22D— C23D—C24D	-0.7 (4)
N2B—C3B— C4B—C5B	-0.8 (4)	C22D—C23D— C24D—C25D	0.4 (4)
N2B—N1B— C5B—C4B	0.8 (3)	C23D—C24D— C25D—C26D	0.1 (4)
C6B—N1B— C5B—C4B	172.5 (3)	C24D—C25D— C26D—C21D	-0.4 (4)
C3B—C4B— C5B—N1B	0.0 (3)	C22D—C21D— C26D—C25D	0.1 (4)
C5B—N1B— C6B—C7B	-97.4 (3)	B1—C21D— C26D—C25D	-178.2 (2)
N2B—N1B— C6B—C7B	73.7 (3)	C21D—B1— C31D—C32D	1.0 (4)
C2—N1—C7B— C6B	76.3 (3)	C41D—B1— C31D—C32D	121.1 (3)
C5—N1—C7B— C6B	-89.8 (3)	C11D—B1— C31D—C32D	-120.6 (3)
N1B—C6B— C7B—N1	52.2 (3)	C21D—B1— C31D—C36D	-174.8 (2)
C2—Rh1—C1C—	-93.77 (15)	C41D—B1—	-54.6 (3)

C2C		C31D—C36D	
N2A—Rh1— C1C—C2C	177.86 (14)	C11D—B1— C31D—C36D	63.6 (3)
C5C—Rh1— C1C—C2C	67.04 (15)	C36D—C31D— C32D—C33D	-0.2 (4)
C6C—Rh1— C1C—C2C	99.75 (15)	B1—C31D— C32D—C33D	-176.3 (3)
C2—Rh1—C1C— C8C	142.17 (18)	C31D—C32D— C33D—C34D	-2.7 (5)
N2A—Rh1— C1C—C8C	53.8 (3)	C32D—C33D— C34D—C35D	2.9 (5)
C2C—Rh1— C1C—C8C	-124.1 (2)	C33D—C34D— C35D—C36D	-0.4 (4)
C5C—Rh1— C1C—C8C	-57.01 (19)	C34D—C35D— C36D—C31D	-2.6 (5)
C6C—Rh1— C1C—C8C	-24.30 (18)	C32D—C31D— C36D—C35D	2.8 (4)
C8C—C1C— C2C—C3C	-3.2 (4)	B1—C31D— C36D—C35D	178.9 (3)
Rh1—C1C— C2C—C3C	-103.4 (2)	C21D—B1— C41D—C46D	-69.2 (3)
C8C—C1C— C2C—Rh1	100.1 (2)	C31D—B1— C41D—C46D	170.0 (2)
C2—Rh1—C2C— C1C	89.75 (15)	C11D—B1— C41D—C46D	49.2 (3)
N2A—Rh1— C2C—C1C	-168.9 (7)	C21D—B1— C41D—C42D	106.1 (3)
C5C—Rh1— C2C—C1C	-112.65 (16)	C31D—B1— C41D—C42D	-14.8 (3)

C6C—Rh1— C2C—C1C	-77.32 (15)	C11D—B1— C41D—C42D	-135.6 (3)
C2—Rh1—C2C— C3C	-150.70 (18)	C46D—C41D— C42D—C43D	-0.5 (4)
N2A—Rh1— C2C—C3C	-49.3 (9)	B1—C41D— C42D—C43D	-175.9 (2)
C1C—Rh1— C2C—C3C	119.6 (2)	C41D—C42D— C43D—C44D	1.1 (4)
C5C—Rh1— C2C—C3C	6.90 (18)	C42D—C43D— C44D—C45D	-0.2 (4)
C6C—Rh1— C2C—C3C	42.23 (19)	C43D—C44D— C45D—C46D	-1.2 (4)
C1C—C2C— C3C—C4C	90.5 (3)	C44D—C45D— C46D—C41D	1.9 (4)
Rh1—C2C— C3C—C4C	10.9 (3)	C42D—C41D— C46D—C45D	-1.0 (4)
C2C—C3C— C4C—C5C	-31.8 (3)	B1—C41D— C46D—C45D	174.7 (2)



**Table 1. Experimental details**

Crystal data	
Chemical formula	$\text{C}_{72}\text{H}_{64}\text{B}_2\text{N}_{12}\text{O}_2\text{Rh}_2$
M_r	707.44
Crystal system, space group	Monoclinic, $P2_1/n$
Temperature (K)	150
a, b, c (Å)	12.6272 (4), 26.3368 (8), 22.9366 (7)
β (°)	91.129 (1)
V (Å ³)	7626.3 (4)
Z	8
Radiation type	Mo $K\alpha$
μ (mm ⁻¹)	0.48
Crystal size (mm)	$0.13 \times 0.09 \times 0.07$
Data collection	
Diffractometer	Bruker kappa APEXII CCD Diffractometer

Absorption correction	Multi-scan <i>SADABS</i> (Bruker, 2001)
T_{\min}, T_{\max}	0.939, 0.968
No. of measured, independent and observed [$I > 2s(I)$] reflections	80179, 13379, 6866
R_{int}	0.115
$(\sin \theta/\lambda)_{\text{max}}$ (\AA^{-1})	0.595
Refinement	
$R[F^2 > 2s(F^2)], wR(F^2), S$	0.065, 0.194, 1.03
No. of reflections	13379
No. of parameters	884
No. of restraints	39
H-atom treatment	H-atom parameters constrained
$D\rho_{\text{max}}, D\rho_{\text{min}}$ (e \AA^{-3})	0.75, -0.46

Computer programs: *APEX2* (Bruker, 2007), *SHELXS-97* (Sheldrick, 2008), *SHELXL-97* (Sheldrick, 2008), *SHELXTL-Plus* (Sheldrick, 2008).

Table 2. Selected geometric parameters (\AA , $^\circ$)

Rh1—C1E	1.783 (8)	C31C—C32C	1.377 (10)
Rh1—C6B	1.975 (7)	C31C—C36C	1.411 (10)
Rh1—N1B	2.074 (5)	C32C—C33C	1.380 (12)
Rh1—N5A	2.098 (6)	C32C—H32C	0.9500
O1E—C1E	1.150 (8)	C33C—C34C	1.381 (13)
Rh2—C2E	1.808 (9)	C33C—H33C	0.9500
Rh2—C6A	1.992 (7)	C34C—C35C	1.377 (12)

Rh2—N1A	2.100 (6)	C34C—H34C	0.9500
Rh2—N6B	2.103 (6)	C35C—C36C	1.370 (11)
O2E—C2E	1.135 (9)	C35C—H35C	0.9500
N1A—C5A	1.317 (9)	C36C—H36C	0.9500
N1A—N2A	1.352 (8)	C41C—C42C	1.399 (9)
N2A—C3A	1.307 (10)	C41C—C46C	1.399 (9)
N2A—C1M	1.436 (10)	C42C—C43C	1.397 (10)
N3A—C6A	1.350 (8)	C42C—H42C	0.9500
N3A—C7A	1.405 (9)	C43C—C44C	1.383 (11)
N3A—C1M	1.431 (9)	C43C—H43C	0.9500
N4A—C6A	1.370 (9)	C44C—C45C	1.339 (10)
N4A—C8A	1.383 (8)	C44C—H44C	0.9500
N4A—C2M	1.430 (9)	C45C—C46C	1.422 (10)
N5A—C11A	1.331 (9)	C45C—H45C	0.9500
N5A—N6A	1.366 (7)	C46C—H46C	0.9500
N6A—C9A	1.344 (9)	B1D—C21D	1.640 (11)
N6A—C2M	1.435 (9)	B1D—C41D	1.650 (10)
C3A—C4A	1.339 (12)	B1D—C31D	1.650 (11)
C3A—H3A	0.9500	B1D—C11D	1.670 (10)
C4A—C5A	1.390 (11)	C11D—C16D	1.397 (10)
C4A—H4A	0.9500	C11D—C12D	1.426 (10)
C5A—H5A	0.9500	C12D—C13D	1.373 (11)
C7A—C8A	1.320 (11)	C12D—H12D	0.9500
C7A—H7A	0.9500	C13D—C14D	1.374 (12)
C8A—H8A	0.9500	C13D—H13D	0.9500
C9A—C10A	1.338 (12)	C14D—C15D	1.354 (12)

C9A—H9A	0.9500	C14D—H14D	0.9500
C10A—C11A	1.367 (12)	C15D—C16D	1.386 (10)
C10A—H10A	0.9500	C15D—H15D	0.9500
C11A—H11A	0.9500	C16D—H16D	0.9500
N1B—C5B	1.320 (8)	C21D—C22D	1.396 (9)
N1B—N2B	1.363 (7)	C21D—C26D	1.400 (9)
N2B—C3B	1.345 (9)	C22D—C23D	1.397 (10)
N2B—C1N	1.443 (8)	C22D—H22D	0.9500
N3B—C6B	1.368 (8)	C23D—C24D	1.370 (10)
N3B—C7B	1.389 (9)	C23D—H23D	0.9500
N3B—C1N	1.448 (8)	C24D—C25D	1.362 (10)
N4B—C6B	1.363 (8)	C24D—H24D	0.9500
N4B—C8B	1.401 (9)	C25D—C26D	1.377 (9)
N4B—C2N	1.442 (8)	C25D—H25D	0.9500
N5B—N6B	1.339 (7)	C26D—H26D	0.9500
N5B—C11B	1.347 (9)	C31D—C36D	1.382 (10)
N5B—C2N	1.440 (9)	C31D—C32D	1.387 (10)
N6B—C9B	1.288 (9)	C32D—C33D	1.349 (11)
C3B—C4B	1.361 (11)	C32D—H32D	0.9500
C3B—H3B	0.9500	C33D—C34D	1.371 (14)
C4B—C5B	1.392 (10)	C33D—H33D	0.9500
C4B—H4B	0.9500	C34D—C35D	1.383 (14)
C5B—H5B	0.9500	C34D—H34D	0.9500
C7B—C8B	1.334 (10)	C35D—C36D	1.416 (11)
C7B—H7B	0.9500	C35D—H35D	0.9500
C8B—H8B	0.9500	C36D—H36D	0.9500

C9B—C10B	1.397 (11)	C41D—C46D	1.382 (9)
C9B—H9B	0.9500	C41D—C42D	1.383 (10)
C10B—C11B	1.350 (11)	C42D—C43D	1.401 (10)
C10B—H10B	0.9500	C42D—H42D	0.9500
C11B—H11B	0.9500	C43D—C44D	1.370 (11)
C1M—H1M1	0.9900	C43D—H43D	0.9500
C1M—H1M2	0.9900	C44D—C45D	1.374 (12)
C2M—H2M1	0.9900	C44D—H44D	0.9500
C2M—H2M2	0.9900	C45D—C46D	1.362 (10)
C1N—H1N1	0.9900	C45D—H45D	0.9500
C1N—H1N2	0.9900	C46D—H46D	0.9500
C2N—H2N1	0.9900	C1F—C2F	1.473 (9)
C2N—H2N2	0.9900	C1F—H1F1	0.9800
B1C—C31C	1.627 (11)	C1F—H1F2	0.9800
B1C—C21C	1.641 (10)	C1F—H1F3	0.9800
B1C—C41C	1.647 (10)	C2F—O1F	1.195 (9)
B1C—C11C	1.653 (10)	C2F—C3F	1.477 (9)
C11C—C16C	1.387 (10)	C3F—H3F1	0.9800
C11C—C12C	1.404 (10)	C3F—H3F2	0.9800
C12C—C13C	1.358 (10)	C3F—H3F3	0.9800
C12C—H12C	0.9500	C1G—C2G	1.475 (10)
C13C—C14C	1.345 (12)	C1G—H1G1	0.9800
C13C—H13C	0.9500	C1G—H1G2	0.9800
C14C—C15C	1.357 (12)	C1G—H1G3	0.9800
C14C—H14C	0.9500	C2G—O1G	1.189 (9)
C15C—C16C	1.411 (11)	C2G—C3G	1.479 (10)

C15C—H15C	0.9500	C3G—H3G1	0.9800
C16C—H16C	0.9500	C3G—H3G2	0.9800
C21C—C26C	1.384 (9)	C3G—H3G3	0.9800
C21C—C22C	1.413 (10)	C2H—O1H	1.189 (9)
C22C—C23C	1.399 (11)	C2H—C3H	1.476 (10)
C22C—H22C	0.9500	C2H—C1H	1.486 (10)
C23C—C24C	1.356 (12)	C3H—H3H1	0.9800
C23C—H23C	0.9500	C3H—H3H2	0.9800
C24C—C25C	1.338 (11)	C3H—H3H3	0.9800
C24C—H24C	0.9500	C1H—H1H1	0.9800
C25C—C26C	1.404 (10)	C1H—H1H2	0.9800
C25C—H25C	0.9500	C1H—H1H3	0.9800
C26C—H26C	0.9500		
C1E—Rh1—C6B	94.4 (3)	C24C—C25C— H25C	120.0
C1E—Rh1—N1B	176.5 (3)	C26C—C25C— H25C	120.0
C6B—Rh1—N1B	87.7 (3)	C21C—C26C— C25C	124.0 (8)
C1E—Rh1—N5A	92.3 (3)	C21C—C26C— H26C	118.0
C6B—Rh1—N5A	170.5 (3)	C25C—C26C— H26C	118.0
N1B—Rh1—N5A	85.4 (2)	C32C—C31C— C36C	111.7 (8)
O1E—C1E—Rh1	176.0 (7)	C32C—C31C—	127.9 (7)

		B1C	
C2E—Rh2—C6A	91.5 (3)	C36C—C31C— B1C	120.3 (7)
C2E—Rh2—N1A	170.8 (3)	C31C—C32C— C33C	125.2 (9)
C6A—Rh2—N1A	87.3 (3)	C31C—C32C— H32C	117.4
C2E—Rh2—N6B	93.3 (3)	C33C—C32C— H32C	117.4
C6A—Rh2—N6B	171.6 (3)	C32C—C33C— C34C	119.9 (9)
N1A—Rh2—N6B	86.9 (2)	C32C—C33C— H33C	120.1
O2E—C2E—Rh2	176.4 (9)	C34C—C33C— H33C	120.1
C5A—N1A—N2A	105.2 (6)	C35C—C34C— C33C	118.4 (9)
C5A—N1A—Rh2	133.2 (5)	C35C—C34C— H34C	120.8
N2A—N1A—Rh2	121.6 (5)	C33C—C34C— H34C	120.8
C3A—N2A—N1A	111.7 (8)	C36C—C35C— C34C	119.2 (9)
C3A—N2A—C1M	130.4 (8)	C36C—C35C— H35C	120.4
N1A—N2A— C1M	117.8 (7)	C34C—C35C— H35C	120.4
C6A—N3A—C7A	110.6 (7)	C35C—C36C— C31C	125.6 (8)

C6A—N3A—C1M	123.2 (7)	C35C—C36C— H36C	117.2
C7A—N3A—C1M	126.0 (7)	C31C—C36C— H36C	117.2
C6A—N4A—C8A	110.4 (7)	C42C—C41C— C46C	115.8 (7)
C6A—N4A—C2M	125.3 (6)	C42C—C41C— B1C	119.8 (6)
C8A—N4A—C2M	123.9 (7)	C46C—C41C— B1C	124.4 (6)
C11A—N5A— N6A	104.9 (6)	C43C—C42C— C41C	121.1 (8)
C11A—N5A— Rh1	126.2 (6)	C43C—C42C— H42C	119.5
N6A—N5A—Rh1	128.7 (5)	C41C—C42C— H42C	119.5
C9A—N6A—N5A	109.6 (7)	C44C—C43C— C42C	122.9 (7)
C9A—N6A—C2M	129.1 (7)	C44C—C43C— H43C	118.6
N5A—N6A— C2M	120.0 (6)	C42C—C43C— H43C	118.6
N2A—C3A—C4A	107.6 (9)	C45C—C44C— C43C	116.3 (8)
N2A—C3A—H3A	126.2	C45C—C44C— H44C	121.8
C4A—C3A—H3A	126.2	C43C—C44C— H44C	121.8
C3A—C4A—C5A	106.1 (9)	C44C—C45C—	123.2 (8)

		C46C	
C3A—C4A—H4A	127.0	C44C—C45C— H45C	118.4
C5A—C4A—H4A	127.0	C46C—C45C— H45C	118.4
N1A—C5A—C4A	109.4 (8)	C41C—C46C— C45C	120.7 (7)
N1A—C5A—H5A	125.3	C41C—C46C— H46C	119.7
C4A—C5A—H5A	125.3	C45C—C46C— H46C	119.7
N3A—C6A—N4A	104.4 (6)	C21D—B1D— C41D	111.2 (6)
N3A—C6A—Rh2	119.6 (6)	C21D—B1D— C31D	112.9 (6)
N4A—C6A—Rh2	135.9 (5)	C41D—B1D— C31D	108.0 (6)
C8A—C7A—N3A	106.7 (7)	C21D—B1D— C11D	109.3 (6)
C8A—C7A—H7A	126.6	C41D—B1D— C11D	106.7 (5)
N3A—C7A—H7A	126.6	C31D—B1D— C11D	108.5 (6)
C7A—C8A—N4A	107.9 (8)	C16D—C11D— C12D	114.7 (7)
C7A—C8A—H8A	126.1	C16D—C11D— B1D	123.6 (7)
N4A—C8A—H8A	126.1	C12D—C11D— B1D	121.5 (7)

C10A—C9A— N6A	108.5 (8)	C13D—C12D— C11D	121.5 (8)
C10A—C9A— H9A	125.7	C13D—C12D— H12D	119.2
N6A—C9A—H9A	125.7	C11D—C12D— H12D	119.2
C9A—C10A— C11A	105.8 (9)	C12D—C13D— C14D	121.5 (9)
C9A—C10A— H10A	127.1	C12D—C13D— H13D	119.3
C11A—C10A— H10A	127.1	C14D—C13D— H13D	119.3
N5A—C11A— C10A	111.3 (9)	C15D—C14D— C13D	118.7 (9)
N5A—C11A— H11A	124.4	C15D—C14D— H14D	120.7
C10A—C11A— H11A	124.4	C13D—C14D— H14D	120.7
C5B—N1B—N2B	104.2 (6)	C14D—C15D— C16D	121.1 (9)
C5B—N1B—Rh1	133.0 (5)	C14D—C15D— H15D	119.5
N2B—N1B—Rh1	122.1 (4)	C16D—C15D— H15D	119.5
C3B—N2B—N1B	111.1 (6)	C15D—C16D— C11D	122.5 (8)
C3B—N2B—C1N	130.5 (7)	C15D—C16D— H16D	118.8
N1B—N2B—C1N	118.2 (5)	C11D—C16D—	118.8

		H16D	
C6B—N3B—C7B	112.9 (6)	C22D—C21D— C26D	113.5 (7)
C6B—N3B—C1N	122.4 (6)	C22D—C21D— B1D	121.3 (6)
C7B—N3B—C1N	124.7 (7)	C26D—C21D— B1D	125.0 (7)
C6B—N4B—C8B	111.5 (6)	C23D—C22D— C21D	123.0 (7)
C6B—N4B—C2N	125.7 (6)	C23D—C22D— H22D	118.5
C8B—N4B—C2N	122.1 (7)	C21D—C22D— H22D	118.5
N6B—N5B— C11B	110.8 (7)	C24D—C23D— C22D	120.7 (8)
N6B—N5B—C2N	120.6 (6)	C24D—C23D— H23D	119.6
C11B—N5B— C2N	127.6 (7)	C22D—C23D— H23D	119.6
C9B—N6B—N5B	105.4 (7)	C25D—C24D— C23D	118.0 (8)
C9B—N6B—Rh2	124.1 (6)	C25D—C24D— H24D	121.0
N5B—N6B—Rh2	130.1 (5)	C23D—C24D— H24D	121.0
N2B—C3B—C4B	108.0 (7)	C24D—C25D— C26D	121.1 (7)
N2B—C3B—H3B	126.0	C24D—C25D— H25D	119.4

C4B—C3B—H3B	126.0	C26D—C25D— H25D	119.4
C3B—C4B—C5B	104.1 (7)	C25D—C26D— C21D	123.7 (7)
C3B—C4B—H4B	127.9	C25D—C26D— H26D	118.2
C5B—C4B—H4B	127.9	C21D—C26D— H26D	118.2
N1B—C5B—C4B	112.5 (7)	C36D—C31D— C32D	114.3 (8)
N1B—C5B—H5B	123.7	C36D—C31D— B1D	123.3 (7)
C4B—C5B—H5B	123.7	C32D—C31D— B1D	122.4 (7)
N4B—C6B—N3B	102.4 (6)	C33D—C32D— C31D	125.6 (9)
N4B—C6B—Rh1	136.6 (5)	C33D—C32D— H32D	117.2
N3B—C6B—Rh1	121.0 (5)	C31D—C32D— H32D	117.2
C8B—C7B—N3B	105.8 (7)	C32D—C33D— C34D	118.8 (10)
C8B—C7B—H7B	127.1	C32D—C33D— H33D	120.6
N3B—C7B—H7B	127.1	C34D—C33D— H33D	120.6
C7B—C8B—N4B	107.4 (7)	C33D—C34D— C35D	120.3 (10)
C7B—C8B—H8B	126.3	C33D—C34D—	119.8

		H34D	
N4B—C8B—H8B	126.3	C35D—C34D— H34D	119.8
N6B—C9B— C10B	112.4 (8)	C34D—C35D— C36D	118.2 (10)
N6B—C9B—H9B	123.8	C34D—C35D— H35D	120.9
C10B—C9B— H9B	123.8	C36D—C35D— H35D	120.9
C11B—C10B— C9B	103.7 (8)	C31D—C36D— C35D	122.7 (9)
C11B—C10B— H10B	128.1	C31D—C36D— H36D	118.6
C9B—C10B— H10B	128.1	C35D—C36D— H36D	118.6
N5B—C11B— C10B	107.6 (8)	C46D—C41D— C42D	114.7 (7)
N5B—C11B— H11B	126.2	C46D—C41D— B1D	123.3 (6)
C10B—C11B— H11B	126.2	C42D—C41D— B1D	122.0 (7)
N3A—C1M— N2A	110.9 (6)	C41D—C42D— C43D	123.0 (8)
N3A—C1M— H1M1	109.5	C41D—C42D— H42D	118.5
N2A—C1M— H1M1	109.5	C43D—C42D— H42D	118.5
N3A—C1M— H1M2	109.5	C44D—C43D— C42D	119.0 (8)

N2A—C1M— H1M2	109.5	C44D—C43D— H43D	120.5
H1M1—C1M— H1M2	108.0	C42D—C43D— H43D	120.5
N4A—C2M— N6A	109.8 (6)	C43D—C44D— C45D	119.4 (8)
N4A—C2M— H2M1	109.7	C43D—C44D— H44D	120.3
N6A—C2M— H2M1	109.7	C45D—C44D— H44D	120.3
N4A—C2M— H2M2	109.7	C46D—C45D— C44D	119.8 (8)
N6A—C2M— H2M2	109.7	C46D—C45D— H45D	120.1
H2M1—C2M— H2M2	108.2	C44D—C45D— H45D	120.1
N2B—C1N—N3B	109.7 (5)	C45D—C46D— C41D	124.0 (8)
N2B—C1N— H1N1	109.7	C45D—C46D— H46D	118.0
N3B—C1N— H1N1	109.7	C41D—C46D— H46D	118.0
N2B—C1N— H1N2	109.7	C2F—C1F—H1F1	109.5
N3B—C1N— H1N2	109.7	C2F—C1F—H1F2	109.5
H1N1—C1N— H1N2	108.2	H1F1—C1F— H1F2	109.5
N5B—C2N—N4B	111.7 (6)	C2F—C1F—H1F3	109.5

N5B—C2N— H2N1	109.3	H1F1—C1F— H1F3	109.5
N4B—C2N— H2N1	109.3	H1F2—C1F— H1F3	109.5
N5B—C2N— H2N2	109.3	O1F—C2F—C1F	121.5 (15)
N4B—C2N— H2N2	109.3	O1F—C2F—C3F	123.6 (16)
H2N1—C2N— H2N2	107.9	C1F—C2F—C3F	114.8 (13)
C31C—B1C— C21C	112.5 (6)	C2F—C3F—H3F1	109.5
C31C—B1C— C41C	106.5 (6)	C2F—C3F—H3F2	109.5
C21C—B1C— C41C	110.5 (6)	H3F1—C3F— H3F2	109.5
C31C—B1C— C11C	111.0 (6)	C2F—C3F—H3F3	109.5
C21C—B1C— C11C	109.0 (6)	H3F1—C3F— H3F3	109.5
C41C—B1C— C11C	107.2 (6)	H3F2—C3F— H3F3	109.5
C16C—C11C— C12C	114.6 (7)	C2G—C1G— H1G1	109.5
C16C—C11C— B1C	123.3 (6)	C2G—C1G— H1G2	109.5
C12C—C11C— B1C	121.9 (7)	H1G1—C1G— H1G2	109.5
C13C—C12C—	123.3 (9)	C2G—C1G—	109.5

C11C		H1G3	
C13C—C12C— H12C	118.4	H1G1—C1G— H1G3	109.5
C11C—C12C— H12C	118.4	H1G2—C1G— H1G3	109.5
C14C—C13C— C12C	121.4 (9)	O1G—C2G—C1G	128.3 (18)
C14C—C13C— H13C	119.3	O1G—C2G—C3G	131.7 (19)
C12C—C13C— H13C	119.3	C1G—C2G—C3G	99 (2)
C13C—C14C— C15C	118.4 (9)	C2G—C3G— H3G1	109.5
C13C—C14C— H14C	120.8	C2G—C3G— H3G2	109.5
C15C—C14C— H14C	120.8	H3G1—C3G— H3G2	109.5
C14C—C15C— C16C	121.3 (9)	C2G—C3G— H3G3	109.5
C14C—C15C— H15C	119.4	H3G1—C3G— H3G3	109.5
C16C—C15C— H15C	119.4	H3G2—C3G— H3G3	109.5
C11C—C16C— C15C	120.9 (8)	O1H—C2H—C3H	127.7 (14)
C11C—C16C— H16C	119.5	O1H—C2H—C1H	126.3 (13)
C15C—C16C— H16C	119.5	C3H—C2H—C1H	105.9 (19)

C26C—C21C— C22C	112.8 (7)	C2H—C3H— H3H1	109.5
C26C—C21C— B1C	125.9 (6)	C2H—C3H— H3H2	109.5
C22C—C21C— B1C	121.2 (7)	H3H1—C3H— H3H2	109.5
C23C—C22C— C21C	123.3 (8)	C2H—C3H— H3H3	109.5
C23C—C22C— H22C	118.4	H3H1—C3H— H3H3	109.5
C21C—C22C— H22C	118.4	H3H2—C3H— H3H3	109.5
C24C—C23C— C22C	119.8 (9)	C2H—C1H— H1H1	109.5
C24C—C23C— H23C	120.1	C2H—C1H— H1H2	109.5
C22C—C23C— H23C	120.1	H1H1—C1H— H1H2	109.5
C25C—C24C— C23C	120.0 (9)	C2H—C1H— H1H3	109.5
C25C—C24C— H24C	120.0	H1H1—C1H— H1H3	109.5
C23C—C24C— H24C	120.0	H1H2—C1H— H1H3	109.5
C24C—C25C— C26C	120.1 (8)		
C6B—Rh1— C1E—O1E	170 (11)	C6B—N3B— C1N—N2B	58.3 (8)

N1B—Rh1— C1E—O1E	-64 (13)	C7B—N3B— C1N—N2B	-123.6 (7)
N5A—Rh1— C1E—O1E	-17 (11)	N6B—N5B— C2N—N4B	74.6 (8)
C6A—Rh2— C2E—O2E	-111 (12)	C11B—N5B— C2N—N4B	-92.5 (8)
N1A—Rh2— C2E—O2E	-28 (13)	C6B—N4B— C2N—N5B	-106.3 (8)
N6B—Rh2— C2E—O2E	62 (12)	C8B—N4B— C2N—N5B	63.1 (8)
C2E—Rh2— N1A—C5A	133.6 (18)	C31C—B1C— C11C—C16C	150.6 (7)
C6A—Rh2— N1A—C5A	-143.6 (7)	C21C—B1C— C11C—C16C	26.1 (9)
N6B—Rh2— N1A—C5A	42.4 (7)	C41C—B1C— C11C—C16C	-93.5 (7)
C2E—Rh2— N1A—N2A	-50 (2)	C31C—B1C— C11C—C12C	-35.8 (9)
C6A—Rh2— N1A—N2A	33.2 (5)	C21C—B1C— C11C—C12C	-160.3 (6)
N6B—Rh2— N1A—N2A	-140.8 (5)	C41C—B1C— C11C—C12C	80.1 (8)
C5A—N1A— N2A—C3A	-0.3 (8)	C16C—C11C— C12C—C13C	3.7 (11)
Rh2—N1A— N2A—C3A	-177.8 (5)	B1C—C11C— C12C—C13C	-170.4 (7)
C5A—N1A— N2A—C1M	-176.0 (6)	C11C—C12C— C13C—C14C	0.1 (13)
Rh2—N1A—	6.4 (8)	C12C—C13C—	-2.8 (14)

N2A—C1M		C14C—C15C	
C1E—Rh1— N5A—C11A	-116.7 (6)	C13C—C14C— C15C—C16C	1.5 (13)
C6B—Rh1— N5A—C11A	17.4 (17)	C12C—C11C— C16C—C15C	-4.8 (10)
N1B—Rh1— N5A—C11A	60.7 (6)	B1C—C11C— C16C—C15C	169.2 (7)
C1E—Rh1— N5A—N6A	56.3 (6)	C14C—C15C— C16C—C11C	2.5 (12)
C6B—Rh1— N5A—N6A	-169.6 (12)	C31C—B1C— C21C—C26C	119.8 (8)
N1B—Rh1— N5A—N6A	-126.3 (5)	C41C—B1C— C21C—C26C	1.0 (10)
C11A—N5A— N6A—C9A	-0.8 (8)	C11C—B1C— C21C—C26C	-116.6 (7)
Rh1—N5A— N6A—C9A	-174.9 (5)	C31C—B1C— C21C—C22C	-63.0 (9)
C11A—N5A— N6A—C2M	-168.5 (6)	C41C—B1C— C21C—C22C	178.1 (7)
Rh1—N5A— N6A—C2M	17.3 (9)	C11C—B1C— C21C—C22C	60.5 (9)
N1A—N2A— C3A—C4A	1.1 (10)	C26C—C21C— C22C—C23C	-0.2 (12)
C1M—N2A— C3A—C4A	176.2 (8)	B1C—C21C— C22C—C23C	-177.7 (8)
N2A—C3A— C4A—C5A	-1.4 (10)	C21C—C22C— C23C—C24C	-1.3 (14)
N2A—N1A— C5A—C4A	-0.6 (8)	C22C—C23C— C24C—C25C	2.7 (15)

Rh2—N1A— C5A—C4A	176.5 (5)	C23C—C24C— C25C—C26C	-2.6 (13)
C3A—C4A— C5A—N1A	1.3 (10)	C22C—C21C— C26C—C25C	0.3 (11)
C7A—N3A— C6A—N4A	0.6 (7)	B1C—C21C— C26C—C25C	177.6 (7)
C1M—N3A— C6A—N4A	175.6 (6)	C24C—C25C— C26C—C21C	1.1 (12)
C7A—N3A— C6A—Rh2	178.5 (5)	C21C—B1C— C31C—C32C	20.3 (10)
C1M—N3A— C6A—Rh2	-6.4 (9)	C41C—B1C— C31C—C32C	141.5 (8)
C8A—N4A— C6A—N3A	0.8 (7)	C11C—B1C— C31C—C32C	-102.2 (9)
C2M—N4A— C6A—N3A	173.2 (6)	C21C—B1C— C31C—C36C	-159.7 (6)
C8A—N4A— C6A—Rh2	-176.6 (5)	C41C—B1C— C31C—C36C	-38.4 (9)
C2M—N4A— C6A—Rh2	-4.2 (11)	C11C—B1C— C31C—C36C	77.9 (8)
C2E—Rh2— C6A—N3A	138.4 (6)	C36C—C31C— C32C—C33C	-2.2 (13)
N1A—Rh2— C6A—N3A	-32.4 (5)	B1C—C31C— C32C—C33C	177.9 (9)
N6B—Rh2— C6A—N3A	14 (2)	C31C—C32C— C33C—C34C	1.5 (17)
C2E—Rh2— C6A—N4A	-44.4 (7)	C32C—C33C— C34C—C35C	0.2 (16)
N1A—Rh2—	144.7 (7)	C33C—C34C—	-1.0 (15)

C6A—N4A		C35C—C36C	
N6B—Rh2— C6A—N4A	-169.3 (13)	C34C—C35C— C36C—C31C	0.2 (14)
C6A—N3A— C7A—C8A	-1.8 (8)	C32C—C31C— C36C—C35C	1.3 (12)
C1M—N3A— C7A—C8A	-176.6 (7)	B1C—C31C— C36C—C35C	-178.7 (7)
N3A—C7A— C8A—N4A	2.2 (8)	C31C—B1C— C41C—C42C	-63.7 (8)
C6A—N4A— C8A—C7A	-1.9 (9)	C21C—B1C— C41C—C42C	58.8 (8)
C2M—N4A— C8A—C7A	-174.5 (7)	C11C—B1C— C41C—C42C	177.4 (6)
N5A—N6A— C9A—C10A	0.6 (9)	C31C—B1C— C41C—C46C	113.4 (7)
C2M—N6A— C9A—C10A	167.0 (7)	C21C—B1C— C41C—C46C	-124.1 (7)
N6A—C9A— C10A—C11A	-0.2 (10)	C11C—B1C— C41C—C46C	-5.5 (9)
N6A—N5A— C11A—C10A	0.6 (9)	C46C—C41C— C42C—C43C	1.6 (10)
Rh1—N5A— C11A—C10A	175.0 (5)	B1C—C41C— C42C—C43C	178.9 (6)
C9A—C10A— C11A—N5A	-0.3 (10)	C41C—C42C— C43C—C44C	-2.1 (11)
C1E—Rh1— N1B—C5B	95 (5)	C42C—C43C— C44C—C45C	0.8 (11)
C6B—Rh1— N1B—C5B	-139.6 (7)	C43C—C44C— C45C—C46C	0.9 (11)

N5A—Rh1— N1B—C5B	46.9 (7)	C42C—C41C— C46C—C45C	0.0 (10)
C1E—Rh1— N1B—N2B	-96 (5)	B1C—C41C— C46C—C45C	-177.2 (6)
C6B—Rh1— N1B—N2B	29.7 (5)	C44C—C45C— C46C—C41C	-1.3 (11)
N5A—Rh1— N1B—N2B	-143.8 (5)	C21D—B1D— C11D—C16D	34.1 (9)
C5B—N1B— N2B—C3B	-1.3 (7)	C41D—B1D— C11D—C16D	-86.3 (8)
Rh1—N1B— N2B—C3B	-173.2 (5)	C31D—B1D— C11D—C16D	157.6 (6)
C5B—N1B— N2B—C1N	-176.2 (6)	C21D—B1D— C11D—C12D	-151.1 (6)
Rh1—N1B— N2B—C1N	11.9 (7)	C41D—B1D— C11D—C12D	88.6 (7)
C11B—N5B— N6B—C9B	-2.3 (8)	C31D—B1D— C11D—C12D	-27.5 (9)
C2N—N5B— N6B—C9B	-171.4 (6)	C16D—C11D— C12D—C13D	1.7 (11)
C11B—N5B— N6B—Rh2	-175.4 (5)	B1D—C11D— C12D—C13D	-173.6 (7)
C2N—N5B— N6B—Rh2	15.6 (9)	C11D—C12D— C13D—C14D	-0.7 (13)
C2E—Rh2— N6B—C9B	-107.2 (7)	C12D—C13D— C14D—C15D	1.0 (15)
C6A—Rh2— N6B—C9B	18 (2)	C13D—C14D— C15D—C16D	-2.3 (14)
N1A—Rh2—	63.6 (6)	C14D—C15D—	3.5 (13)

N6B—C9B		C16D—C11D	
C2E—Rh2— N6B—N5B	64.7 (6)	C12D—C11D— C16D—C15D	-3.0 (11)
C6A—Rh2— N6B—N5B	-170.5 (15)	B1D—C11D— C16D—C15D	172.2 (7)
N1A—Rh2— N6B—N5B	-124.5 (6)	C41D—B1D— C21D—C22D	40.2 (8)
N1B—N2B— C3B—C4B	1.1 (9)	C31D—B1D— C21D—C22D	161.7 (6)
C1N—N2B— C3B—C4B	175.1 (7)	C11D—B1D— C21D—C22D	-77.4 (8)
N2B—C3B— C4B—C5B	-0.4 (9)	C41D—B1D— C21D—C26D	-145.2 (6)
N2B—N1B— C5B—C4B	1.0 (8)	C31D—B1D— C21D—C26D	-23.6 (9)
Rh1—N1B— C5B—C4B	171.6 (5)	C11D—B1D— C21D—C26D	97.2 (7)
C3B—C4B— C5B—N1B	-0.4 (9)	C26D—C21D— C22D—C23D	0.1 (9)
C8B—N4B— C6B—N3B	1.6 (7)	B1D—C21D— C22D—C23D	175.3 (6)
C2N—N4B— C6B—N3B	172.0 (6)	C21D—C22D— C23D—C24D	-1.2 (10)
C8B—N4B— C6B—Rh1	-177.8 (5)	C22D—C23D— C24D—C25D	1.8 (10)
C2N—N4B— C6B—Rh1	-7.4 (10)	C23D—C24D— C25D—C26D	-1.4 (10)
C7B—N3B— C6B—N4B	-1.4 (7)	C24D—C25D— C26D—C21D	0.3 (10)

C1N—N3B— C6B—N4B	176.8 (6)	C22D—C21D— C26D—C25D	0.4 (9)
C7B—N3B— C6B—Rh1	178.1 (5)	B1D—C21D— C26D—C25D	-174.7 (6)
C1N—N3B— C6B—Rh1	-3.6 (8)	C21D—B1D— C31D—C36D	-117.9 (8)
C1E—Rh1— C6B—N4B	-36.6 (7)	C41D—B1D— C31D—C36D	5.5 (9)
N1B—Rh1— C6B—N4B	146.2 (7)	C11D—B1D— C31D—C36D	120.8 (7)
N5A—Rh1— C6B—N4B	-170.6 (11)	C21D—B1D— C31D—C32D	64.0 (9)
C1E—Rh1— C6B—N3B	144.0 (5)	C41D—B1D— C31D—C32D	-172.6 (6)
N1B—Rh1— C6B—N3B	-33.1 (5)	C11D—B1D— C31D—C32D	-57.3 (9)
N5A—Rh1— C6B—N3B	10.1 (17)	C36D—C31D— C32D—C33D	3.6 (12)
C6B—N3B— C7B—C8B	0.7 (8)	B1D—C31D— C32D—C33D	-178.2 (8)
C1N—N3B— C7B—C8B	-177.5 (6)	C31D—C32D— C33D—C34D	-4.1 (14)
N3B—C7B— C8B—N4B	0.4 (8)	C32D—C33D— C34D—C35D	1.9 (15)
C6B—N4B— C8B—C7B	-1.3 (8)	C33D—C34D— C35D—C36D	0.2 (14)
C2N—N4B— C8B—C7B	-172.1 (6)	C32D—C31D— C36D—C35D	-1.2 (11)
N5B—N6B—	2.5 (9)	B1D—C31D—	-179.4 (7)

C9B—C10B		C36D—C35D	
Rh2—N6B— C9B—C10B	176.1 (5)	C34D—C35D— C36D—C31D	-0.6 (12)
N6B—C9B— C10B—C11B	-1.8 (10)	C21D—B1D— C41D—C46D	-144.3 (7)
N6B—N5B— C11B—C10B	1.3 (9)	C31D—B1D— C41D—C46D	91.3 (8)
C2N—N5B— C11B—C10B	169.4 (7)	C11D—B1D— C41D—C46D	-25.2 (9)
C9B—C10B— C11B—N5B	0.2 (9)	C21D—B1D— C41D—C42D	38.9 (9)
C6A—N3A— C1M—N2A	61.3 (9)	C31D—B1D— C41D—C42D	-85.5 (8)
C7A—N3A— C1M—N2A	-124.5 (7)	C11D—B1D— C41D—C42D	158.0 (7)
C3A—N2A— C1M—N3A	126.9 (8)	C46D—C41D— C42D—C43D	-2.3 (12)
N1A—N2A— C1M—N3A	-58.3 (8)	B1D—C41D— C42D—C43D	174.8 (8)
C6A—N4A— C2M—N6A	-110.0 (7)	C41D—C42D— C43D—C44D	2.7 (14)
C8A—N4A— C2M—N6A	61.5 (8)	C42D—C43D— C44D—C45D	-2.2 (15)
C9A—N6A— C2M—N4A	-90.1 (9)	C43D—C44D— C45D—C46D	1.5 (16)
N5A—N6A— C2M—N4A	75.0 (8)	C44D—C45D— C46D—C41D	-1.2 (15)
C3B—N2B— C1N—N3B	125.5 (8)	C42D—C41D— C46D—C45D	1.5 (12)

N1B—N2B— C1N—N3B	-60.8 (8)	B1D—C41D— C46D—C45D	-175.5 (8)
---------------------	-----------	------------------------	------------

[Ir(NCN^{Me})(PPh₃)₂(CO)BPh₄ (2.1V)]

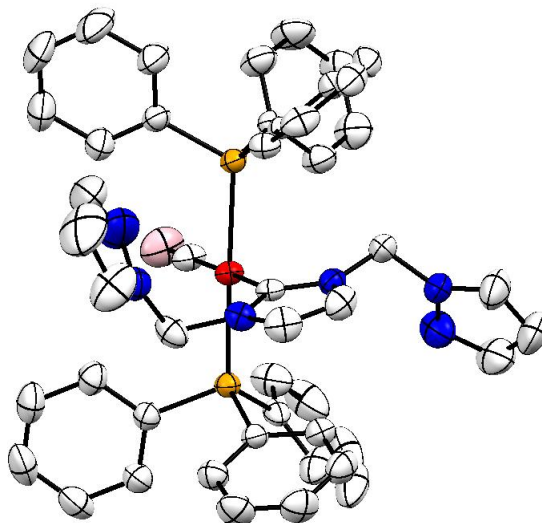


Table 1. Experimental details

Crystal data	
Chemical formula	C ₇₂ H ₆₂ BIrN ₆ OP ₂
<i>M</i> _r	1232.75
Crystal system, space group	?, ?
Temperature (K)	293
<i>a</i> , <i>b</i> , <i>c</i> (Å)	13.4663 (3), 13.9568 (4), 17.4852 (4)
<i>a</i> , <i>b</i> , <i>g</i> (°)	88.321 (1), 88.690 (1), 68.105 (1)
<i>V</i> (Å ³)	3047.68 (13)
<i>Z</i>	2
Radiation type	Mo <i>K</i> α
<i>m</i> (mm ⁻¹)	2.29
Crystal size (mm)	××
Data collection	

Diffractometer	?
Absorption correction	—
No. of measured, independent and observed [$I > 2s(I)$] reflections	66139, 10696, 10056
R_{int}	0.028
$(\sin \theta/\lambda)_{\text{max}}$ (\AA^{-1})	0.595
Refinement	
$R[F^2 > 2s(F^2)]$, $wR(F^2)$, S	0.018, 0.044, 1.96
No. of reflections	10696
No. of parameters	748
No. of restraints	0
H-atom treatment	H atoms treated by a mixture of independent and constrained refinement
$D\rho_{\text{max}}$, $D\rho_{\text{min}}$ (e \AA^{-3})	0.54, -0.39

Computer programs: *SHELXS97* (Sheldrick, 2008), *SHELXL97* (Sheldrick, 2008).

Table 2. Selected geometric parameters (\AA , $^\circ$)

Ir1—C1D	1.863 (2)	N1C—C4C	1.376 (2)
Ir1—C3C	2.0711 (19)	N1C—C2M	1.465 (2)
Ir1—P1A	2.3240 (5)	N2C—C3C	1.359 (2)
Ir1—P1B	2.3416 (5)	N2C—C5C	1.379 (2)
C1D—O1D	1.145 (2)	N2C—C1M	1.450 (2)
P1A—C7A	1.821 (2)	C4C—C5C	1.328 (3)
P1A—C13A	1.8267 (19)	C4C—H4C	0.9300
P1A—C1A	1.8313 (19)	C5C—H5C	0.9300
C1A—C2A	1.382 (3)	N3C—N4C	1.332 (3)

C1A—C6A	1.392 (3)	N3C—C8C	1.333 (3)
C2A—C3A	1.387 (3)	N3C—C1M	1.427 (3)
C2A—H2A	0.9300	N4C—C6C	1.326 (5)
C3A—C4A	1.376 (3)	C6C—C7C	1.361 (5)
C3A—H3A	0.9300	C6C—H6C	0.9300
C4A—C5A	1.363 (3)	C7C—C8C	1.356 (4)
C4A—H4A	0.9300	C7C—H7C	0.9300
C5A—C6A	1.381 (3)	C8C—H8C	0.9300
C5A—H5A	0.9300	N5C—N6C	1.342 (2)
C6A—H6A	0.9300	N5C—C11C	1.347 (3)
C7A—C8A	1.384 (3)	N5C—C2M	1.428 (2)
C7A—C12A	1.390 (3)	N6C—C9C	1.322 (3)
C8A—C9A	1.380 (3)	C9C—C10C	1.375 (4)
C8A—H8A	0.9300	C9C—H9C	0.9300
C9A—C10A	1.360 (3)	C10C—C11C	1.338 (3)
C9A—H9A	0.9300	C10C—H10C	0.9300
C10A—C11A	1.366 (3)	C11C—H11C	0.9300
C10A—H10A	0.9300	C1M—H1M1	0.9700
C11A—C12A	1.370 (3)	C1M—H1M2	0.9700
C11A—H11A	0.9300	C2M—H2M1	0.9700
C12A—H12A	0.9300	C2M—H2M2	0.9700
C13A—C18A	1.376 (3)	B1E—C21E	1.639 (3)
C13A—C14A	1.383 (3)	B1E—C37E	1.646 (3)
C14A—C15A	1.380 (3)	B1E—C11E	1.655 (3)
C14A—H14A	0.9300	B1E—C31E	1.657 (3)
C15A—C16A	1.375 (4)	C11E—C16E	1.388 (3)

C15A—H15A	0.9300	C11E—C12E	1.394 (3)
C16A—C17A	1.365 (3)	C12E—C13E	1.386 (3)
C16A—H16A	0.9300	C12E—H12E	0.9300
C17A—C18A	1.385 (3)	C13E—C14E	1.375 (3)
C17A—H17A	0.9300	C13E—H13E	0.9300
C18A—H18A	0.9300	C14E—C15E	1.370 (3)
P1B—C13B	1.8212 (19)	C14E—H14E	0.9300
P1B—C1B	1.8217 (19)	C15E—C16E	1.388 (3)
P1B—C7B	1.8339 (19)	C15E—H15E	0.9300
C1B—C2B	1.383 (3)	C16E—H16E	0.9300
C1B—C6B	1.399 (3)	C21E—C26E	1.391 (3)
C2B—C3B	1.384 (3)	C21E—C22E	1.401 (3)
C2B—H2B	0.9300	C22E—C23E	1.386 (3)
C3B—C4B	1.366 (3)	C22E—H22E	0.9300
C3B—H3B	0.9300	C23E—C24E	1.373 (4)
C4B—C5B	1.378 (3)	C23E—H23E	0.9300
C4B—H4B	0.9300	C24E—C25E	1.363 (4)
C5B—C6B	1.373 (3)	C24E—H24E	0.9300
C5B—H5B	0.9300	C25E—C26E	1.391 (3)
C6B—H6B	0.9300	C25E—H25E	0.9300
C7B—C8B	1.375 (3)	C26E—H26E	0.9300
C7B—C12B	1.385 (3)	C31E—C36E	1.391 (3)
C8B—C9B	1.399 (3)	C31E—C32E	1.404 (3)
C8B—H8B	0.9300	C32E—C33E	1.384 (3)
C9B—C10B	1.363 (4)	C32E—H32E	0.9300
C9B—H9B	0.9300	C33E—C34E	1.353 (3)

C10B—C11B	1.342 (4)	C33E—H33E	0.9300
C10B—H10B	0.9300	C34E—C35E	1.368 (3)
C11B—C12B	1.385 (3)	C34E—H34E	0.9300
C11B—H11B	0.9300	C35E—C36E	1.394 (3)
C12B—H12B	0.9300	C35E—H35E	0.9300
C13B—C18B	1.382 (3)	C36E—H36E	0.9300
C13B—C14B	1.391 (3)	C37E—C42E	1.391 (3)
C14B—C15B	1.384 (3)	C37E—C38E	1.409 (3)
C14B—H14B	0.9300	C38E—C39E	1.369 (3)
C15B—C16B	1.366 (3)	C38E—H38E	0.9300
C15B—H15B	0.9300	C39E—C40E	1.374 (3)
C16B—C17B	1.374 (3)	C39E—H39E	0.9300
C16B—H16B	0.9300	C40E—C41E	1.369 (3)
C17B—C18B	1.385 (3)	C40E—H40E	0.9300
C17B—H17B	0.9300	C41E—C42E	1.387 (3)
C18B—H18B	0.9300	C41E—H41E	0.9300
N1C—C3C	1.354 (2)	C42E—H42E	0.9300
C1D—Irl—C3C	177.49 (8)	C4C—N1C—C2M	123.93 (17)
C1D—Irl—P1A	87.28 (6)	C3C—N2C—C5C	111.20 (17)
C3C—Irl—P1A	92.56 (5)	C3C—N2C—C1M	124.82 (16)
C1D—Irl—P1B	90.22 (6)	C5C—N2C—C1M	123.94 (17)
C3C—Irl—P1B	90.05 (5)	N1C—C3C—N2C	103.40 (15)
P1A—Irl—P1B	176.319 (15)	N1C—C3C—Irl	130.10 (14)
O1D—C1D—Irl	177.4 (2)	N2C—C3C—Irl	126.41 (14)
C7A—P1A—	105.55 (9)	C5C—C4C—N1C	106.88 (18)

C13A			
C7A—P1A—C1A	102.86 (9)	C5C—C4C—H4C	126.6
C13A—P1A— C1A	101.49 (9)	N1C—C4C—H4C	126.6
C7A—P1A—Irl	109.34 (6)	C4C—C5C—N2C	106.93 (19)
C13A—P1A—Irl	117.18 (7)	C4C—C5C—H5C	126.5
C1A—P1A—Irl	118.78 (6)	N2C—C5C—H5C	126.5
C2A—C1A—C6A	118.60 (18)	N4C—N3C—C8C	112.1 (2)
C2A—C1A—P1A	119.14 (15)	N4C—N3C—C1M	120.5 (2)
C6A—C1A—P1A	122.26 (15)	C8C—N3C—C1M	127.3 (2)
C1A—C2A—C3A	120.5 (2)	C6C—N4C—N3C	104.6 (3)
C1A—C2A—H2A	119.7	N4C—C6C—C7C	110.9 (3)
C3A—C2A—H2A	119.7	N4C—C6C—H6C	124.5
C4A—C3A—C2A	120.0 (2)	C7C—C6C—H6C	124.5
C4A—C3A—H3A	120.0	C8C—C7C—C6C	106.1 (3)
C2A—C3A—H3A	120.0	C8C—C7C—H7C	127.0
C5A—C4A—C3A	120.0 (2)	C6C—C7C—H7C	127.0
C5A—C4A—H4A	120.0	N3C—C8C—C7C	106.1 (3)
C3A—C4A—H4A	120.0	N3C—C8C—H8C	126.9
C4A—C5A—C6A	120.5 (2)	C7C—C8C—H8C	126.9
C4A—C5A—H5A	119.7	N6C—N5C— C11C	112.08 (18)
C6A—C5A—H5A	119.7	N6C—N5C—C2M	119.93 (18)
C5A—C6A—C1A	120.3 (2)	C11C—N5C— C2M	127.97 (19)
C5A—C6A—H6A	119.8	C9C—N6C—N5C	103.2 (2)
C1A—C6A—H6A	119.8	N6C—C9C—	112.7 (2)

		C10C	
C8A—C7A— C12A	117.79 (19)	N6C—C9C—H9C	123.6
C8A—C7A—P1A	118.91 (15)	C10C—C9C— H9C	123.6
C12A—C7A— P1A	123.19 (15)	C11C—C10C— C9C	104.9 (2)
C9A—C8A—C7A	120.8 (2)	C11C—C10C— H10C	127.6
C9A—C8A—H8A	119.6	C9C—C10C— H10C	127.6
C7A—C8A—H8A	119.6	C10C—C11C— N5C	107.1 (2)
C10A—C9A— C8A	120.5 (2)	C10C—C11C— H11C	126.4
C10A—C9A— H9A	119.7	N5C—C11C— H11C	126.4
C8A—C9A—H9A	119.7	N3C—C1M—N2C	112.75 (17)
C9A—C10A— C11A	119.5 (2)	N3C—C1M— H1M1	109.0
C9A—C10A— H10A	120.3	N2C—C1M— H1M1	109.0
C11A—C10A— H10A	120.3	N3C—C1M— H1M2	109.0
C10A—C11A— C12A	120.9 (2)	N2C—C1M— H1M2	109.0
C10A—C11A— H11A	119.6	H1M1—C1M— H1M2	107.8
C12A—C11A—	119.6	N5C—C2M—N1C	113.15 (16)

H11A			
C11A—C12A— C7A	120.6 (2)	N5C—C2M— H2M1	108.9
C11A—C12A— H12A	119.7	N1C—C2M— H2M1	108.9
C7A—C12A— H12A	119.7	N5C—C2M— H2M2	108.9
C18A—C13A— C14A	118.37 (18)	N1C—C2M— H2M2	108.9
C18A—C13A— P1A	120.76 (15)	H2M1—C2M— H2M2	107.8
C14A—C13A— P1A	120.85 (16)	C21E—B1E— C37E	109.06 (18)
C15A—C14A— C13A	120.8 (2)	C21E—B1E— C11E	110.45 (17)
C15A—C14A— H14A	119.6	C37E—B1E— C11E	106.27 (17)
C13A—C14A— H14A	119.6	C21E—B1E— C31E	110.18 (17)
C16A—C15A— C14A	120.0 (2)	C37E—B1E— C31E	111.09 (17)
C16A—C15A— H15A	120.0	C11E—B1E— C31E	109.72 (17)
C14A—C15A— H15A	120.0	C16E—C11E— C12E	114.56 (19)
C17A—C16A— C15A	120.0 (2)	C16E—C11E— B1E	123.31 (18)
C17A—C16A— H16A	120.0	C12E—C11E— B1E	121.75 (18)

C15A—C16A— H16A	120.0	C13E—C12E— C11E	122.9 (2)
C16A—C17A— C18A	119.9 (2)	C13E—C12E— H12E	118.6
C16A—C17A— H17A	120.1	C11E—C12E— H12E	118.6
C18A—C17A— H17A	120.1	C14E—C13E— C12E	120.5 (2)
C13A—C18A— C17A	121.0 (2)	C14E—C13E— H13E	119.7
C13A—C18A— H18A	119.5	C12E—C13E— H13E	119.7
C17A—C18A— H18A	119.5	C15E—C14E— C13E	118.4 (2)
C13B—P1B—C1B	103.74 (9)	C15E—C14E— H14E	120.8
C13B—P1B—C7B	103.49 (8)	C13E—C14E— H14E	120.8
C1B—P1B—C7B	103.83 (9)	C14E—C15E— C16E	120.3 (2)
C13B—P1B—Irl	113.24 (6)	C14E—C15E— H15E	119.8
C1B—P1B—Irl	115.30 (6)	C16E—C15E— H15E	119.8
C7B—P1B—Irl	115.77 (6)	C15E—C16E— C11E	123.3 (2)
C2B—C1B—C6B	118.85 (18)	C15E—C16E— H16E	118.4
C2B—C1B—P1B	122.34 (15)	C11E—C16E—	118.4

		H16E	
C6B—C1B—P1B	118.66 (14)	C26E—C21E— C22E	114.4 (2)
C1B—C2B—C3B	120.0 (2)	C26E—C21E— B1E	124.0 (2)
C1B—C2B—H2B	120.0	C22E—C21E— B1E	121.6 (2)
C3B—C2B—H2B	120.0	C23E—C22E— C21E	122.7 (3)
C4B—C3B—C2B	120.9 (2)	C23E—C22E— H22E	118.7
C4B—C3B—H3B	119.5	C21E—C22E— H22E	118.7
C2B—C3B—H3B	119.5	C24E—C23E— C22E	120.6 (3)
C3B—C4B—C5B	119.5 (2)	C24E—C23E— H23E	119.7
C3B—C4B—H4B	120.3	C22E—C23E— H23E	119.7
C5B—C4B—H4B	120.3	C25E—C24E— C23E	118.9 (3)
C6B—C5B—C4B	120.6 (2)	C25E—C24E— H24E	120.6
C6B—C5B—H5B	119.7	C23E—C24E— H24E	120.6
C4B—C5B—H5B	119.7	C24E—C25E— C26E	120.2 (3)
C5B—C6B—C1B	120.1 (2)	C24E—C25E— H25E	119.9

C5B—C6B—H6B	119.9	C26E—C25E— H25E	119.9
C1B—C6B—H6B	119.9	C21E—C26E— C25E	123.3 (2)
C8B—C7B— C12B	118.36 (19)	C21E—C26E— H26E	118.3
C8B—C7B—P1B	122.17 (17)	C25E—C26E— H26E	118.3
C12B—C7B—P1B	119.45 (16)	C36E—C31E— C32E	113.5 (2)
C7B—C8B—C9B	119.9 (3)	C36E—C31E— B1E	121.93 (18)
C7B—C8B—H8B	120.0	C32E—C31E— B1E	124.53 (19)
C9B—C8B—H8B	120.0	C33E—C32E— C31E	122.9 (2)
C10B—C9B— C8B	120.3 (3)	C33E—C32E— H32E	118.6
C10B—C9B— H9B	119.8	C31E—C32E— H32E	118.6
C8B—C9B—H9B	119.8	C34E—C33E— C32E	121.2 (2)
C11B—C10B— C9B	120.2 (2)	C34E—C33E— H33E	119.4
C11B—C10B— H10B	119.9	C32E—C33E— H33E	119.4
C9B—C10B— H10B	119.9	C33E—C34E— C35E	118.7 (2)
C10B—C11B—	120.6 (3)	C33E—C34E—	120.6

C12B		H34E	
C10B—C11B— H11B	119.7	C35E—C34E— H34E	120.6
C12B—C11B— H11B	119.7	C34E—C35E— C36E	119.9 (2)
C11B—C12B— C7B	120.6 (2)	C34E—C35E— H35E	120.0
C11B—C12B— H12B	119.7	C36E—C35E— H35E	120.0
C7B—C12B— H12B	119.7	C31E—C36E— C35E	123.7 (2)
C18B—C13B— C14B	118.62 (18)	C31E—C36E— H36E	118.2
C18B—C13B— P1B	121.24 (15)	C35E—C36E— H36E	118.2
C14B—C13B— P1B	120.07 (16)	C42E—C37E— C38E	113.5 (2)
C15B—C14B— C13B	120.4 (2)	C42E—C37E— B1E	123.14 (19)
C15B—C14B— H14B	119.8	C38E—C37E— B1E	123.21 (19)
C13B—C14B— H14B	119.8	C39E—C38E— C37E	123.4 (2)
C16B—C15B— C14B	120.1 (2)	C39E—C38E— H38E	118.3
C16B—C15B— H15B	119.9	C37E—C38E— H38E	118.3
C14B—C15B— H15B	119.9	C38E—C39E— C40E	120.7 (2)

C15B—C16B— C17B	120.4 (2)	C38E—C39E— H39E	119.6
C15B—C16B— H16B	119.8	C40E—C39E— H39E	119.6
C17B—C16B— H16B	119.8	C41E—C40E— C39E	118.5 (2)
C16B—C17B— C18B	119.8 (2)	C41E—C40E— H40E	120.7
C16B—C17B— H17B	120.1	C39E—C40E— H40E	120.7
C18B—C17B— H17B	120.1	C40E—C41E— C42E	120.1 (2)
C13B—C18B— C17B	120.7 (2)	C40E—C41E— H41E	120.0
C13B—C18B— H18B	119.7	C42E—C41E— H41E	120.0
C17B—C18B— H18B	119.7	C41E—C42E— C37E	123.8 (2)
C3C—N1C—C4C	111.59 (16)	C41E—C42E— H42E	118.1
C3C—N1C—C2M	124.18 (16)	C37E—C42E— H42E	118.1
C3C—Irl—C1D— O1D	26 (6)	C15B—C16B— C17B—C18B	0.4 (4)
P1A—Irl—C1D— O1D	-61 (5)	C14B—C13B— C18B—C17B	-0.4 (3)
P1B—Irl—C1D— O1D	122 (5)	P1B—C13B— C18B—C17B	176.55 (17)

C1D—Ir1—P1A— C7A	-53.45 (9)	C16B—C17B— C18B—C13B	0.2 (3)
C3C—Ir1—P1A— C7A	129.06 (8)	C4C—N1C— C3C—N2C	0.5 (2)
P1B—Ir1—P1A— C7A	-6.1 (3)	C2M—N1C— C3C—N2C	-173.38 (16)
C1D—Ir1—P1A— C13A	66.53 (10)	C4C—N1C— C3C—Ir1	-176.16 (14)
C3C—Ir1—P1A— C13A	-110.97 (9)	C2M—N1C— C3C—Ir1	10.0 (3)
P1B—Ir1—P1A— C13A	113.9 (2)	C5C—N2C— C3C—N1C	-0.6 (2)
C1D—Ir1—P1A— C1A	-170.96 (10)	C1M—N2C— C3C—N1C	177.20 (16)
C3C—Ir1—P1A— C1A	11.54 (9)	C5C—N2C— C3C—Ir1	176.18 (13)
P1B—Ir1—P1A— C1A	-123.6 (2)	C1M—N2C— C3C—Ir1	-6.0 (3)
C7A—P1A— C1A—C2A	180.00 (14)	C1D—Ir1—C3C— N1C	-159.2 (16)
C13A—P1A— C1A—C2A	70.92 (16)	P1A—Ir1—C3C— N1C	-72.86 (16)
Ir1—P1A—C1A— C2A	-59.13 (16)	P1B—Ir1—C3C— N1C	104.55 (16)
C7A—P1A— C1A—C6A	-0.17 (17)	C1D—Ir1—C3C— N2C	24.9 (17)
C13A—P1A— C1A—C6A	-109.26 (16)	P1A—Ir1—C3C— N2C	111.18 (15)
Ir1—P1A—C1A—	120.69 (14)	P1B—Ir1—C3C—	-71.42 (15)

C6A		N2C	
C6A—C1A— C2A—C3A	-0.6 (3)	C3C—N1C— C4C—C5C	-0.2 (2)
P1A—C1A— C2A—C3A	179.21 (15)	C2M—N1C— C4C—C5C	173.71 (18)
C1A—C2A— C3A—C4A	0.4 (3)	N1C—C4C— C5C—N2C	-0.2 (2)
C2A—C3A— C4A—C5A	0.3 (3)	C3C—N2C— C5C—C4C	0.6 (2)
C3A—C4A— C5A—C6A	-0.7 (3)	C1M—N2C— C5C—C4C	-177.31 (18)
C4A—C5A— C6A—C1A	0.4 (3)	C8C—N3C— N4C—C6C	3.6 (3)
C2A—C1A— C6A—C5A	0.2 (3)	C1M—N3C— N4C—C6C	-177.2 (2)
P1A—C1A— C6A—C5A	-179.59 (15)	N3C—N4C— C6C—C7C	-3.0 (4)
C13A—P1A— C7A—C8A	-158.52 (16)	N4C—C6C— C7C—C8C	1.5 (5)
C1A—P1A— C7A—C8A	95.49 (17)	N4C—N3C— C8C—C7C	-2.8 (3)
Ir1—P1A—C7A— C8A	-31.64 (18)	C1M—N3C— C8C—C7C	178.0 (2)
C13A—P1A— C7A—C12A	25.4 (2)	C6C—C7C— C8C—N3C	0.8 (4)
C1A—P1A— C7A—C12A	-80.61 (19)	C11C—N5C— N6C—C9C	0.8 (3)
Ir1—P1A—C7A— C12A	152.27 (17)	C2M—N5C— N6C—C9C	179.13 (19)

C12A—C7A— C8A—C9A	1.8 (3)	N5C—N6C— C9C—C10C	-0.8 (3)
P1A—C7A— C8A—C9A	-174.52 (18)	N6C—C9C— C10C—C11C	0.6 (4)
C7A—C8A— C9A—C10A	-0.8 (4)	C9C—C10C— C11C—N5C	0.0 (3)
C8A—C9A— C10A—C11A	-0.3 (4)	N6C—N5C— C11C—C10C	-0.5 (3)
C9A—C10A— C11A—C12A	0.4 (4)	C2M—N5C— C11C—C10C	-178.7 (2)
C10A—C11A— C12A—C7A	0.6 (4)	N4C—N3C— C1M—N2C	79.0 (3)
C8A—C7A— C12A—C11A	-1.7 (3)	C8C—N3C— C1M—N2C	-101.8 (3)
P1A—C7A— C12A—C11A	174.45 (19)	C3C—N2C— C1M—N3C	-100.7 (2)
C7A—P1A— C13A—C18A	96.64 (18)	C5C—N2C— C1M—N3C	76.9 (2)
C1A—P1A— C13A—C18A	-156.36 (17)	N6C—N5C— C2M—N1C	83.7 (2)
Ir1—P1A— C13A—C18A	-25.32 (19)	C11C—N5C— C2M—N1C	-98.2 (3)
C7A—P1A— C13A—C14A	-81.73 (19)	C3C—N1C— C2M—N5C	-121.90 (19)
C1A—P1A— C13A—C14A	25.3 (2)	C4C—N1C— C2M—N5C	65.0 (2)
Ir1—P1A— C13A—C14A	156.31 (16)	C21E—B1E— C11E—C16E	-26.4 (3)
C18A—C13A—	-0.3 (4)	C37E—B1E—	91.7 (2)

C14A—C15A		C11E—C16E	
P1A—C13A— C14A—C15A	178.1 (2)	C31E—B1E— C11E—C16E	-148.1 (2)
C13A—C14A— C15A—C16A	-0.2 (4)	C21E—B1E— C11E—C12E	160.97 (19)
C14A—C15A— C16A—C17A	-0.1 (4)	C37E—B1E— C11E—C12E	-80.9 (2)
C15A—C16A— C17A—C18A	0.9 (4)	C31E—B1E— C11E—C12E	39.3 (3)
C14A—C13A— C18A—C17A	1.1 (3)	C16E—C11E— C12E—C13E	-2.2 (3)
P1A—C13A— C18A—C17A	-177.28 (18)	B1E—C11E— C12E—C13E	171.0 (2)
C16A—C17A— C18A—C13A	-1.5 (4)	C11E—C12E— C13E—C14E	1.8 (3)
C1D—Irl—P1B— C13B	-54.63 (9)	C12E—C13E— C14E—C15E	-0.1 (3)
C3C—Irl—P1B— C13B	122.88 (8)	C13E—C14E— C15E—C16E	-1.1 (3)
P1A—Irl—P1B— C13B	-101.9 (2)	C14E—C15E— C16E—C11E	0.7 (4)
C1D—Irl—P1B— C1B	-173.90 (9)	C12E—C11E— C16E—C15E	0.9 (3)
C3C—Irl—P1B— C1B	3.61 (8)	B1E—C11E— C16E—C15E	-172.1 (2)
P1A—Irl—P1B— C1B	138.8 (2)	C37E—B1E— C21E—C26E	15.7 (3)
C1D—Irl—P1B— C7B	64.65 (10)	C11E—B1E— C21E—C26E	132.2 (2)

C3C—Ir1—P1B— C7B	-117.84 (9)	C31E—B1E— C21E—C26E	-106.4 (2)
P1A—Ir1—P1B— C7B	17.4 (3)	C37E—B1E— C21E—C22E	-165.6 (2)
C13B—P1B— C1B—C2B	-14.56 (19)	C11E—B1E— C21E—C22E	-49.1 (3)
C7B—P1B— C1B—C2B	-122.47 (17)	C31E—B1E— C21E—C22E	72.2 (3)
Ir1—P1B—C1B— C2B	109.83 (16)	C26E—C21E— C22E—C23E	-0.1 (4)
C13B—P1B— C1B—C6B	170.02 (15)	B1E—C21E— C22E—C23E	-178.9 (2)
C7B—P1B— C1B—C6B	62.11 (16)	C21E—C22E— C23E—C24E	0.2 (4)
Ir1—P1B—C1B— C6B	-65.59 (16)	C22E—C23E— C24E—C25E	-0.3 (4)
C6B—C1B— C2B—C3B	-0.3 (3)	C23E—C24E— C25E—C26E	0.3 (4)
P1B—C1B— C2B—C3B	-175.74 (16)	C22E—C21E— C26E—C25E	0.2 (3)
C1B—C2B— C3B—C4B	0.6 (3)	B1E—C21E— C26E—C25E	178.9 (2)
C2B—C3B— C4B—C5B	-0.7 (4)	C24E—C25E— C26E—C21E	-0.2 (4)
C3B—C4B— C5B—C6B	0.7 (4)	C21E—B1E— C31E—C36E	148.8 (2)
C4B—C5B— C6B—C1B	-0.5 (3)	C37E—B1E— C31E—C36E	27.9 (3)
C2B—C1B—	0.3 (3)	C11E—B1E—	-89.4 (2)

C6B—C5B		C31E—C36E	
P1B—C1B— C6B—C5B	175.88 (16)	C21E—B1E— C31E—C32E	-31.6 (3)
C13B—P1B— C7B—C8B	-100.88 (18)	C37E—B1E— C31E—C32E	-152.5 (2)
C1B—P1B— C7B—C8B	7.22 (19)	C11E—B1E— C31E—C32E	90.2 (2)
Ir1—P1B—C7B— C8B	134.63 (16)	C36E—C31E— C32E—C33E	-1.1 (3)
C13B—P1B— C7B—C12B	77.29 (18)	B1E—C31E— C32E—C33E	179.3 (2)
C1B—P1B— C7B—C12B	-174.61 (16)	C31E—C32E— C33E—C34E	0.5 (4)
Ir1—P1B—C7B— C12B	-47.20 (18)	C32E—C33E— C34E—C35E	0.7 (4)
C12B—C7B— C8B—C9B	1.3 (3)	C33E—C34E— C35E—C36E	-1.3 (4)
P1B—C7B— C8B—C9B	179.50 (18)	C32E—C31E— C36E—C35E	0.5 (3)
C7B—C8B— C9B—C10B	-0.8 (4)	B1E—C31E— C36E—C35E	-179.8 (2)
C8B—C9B— C10B—C11B	-1.1 (4)	C34E—C35E— C36E—C31E	0.6 (4)
C9B—C10B— C11B—C12B	2.4 (4)	C21E—B1E— C37E—C42E	92.9 (2)
C10B—C11B— C12B—C7B	-1.8 (4)	C11E—B1E— C37E—C42E	-26.1 (3)
C8B—C7B— C12B—C11B	0.0 (3)	C31E—B1E— C37E—C42E	-145.4 (2)

P1B—C7B— C12B—C11B	-178.27 (18)	C21E—B1E— C37E—C38E	-83.0 (2)
C1B—P1B— C13B—C18B	-65.80 (18)	C11E—B1E— C37E—C38E	157.88 (19)
C7B—P1B— C13B—C18B	42.36 (18)	C31E—B1E— C37E—C38E	38.6 (3)
Ir1—P1B— C13B—C18B	168.48 (14)	C42E—C37E— C38E—C39E	1.6 (3)
C1B—P1B— C13B—C14B	111.14 (17)	B1E—C37E— C38E—C39E	178.0 (2)
C7B—P1B— C13B—C14B	-140.69 (17)	C37E—C38E— C39E—C40E	-2.2 (4)
Ir1—P1B— C13B—C14B	-14.57 (18)	C38E—C39E— C40E—C41E	0.9 (4)
C18B—C13B— C14B—C15B	0.0 (3)	C39E—C40E— C41E—C42E	0.6 (4)
P1B—C13B— C14B—C15B	-177.04 (16)	C40E—C41E— C42E—C37E	-1.1 (4)
C13B—C14B— C15B—C16B	0.7 (3)	C38E—C37E— C42E—C41E	0.0 (3)
C14B—C15B— C16B—C17B	-0.9 (4)	B1E—C37E— C42E—C41E	-176.3 (2)